INFORMATION TO USERS

This manuscript has been reproduced from the microfilm master. UMI films the text directly from the original or copy submitted. Thus, some thesis and dissertation copies are in typewriter face, while others may be from any type of computer printer.

The quality of this reproduction is dependent upon the quality of the copy submitted. Broken or indistinct print, colored or poor quality illustrations and photographs, print bleedthrough, substandard margins, and improper alignment can adversely affect reproduction.

In the unlikely event that the author did not send UMI a complete manuscript and there are missing pages, these will be noted. Also, if unauthorized copyright material had to be removed, a note will indicate the deletion.

Oversize materials (e.g., maps, drawings, charts) are reproduced by sectioning the original, beginning at the upper left-hand corner and continuing from left to right in equal sections with small overlaps. Each original is also photographed in one exposure and is included in reduced form at the back of the book.

Photographs included in the original manuscript have been reproduced xerographically in this copy. Higher quality 6" x 9" black and white photographic prints are available for any photographs or illustrations appearing in this copy for an additional charge. Contact UMI directly to order.

UMI

A Bell & Howell Information Company
300 North Zeeb Road, Ann Arbor MI 48106-1346 USA
313/761-4700 800/521-0600

Study on Homogeneous Polymerization of 1-Hexene with Zirconocene/Methylaluminoxane Catalysis and Synthesis of Oscillating Zirconocene Catalysts

by

Xia Zhao

A dissertation submitted to the Graduate Faculty in Chemistry in partial fulfillment of the requirements for the degree of Doctor of Philosophy, The City University of New York.

1997

This manuscript has been read and accepted for the Graduate Faculty in Chemistry in satisfaction for the dissertation requirement for the degree of Doctor of Philosophy.

4/30/97
Date

George Odian
Chairman of Examining Committee

4/30/97
Date

Executive Officer

George Odian
Dr. George Odian

Howard Haubenstock
Dr. Howard Haubenstock

Norman Indictor
Dr. Norman Indictor

Supervisory Committee
The City University of New York

Abstract

Study *on* Homogeneous Polymerization *of* 1-Hexene with Zirconocene/Methylaluminoxane Catalysis and Synthesis of Oscillating Zirconocene Catalysts

By: Xia Zhao

Adviser: Professor George Odian

Part A: Homogeneous Polymerization of 1-Hexene with Zirconocene/MAO catalysis

The kinetics of 1-hexene polymerization initiated by *rac*-dimethylsilyl bis[4,5,6,7-tetrahydro-1-indenyl]zirconium dichloride / methyaluminoxane (MAO) catalysis was investigated. Polymerization rate was proportional to $[Zr][MAO]^{1-2}$ $[M]^{1-2}$. The fractional orders to which polymerization rate depends on monomer and MAO concentrations changed with temperature. Polymerization rate constant k_p and activation energy E_p were determined. Three types of unsaturated end groups were studied. The relationships between chain transfer rates to form these three types of end groups and zirconocene concentration, MAO concentration and monomer concentration were determined. Chain transfer to the coordinated monomer was predominating. At low temperature, catalyst species participated chain transfer reactions. The MAO effect on chain transfer was complicated as that in propagation. Kinetic model of polymerization and chain transfers was proposed based on the kinetic results. The results of

polymer molecular weight support the kinetic results.

Isotacticity was investigated on both %mmmm and %mmmmmm levels. Isotacticity decreased tremendously with the increase of temperature. With the increase of monomer concentration, isotacticity increased and then leveled off. Isotacticity decreased with the increase of zirconocene concentration and MAO concentration. Regioreglarity was only slightly affected by reaction conditions.

Part B: Synthesis of Oscillating Zirconocene catalysts

Bis[2-phenylindenyl]zirconium dichloride (Cat.1), bis[1,2-diphenyl]zirconium dichloride (Cat.2), bis[2-methyl-1-phenyl]zirconium dichloride (Cat.3), [2-phenylindenyl][1,2,3-triphenylindenyl]zirconium dichloride (Cat.4) and bis[1,2-dimethylindenyl]zirconium dichloride (Cat.5) were synthesized as oscillating metallocene catalysts and were characterized. The polymerization of 1-hexene with the catalysis of the above catalysts was performed at different temperatures, respectively. The isotacticity of polymers was investigated by ^{13}C NMR at both pentad and heptad levels. Cat.1 could only produce atactic polymer at higher temperature and stereoblock polymer with small to medium amount of isotactic sequances at 20 and 0 °C. Cat.2 could produce polymer with almost the same high amount of isotactic sequances at 20, 50 and 80 °C. Cat.3 produced polymers with isotactic sequances and syndiotactic sequances at both 0 °C and 80 °C, but produced polymer only with syndiotactic sequances at 20 °C. Cat.4 could produce polymer with high amount of isotactic sequances. Cat.5 could only produce atactic polymer at all temperatures. However, the activities of Cat.2, Cat.3 and Cat.4 were pretty low.

Acknowledgment

I would like to express my sincere gratitude to Dr. George Odian for his generous help, guidance and patience during the course of this research.

I also want to thank Dr. Howard Haubenstock and Dr. Norman Indictor for their valuable suggestions and being so generous on their time. I am most appreciative of the many useful conversations with Dr. Jianhua Dong, Dr. Yongliang Zhang, as well as other graduate students, post doctoral associates and faculty. Thanks is also due to Dr. Boris Arshava for helping me in NMR experiments.

I gratefully acknowledge financial support of this work by grants from Exxon Chemical Co. as well as teaching appointments from the College of Staten Island. I would like to especially thank Dr. Albert Rossi of Exxon Chemical Co. for supplying catalysts and also for his guidance and friendship.

Without the support of my family this work could not have been accomplished. To my mother Weijun Wu, who helped me during the course of a difficult pregnancy and helped take care of my baby so I would have more time to work on my dissertation; to my daughter Sarah, who let me have some time to work on my dissertation; and to my husband David, who did certain things necessary to keep me on track; I say thank you and dedicate this thesis.

CONTENTS

Part. B Synthesis of Oscillating Metallocene Catalysts

LIST OF FIGURES

Part. A Homogeneous Polymerization of 1-Hexene with Zirconocene/MAO Catalysis

Part. B Synthesis of Oscillating Metallocene Catalysts

LIST OF TABLES

Part. B Synthesis of Oscillating Metallocene Catalysts

Part. A Homogenous Polymerization of 1-Hexene with Zirconocene/MAO Catalysis

1.0 Introduction

1.1 Potential of Metallocene Catalysts

In 1950's and 1960's, the discovery of Ziegler-Natta catalysts caused the plastics industry to flourish. These catalysts made possible the inexpensive and easily controlled production of linear polyethylene, stereospecific polypropylene and various poly(α-olefins)[1-6]. The Ziegler-Natta catalysis systems have developed quickly. They were developed by the interaction of an organometallic compound or hydride of a Group I-III metal with a halide, hydroxide, alkoxide or other derivative of a Group IV-VIII transition metal[7-9]. Ziegler-Natta catalysts are also called coordination initiators, which show the greatest power in stereospecific polymerization. There are two most remarkable successes for Ziegler-Natta catalysts: accomplishment of polymerization of α-olefins and creation of the stereospecific polymerization. Propylene is an oil-derived gas which is plentiful and inexpensive. Before the discovery of the Ziegler-Natta catalysis system, it was only a useless gas. But today, our daily contact with stereospecific polypropylene is inevitable. It is found in appliances, bottles, carpeting, clothing, insulation, drinking glasses and everywhere. More than 80 billion pounds of polymers are produced worldwide with Ziegler-Natta technology Therefore, these two great successes ushered in the tremendous development of the plastics industry since the 1950's and won the 1963 Nobel Prize for

Ziegler and Natta.

While Ziegler-Natta catalysts have been useful, some newer catalysts, such as homogeneous metallocene catalysts, may be even more efficient. Homogeneous metallocene catalysts are being developed with the hope to improve upon Ziegler-Natta catalysts. The typical metallocene catalysts consist of a transition-metal atom sandwiched between ring structures to form a sterically hindered site. Metallocene catalysts have several potential advantages over Ziegler-Natta catalysts. First, because Ziegler-Natta catalysts are heterogeneous catalysts, only the catalyst molecules on the surface are used. So, instead of using 100% of the catalysts in the polymerization, only some of the catalysts are used. The use of catalysts soluble in polymerization solution, also called homogeneous, may increase the utilization ratio of catalysts to 100%, which will improve the catalyst activity. The second advantage arises from the fact that the chirality of the Ziegler-Natta catalysts results from the chirality of the crystal structure, whereas the chirality of metallocene catalysts results from the chirality of the molecule as a whole because of this, it would be possible to use metallocene catalysts to refine, even design, the structure of the polymer. This would enable controlling the properties of the polymer to a greater degree than is possible with Ziegler-Natta catalysts.

The third advantage arises because metallocene catalysts enable us to more easily control the molecular weight of the polymers. This is because metallocene catalysts have well-defined single catalytic sites and well-

understood molecular structures, while Ziegler-Natta catalysts have multi-catalytic sites and complicated structures related with crystal surface structures. Further, molecular weight distribution is much narrower by using metallocene catalysts instead of Ziegler-Natta catalysts. Usually, MWD is between 2 to 3 for the polymers produced by metallocene catalysts, but is in the range of 5 to 20 for those polymers produced by Ziegler-Natta catalysts. Fourth, it is much easier to study and understand homogeneous catalysis than heterogeneous catalysis. Based on the above advantages, metallocene catalysts are predicted to initiate a new era in polymer synthesis[10]. Polymers synthesized by metallocene catalysts, ranging from crystalline to elastomeric materials, have been available commercially since about 1991. They tend to have features such as increased impact strength and toughness, better melt characteristics (because of the control over molecular structure), and improved clarity in films. Most early applications have been in specialty markets where there is a demand for higher priced, value-added polymers.

The first metallocene catalyst, bis(η^5-cyclopentadienyl)titanium dichloride (Cp_2TiCl_2) (see Scheme I), was discovered by Natta[11] in the 1950's, almost as

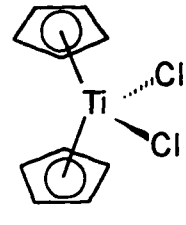

I

Scheme I Bis(η_5-cyclopentadienyl)titanium dichloride

early as the discovery of Ziegler-Natta catalysts. But they were not developed with the same enthusiasm. The homogeneous polymerization by this catalyst with group IA-IIIA metal halide or group IA-IIIA organometallic compounds as cocatalysts showed very low catalyst activity and non-stereospecificity. Meanwhile, in contrast to metallocene catalysts, Zieglar-Natta catalysts were developed with more enthusiasm and speed because they showed superior activity and stereospecificity. It seemed no other catalysts could replace them. From the 1950's through the 1980's, scientists all over the world busily searched for better Ziegler-Natta catalysis systems, rather than spend time or effort developing metallocene catalysts. Still, a few chemists thought it worthwhile to search for homogeneous catalysts. In early 1980s, Walter Kaminsky found that methylaluminoxane (MAO) used as cocatalyst could achieve high catalyst activity[12]. Although the activity of metallocene catalysts was greatly improved, only atactic polypropylene was produced by achiral metallocene[13-16]. Meanwhile, meso metallocene/MAO catalysis systems, namely meso-ethylene bis(η^5-indenyl)zirconium dichloride/MAO[17] and meso-ethylene bis(η^5-indenyl) titanium dichloride/MAO[18], produced only atactic polypropylene. But the atactic polypropylene was of little value.

The breakthrough in homogeneous isospecific polymerization was brought by Kaminsky and Külper's work in 1985. Highly isotactic polypropylene was obtained by using rac-ethylene bis(η^5-tetrahydroindenyl) zirconium dichloride (rac-$C_2H_4[H_4Ind]_2ZrCl_2$) as catalyst activated with MAO[19,20]. The isotactic index of

the polypropylene polymerized from -10°C to 20°C was as high as 99% - 99.8%. High-resolution 13C NMR spectroscopy affords an insight into the pattern of the sequences in the polymer chain. Isotactic sequences (mm triads) were found to be present to the extent of 95%, heterotactic sequences (mr triads) to the extent of 3.2 %, and sydiotactic sequences (rr triads) to the extent of 0.9%. On the other hand, the high activity of this chiral catalyst was remarkable. Less than 10^{-5} mols/L sufficed for the production of 7700 kg polypropylene per mole of Zr per hour at 60°C. However, under comparable conditions, only 2,730 kg of atactic polypropylene was formed per mole of Zr per hour with Cp_2ZrCl_2 as catalyst. The chiral zirconocene rac-$C_2H_4[H_4Ind]_2ZrCl_2$ afforded highly isotactic polypropylene, and also had a polymerization activity 2 to 3 times greater towards propylene than those catalysts that formed only atactic polymer. In addition, the properties of the polypropylene thus formed were also very remarkable. In contrast with the industrial polypropylene of that time, which had a molecular weight distribution of at least 5, polypropylene was produced with molecular weight distribution of only 1.9 to 2.6 at the polymerization temperature between ~10°C to 20°C with rac-$C_2H_4[H_4Ind]_2ZrCl_2$ as catalyst. Meanwhile, in independent studies by Ewen with $C_2H_4[H_4Ind]_2TiCl_2$ / MAO, highly isotactic polymer and high polymerization were obtained [14].

Due to the remarkable advantages of homogeneous metallocene catalysts, much research has been done on homogeneous polymerization in the last ten

years. In the following section, we shall briefly talk about the previous work done on the stereospecific polymerization of olefin with metallocene catalysts.

1.2 Stereospecific Polymerization of Olefin with Metallocene Catalysts

Catalyst stereoselectivities were studied by ^{13}C NMR. Isotactic polypropylene produced by modern heterogeneous Ziegler-Natta catalysts[21] is highly stereoregular with above 95% of mmmm pentad. At ambient temperatures, typical MAO-activated chiral ansa-metallocene catalysts yield polypropylene with 80% to 90% of mmmm[19,22,23]. However, at increased polymerization temperatures, most of these homogeneous catalysts are distinctly less stereoselective than typical heterogeneous Ziegler-Natta catalysts[24]. The ^{13}C NMR signals associated with occasional stereoerrors in the isotactic polymers produced by metallocene catalysts indicate that stereoregularity is controlled by the chirality of the metallocene catalyst and not by the asymmetry of the last inserted unit[25].

How the stereoselectivities of chiral catalysts depend on the structures of these catalysts, in particular on different bridging units and substituent patterns, has been the subject of comparative studies in several research groups[26-30]. In investigations of this kind, it is crucial to take into account the polymerization temperature T_p. A short interannular bridge will necessarily restrict rotation of the 5-member ring ligands. Accordingly, high stereoselectivities are with one-atom bridges, at least at lower polymerization temperatures. Incorporation of the ethylene bridge of $C_2H_4[Ind]_2ZrCl_2$ into a carbocyclic system[31] or its replacement

by a one-atom silanediyl or germanediyl bridge[27,32,33] increases stereoselectivities, but only to a limited extent[34].

With respect to the substituent effects on polymer stereoregularities, the substituents in β-position to the bridgehead atom of an ansa-zirconocene are the most interesting. These β-substituents are in close proximity to the coordination sites at which the growing polymer chain and the α-olefin substrate are bound. In the chiral complexes $C_2H_4[Ind]_2ZrCl_2$, $C_2H_4[H_4Ind]_2ZrCl_2$ and $Me_2Si[Ind]_2ZrCl_2$, CH or CH_2 groups of the annelated six member ring function as β-substituents and flank each of the adjacent coordination sites. If the β-substituents are very bulky, as in $Me_2Si[2\text{-}Me\text{-}4\text{-}tBu\text{-}C_5H_2]_2ZrCl_2$[31a] or in $[Me_2Si(2\text{-}SiMe_3\text{-}4\text{-}tBu\text{-}C_5H_2)_2YH]_2$[35], or particularly protruding, as in $Me_2Si[2\text{-}Me\text{-}4\text{-}aryl\text{-}1\text{-}ind]_2ZrCl_2$[27c], polypropylene with stereoregularities of %mmmm above 95% are generated even at polymerization temperatures of 70-80 °C. On the other hand, it was also shown that chirally substituted ansa-zirconocene catalysts with α-CH_3 groups at each 5-member ring do indeed show increased stereoselectivities[28-30].

Chiral ansa-zirconocene complexes with two identical ligand moieties have C_2 symmetry (The molecule possesses only one twofold symmetry axis). Both coordination sites of such a C_2-symmetric complex are thus equivalent; each is framed by the β-substituents in such a manner that olefin insertions at the Zr center occur with equal enantiofacial preference at both sites. Unilateral coverage of each coordination site is essential for this stereoselectivity; this is documented by the observation that atactic polypropylene is produced if both

coordination sites are flanked by two β-substituents, as in C_2H_4[3-Me-ind]$_2ZrCl_2$ or in its silyl-bridged analogue Me_2Si[3-Me-ind]$_2ZrCl_2$[27a,33]. The bilateral coverage of each coordination site in these complexes, by a CH and a CH_3 group, appears to render them indifferent with respect to the enantiofacial orientation of an entering olefin. The same result, production of essentially atactic polymers, was also observed for the meso isomers of each ansa-metallocene catalyst[14].

The relationship between the stereoselectivity of ansa-metallocene catalysts and the spatial disposition of their β-substituents has been discovered by Ewen et al[26] in a series of studies on Me_2C-bridged fluorenyl complexes. Syndiotactic polypropylene was produced by Me_2C(Cp)(9-fluorenyl)$ZrCl_2$/MAO, which is a C_s-symmetric structure (The molecule possesses only one symmetry plane). Introduction of a β-CH_3 on the 5-member ring results in the formation of a hemiisotactic polymer in which every other repeat unit is randomly configured. Introduction of a β-tert-butyl group gives highly isotactic polypropylene.

The mechanisms by which chiral ansa-metallocenes control the stereochemistry of polymer growth are reasonably well-understood today. The first important clues as to the factors governing the stereoselectivity of C_2-symmetric, chiral metallocene catalysts were obtained by Zambelli et al from ^{13}C NMR studies. They followed the course of propylene and 1-butene insertions into ^{13}C-enriched CH_3 and CH_2CH_3 end groups, which were introduced into MAO-activated C_2H_4[Ind]$_2TiMe_2$ catalyst by alkyl exchange with Al($^{13}CH_3$)$_3$ or Al($^{13}CH_2CH_3$)$_3$[36]. The results of these studies can be summarized as following:

1. Propylene inserts into C_2H_4[Ind]$_2$Ti-$^{13}CH_3$ bonds without significant

stereoselectivity, as shown by signals of diastereomeric end groups with almost equal intensity.

2. 1-Butene insertion into $C_2H_4[Ind]_2Ti\text{-}^{13}CH_3$ bonds occurs with slight (2:1) selectivity.

3. Complete stereoselectivity prevails when either propylene or 1-butene inserts into $C_2H_4[Ind]_2Ti\text{-}^{13}CH_2CH_3$ bonds.

4. All these results resemble those obtained before with analogously activated heterogeneous polymerization catalyst systems.

Efficient control of the chiral catalyst over the enantiofacial orientation of the entering olefin is thus clearly contingent on the presence of a metal-alkyl segment with at least two C atoms. The nature of this stereocontrol mechanism was clarified by molecular mechanics calculations by Corradini, Guerra et. al[37]. As previously proposed for heterogeneous Ziegler-Natta catalysis[38], repulsive interactions were shown to force an olefin into that enantiofacial approach to the metal-alkyl unit which places the olefin substituent trans to the β-C atom of the metal-bound alkyl chain. The metal-alkyl chain, in turn, was proposed to favor an orientation in which its C(α)-C(β) segment (see Scheme II) is in the most open sector of the chiral ansa-metallocene ligand framework. Experimental proof for this catalytic-site control by means of chain-segment orientation was provided by Pino et al[39].

The origin of stereoselectivity in ansa- metallocene catalysts was further examined by use of α-deuterated olefins. Stereokinetic isotope effects of k_H/k_D

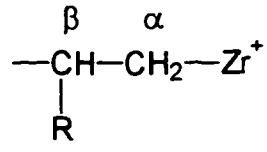

Scheme II C(α)-C(β) segment

about 1.4 were observed for hydrodimerization of (E)- and (Z)-1-[D_1]-1-hexene by chiral ansa-zirconocene and scandocene catalyst systems[40,41]. This indicates that the insertion reaction favors a transition state in which the α-H and not the α-D atom of initially formed Zr-CHD-R unit is in a position suitable for α-agnostic interaction with the metal center (The interaction between the protons on C(α) and the metal center). Recently stereokinetic isotope effects of k_H/k_D about 1.3 were determined directly for isotactic propylene polymerizations catalyzed by $C_2H_4[H_4Ind]_2ZrCl_2$/MAO and other chiral ansa-zirconocene catalysts from the mean chain lengths of polymers produced from either (E)- or (Z)-1-[D_1]-propylene. These results indicate that α-agnostic interactions control the stability of alternative transition states for the insertion of an olefin into a metal-alkyl bond.

Chain-end isomerization was discovered by Leclerc and Brintzinger from a study of D-label distributions in isotactic polypropylene obtained from (E)- or (Z)-1-[D_1]-propylene with chiral ansa-zirconocene catalysts[41]. The appearance of CH_2D instead of CH_3 groups in the mrrm stereoerror positions indicates that most of these errors arise from the isomerization.

It was interesting that the polymerization with chiral ansa-zirconocene catalysts, such as rac-$C_2H_4[H_4Ind]_2ZrCl_2$ and even the sterically strongly

congested chiral catalyst rac-$Me_2Si[2\text{-}Me\text{-}4\text{-}tBu\text{-}C_5H_2]_2ZrCl_2$, showed higher catalyst activity than that of the stereochemically unselective, unsubstituted catalyst Cp_2TiCl_2. Apparently, bridged catalysts have higher activity than unbridged ones. Considering the effects of different bridging units linking the 5-member ring ligands, it is found that zirconocenes with the one-atom bridge Me_2Si yield somewhat more active catalysts than comparable complexes with the

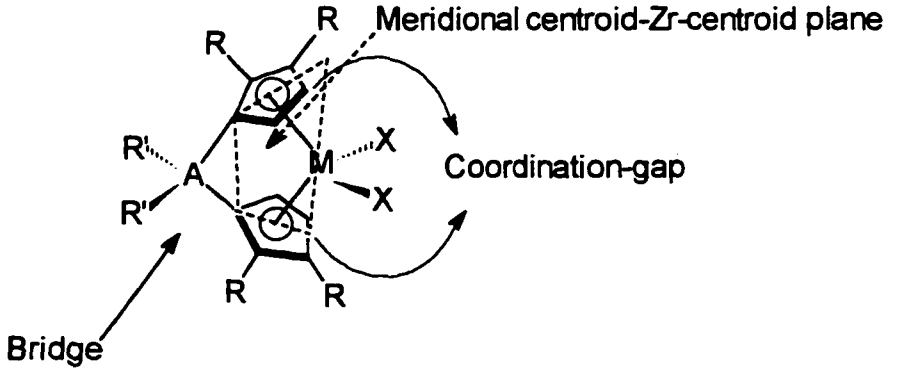

Scheme III Coordination gap and Meridional centroid-Zr-centroid plane

two-atom bridge C_2H_4. And zirconocenes with three-atom or four-atom bridges have so far all been found to be practically inactive for propylene polymerization in the presence of MAO[26b,42]. It seems that a short bridge widens the coordination-gap aperture (see Scheme III. The two unparallel five member rings form a gap in which the transition metal M coordinates with the two rings. This gap is called coodination-gap aperture)[43]. Structural studies on these inactive complexes reveal that a substituent on the five member ring close to the meridional centroid-Zr-centroid plane (see Scheme III. The coordination bond between the center of a five member ring and Zr is called centroid-Zr bond. The plane containing both centroid-Zr bonds, which cuts the catalyst molecule into

two parts, is called meridional centroid-Zr-centroid plane.) appears to block the insertion of α-olefins but not ethylene.

1.3 Addressing the Remaining Problems with Metallocene Catalysts

Lots of kinetic studies have been done on the polymerization of ethylene and propylene by both chiral or achiral metallocenes[44-46]. But so far, no systematic kinetic studies on both chain propagation and termination have been done. In this thesis, the kinetics of one polymerization system will be investigated by determining the rates of polymer propagation and termination as functions of temperature, concentrations of ziconocene, MAO and monomer.

Olefin copolymers whose total production volume is comparable to that of the homopolymers are of great practical interest. LLDPE is obtained by copolymerization of ethylene with 1-butene, 1-hexene and/or 1-octene[47]. Its mechanical properties, which surpass those of the long-chain branched LDPE produced by high-pressure radical polymerization, make LLDPE one of the largest volume polyolefin products. As one of the significant comonomer, 1-hexene will be chosen as the main monomer in the study of this thesis. Understanding its behavior in homopolymerization will help the understanding of its behavior in copolymerization. The main reason why 1-hexene was chosen as monomer in our study was that it was a liquid monomer. It is easier to get reproducible results by using a liquid monomer instead of a gas monomer. Only a little bit has been reported on 1-hexene polymerization by metallocene catalysts so far.

Odain and Zhang[48] once proposed the mechenism for the polymerization of 1-butene with rac-$Me_2Si[H_4Ind]_2ZrCl_2$. It was assumed that MAO methylated the zirconium chloride ligands to form the initial polymerization species with Zr-Me sites. Most polymer chains were subsqently initiated by Zr-H sites which were formed by various β-hydride (or βH) transfer reactions during the polymerization. Propagation involved insertion of 1-butene into Zr-C sites with almost exclusively 1,2-addition coupled with isospecificity. The unsaturated end groups (vinylidene, vinylene and trisubstituted end groups) were formed by βH transfer from propagation sites. Chien et al[49] also proposed a chain termination mechanism for polymerization of 1-hexene with rac-$C_2H_4[Ind]_2ZrCl_2$ catalysis by studying the microstructure of poly(1-hexene). They estimated that the three kinds of end groups (vinylidene, vinylene and trisubstituted end groups) were formed by various rearrangement and βH transfer from the propagation sites (see Scheme IV). But our studies showed the chain transfers in homogeneous polymerization are much more complicated.

The catalyst we used is rac-$Me_2Si[H_4Ind]_2ZrCl_2$ which has high activity and high stereoselectivity. Scheme V shows the two enantimers of this catalyst obtained from the general synthesis in 1:1 ratio. Both of the two enantimers produce isotactic polymer. MAO was used to activate the catalyst to achieve high activity.

Besides kinetics, we will also study end groups of polymers, the molecular weight of polymers and the polymerization condition's effects on the polymer

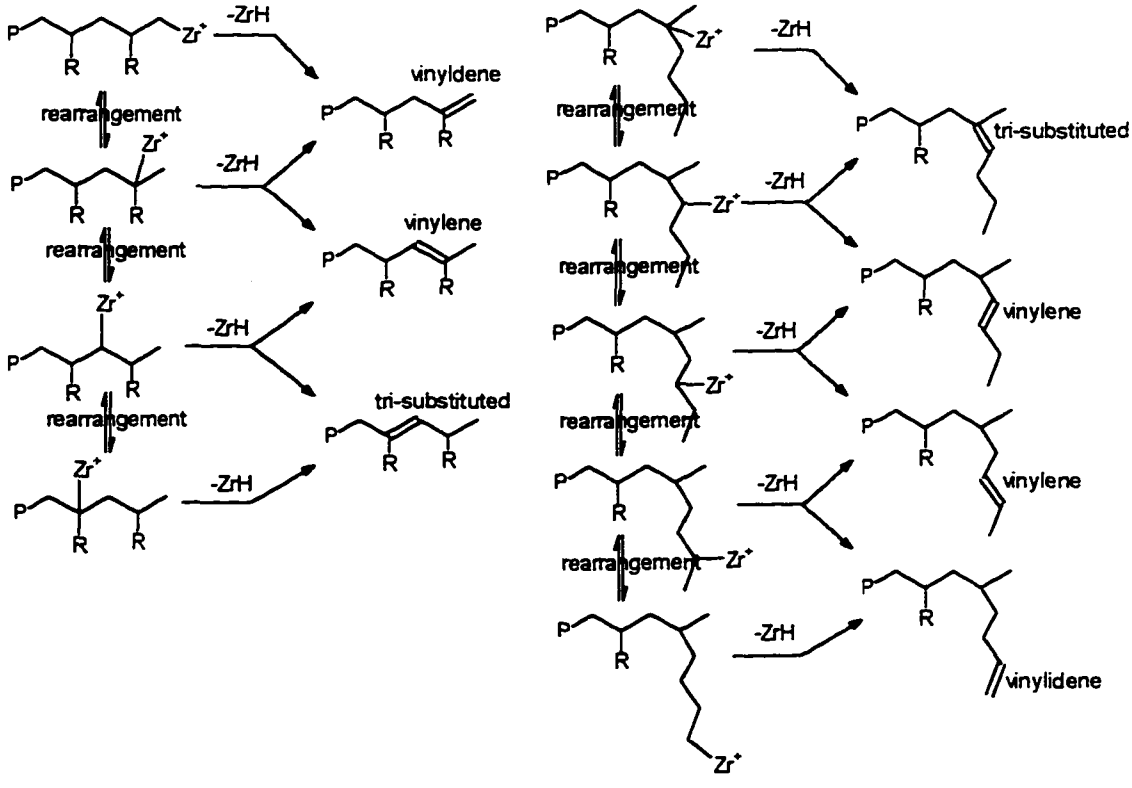

Scheme IV Mechanism of the βH Transfer from Propagation Sites

microstructure in this thesis. We wish that our study will bring a further understanding of homogeneous polymerization of α-olefins by metallocene catalysts.

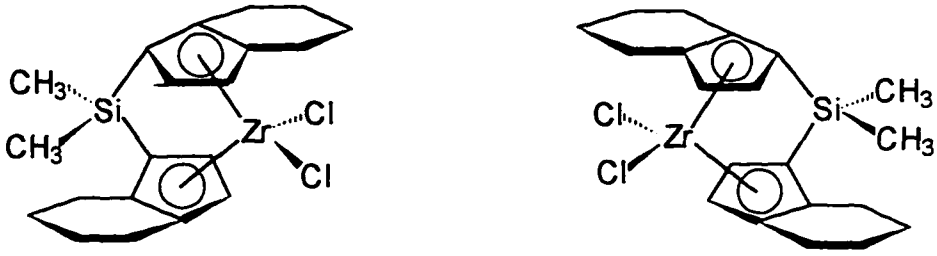

IIa **IIb**

Scheme V rac-$Me_2Si[H_4Ind]_2ZrCl_2$

2.0 Experimental

2.1 Purification of Solvents and Reagents

1-Hexene (b.p 63 - 64 °C, J.T. Baker) was dried overnight over a 3-4 : 1 (w/w) mixture of activated 4Å molecular sieves and aluminum oxide. Anhydrous toluene (Aldrich) was dried overnight over activated 4Å molecular sieves. Dimethylsilyl bis[tetrahydroindenyl]zirconium dichloride (or $Me_2Si[H_4Ind]_2ZrCl_2$) was supplied by Exxon Chemical Company and used directly without further purification. MAO (10wt-% solution in toluene) was purchased from Albemarle Corporation and used without further purification. Hexanes (GR reagent) was purchased from Fisher Scientific Company. Tetrahydrofuran (THF) (HPLC grade, Fisher Scientic) was filtered through 0.5μm filter (FHLP-013-00, Millipore) before used as GPC solvent. Methylene-d_2 chloride (99.9% D) and chloroform-d (99.8% D) were from Cambridge Isotope Laboratory. Sodium hydroxide (Fisher) was used without further purification.

2.2 Preparation of Solutions for Polymerization

All the glasswares here were dried at above 120°C for at least two days and then kept in the glove box for overnight before being used. The following procedures were completed in a glove box (Labconco, Model 51218-00). A nitrogen environment is established inside the drybox. The pressure range inside is between 0.6 to 3.0 inches water column higher that the atmosphere.

MAO washing solution Add 0.5 ml of 10% MAO solution in toluene into 100 ml of dried toluene.

MAO spike solution Add 10 ml of 10% MAO solution in toluene into 100 ml of dried toluene.

Zirconocene catalyst solution Add 10 ml of 10% MAO solution in toluene into 90 ml of dried toluene. Let it stand for 15 minutes. And then dissolve 100mg (0.218 mmols) of catalyst.

2.3 Polymerization of 1-Hexene

Reaction tubes were dried at above 120°C for over 6 hours and then kept in the glove box for overnight before being used. Rinse all the reaction tubes and syringes with MAO washing solution immediately before each experiment. The purpose of this washing is to completely remove all traces of water, which would destroy the catalyst. Add 1-hexene (5ml) into a 15 ml pressure tube (see Figure A-1), which is followed by the addition of the MAO spike solution (100 μl). The purpose of adding spike solution is to completely remove all traces of water from the monomer, which, again, would destroy the catalyst. After thorough mixing, add 10% MAO solution (180μl) and 100 μl of zirconocene catalyst solution. Polymerization were carried out at various temperatures (100°C, 80°C, 50°C, room temperature and 0°C, ± 2°C) for a certain time and was quenched by the addition of 2% NaOH aqueous solution (5ml) into the polymerization tube. The viscous reaction mixture was diluted by hexanes and transferred into a separatory funnel. The diluted mixture was washed with 2% NaOH until no more white solid was left and then washed three times with water. Residual monomer

and solvent were removed overnight in a Speed Vac (Savant, SC110) at ~45°C and 120 millitorr. The poly(1-hexene) was weighed.

2.4 End-group Equilibrium Study

a) 1-Hexene was polymerized at 80°C and 0°C as described in Section 2.3. The polymerizations were terminated at four different times (80°C: 30 mins, 1 week, 2 weeks and 1 month; 0°C: 2 days, 1 week, 2 weeks and 1 month). The shortest time used corresponded to the minimal time for complete conversion. The polymerization mixtures in other tubes were kept at the same temperature for a certain time before termination. The polymer was isolated and dried as has been described before. The double bond end-group compositions were determined by NMR and compared. The polymerization conditions were: [Zr]=56μM, [M]=8.0M and [MAO]=62mM.

b) Polymerizations were finished by keeping the reaction mixture at 80°C for 40 mins and 0°C for 3 days, respectively, as described in Section 2.3. The reaction mixtures polymerized at 80°C were brought to 0°C without isolation of polymer and kept at 0°C for certain time (1 day, 1 week, 2 weeks and 1 month) before 1wt-% aqueous NaOH was introduced and the polymer was isolated.

c) 1 g of dried poly(1-hexene) which was polymerized at 0°C was dissolved into 2 ml of toluene followed by the addition of 60μl of MAO spike solution, 110μl of 10% MAO and 78μl of zirconocene catalyst solution. The mixture was kept at 80°C for 24 hours and washed once with 1% aqueous NaOH and twice with water. The polymer was isolated. The end-group compositions of the polymer

was determined by NMR and compared with the same polymer without this process.

d) Model compounds were used to mix with monomer before polymerization. 2-Heptene was used as the model compound of vinylene double bond, 2-methyl-1-hexene as the model compound of vinylidene double bond and 3-methyl-2-pentene as the model compound of trisubstituted double bond. Since the model compounds caused the precipitation of MAO, toluene was used as polymerization solvent. Polymerizations were run at 0°C, 50°C and 80°C, respectively for a certain time, the total volume of polymerization mixture was 4ml, and the concentration of zirconocene catalyst and MAO were the same with the polymerization in Section 2.3. The vol ratio of monomer, model compound and toluene are listed as the following:

#	Monomer	Model Compound	Toluene
1	1	0	3
2	1	1 (2-heptene)	2
3	1	1 (2-methyl-1-hexene)	2
4	1	1 (3-methyl-2-pentene)	2

The polymer was isolated as before and the end-group compositions were determined by NMR and compared.

2.5 ^{1}H and ^{13}C NMR Spectroscopy

For ^{1}H NMR, samples were dissolved in $CDCl_3$ as 10% (wt/vol) solution, 5mm probe, 40°C, 30° pulse, 1s acquisition time, 2s delay between pulses, 500

scans and TMS as internal reference were used on Varian Unity Plus 600 MHz spectrometer. For ^{13}C NMR, samples were dissolved in $CDCl_3$ as 10% (wt/vol) solutions with 15mg of $Cr(AcAc)_3$ per mililiter added, 10mm probe, 40°C, 90° pulse, inverse gated decoupling with 3s delay between pulses, 10,000 scans and $CDCl_3$ as internal reference were used on Varian Unity Plus 300 MHz spectrometer.

2.6 Molecular Weight Measurements

2.6.1 Gel Permeation Chromatography

The molecular weight and molecular weight distribution of the poly(1-hexene) was measured at 40°C on a Waters 150C instrument using tetrahydrofuran (THF) as the mobile phase at a flow rate of 1.0 ml/min. A set of four ultrastyragel columns (with 10^3, 10^4, 10^5 and 10^6 Angstrom pore sizes) were used as the stationary phase. The GPC calibration for molecular weight determination was based on polystyrene standards with molecular weight ranging from 500 to 290,000.

2.6.2 ^1H NMR Spectroscopy

The conditions of ^1H NMR spectroscopy measurement has been described before. Molecular weight was calculated from the ratio of the integrals of protons on saturated carbons and proton on unsaturated carbons based on the assumption that each polymer chain contains one double bond end group.

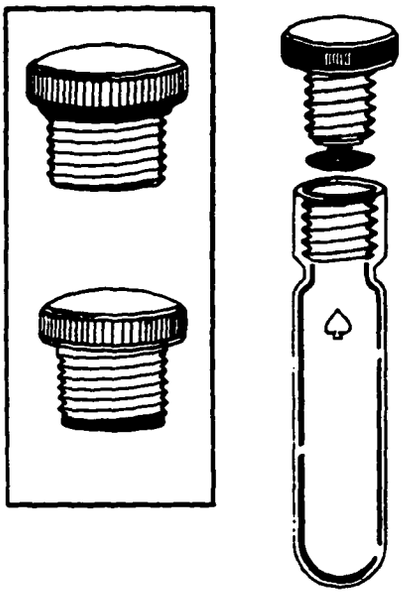

Figure A-1 Pressure Reaction Tube

3.0 Results and Discussion on Kinetic Studies

3.1 Propagation in Polymerization of 1-Hexene

3.1.1 Simplest Propagation Rate Expression

From the experiments, it was found that the propagating rate of homogeneous polymerization is dependent on the catalyst (zirconocene) concentration, cocatalyst (MAO) concentration, and monomer (1-hexene) concentration. In the following sections, we will discuss respectively the effects of catalyst concentration, cocatalyst concentration and monomer concentration in detail.

Assume that there is the following expression for R_p:

$$R_p = -\frac{d[M]}{dt} = k_p[Zr]^A[MAO]^B[M]^C \qquad (1)$$

R_p = propagation rate [MAO] = cocatalyst concentration

[Zr] = catalyst cocentration [M] = monomer concentration

The value k_p, A, B and C are all called pseudo values because the rate expression here only shows the overall relationship between R_p and [Zr], [MAO] and [M]. However, it is possible that there are several successive or/and parallel simple kinetic steps involved, which are called elemental kinetic steps. An equation like Equation (1) does not show how many elemental kinetic steps involved in propagation and what these elemental kinetic steps are. In fact, from the discussion in the following sections, it can be proven that more than one kind of mechanism is involved in propagation.

3.1.2 The Effect of Catalyst Concentration on Propagation

At certain temperatures, the polymerization of 1-hexene was run at different catalyst concentrations with other conditions remaining the same. The polymerization was quenched after a certain time. Figures A-2 - A-5 show the relationship of monomer concentration decrease versus time at different catalyst concentrations and at temperatures of 100°C, 80°C, 50°C and 0°C, respectively. In these figures, only the linear part was considered as the initial propagation rate because the propagation rate slowed down significantly after a certain time when monomer concentration decreased to a certain level. The slope of each curve is the propagation rate (R_p). Table A-1 lists the propagation rates at different temperatures and catalyst concentrations. Figure A-6 shows the relationship of LnR_p and Ln[Zr] at the four different temperatures. The slope of each curve gives the A value in Equation 1 at the corresponding temperature. All the A values are listed in Tables A-2. B and C values in Equation 1 are also listed in Table A-2, which will be discussed later.

Table A-2 shows that there is first-order dependency of propagation rate on catalyst concentration at all these four temperatures, which means that each propagating species contains only one catalyst species.

Experiments showed that there is a minimum concentration of catalyst below which polymerization could not go to high conversion. This minimum concentration changes with temperature. For example, when the catalyst concentration was decreased to 1.0 μM, polymerization did not go further than

10% conversion at 50°C, but to as high as 60% conversion at both 100°C and 80°C. It is possible that small amounts of catalyst poison(s) exist(s) in the reaction system which show(s) higher inhibiting capability at lower temperature than at higher temperature.

3.1.3 The Effect of Monomer Concentration on Propagation

The polymerization of 1-hexene was run at certain temperatures with different monomer concentrations and with other conditions remaining the same. Figures A-7 - A-10 show the relationship of the monomer concentration decrease versus time at different monomer concentrations and temperatures of 100°C, 80°C, 50°C and 0°C, respectively. The slope of each line is the propagating rate (R_p) at certain conditions. Table A-3 lists R_p values obtained from Figure A-7 to Figure A-10. And Figure A-11 shows that $Ln(R_p)$ changes as a linear function of Ln[M] at different temperatures. The slope of each line gives the C value in Equation 1. The C values at different temperatures are listed in Table A-2.

It can been seen that C is about 1.0 at 0°C but 1.3 at higher temperature. There are several possible explanations for it. First, propagation step consists of the growth of propagation species by the succesive additions of large numbers of monomer molecules. It is possible that at temperature higher than 0°C, the addition of first monomer molecule is slower than the additions of other monomer molecule. In that case, C becomes more than 1.0. The second possibility is that the propagating rate is so fast at these higher temperatures relative to low

temperatures, such as 0°C here, that the monomer concentration around propagating species is lower than the overall monomer concentration in the reaction system. At this moment, the monomer diffusion rate is slower than the propagating rate. The rate determination step is not only propagation but also monomer diffusion. This result is consistent with Herfert and Fink's results[50b]. They found that the order of the propylene polymerization reaction concerning the monomer concentration is 1.3 at a constant ratio of [MAO] to [Zr] and 25°C. Other literature[50a, 51] also showed that the order of propagating rate in α-olefin polymerization with respect to monomer concentration was between one and two, even in different catalysts/MAO systems.

Another possible explanation for the above result is that, at a temperature higher than a certain value, the insertion reaction of monomer into Al-C bond occurs as shown in (2). Therefore some **V** participates in the alkylation of zirconocene catalyst.

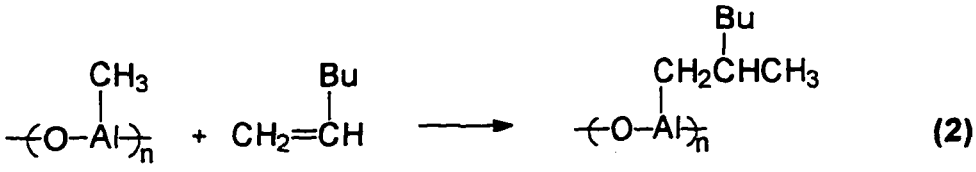

III **IV** **V** **(2)**

This assumption is supported by the following observed reactions[52]:

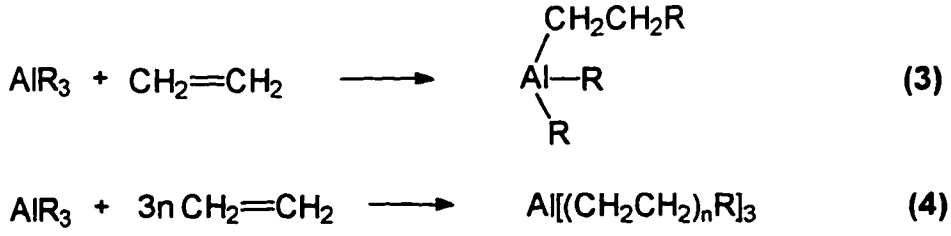

$$AlR_3 + CH_2{=}CH_2 \longrightarrow Al(CH_2CH_2R)(R)(R) \quad (3)$$

$$AlR_3 + 3n\,CH_2{=}CH_2 \longrightarrow Al[(CH_2CH_2)_nR]_3 \quad (4)$$

The insertion reaction of monomer into MAO can also give a possible reason for high kinetic order of propagation rate with respect to MAO concentration, which will be further discussed in the next section.

3.1.4 The Effect of MAO Concentration on the Propagation

The polymerization of 1-hexene was run at different MAO concentrations. Figures A-12 - A-15 show the relationship between monomer concentration decrease and time. The slope of each straight line is the propagating rate at certain conditions. Table A-4 is the summary of the R_p data from Figures A-12 to A-15. Figure A-16 shows the relationship of Ln(R_p) and Ln[MAO] based on the data in Table A-4.

It is very interesting to see in Figure A-16 that at high temperatures, R_p increases with MAO quickly in the beginning, and then levels off with further increases of MAO concentration, after the ratio of MAO to catalyst is about 600. At 50°C, R_p is proportional to MAO. However at high temperatures like 80°C and 100°C, the relationship of R_p and [MAO] can be expressed as a quadratic equation. The B values in Table A-2 were obtained by the slopes in the linear part of these curves. B changes with temperature. It is 0.59 at 0°C, increases with temperature, and becomes 1.8 at 100°C. The possible explanation is that

there are two equilibriums in the initiation step (see section 3.1.6). Because there are two chlorides on the catalyst, it is possible that during the initiation, one chloride is methylated by a MAO molecule to form $Me_2Si[H_4Ind]_2ZrClCH_3$, and the other one is activated by another MAO molecule to form a zirconium cation, $Me_2Si[H_4Ind]_2ZrCH_3^+$·($ClMAO^-$). At low temperature, one equilibrium is much faster than the other, therefore, only one equilibium is the rate-determining step. However at high temperature, the two eqilibriums have similar rates, and so both of them become rate-determining steps. Another explanation is that reaction (2) occurs at high temperature and **V** acts as activated monoomer.

Although B value at 0°C is obtained as 0.59, it will be roughly treated as 1 in the further calculation of k_p and E_p because at this temperature, R_p is very small (~ 10^{-3} M/min) and the order cannot be determined to good.

The ratio of [MAO] to [Zr] is needed to be much higher than 1:1. Experiments showed that no polymerization occurred when the ratio of [MAO] to [Zr] was lowered to 141:1 at both 80°C and 100°C. The result of Chien's[53] investigation of propylene polymerization by $C_2H_4[Ind]_2ZrCl_2$ catalysis system was that no polymerization occurred when the ratio of [Al]:[Zr] was lower than 350:1. However, with this ratio, polymerization occurred at 50°C but with no more than a 20% conversion in our experiment. MAO exists as an oligmer $(MAO)_n$ with n around 4 to 26[54]. In addition, unlike the catalyst which can be recycled, MAO is a reagent which is used up during the polymerization.

Although MAO is a powerful cocatalyst for metallocene catalysts, it still remains a "black box" due to the presence of multiple equilibria in solution. TMA is used to produce MAO. It was reported by Howie[55] that there were always equilibria between MAO and TMA in toluene solution and the relative compositions of MAO and TMA change with time and temperature. MAO composition increases with time and decreases with increasing temperature. Resconi et al[56] reported that the equilibrium shown in Equation (5) must occur in toluene solution.

$$MAO{\cdot}nTMA \Leftrightarrow MAO{\cdot}(n-m)TMA + (m/2)(TMA)_2 \qquad \textbf{(5)}$$

They also proposed that the actual cocatalyst in the metallocene-MAO system was TMA itself, with MAO acting as a soluble carrier-activator of the ion pair formed upon reaction of the metallocene with TMA.

Giannini et al[57] reported the exist of Equation (6) also with ^1H NMR study.

$$Cp_2ZrCl_2 + MAO{\cdot}xAl(CH_3)_3 \rightarrow$$

$$(1-x)Cp_2ZrCl_2 + xCp_2ZrCH_3Cl + MAO{\cdot}xAl(CH_3)_2Cl \qquad \textbf{(6)}$$

They proved that Cp_2ZrCl_2 was monoalkylated by $Al_2(CH_3)_6$ present in MAO. Meanwhile, they found that the Cp_2ZrCH_3Cl likely formed, with an excess of MAO, highly polarized species, which were decomposed by a complexing agent of MAO such as KCl.

If it is true that Cp_2MCl_2 is monoalkylated to form Cp_2MCH_3Cl during the polymerization, Cp_2MCl_2 and Cp_2MCH_3Cl should have almost the same activities.

However, Kaminsky[58] once reported that the activity of Cp_2TiCH_3Cl was only as high as half of the activity of Cp_2TiCl_2.

3.1.5 Effect of Temperature on Propagation

As with most polymerizations, the propagation rate of 1-hexene polymerization increases with temperature increases. The k_p's at different temperatures are obtained and listed in Table A-5. Figure A-17 shows the relationship between Lnk_p versus the reciprocal of temperature (1/T). E_p and A_p are obtained from Figure A-17 according to the following Equation 5 and are listed in the same table.

$$Lnk_p = -E_p/RT + LnA_p \qquad (7)$$

The overall activation energy E_p here is reasonable compared with the other research results. The E_p in the polymerization of 1-propylene using $C_2H_4[H_4Ind]_2ZrCl_2$ catalyst system was 10.6 kcal/mol[53]. Actually, the E_p value changes with monomer and catalyst used. In the polymerization of propylene, it was 12.9 kcal/mol catalyzed by $Me_2Si[2\text{-}Me\text{-}Benzindenyl]_2ZrCl_2$, and was 6.7 kcal/mol catalyzed by $Me_2Si[Benzindenyl]_2ZrCl_2$[51b]. And E_p was 7.4 kcal/mol for ethylene polymerization by η^5-$(NMeCp)_2ZrCl_2$[44b]. In radical polymerization E_p is 4.4 kcal/mol for ethylene and 6.2 kcal/mol for styrene in their radical polymerization[59a]. E_p is higher in stereospecific homogeneous polymerization than that in radical polymerization, but is comparable with Ziegler-Natta polymerization. The overall E_p for the rates of most Ziegler-Natta polymerizations fall in the range 4.8 kcal/mol - 16.7 kcal/mol[59b]. However, E_p and A_p are not real in our case because B and C vary with temperature.

A_p is comparable with those in radical polymerization. It is 3.3 x 10^6 $M^{-1}s^{-1}$ for vinyl chloride and is 4.5 x 10^6 $M^{-1}s^{-1}$ for styrene.

3.1.6 Mechanism of Initiation and Propagation

No previous literature have reported in determining the rate of polymer formation as a function of the concentrations of zirconocene, MAO and monomers so far, though some literatures reported that polymerization rates depend on olefin concentration to a fractional order between 1 and 2 (see Section 3.1.3).

We tried to determine the propagation rate as a function of the concentrations of zirconocene, MAO and monomer and get the following equation (1):

$$R_p = [Zr]^A[MAO]^B[M]^C \qquad (1)$$

A, B and C constants at four different temperatures are listed in Table A-2. From this table, we can see that at all these four temperatures, the fractional order to which R_p depends on zirconocene concentration is always around 1. This tells us that only one molecule of catalyst is involved in the propagation transition states.

However, the fractional order to which R_p depends on monomer concentration changes with temperature. It is 1 at 0°C, but between 1 and 2 at the other three higher temperatures. We have discussed the possible reasons in section 3.1.3.

The fractional order to which R_p depends on MAO concentration is very complicated. At 0°C and 50°C, it is almost 1, and at 80°C and 100°C, it is between 1 and 2. Besides, it increases with the increase of temperature. It is possible that the activation of catalyst consists of more than one step, possibly two steps as dicussed in section 3.1.4. MAO is needed in each step. The relative reaction rates are controlled by reaction temperature. At lower temperature, one reaction is much faster than the other and only the slow reaction is the rate-determining step. As the increase of temperature, the difference between the two reaction rates decreases. So, at certain high temperature, the two reaction rates become comparable and both steps are rate-determining steps.

Based on the above observed results and concerned discussion, we tried to make the kinetic model for the initiation and propagation of homogeneous polymerization. In the initiation (see Scheme VI), we assume that there are three steps. The first two steps are equilibria which involve in the activation of catalyst. The first equilibrium is the monomethylation of catalyst by MAO. Maybe the methylation agent is $Al(CH_3)_3$. Since there is direct equilibrium between MAO and $Al(CH_3)_3$, we may just use MAO to represent the methylation agent here.

Scheme VI

$$ZrCl_2 + MAO \underset{}{\overset{K_{i1}}{\rightleftharpoons}} ZrCH_3Cl \qquad (8)$$

$$ZrCH_3Cl + MAO \overset{K_{i2}}{\rightleftharpoons} CH_3Zr^+\cdot MAOCl^- \qquad (9)$$

$$CH_3Zr^+\cdot MAOCl^- + \underset{\underset{Bu}{|}}{CH}{=}CH_2 \xrightarrow{k_i} CH_3\underset{\underset{Bu}{|}}{C}HCH_2Zr^+\cdot MAOCl^- \qquad (10)$$

At low temperature, (8) is much slower than (9), (8) and (10) will be rate-determining steps and initiation rate R_i can be expressed by

$$R_i = k_i K_{i1}[ZrCl_2][MAO][M] \quad (11)$$

At very high temperature, (8) and (9) occur in comparable rates, initiation rate R_i can be expressed by

$$R_i = k_i K_{i1} K_{i2}[ZrCl_2][MAO]^2[M] \quad (12)$$

At mediate temperature, initiation rate R_i can be expressed by

$$R_i = k_i K_{i1} K_{i2}[ZrCl_2][MAO]^{1\text{-}2}[M] \quad (13)$$

Propagation consists of the growth of $CH_3BuCHCH_2Zr^+ \cdot MAOCl^-$ in Equation (10) by the successive additions of monomer molecules. It is shown in Scheme VII. Each addition creats a new propagation species which has the same identity as the one previously, except that it is larger by one monomer unit. Also the rate constants for all the propagation steps are the same.

Scheme VII

$$\sim\!\!\sim CHCH_2Zr^+ \cdot MAOCl^- + CH{=}CH_2 \xrightarrow{k_p} \sim\!\!\sim CHCH_2CHCH_2Zr^+ \cdot MAOCl^- \quad (14)$$

(Bu) (Bu) (Bu)

At low temperature like 0°C, two possible situations can be concerned to result in the propagation rate expression obtained from the experimental result. One is that k_i and k_p are almost the same. Then the propagation rate can be simply expressed by

$$R_p = k_p K_{i1}[ZrCl_2][MAO][M] \quad (15)$$

The other possibility is that between k_i and k_p, one is much bigger than the other. In this case only one reaction out of these two is the rate-determining step. We can also get Equation (15), except that the rate constant could be either k_pK_{i1} or k_iK_{i1}. Equation (10) and Equation (14) are similar in enthalpy change because in each of these two equations, a C-Zr bond and a C-C π bond are broken followed by the formation of a new C-Zr bond and a C-C σ bond. The first possibility seems more reasonable here.

However, at higher temperature, it is possible that the reaction (10) became slightly slower than reaction (14). The fractional order to which R_p depends on monomer concentration becomes bigger than 1. R_p can be expressed by

$$R_p = k_pk_iK_{i1}K_{i2}[ZrCl_2][MAO]^{1\text{-}2}[M]^{>1} \qquad \textbf{(16)}$$

3.2 Chain Transfers in Polymerization of 1-Hexene

3.2.1 ^{1}H NMR Assignments of Double Bond End Groups

Figure A-18 is a ^{1}H NMR spectrum of poly(1-hexene). The resonances between 0.9 ppm to 1.4 ppm are from three kinds of saturated protons in the polymer: -C<u>H</u>$_3$, -C<u>H</u>$_2$- and -C<u>H</u><. Chemical shifts depend on chemical environments around protons. Usually, methyl group appears at higher field which shows at 0.9 ppm here, and methylene and methine protons appear at 1.0-1.4 ppm.

Besides the saturated resonances, there are three kinds of very small resonances appearing in the double bond proton range 4.0-6.0 ppm. Figure A-19 shows the expanded spectrum. The relative integral ratios between these

three kinds of double bonds vary with polymerization conditions. These three kinds of double bonds are assumed to be the end-groups of poly(1-hexene) which result from various chain transfer reactions.

The studies on model alkene compounds provide a detailed chemical shift assignments of different types of double bond protons. The terminologies used for double bond groups which contain proton(s) are: vinyl for CH_2=CH-, vinylidene for CH_2=C<, vinylene for -CH=CH- and trisubstituted for -CH=C<. Table A-6[60] shows the detailed chemical shift ranges for different types of double bond protons.

Double bond end groups of poly(1-hexene) were assigned according to the assignments in Table A-6 (see Figure A-19). Vinylidene end group appears as a doublet at 4.68 ppm and 4.74 ppm, trisubstituted end-group appears as a triplet at 5.11 ppm and as a multiplet at 5.16 ppm, and vinylene end group appears as a broad multiplet at 5.30-5.41 ppm. It seems there are two kinds of trisubstituted end groups. At low temperature, only the triplet at 5.11 ppm appears, which seems that the double bond is next to -CH_2-; And at higher temperature both signals appear. The previous mechanism described for vinylidene, vinylene and trisubstituted end group was shown in Scheme IV.

3.2.2 Pseudo Expression Equation for Chain Transfer Reactions

The experiments showed that the ratios of three kinds of end-groups varied significantly with changes in the polymerization conditions such as zirconocene catalyst concentration, monomer concentration, MAO concentration and

temperature. Assume the following relationship between chain transfer rates and conditions:

$$R_{tr} = k_{tr}[Zr]^X[MAO]^Y[M]^Z \qquad (17)$$

From Equation (17), we can not see how many kinds of chain transfers involved and how many elemental kinetic steps occur in each chain transfer. In the following several sections, we will discuss the effects of polymerization conditions on chain transfers.

According to the previously proposed chain termination mechanism[48, 49], which is simplified and shown in Scheme VIII, X=1, Y=1 and Z=0-1 are expected.

Scheme VIII

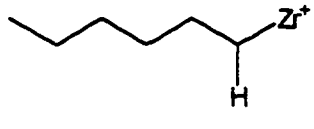

$\longrightarrow$ HZr + Polymer with C=C **(18)**

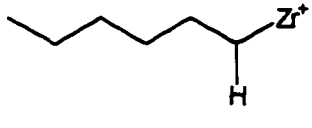

$\xrightarrow{+M}$ HMZr + Polymer with C=C **(19)**

However, we got some unexpected X, Y and Z data in our experiment, which are shown in Table A-8. In the following several sections, we will discuss them respectively.

3.2.3 The Effect of Zirconocene Catalyst Concentration on Chain Transfers

Figures A-20 - A-22 show the concentrations of three kinds of end groups versus time at 100°C and different catalyst concentrations, respectively. Figures A-23 - A-25, A-26 - A-28 and A-29 - A-31 are for 80°C, 50°C and 0°C,

respectively. The slope of each curve is the value of one kind of chain transfer rate R_{tr}. Table A-7 is the summary of catalyst concentration effect on chain transfer rates at the above four temperatures. Figures A-32 to A-35 show the relationship between LnR_{tr} versus Ln[Zr] for three types of end-groups at these temperatures, respectively. The slopes are the X values in Equation (17), which are listed in Table A-8.

In Table A-8, the dependency of three kinds of chain transfer rates on catalyst concentration are varied with temperature. At high temperature such as 100°C and 80°C, the fractional kinetic orders of three kinds of chain transfer rates with respect to catalyst concentration are all almost one, which is expected. However, these fractional kinetic orders are increased with the decrease of temperature. This is especially so with the formation of vinylidene end group. The fractional order of the chain transfer rate to form vinylidene end group with respect to catalyst concentration increases from 1.1 at 100°C to 2.4 at 0°C. Whereas the kinetic study on propagation shows the first-order of propagation rate on catalyst concentration at all of these four temperatures. The first conclusion which can be made here is that catalyst molecules must participate in chain transfer reactions at a low temperature but not at a high temperature.

At high temperatures, the molecular motion is so fast that the bulky catalyst species have difficulty attacking the active polymer chain. On the other hand, at high temperature, βC-H bond and C-Zr bond are easily broken, which is called

and βH elimination mechanism (see Scheme IV in section 1.3 and Scheme VIII). Therefore at high temperature, βH elimination[49] could be the main chain transfer mechanism. But at lower temperatures, βC-H, C-Zr bonds are harder to break and βH elimination becomes very difficult. In addition, the reaction mixture becomes so viscous (The solutions became thick in the experiments at 0°C.) that the molecular motion slows down. Although in this situation, another catalyst species have less chance to 'meet' a polymer propagating chains, they have a longer time to stay together once they meet. This would give the catalyst species enough time to find its attacking target on the propagating chains and result in a chain transfer. If another catalyst species may attack the polymer chain, the question is where it will attack the chain. It could be βH. βH is more nucleophilic than other hydrogens on the polymer chain because the αC, which is directly connected with Zr of the catalyst species, has partially negative charge. The difference from the βH elimination mechanism shown in Scheme IV and VIII is that βH elimination here occurs under the help of another zirconocene species companied with the leaving of the catalyst species which is connected with αC. The main question for this mechanism is whether it is possible in space because it would be very crowded for two catalyst species to be so close. By considering the spatial effect, it is more likely that the catalyst species drops from the end of propagating chain first followed by the leaving of βH under the help of another catalyst species.

The dependency on catalyst concentration varies for different kinds of chain transfer reactions; even for the same type of chain transfer reaction, it varies with temperature. This indicates that different chain transfer reactions are involved with different orders with respect to catalyst concentration to form the same type of end group. Because different reactions show different temperature dependency, the overall dependency of one kind of chain transfer rate on catalyst concentration changes with temperature. The possible mechanism will be derived later.

3.2.4 The Effect of Monomer Concentration on Chain Transfers

Figures A-36 - A-38 show the concentrations of three types of end-groups versus time, respectively, at 100°C and different monomer concentrations. Figures A-39 - A-41, A-42 - A-44 and A-45 - A-47 show the same relationship at 80°C, 50°C and 0°C. R_{tr} obtained from these figures are listed in Table A-9. And Figures A-48 to A-51 show the relationship between LnR_{tr} and Ln[M] for three kinds of end-groups at the above four temperatures, respectively. The slope of each line is a Z value in Equation (17), which is listed in Table A-8.

Table A-8 shows that Z is close to one in most of the cases. The exceptions are that Z is bigger than one in the chain transfer to form vinylene at 100°C, 80°C and 50°C, and Z is smaller than one in the chain transfer to form vinylidene at 50°C and 0°C and in the chain transfer to form trisubstituted end group at 0°C.

Since it is a coordination polymerization, there are two coordinating positions in each catalyst molecule. One is connected with a polymer

propagating chain and the other is with a monomer molecule. Therefore, there are two kinds of 'active' propagating species existing in this polymerization mixture. One is the catalyst connecting with both a polymer chain and a monomer molecule, which can be expressed as MZrP; And the other is the catalyst only connecting with a polymer chain with an unoccupied site, which can also be called semi active propagating species and expressed as PZr. The latter has to catch a monomer molecule before another step of propagation occurs. The chain transfer reactions, however, could happen for both kinds of these species. It is likely that in most cases in Table A-8, chain transfer reactions occur on MZrP in which chains transfer to the coordinated monomer because the kinetic orders of chain transfer reaction rates with respect to monomer concentration are one. Only in those cases in which these orders are between 0 and 1, chain transfer reactions occur for not only MZrP but PZr. Under the range we studied, no 0 order of chain transfer reaction rate was obtained. In the cases in which these orders are bigger than one, chain transfer could happen between a MZrP and a noncoordinated monomer.

On the other hand, like X, Z varies with temperature. This also indicates that there are multiple kinds of reactions, with different kinetic orders, with respect to monomer concentration, to form the same type of end-group.

3.2.5 The Effect of MAO Concentration on Chain Transfers

Figures A-52 - A-54 show the relationship between the concentration of three types of end groups versus time at 100°C and different MAO

concentrations, respectively. In the same way, Figures A-55 - A-57, A-58 - A-60 and A-61 - A-63 show the situation at 80°C, 50°C and 0°C, respectively. R_{tr} values are listed in Table A-10.

From Figures A-64 - A-67, we can see R_{tr} is not no longer directly proportional to $[MAO]^Y$ at high temperatures. This is why no Y value can be listed in Table A-8 at 80 and 100 °C. This is similar with the MAO effect on propagation rate. Rather, R_{tr} can be roughly expressed as a function of MAO concentration with some quadratic equations. There seems to be some maximum for R_{tr} at certain MAO concentration value. In additions, the MAO concentration values at which R_{tr} reaches maximum value are various with temperature. The MAO concentration we use here is very big compared with the catalyst concentration, which could be the reason why the reactions are not sensitive to MAO concentration.

3.2.6 Temperature Effect on Chain Transfers

Table A-11 shows temperature effect on chain transfer rates. k_{tr} values at 50°C and 0°C can be calculated according to Equation (17) and Table A-8, respectively, and are listed here. We can not get k_{tr} for 80 and 100 °C because there are no Y values for these two temperatures in Table A-8. Although there is no doubt that R_{tr} for a specific type of end group is increased with the increase of temperature, k_{tr} does not change in the same way with R_{tr}, which further proves that the mechanism at high temperature is different than that at low temperature. It is hard to believe that there are absolutely different chain transfer mechanism

at different temperatures,.However it is very possible that there are several parallel chain transfer reactions to form the same type of end-group. Because they have different dependencies on catalyst concentration, monomer concentration, MAO concentration and temperature, the overall dependencies show different behaviors from the normal radical, ionic or step polymerization. k_{tr} values obtained are only pseudo values which are the overall value of different chain transfer reactions. They cannot supply any valuable information about the k_{tr} in the real mechanism but from them, we can derive the possible mechanism of chain transfer.

3.2.7 Mechanism for Chain Transfer Reactions

From our kinetic study on the chain transfer reactions of homogeneous polymerization, it is seen that the chain transfer mechanism for homogeneous polymerization is different from, and much more complicated than, either chain or step polymerization. Through the results we obtained, the kinetic model of chain transfer reactions can be constituted. All these three kinds of chain transfers will be derived as the same general model first and then discussed individually.

Based on the discussion through section 3.2.1 to section 3.2.6, we can conclude that there are three types of end groups caused by chain transfers. The mechanisms of chain transfers to form these three kinds of end groups are different somehow because the relationships between R_{tr} and reaction conditions are different. Chain transfer to monomer is exclusive at higher

temperature and predominating at lower temperature. The chain transfer to monomer could occur inside MZrP or between PZr and M, or even between MZrP and M. M means monomer here. At lower temperature, chain transfer to catalyst species (expressed as Zr here) occurs and even becomes predominating. Scheme IX proposes the possibilities of chain transfers as general model. Equation (20) to (22) are chain transfers to monomer. Equation (23) and (24) are chain transfers to catalyst. Equation (20) is the chain transfer to the coordinated monomer within the active propagation species MZrP. Equation (21) is the chain transfer from semi active propagation species PZr to

Scheme IX

$$MZrP \longrightarrow HMZr + P \text{ with } C{=}C \qquad (20)$$

$$PZr + M \longrightarrow HMZr + P \text{ with } C{=}C \qquad (21)$$

$$MZrP + M \longrightarrow HMZrM + P \text{ with } C{=}C \qquad (22)$$

$$MZrP \xrightarrow{-MZr^+} P^- \xrightarrow{+Zr^+} HZr + P \text{ with } C{=}C \qquad (23)$$

$$PZr \xrightarrow{-Zr^+} P^- \xrightarrow{+Zr^+} HZr + P \text{ with } C{=}C \qquad (24)$$

noncoordinated monomer. Equation (22) is the chain transfer from active propagation species to noncoordinated moonomer. Equaion (23) is chain transfer to catalyst species starting from active propagation species MZrP. Equaion (24) is chain transfer to catalyst species starting from semi active propagation species PZr.

a) Chain transfers to form vinylidene end group

Equation (20), (21) (23) and (24) seem to be the possible chain transfer reactions to form vinylidene end group because X is between 1 to 2 and Z is between 0 and 1. Equation (22) is not considered as a possibility in which Z is 2. Within the possible four reactions, different reactions are favored at different temperatures. At high temperature like 80 and 100 °C, chain transfers to monomer, reaction (20) and (21), are favored and R_{tr} is proportional to $[Zr]^1[M]^{-1}$. At low temperature like 0 °C, chain transfers to catalyst, reaction (23) and (24), are mainly favored and R_{tr} is proportional to $[Zr]^2[M]^{-0}$. At medium temperature like 50 °C, chain transfers to catalyst and chain transfers to monomer are equally favored and R_{tr} is proportional to $[Zr]^{1-2}[M]^{0-1}$.

b) Chain transfers to form vinylene end group

Equation (20), (21) and (22) seem to be favored in chain transfer to form vinylene end group because X is around 1 at all temperatures and Z is between 1 and 2. At temperature as low as 0 °C, reaction (20) and (21) seem to be the only possibilities which make R_{tr} proportional to $[Zr]^1[M]^1$. At temperature higher than 0 °C, all three reactions are possible and R_{tr} is proportional to $[Zr]^1[M]^{1-2}$. The reason why chain transfer to catalyst species could not occur to form vinylene end group is probably the steric hindrance on both carbons.

c) Chain transfers to form trisubstituted end group

Equation (20) to (24) all seem to be possible for chain transfer to form trisubstituted end group because X is between 1 and 2 and Z is between around

1. At high temperature like 80 and 100 °C, reaction (20) and (21) are predominating and reaction (22) is possible at 80 °C because R_{tr} proportional to $[Zr]^1[M]^1$ at 100 °C and to $[Zr]^1[M]^{1-1.5}$ at 80 °C. At low temperature, all five reactions seem to be possible and R_{tr} is proportional to $[Zr]^{1-2}[M]^{0.5-1.5}$.

Table A-1. Catalyst Concentration effect on R_p

T (°C)	[Zr] (μM)	R_p (M/min)
100	52	1.7×10^{0}
	26	5.8×10^{-1}
	5.2	1.5×10^{-1}
	1.0	2.7×10^{-2}
80	52	9.4×10^{-1}
	26	5.1×10^{-1}
	5.2	8.2×10^{-2}
	1.0	2.5×10^{-2}
50	99	8.7×10^{-1}
	26	2.9×10^{-1}
	13	8.7×10^{-2}
	5.2	2.6×10^{-2}
0	99	2.0×10^{-2}
	52	9.1×10^{-3}
	26	5.5×10^{-3}

*Note: The other polymerization conditions are: [M]=8.0 M and [MAO]=62 mM.

Table A-2. Summary of A, B and C's in Eq.(1)

T (°C)	A	B	C
100	1.0	1.8	1.3
80	0.95	1.5	1.4
50	1.1	0.98	1.3
0	0.94	0.59	.96

Table A-3. Monomer Concentration Effect on R_p

T (°C)	[M] (M)	R_p (M/min)
100	8.0	1.7×10^{0}
	4.0	6.2×10^{-1}
	2.0	2.9×10^{-1}
	0.80	8.4×10^{-2}
80	8.0	9.4×10^{-1}
	4.0	3.9×10^{-1}
	0.80	4.8×10^{-2}
50	8.0	4.9×10^{-1}
	4.0	1.6×10^{-1}
	2.0	7.0×10^{-2}
	0.80	2.4×10^{-2}
0	8.0	9.1×10^{-3}
	4.0	5.3×10^{-3}
	2.0	3.2×10^{-3}
	0.80	1.0×10^{-3}

*Note: the other polymerization conditions are: [Zr]=52 μM and [MAO]=62 mM.

Table A-4. MAO Concentration Effect on R_p

T (°C)	[MAO] (mM)	R_p (M/min)
100	62	1.7×10^{0}
	34	1.5×10^{0}
	18	4.8×10^{-1}
80	62	9.4×10^{-1}
	34	8.8×10^{-1}
	18	3.5×10^{-1}
50	62	4.9×10^{-1}
	31	2.5×10^{-1}
	16	1.6×10^{-1}
	3.9	3.2×10^{-2}
0	62	9.1×10^{-3}
	34	8.4×10^{-3}
	18	4.5×10^{-3}

*Note: The other polymerization conditions are: [Zr]=52 μM and [M]=8.0 M.

Table A-5 List of k_p, A and E_a

T (°C)	R_p (M/min)	k_p	A_p	E_p (kcal/mol)
100	1.7×10^{0}	3.3×10^{5}	3.6×10^{6}	1.4×10^{1}
80	9.4×10^{-1}	4.8×10^{4}		
50	4.9×10^{-1}	2.6×10^{4}		
0	9.1×10^{-3}	2.1×10^{2}		

*Note: The other polymerization conditions are: [Zr]=52 μM, [M]=8.0 M and [MAO]=62 mM.

Table A-6 ^{1}H Chemical Shifts of H of Double Bonds

Structure	^{1}H Chemical Shift
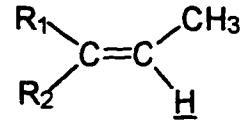	5.2 ppm
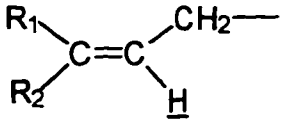	5.1 ppm
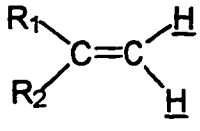	4.6-4.9 ppm
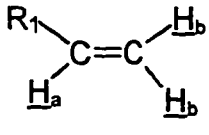	5.6-5.9 ppm ($1H_a$) 4.8-5.0 ppm ($2H_b$)
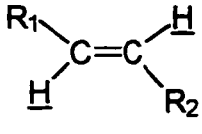	5.4 ppm

Table A-7. [Zr] Effect on Chain Transfer Rates at 100°C, 80°C, 50°C & 0°C*

T (°C)	[Zr] (μM)	$R_{tr,vd}$ (M/min)**	$R_{tr,vn}$ (M/min)**	$R_{tr,tri}$ (M/min)**
100	52	4.6×10^{-2}	8.9×10^{-3}	7.8×10^{-3}
	26	2.8×10^{-2}	1.9×10^{-3}	4.8×10^{-3}
	5.2	4.8×10^{-3}	4.6×10^{-4}	9.6×10^{-4}
	1.0	7.2×10^{-4}	7.5×10^{-5}	1.6×10^{-4}
80	52	3.8×10^{-2}	5.3×10^{-3}	5.6×10^{-3}
	26	5.9×10^{-3}	1.0×10^{-3}	1.1×10^{-3}
	5.2	1.3×10^{-3}	2.9×10^{-4}	2.7×10^{-4}
	1.0	2.1×10^{-4}	6.9×10^{-5}	1.0×10^{-4}
50	99	7.9×10^{-3}	2.9×10^{-3}	1.6×10^{-3}
	52	2.3×10^{-3}	2.8×10^{-3}	1.1×10^{-3}
	26	5.0×10^{-4}	4.0×10^{-4}	1.9×10^{-4}
	5.2	8.1×10^{-5}	7.1×10^{-5}	3.0×10^{-5}
0	99	2.1×10^{-5}	9.3×10^{-5}	1.2×10^{-5}
	52	6.0×10^{-6}	4.3×10^{-5}	3.0×10^{-6}
	26	8.4×10^{-7}	2.0×10^{-5}	1.6×10^{-6}

*Other polymerization conditions: [MAO]=62 mM, [M]=8.0 M.
**$R_{tr,vd}$: chain transfer rate to form vinylidene end-group; $R_{tr,vn}$: chain transfer rate to form vinylene end-group; $R_{tr,tri}$: chain transfer rate to form tri-substituted end-group.

Table A-8. X, Y and Z at 100°C, 80°C, 50°C and 0°C

T (°C)	End Group	X	Y	Z
100	CH_2=C<	1.1		0.80
	-CH=CH-	1.2		1.6
	-CH=C<	1.0		1.0
80	CH_2=C<	1.2		1.0
	-CH=CH-	1.0		1.3
	-CH=C<	1.0		1.2
50	CH_2=C<	1.6	0.37	0.60
	-CH=CH-	1.2	0.64	1.5
	-CH=C<	1.4	0.84	1.1
0	CH_2=C<	2.4	0.46	0.28
	-CH=CH-	1.2	0.85	0.99
	-CH=C<	1.5	1.1	0.75

Table A-9 [M] Effect on Chain Transfer Rates at 100°C, 80°C, 50°C & 0°C*

T (°C)	[M] (M)	$R_{tr,vd}$ (M/min)	$R_{tr,vn}$ (M/min)	$R_{tr,tri}$ (M/min)
100	8.0	4.6×10^{-2}	8.9×10^{-3}	7.8×10^{-3}
	4.0	3.4×10^{-2}	1.8×10^{-3}	5.6×10^{-3}
	2.0	1.6×10^{-2}	6.6×10^{-4}	2.3×10^{-3}
	.80	7.8×10^{-3}	2.2×10^{-4}	8.0×10^{-4}
80	8.0	3.8×10^{-2}	5.3×10^{-3}	5.6×10^{-3}
	4.0	1.4×10^{-2}	1.2×10^{-3}	2.2×10^{-3}
	.80	3.2×10^{-3}	2.6×10^{-4}	3.2×10^{-4}
50	8.0	2.3×10^{-3}	2.8×10^{-3}	1.1×10^{-3}
	4.0	1.5×10^{-3}	9.1×10^{-4}	2.8×10^{-4}
	2.0	1.0×10^{-3}	3.1×10^{-4}	1.6×10^{-4}
	.80	5.7×10^{-4}	9.0×10^{-5}	8.4×10^{-5}
0	8.0	6.0×10^{-6}	4.3×10^{-5}	3.0×10^{-6}
	4.0	3.2×10^{-6}	2.9×10^{-5}	2.6×10^{-6}
	2.0	3.6×10^{-6}	2.1×10^{-5}	1.3×10^{-6}
	.80	2.8×10^{-6}	4.2×10^{-6}	5.8×10^{-7}

*Note: Other polymerization conditions: [Zr] = 52 μM, [MAO] = 62 mM.

Table A-10 [MAO] Effect on Chain Transfer Rates at 100°C, 80°C, 50°C & 0°C*

T (°C)	[MAO] (mM)	$R_{tr,vd}$ (M/min)	$R_{tr,vn}$ (M/min)	$R_{tr,tri}$ (M/min)
100	62.0	4.6×10^{-2}	8.9×10^{-3}	7.8×10^{-3}
	34.4	1.1×10^{-1}	8.4×10^{-3}	1.4×10^{-2}
	18.5	4.9×10^{-2}	4.8×10^{-3}	5.6×10^{-3}
80	62.0	3.8×10^{-2}	5.3×10^{-3}	5.6×10^{-3}
	34.4	3.6×10^{-2}	5.1×10^{-3}	4.0×10^{-3}
	18.5	9.0×10^{-3}	1.8×10^{-3}	9.1×10^{-4}
50	62.0	2.3×10^{-3}	2.8×10^{-3}	1.1×10^{-3}
	31.0	1.9×10^{-3}	1.5×10^{-3}	4.7×10^{-4}
	15.5	1.4×10^{-3}	1.2×10^{-3}	3.5×10^{-4}
0	62.0	6.0×10^{-6}	4.3×10^{-5}	3.0×10^{-6}
	34.4	4.7×10^{-6}	3.4×10^{-5}	2.4×10^{-7}
	18.5	3.5×10^{-6}	1.6×10^{-5}	7.5×10^{-8}

*Other polymerization conditions: [M]=8.0 M, [Zr]=52 μM.

Table A-11 Temperature Effect on Chain Transfer Rates*

T (°C)	$R_{tr,vd}$ (M/min)	$R_{tr,vn}$ (M/min)	$R_{tr,tri}$ (M/min)	$k_{tr,vd}$	$k_{tr,vn}$	$k_{tr,tri}$
100	4.6×10^{-2}	8.9×10^{-3}	7.8×10^{-3}			
80	3.8×10^{-2}	5.3×10^{-3}	5.6×10^{-3}			
50	2.3×10^{-3}	2.8×10^{-3}	1.1×10^{-3}	8.2×10^{3}	1.4×10^{3}	1.4×10^{3}
0	6.0×10^{-6}	4.3×10^{-5}	2.6×10^{-7}	2.8×10^{5}	1.0×10^{2}	2.3×10^{0}

*Other polymerization conditions: [M]=8.0 M, [Zr]=52 μM and [MAO]=62 mM.

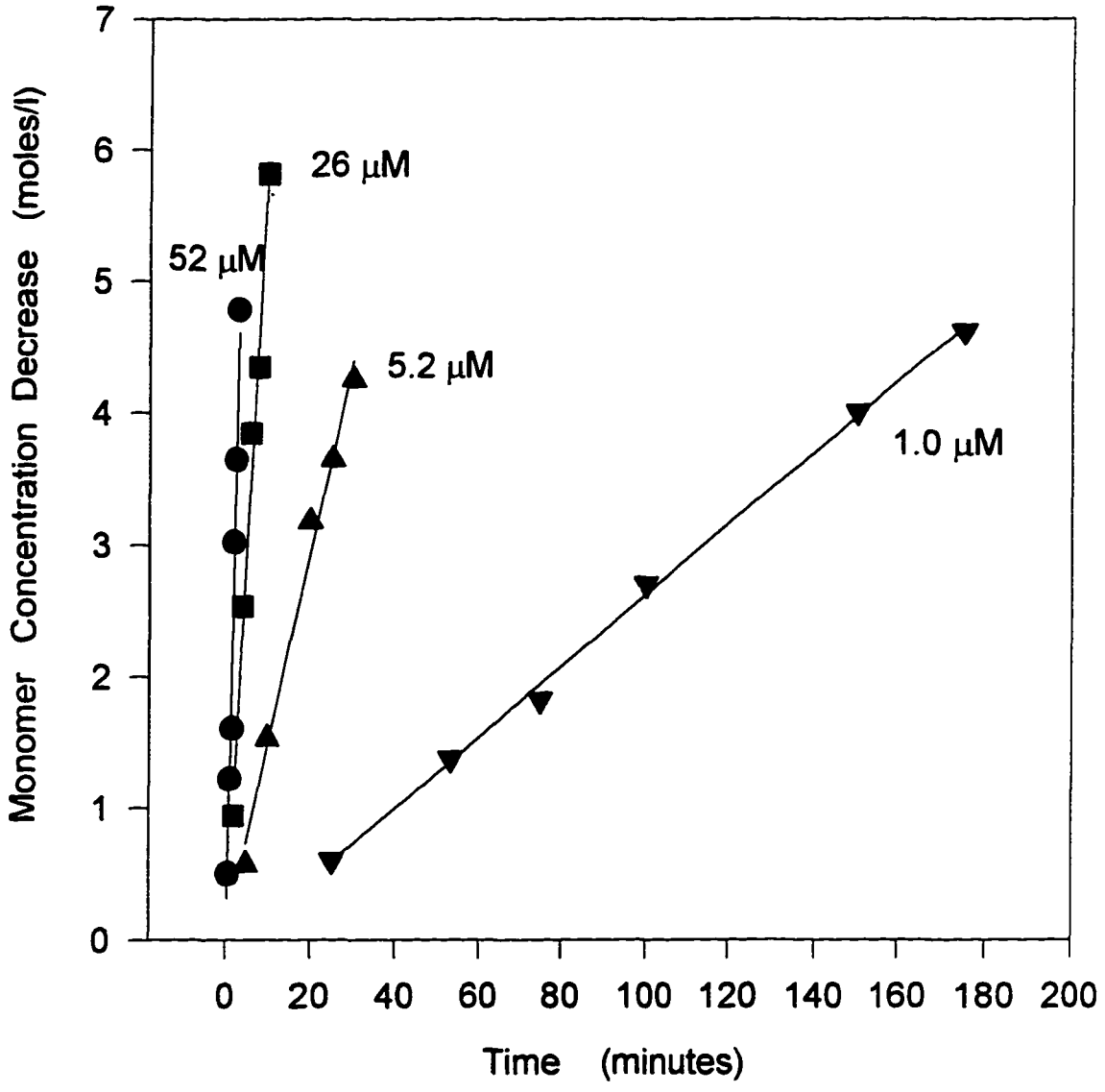

Figure A-2. Monomer concentration decrease as a function of time at 100°C and different catalyst concentrations

Polymerization conditions: [MAO]=62mM, [M]=8.0M, T=100°C
Catalyst concentration is labeled on each curve.

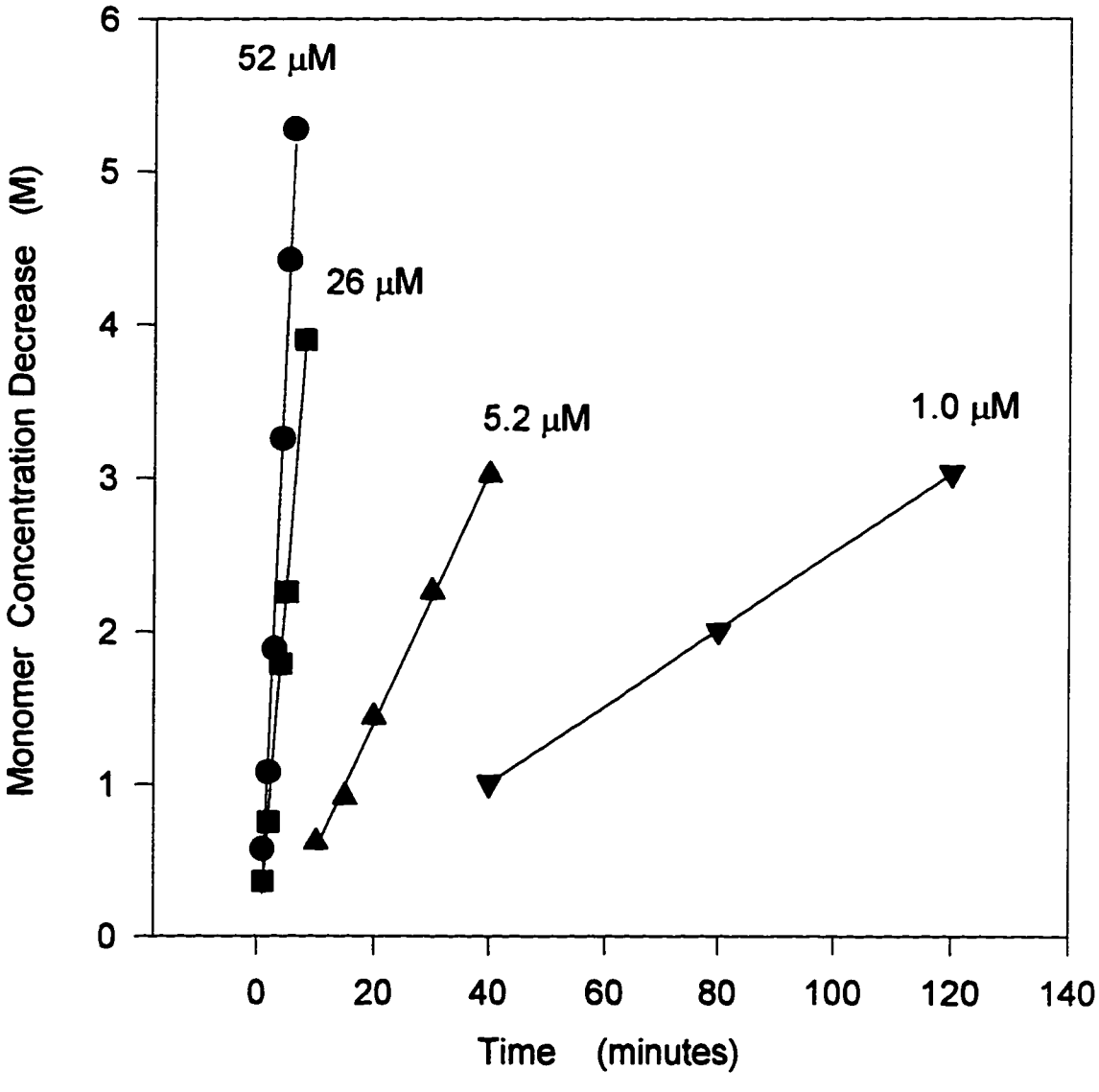

Figure A-3. Monomer concentration decrease as a function of time at 80°C and different catalyst concentrations

Polymerization conditions: [MAO]=62mM, [M]=8.0M, T=80°C
Catalyst concentration is labeled on each curve

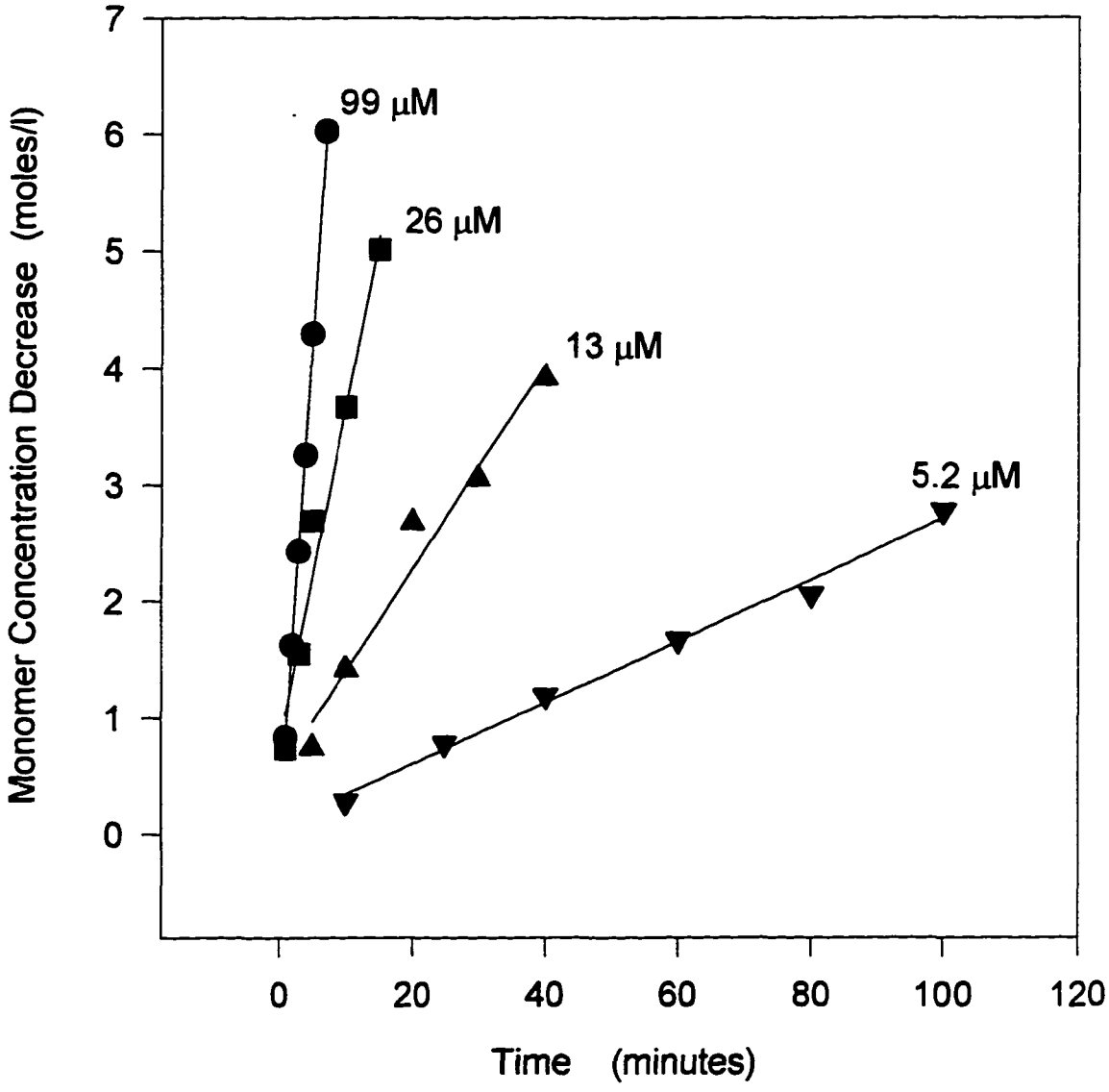

Figure A-4. Monomer concentration decrease as a function of time at 50°C and different catalyst concentrations

Polymerization conditions: [MAO]=62mM, [M]=8.0M, T=50°C
Catalyst concentration is labeled on each curve.

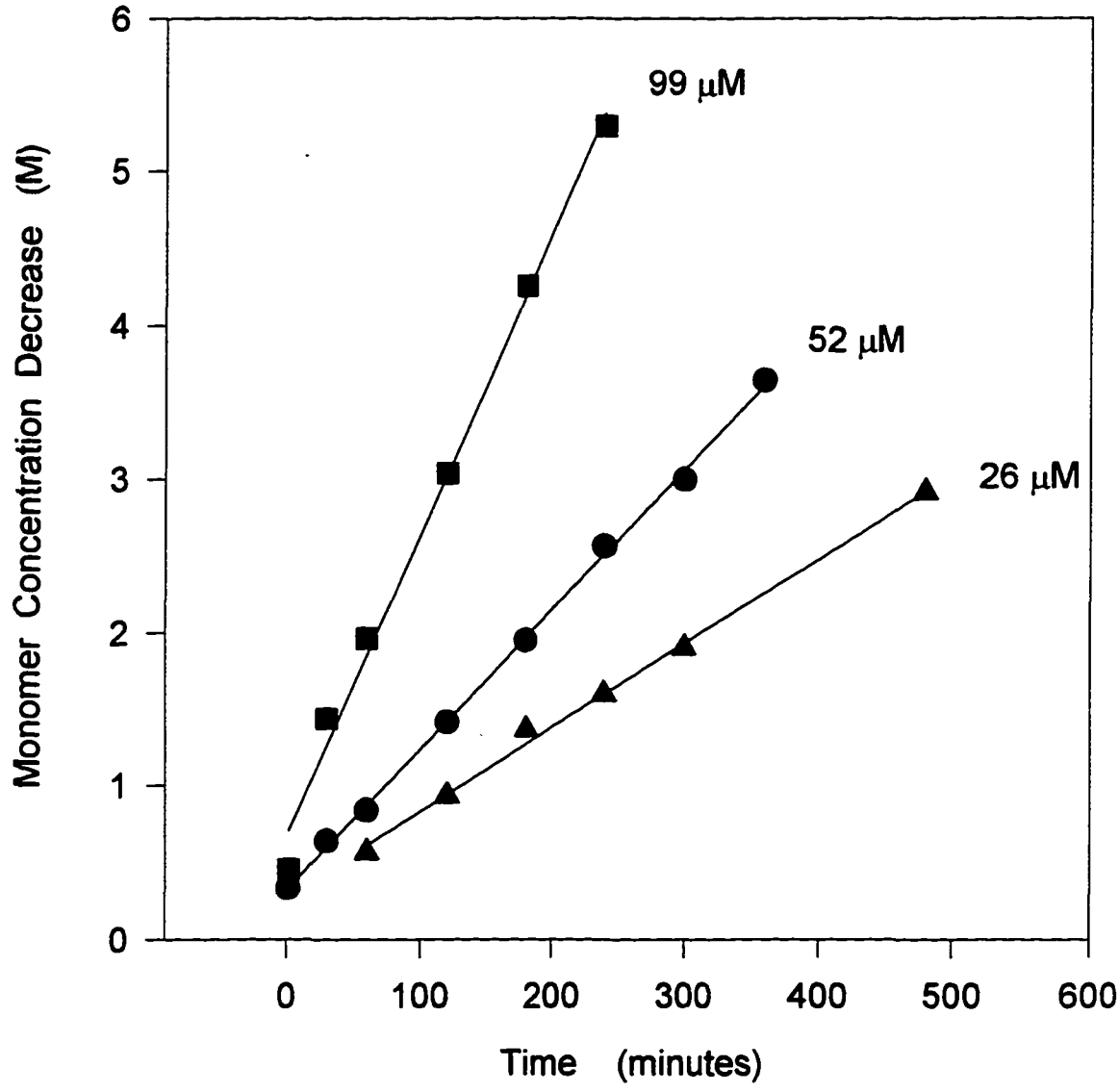

Figure A-5. Monomer concentration decrease as a function of time at 0°C and different catalyst concentrations

Polymerization conditions: [MAO]=62mM, [M]=8.0M, T=0°C. Catalyst concentration is labeled on each curve.

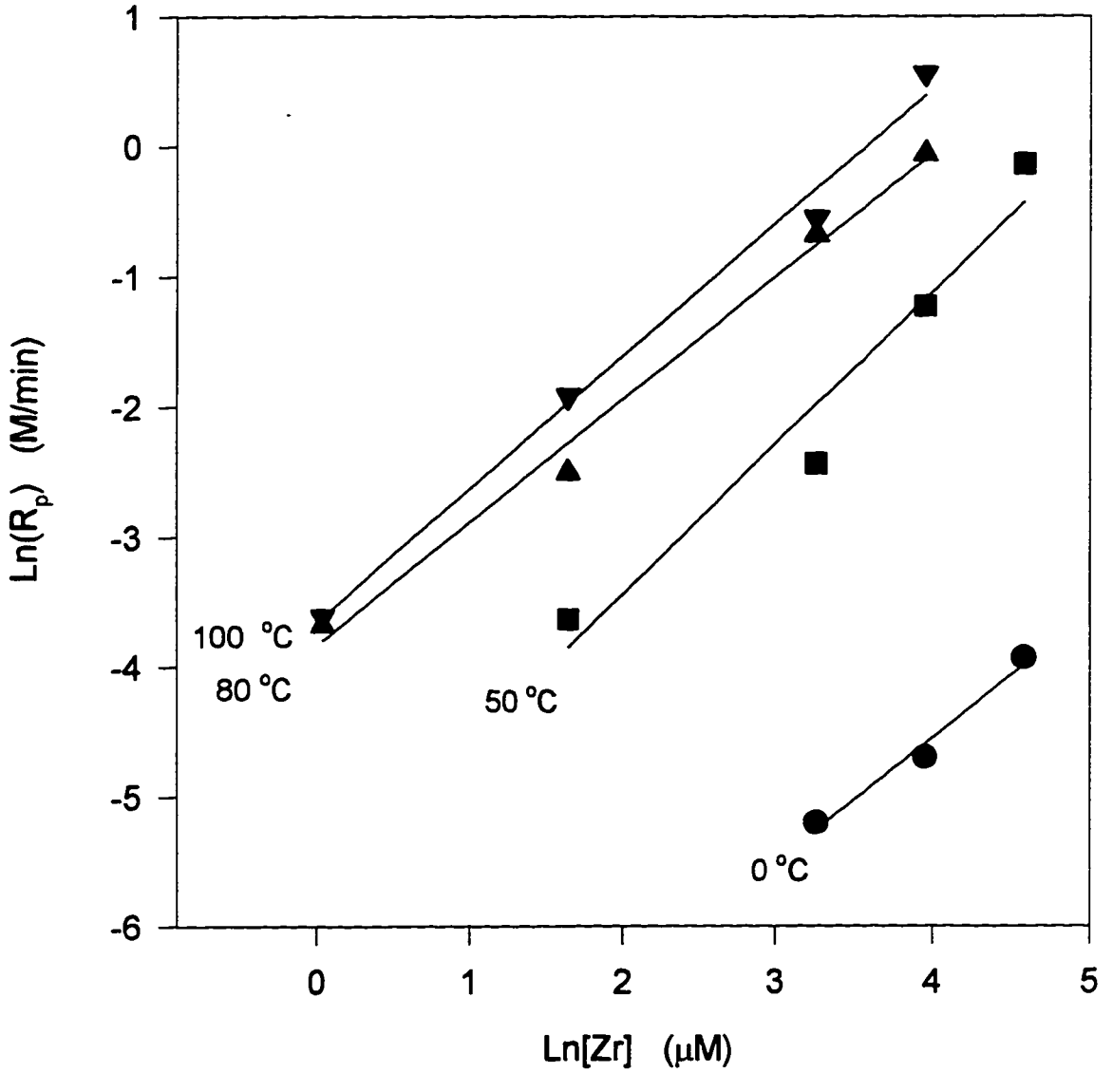

Figure A-6. $Ln(R_p)$ as a function of Ln[Zr] at different temperatures

Polymerization conditions: [MAO] = 62mM, [M] = 8.0M (bulk)

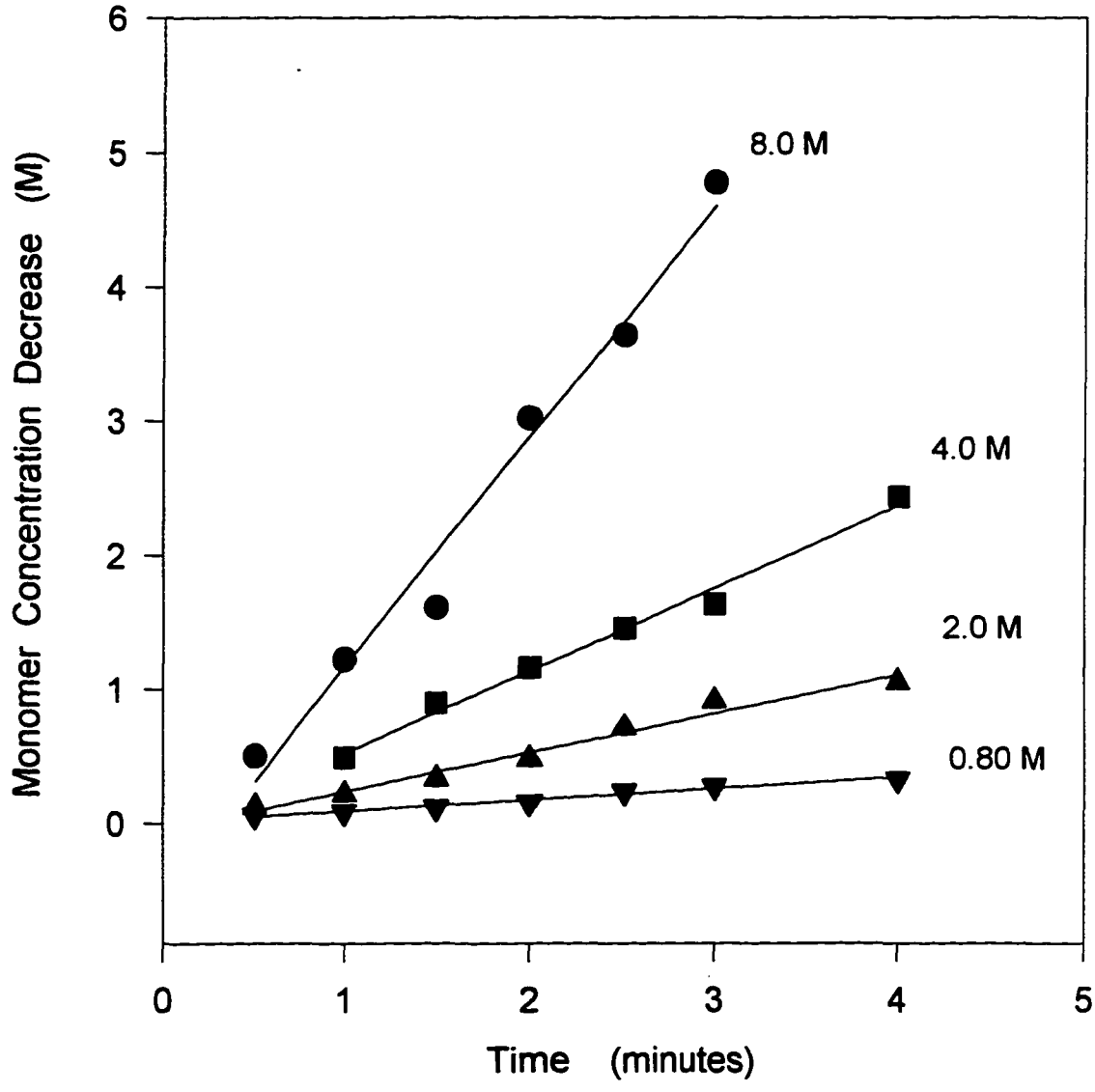

Figure A-7. Monomer concentration decrease as a function of time at 100°C and different monomer concentrations

Polymerization conditions: [Zr]=52μM, [MAO]=62mM, T=100°C
Monomer concentration is labeled on each curve.

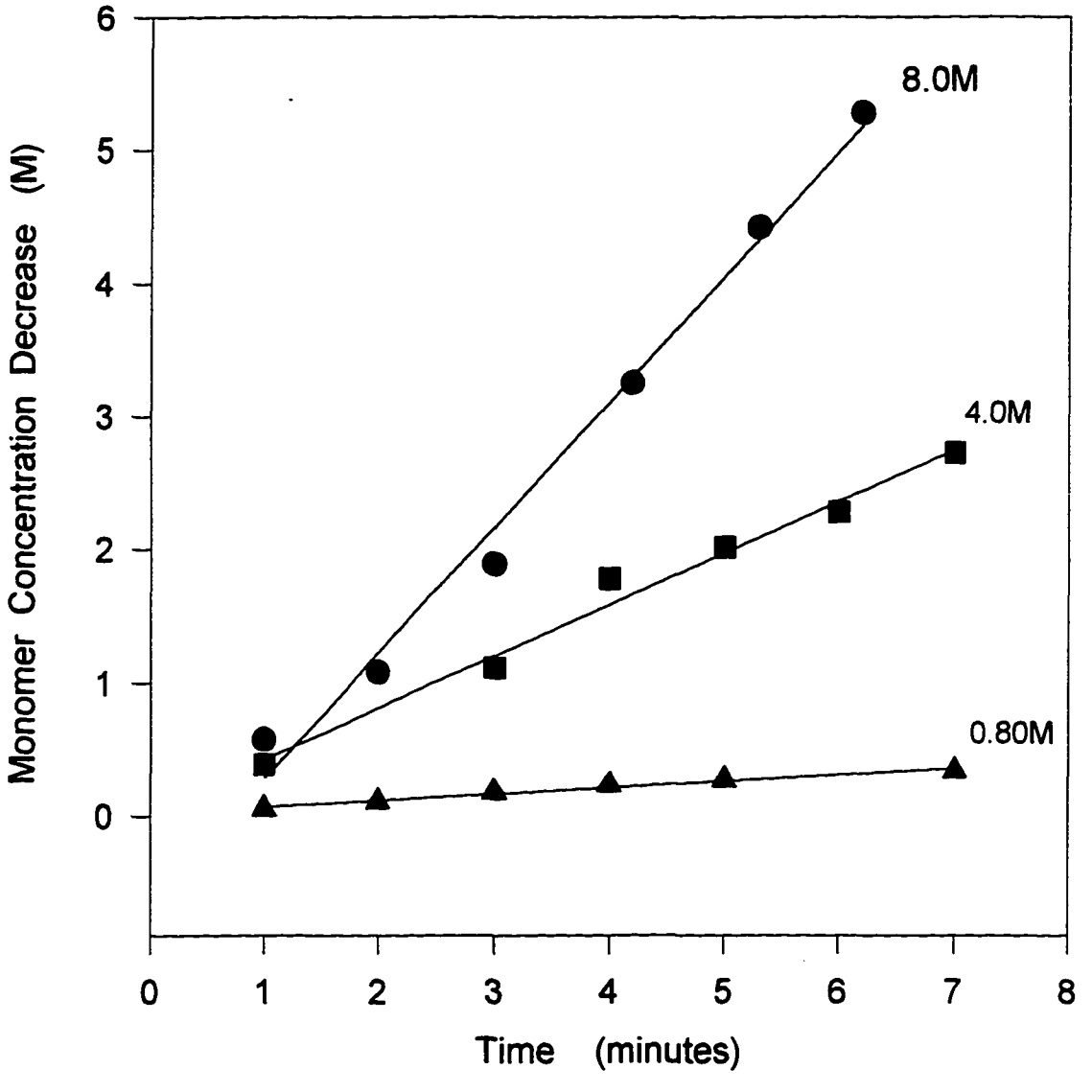

Figure A-8. Monomer concentration decrease as a function of time at 80°C and different monomer concentrations

Polymerization conditions: [MAO]=62mM, [Zr]=52μM, T=80°C
Monomer concentration is labeled on each curve.

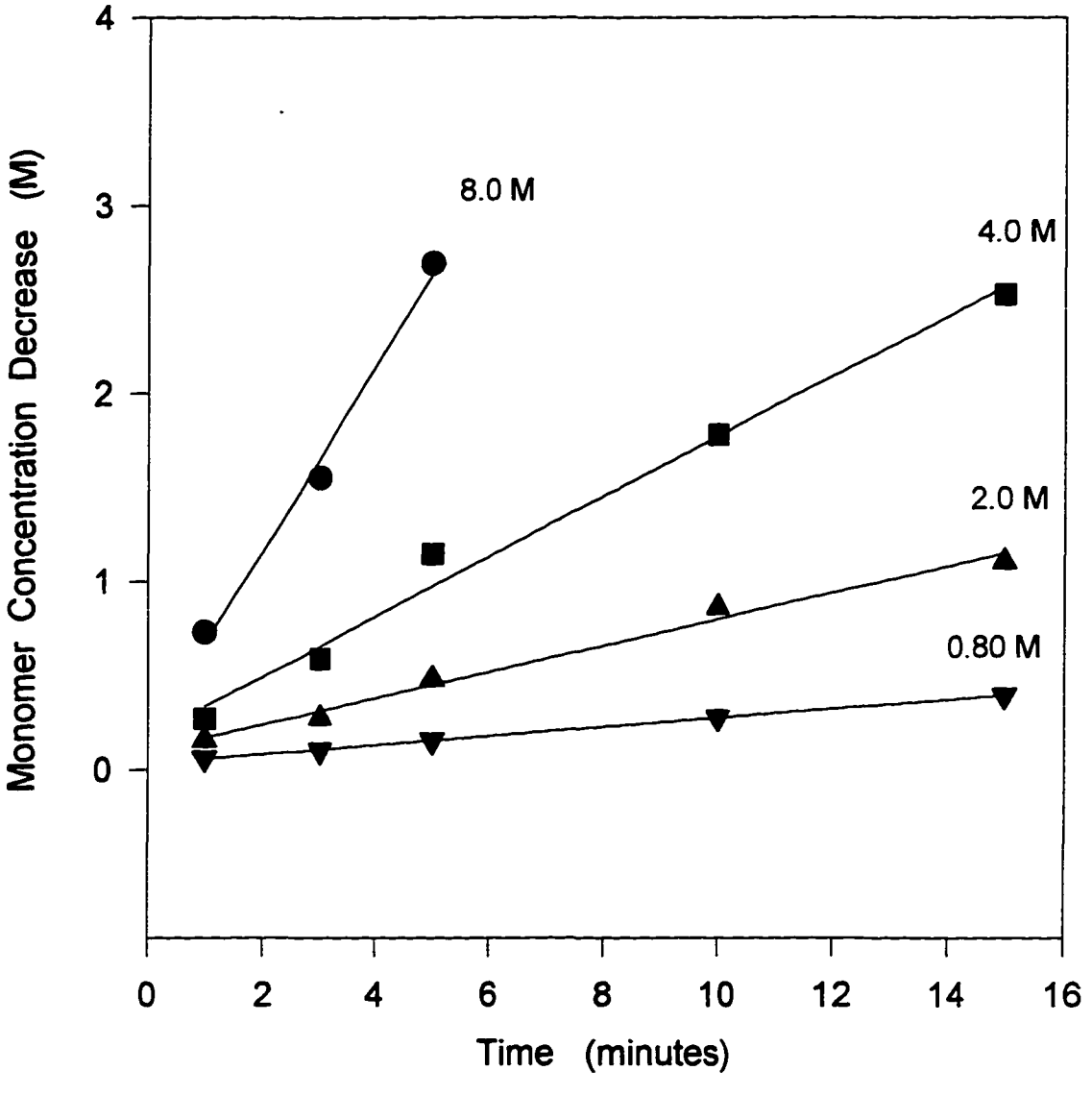

Figure A-9. Monomer concentration decrease as a function of time at 50°C and different monomer concentrations

Polymerization conditions: [MAO]=62mM, [Zr]=52M, T=50°C
Monomer concentration is labeled on each curve.

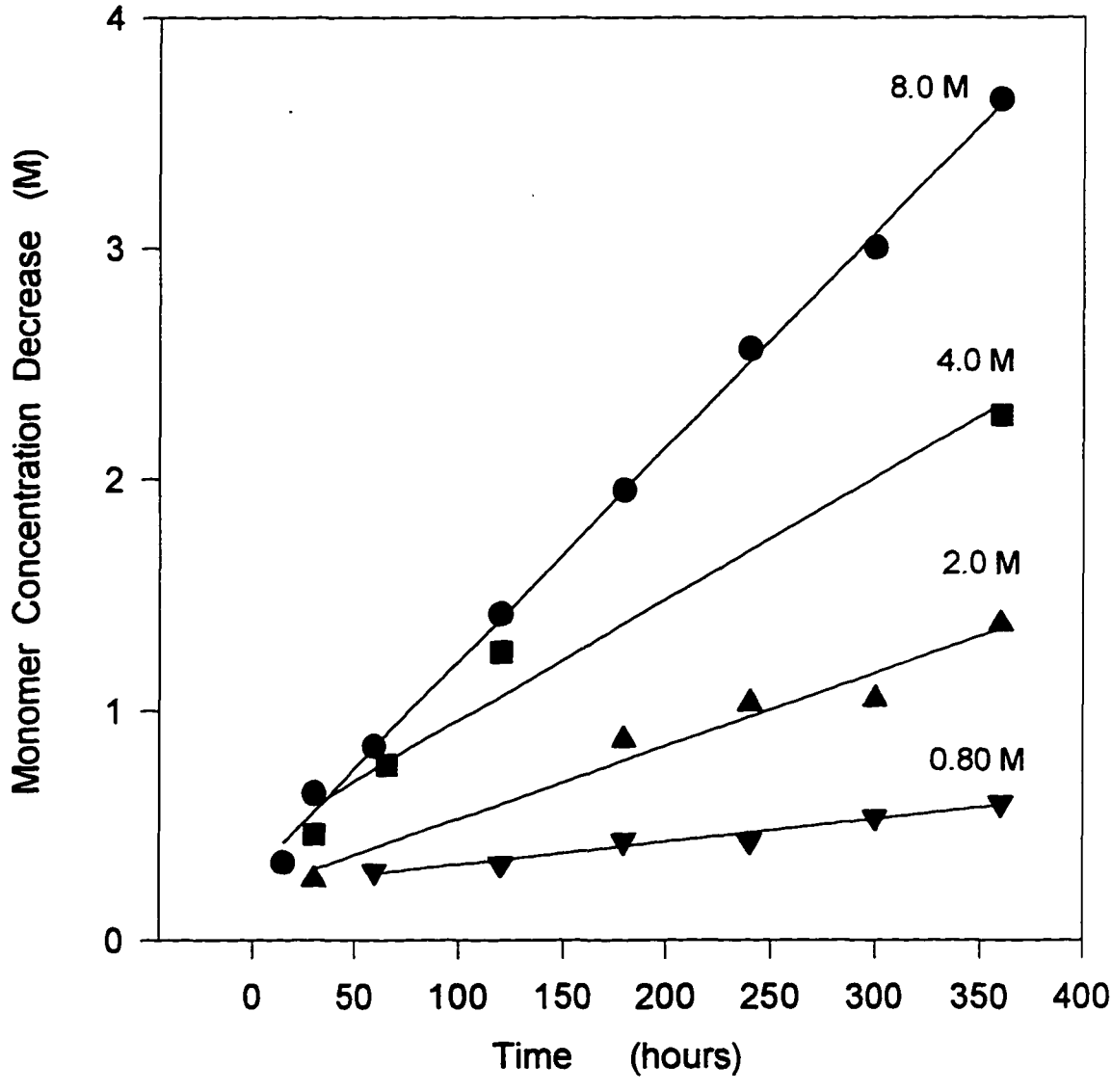

Figure A-10. Monomer concentration decrease as a function of time at 0°C and different monomer concentrations

Polymerization conditions: [Zr]= 52μM, [MAO]=62mM, T=0°C
Monomer concentration is labeled on each curve.

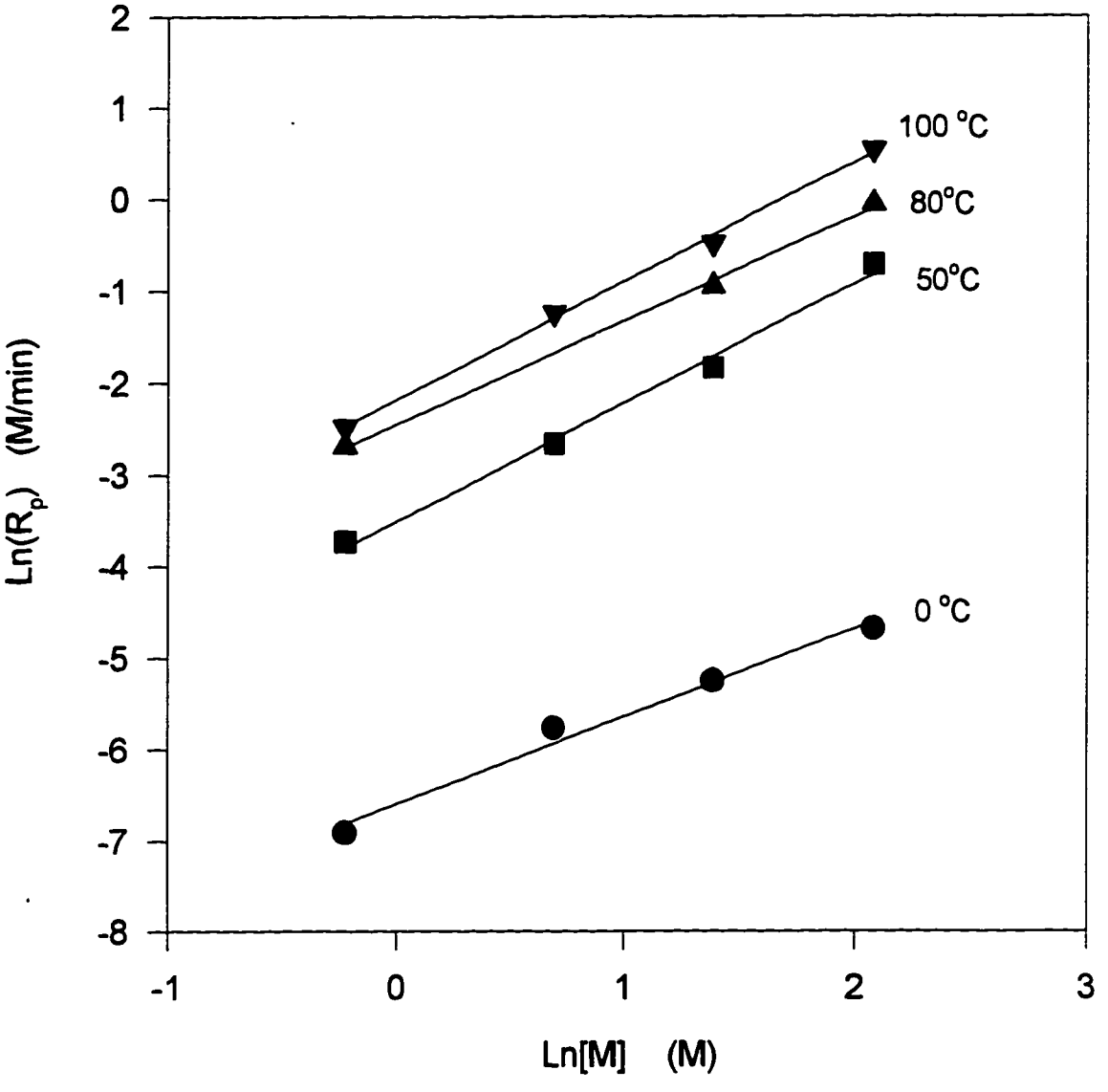

Figure A-11. $Ln(R_p)$ as a function of Ln[M] at different temperatures

Polymerization Conditions: [Zr] = 52μM, [MAO] = 62mM

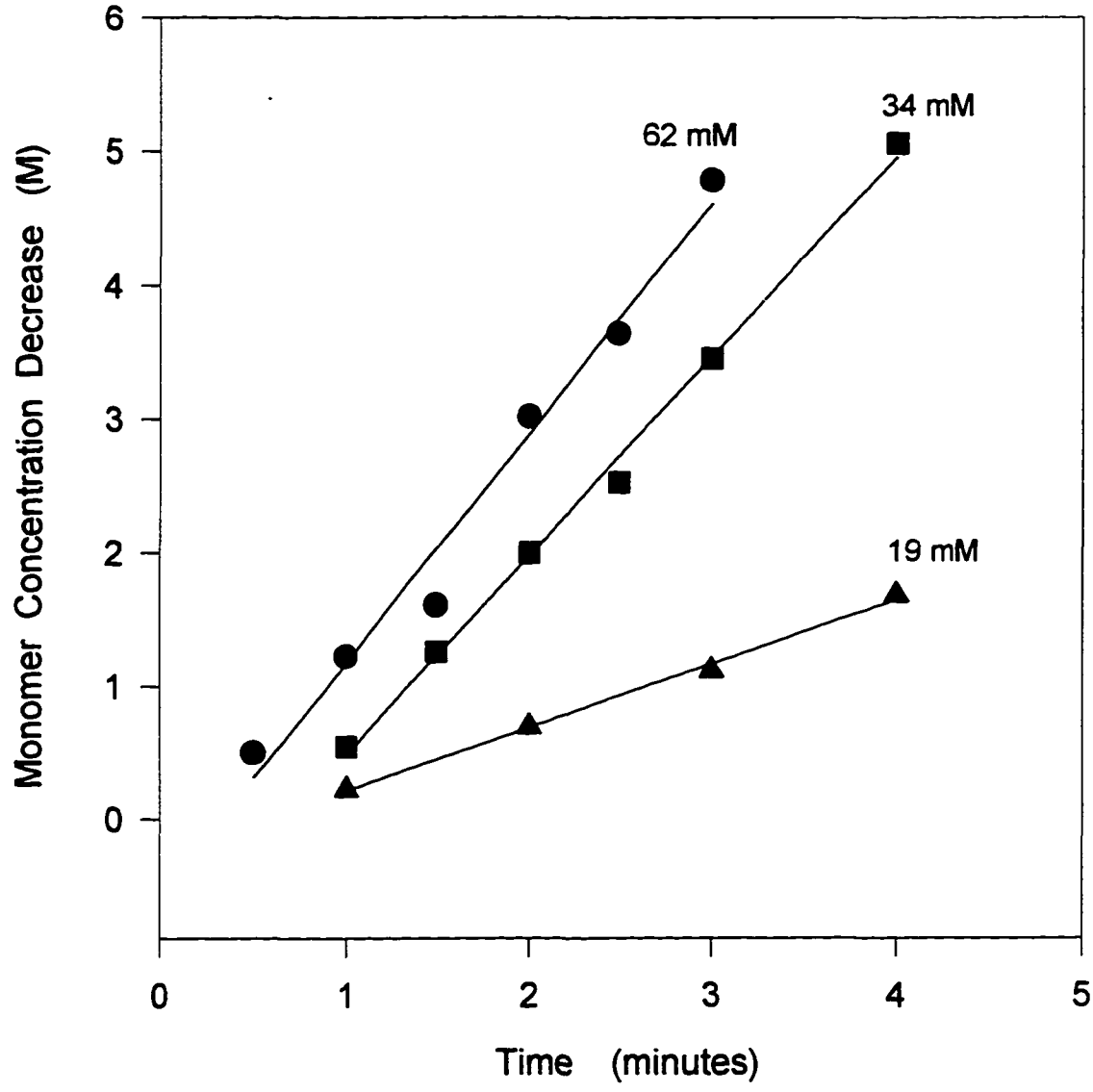

Figure A-12. Monomer concentration decrease as a function of time at 100°C and different MAO concentrations

Polymerization conditions: [Zr]=52μM, [M]=8.0M, T=100°C
MAO concentration is labeled on each curve.

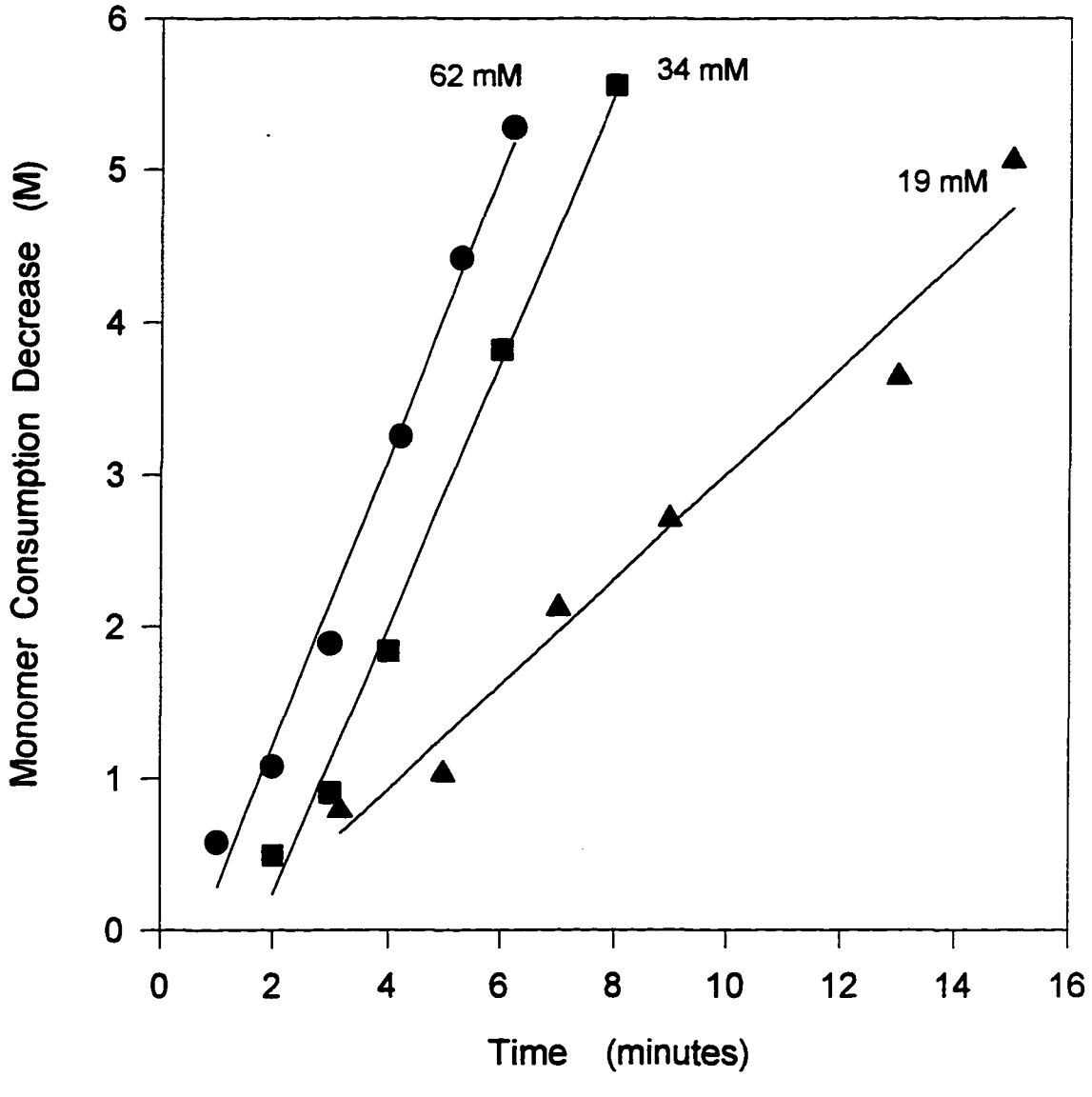

Figure A-13. Monomer concentration decrease as a function of time at 80°C and different MAO concentrations

Polymerization conditions: [Zr]=52μM, [M]=8.0M, T=80°C
MAO concentration is labeled on each curve.

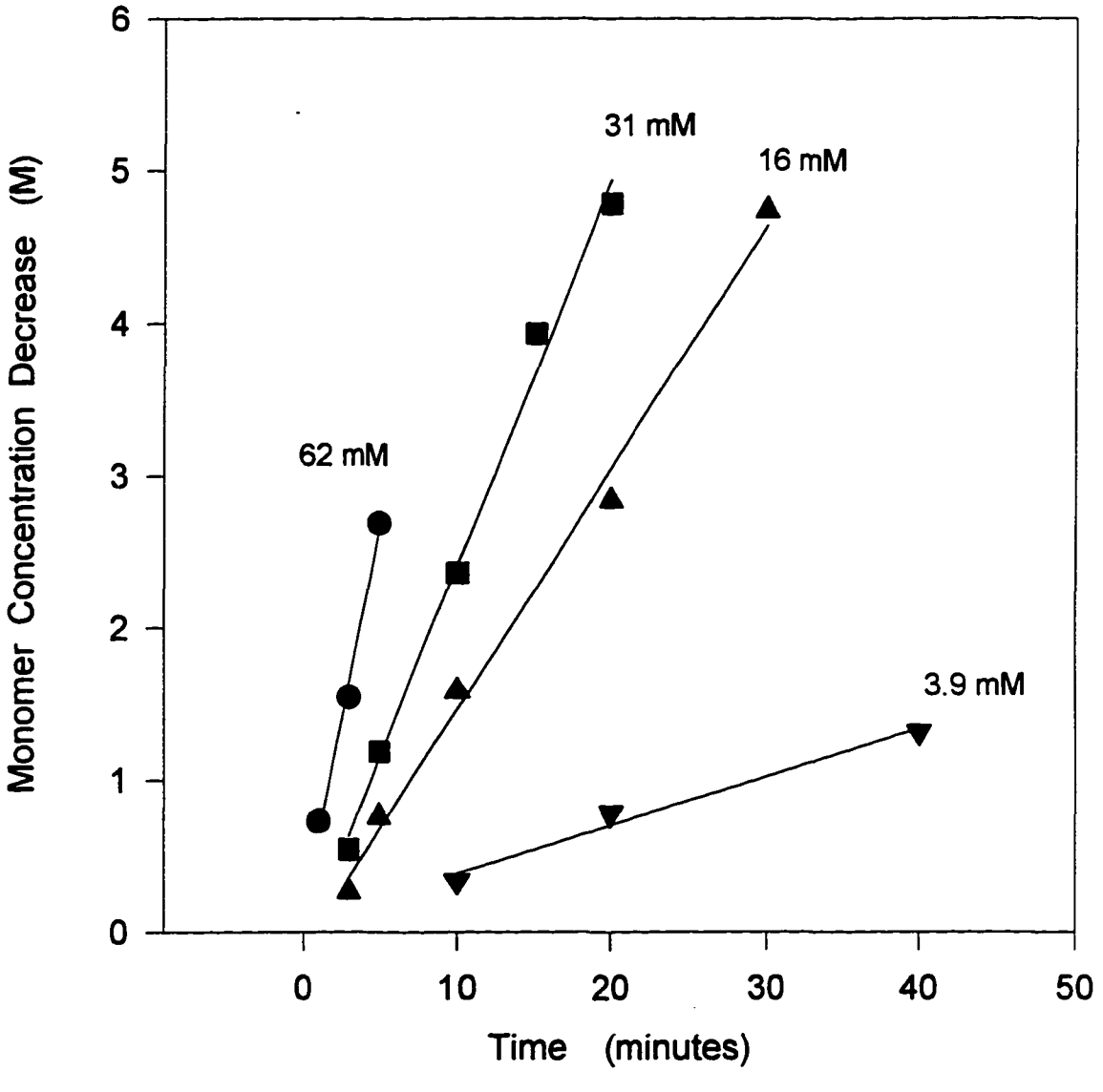

Figure A-14. Monomer concentration decrease as a function of time at 50°C and different MAO concentration

Polymerization conditions: [M]=8.0M, [Zr]=52μM, T=50°C
MAO concentration is labeled on each curve.

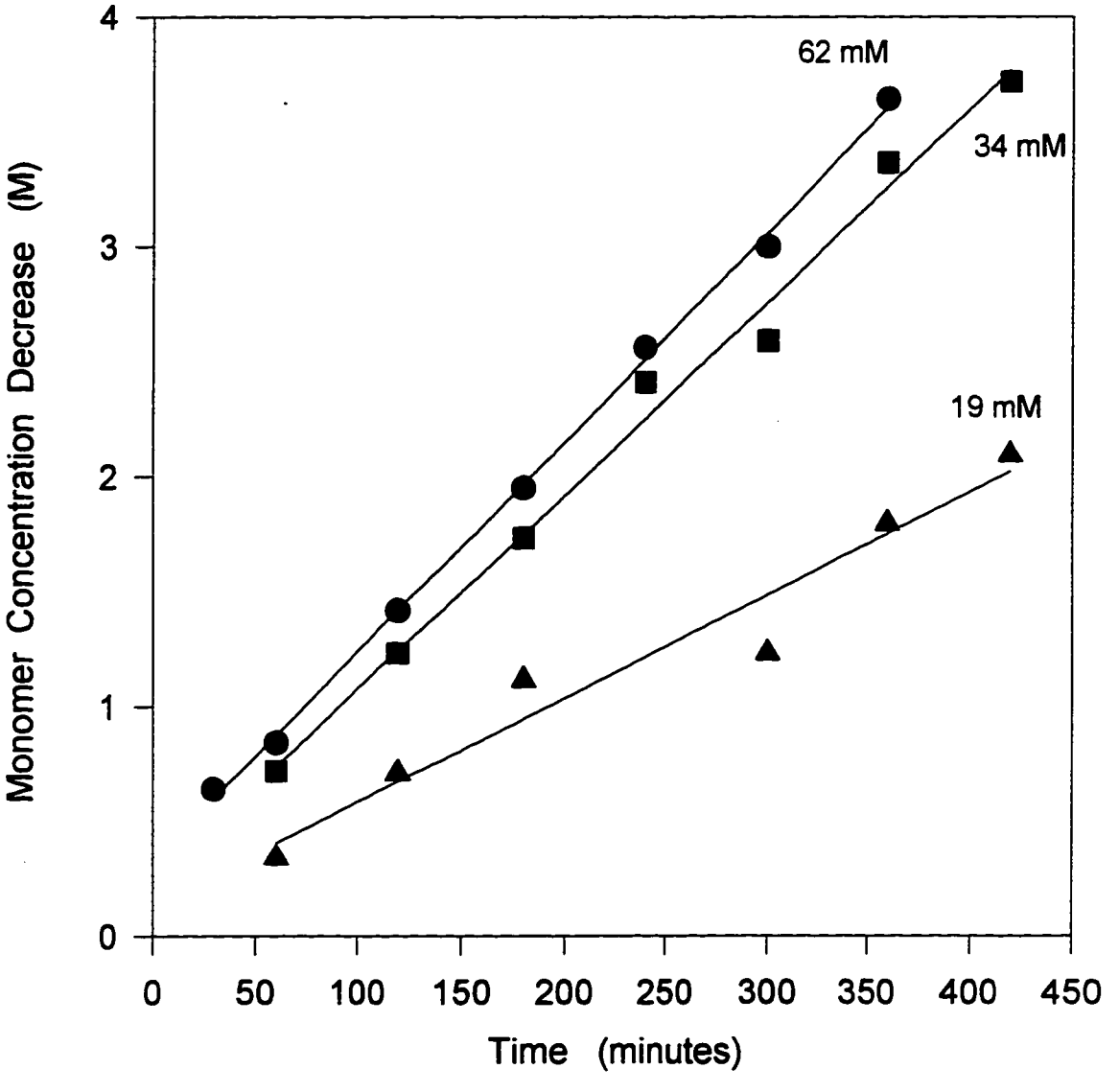

Figure A-15. Monomer concentration decrease as a function of time at 0°C and different MAO concentrations

Polymerization conditions: [Zr]=52μM, [M]=8.0M, T=0°C
MAO concentration is labeled on each curve.

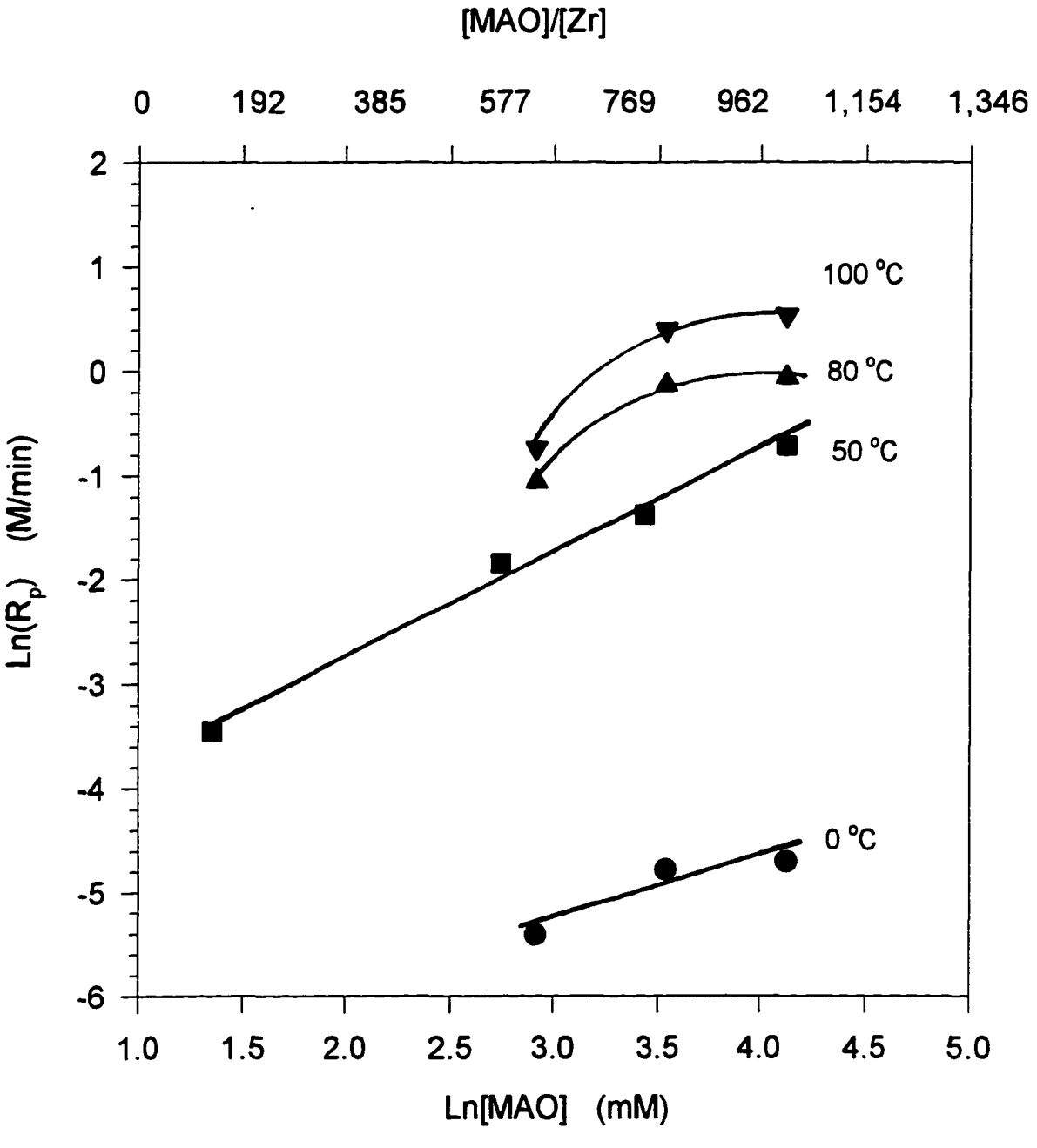

Figure A-16. $Ln(R_p)$ as a function of Ln[MAO]

Polymerization conditions: [Zr] = 52μM, [M] = 8.0M (bulk)

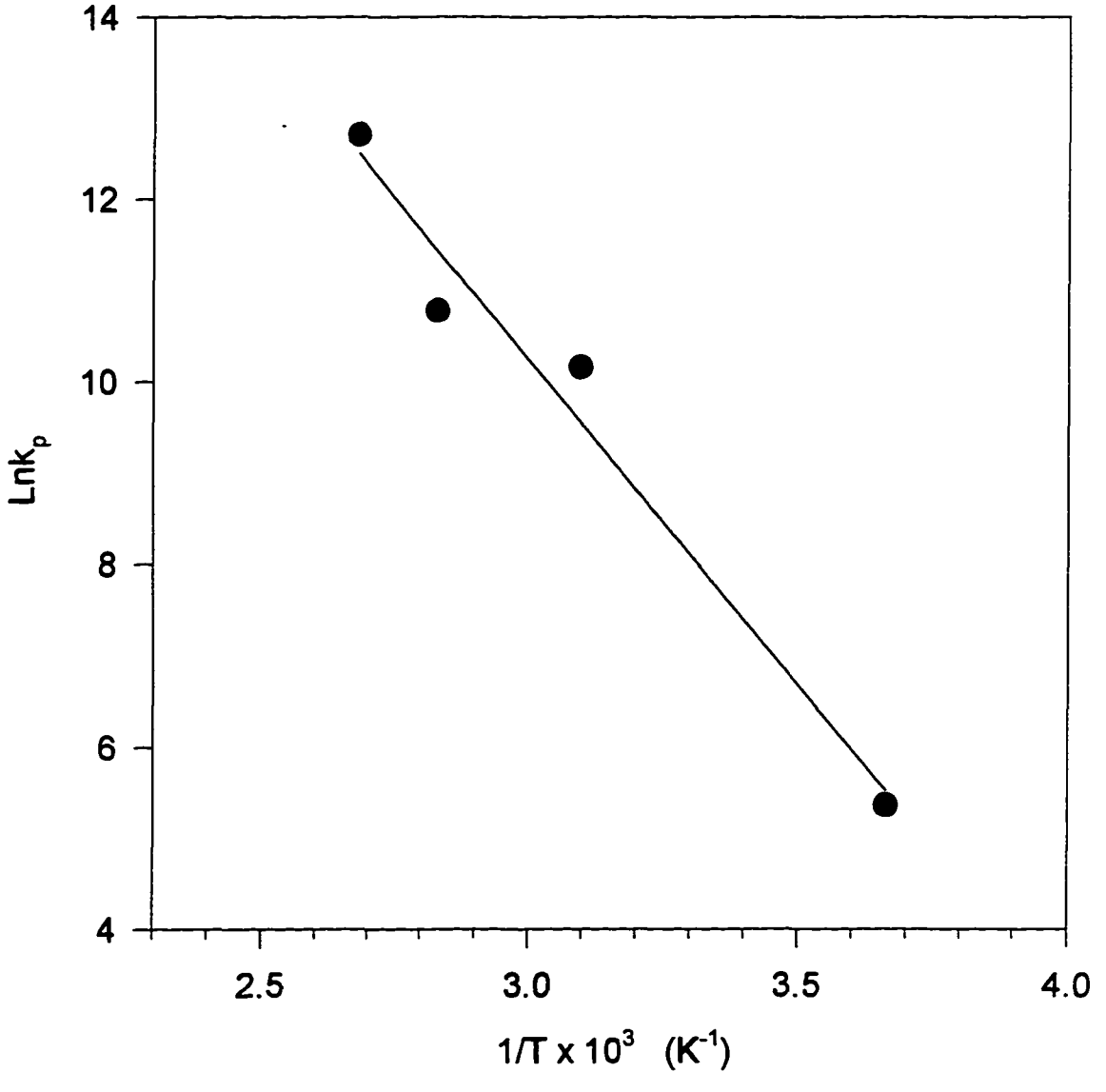

Figure A-17. Lnk$_p$ as a function of 1/T

Polymerization conditions: [Zr]=52 μM, [M]=8.0 M, [MAO]=62 mM.

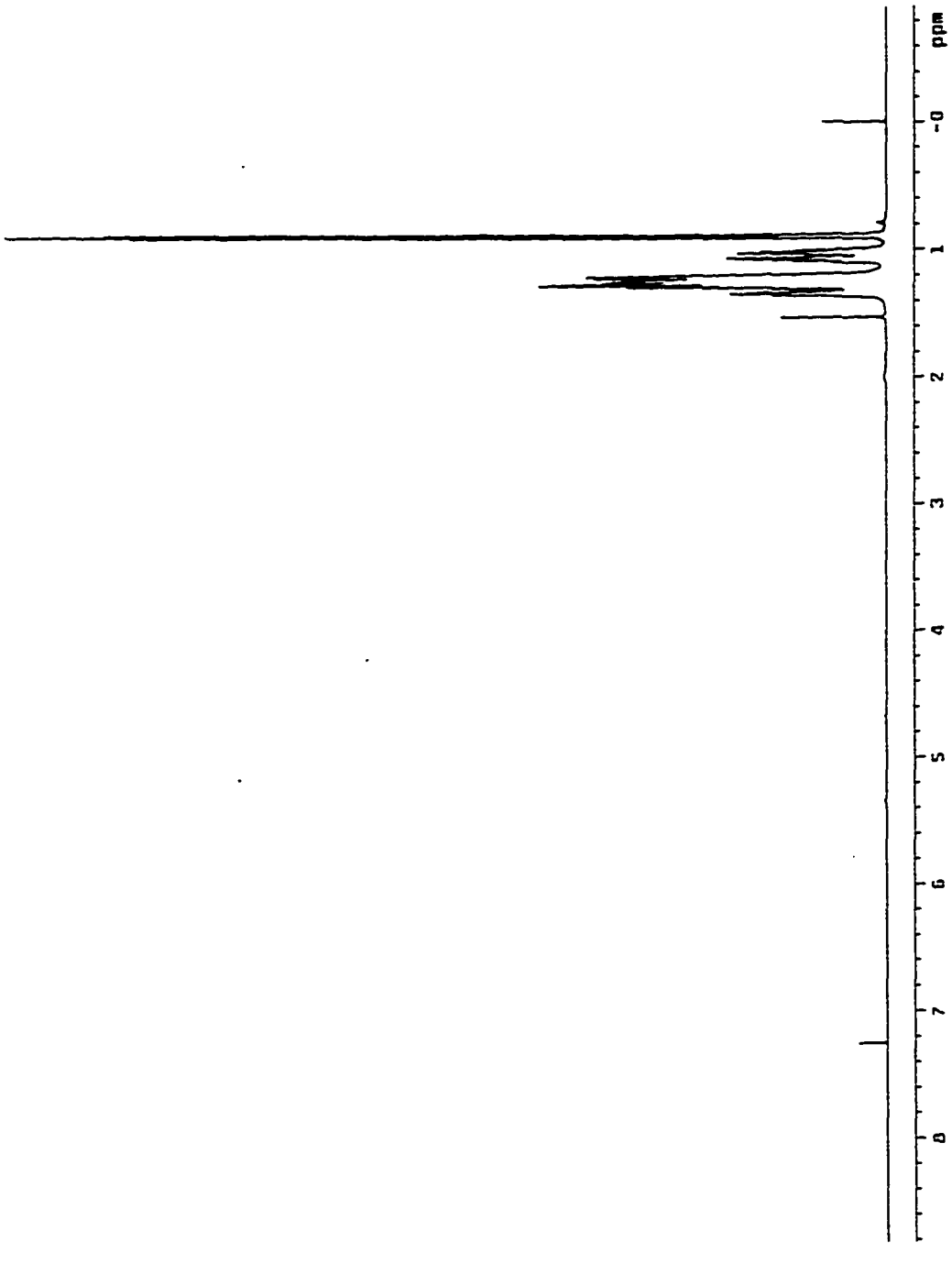

Figure A-18 ^{1}H NMR spectrum of poly(1-hexene)

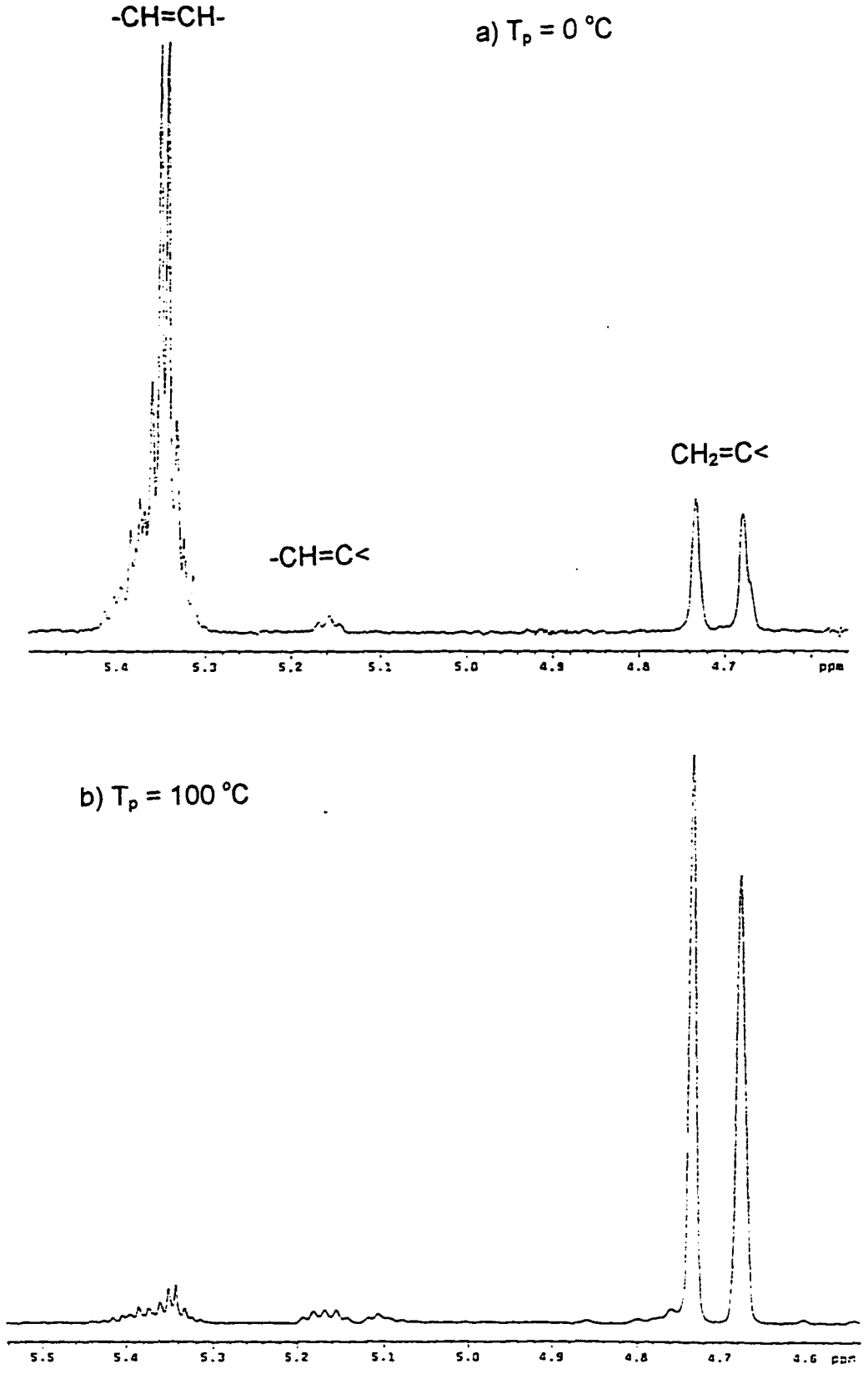

Figure A-19 Double bond end-groups of poly(1-hexene) in ^{1}H NMR spectrum

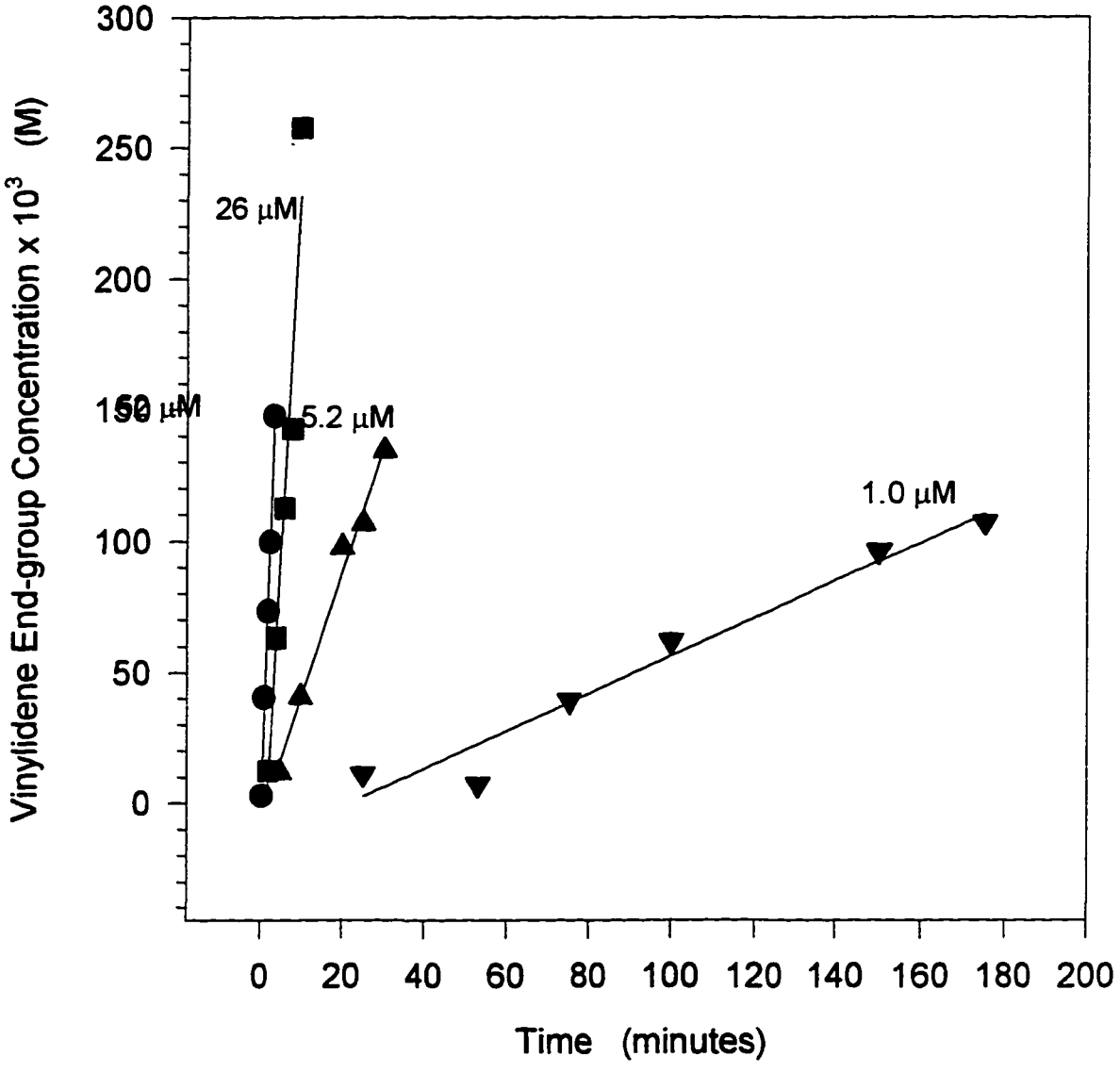

Figure A-20. Vinylidene end-group concentration as a function of time at 100°C and different catalyst concentrations

Polymerization conditions: [MAO=62mM, [M]=8.0M and T=100°C
Catalyst concentration is labeled on each curve.

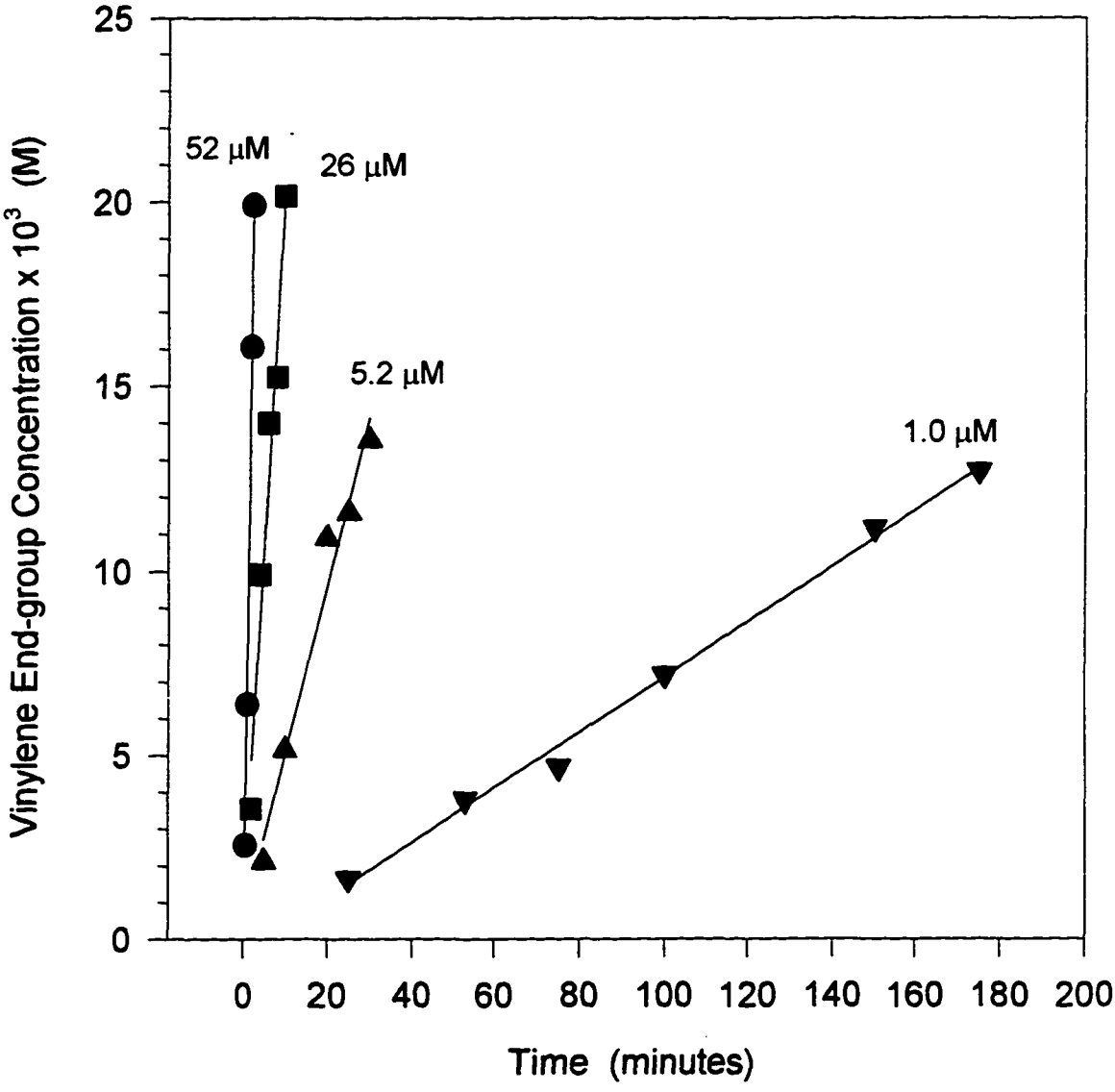

Figure A-21. Vinylene end-group concentration as a function of time at 100°C and different catalyst concentrations

Polymerization conditions: [MAO]=62mM, [M]=8.0M and T=100°C
Catalyst concentration is labeled on each curve.

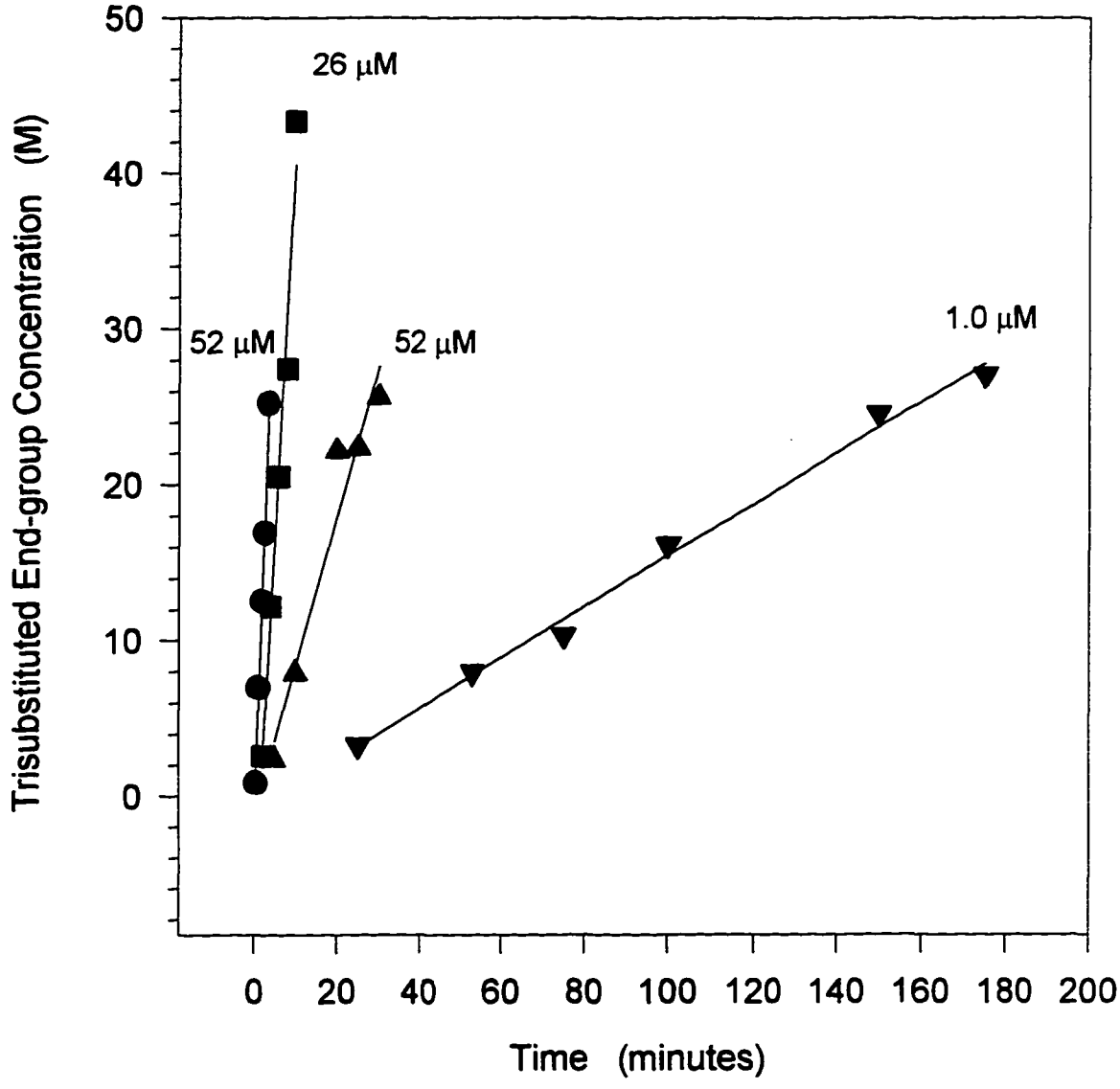

Figure A-22. Trisubstituted end-group concentration as a function of time at 100°C and different catalyst concentrations

Polymerization conditions: [MAO]=62mM, [M]=8.0M and T=100°C
Catalyst concentration is labeled on each curve.

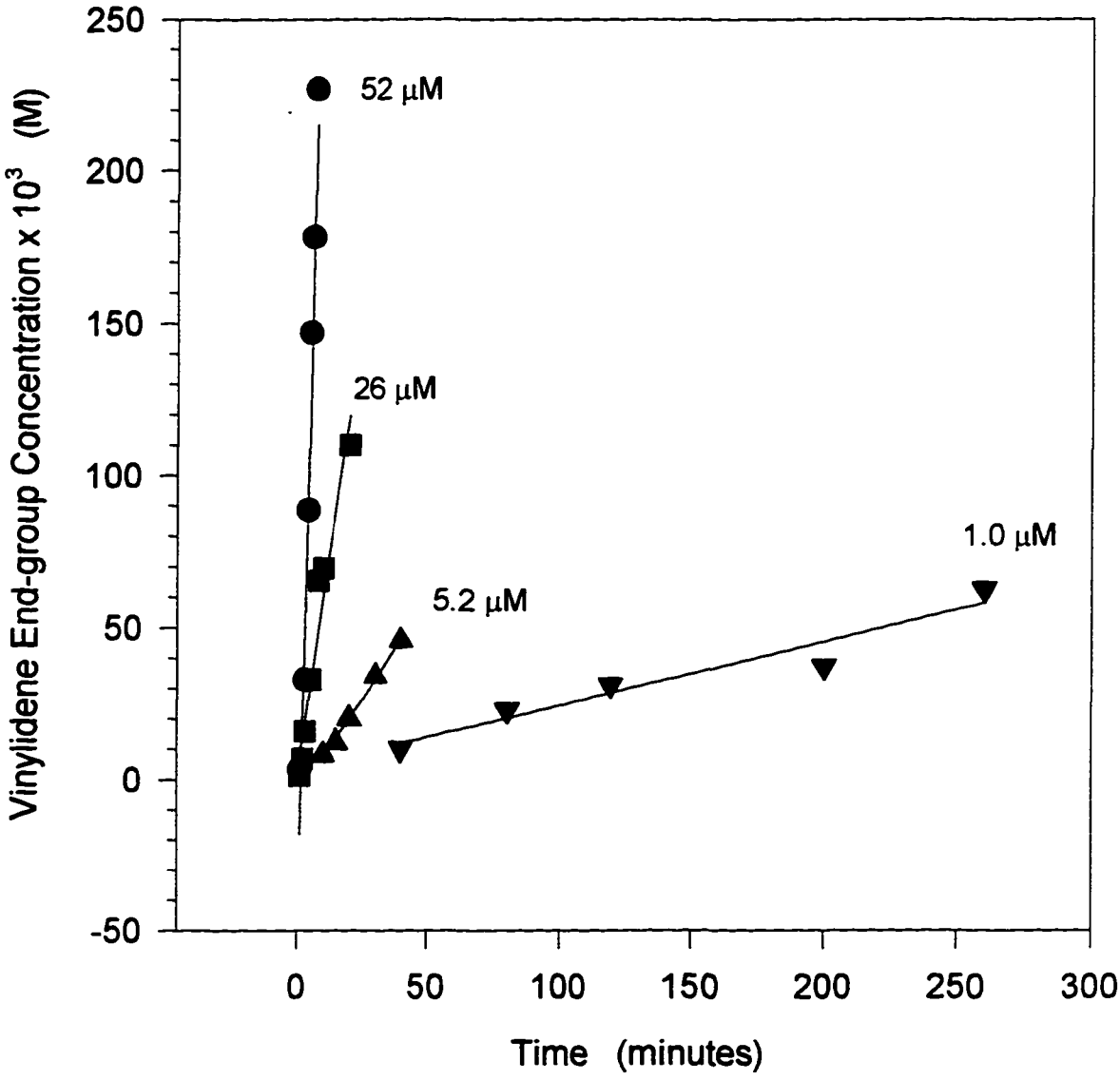

Figure A-23. Vinylidene End-group Concentration as a function of time at 80°C and different catalyst concentrations

Polymerization conditions: [M]=8.0M, [MAO]=62mM and T=80°C
Catalyst concentration is labeled on each curve.

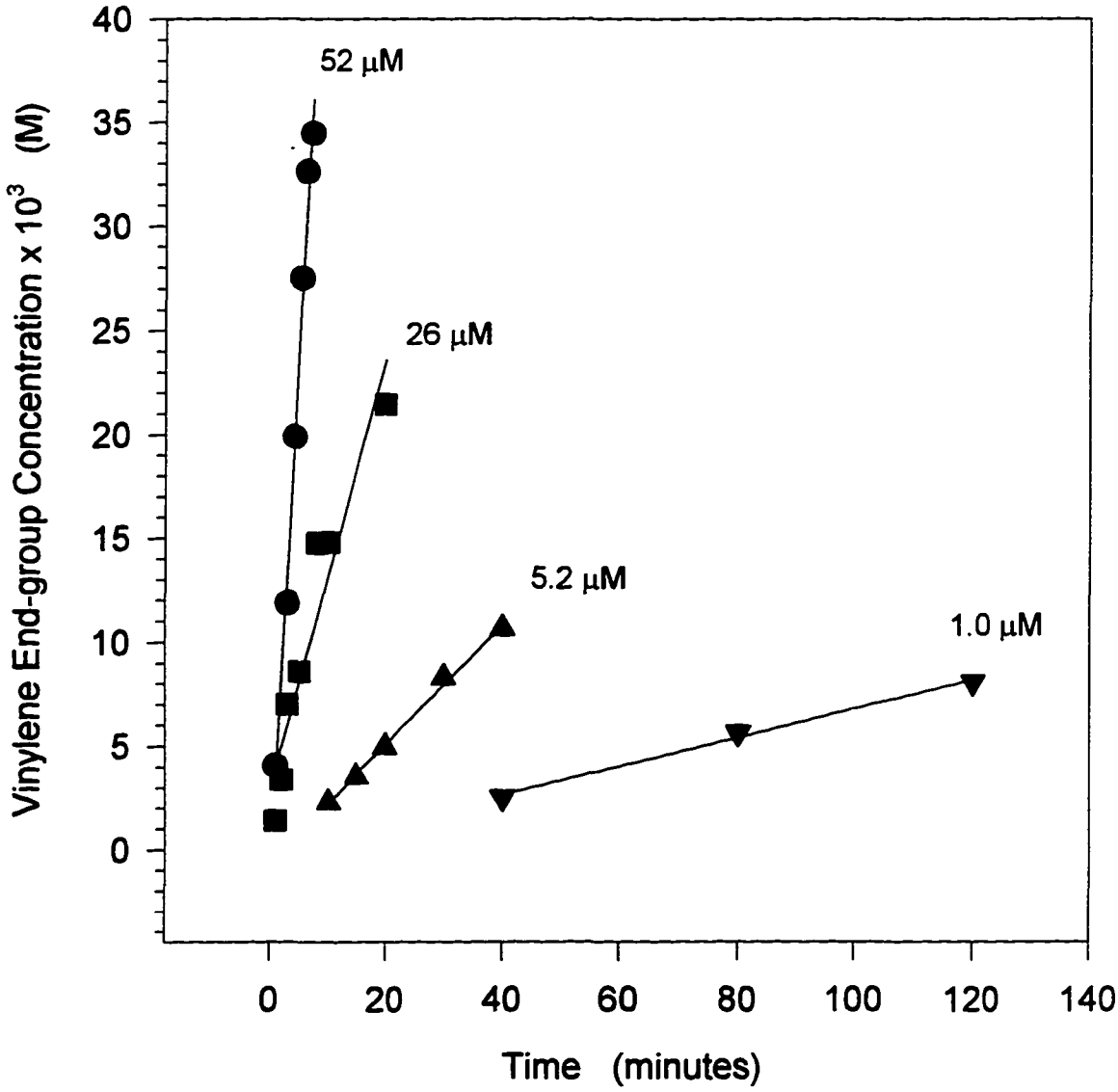

Figure A-24. Vinylene end-group concentration as a function of time at 80°C and different catalyst concentrations

Polymerization conditions: [M]=8.0M, [MAO]=62mM and T=80°C
Catalyst concentration is labeled on each curve.

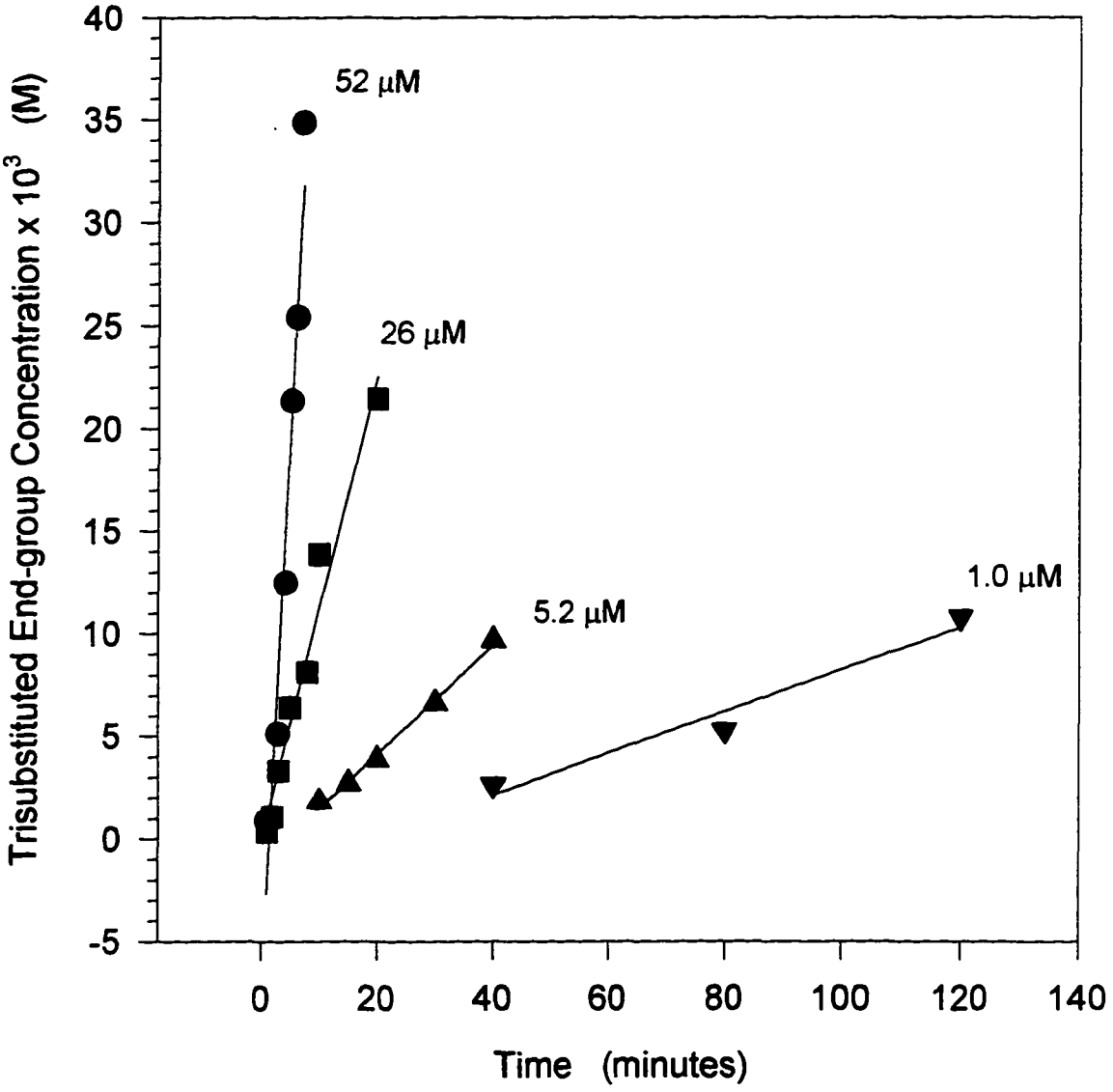

Figure A-25. Trisubstituted end-group concentration as a function of time at 80°C and different catalyst concentrations

Polymerization conditions: [M]=8.0M, [MAO]=62mM and T=80°C
Catalyst concentration is labeled on each curve.

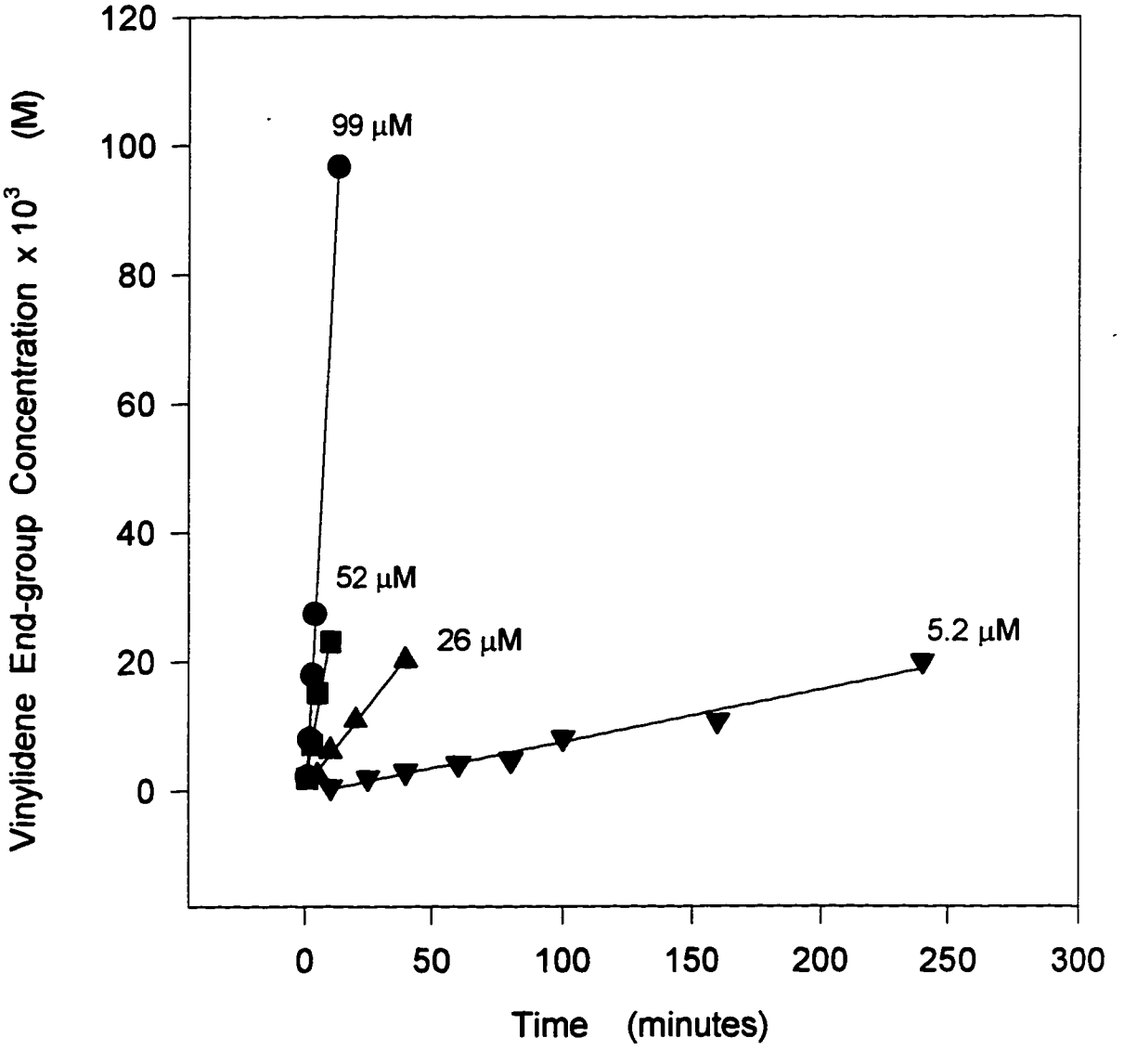

Figure A-26. Vinylidene end-group concentration as a function of time at 50°C and different catalyst concentrations

Polymerization conditions: [MAO]=62mM, [M]=8.0M, T=50°C
Catalyst concentration is labeled on each curve .

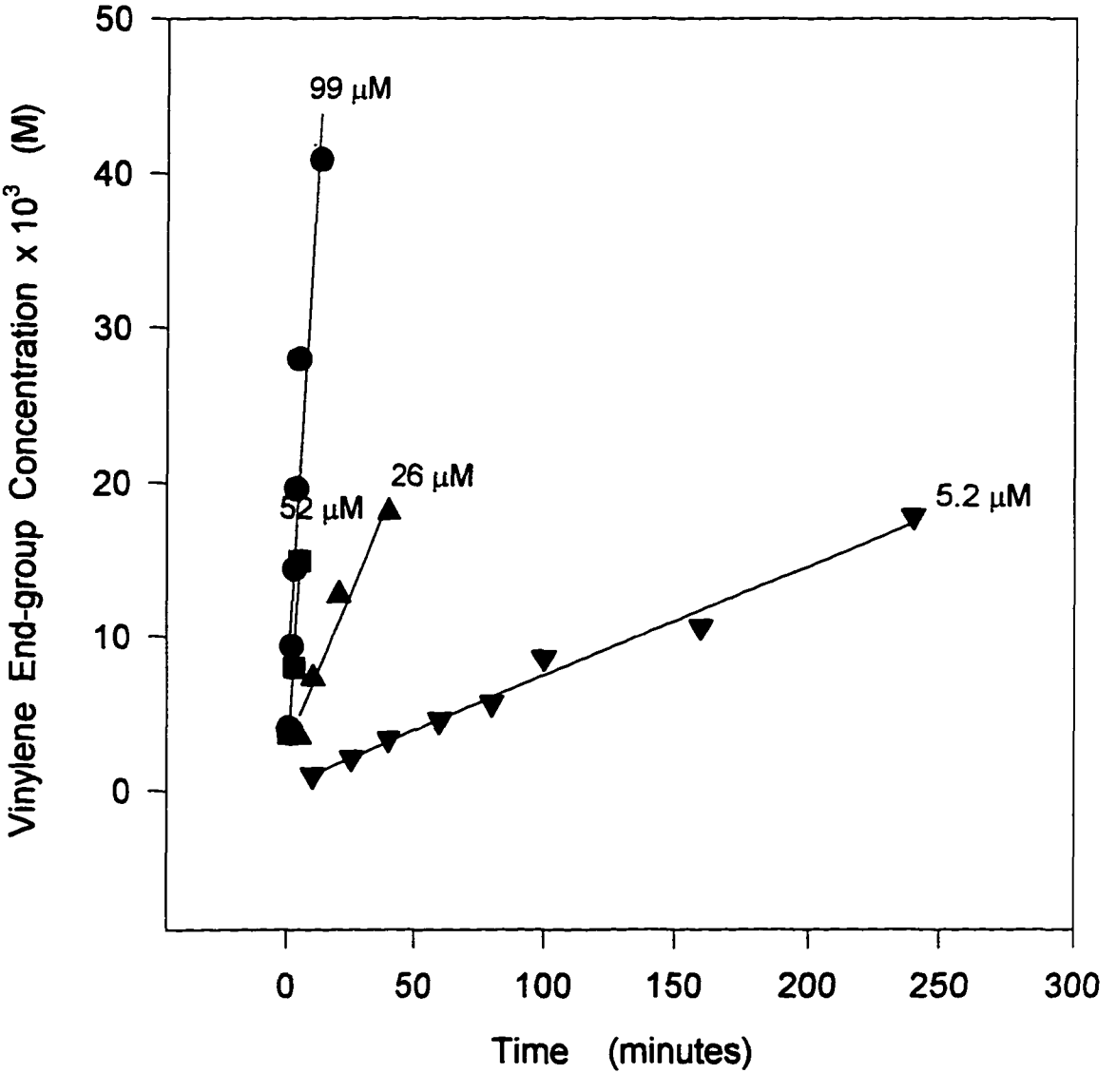

Figure A-27. Vinylene end-group concentration as a function of time at 50°C and different catalyst concentrations

Polymerization conditions: [MAO]=62 mM, [M]=8.0M and T=50°C
Catalyst concentration is labeled on each curve.

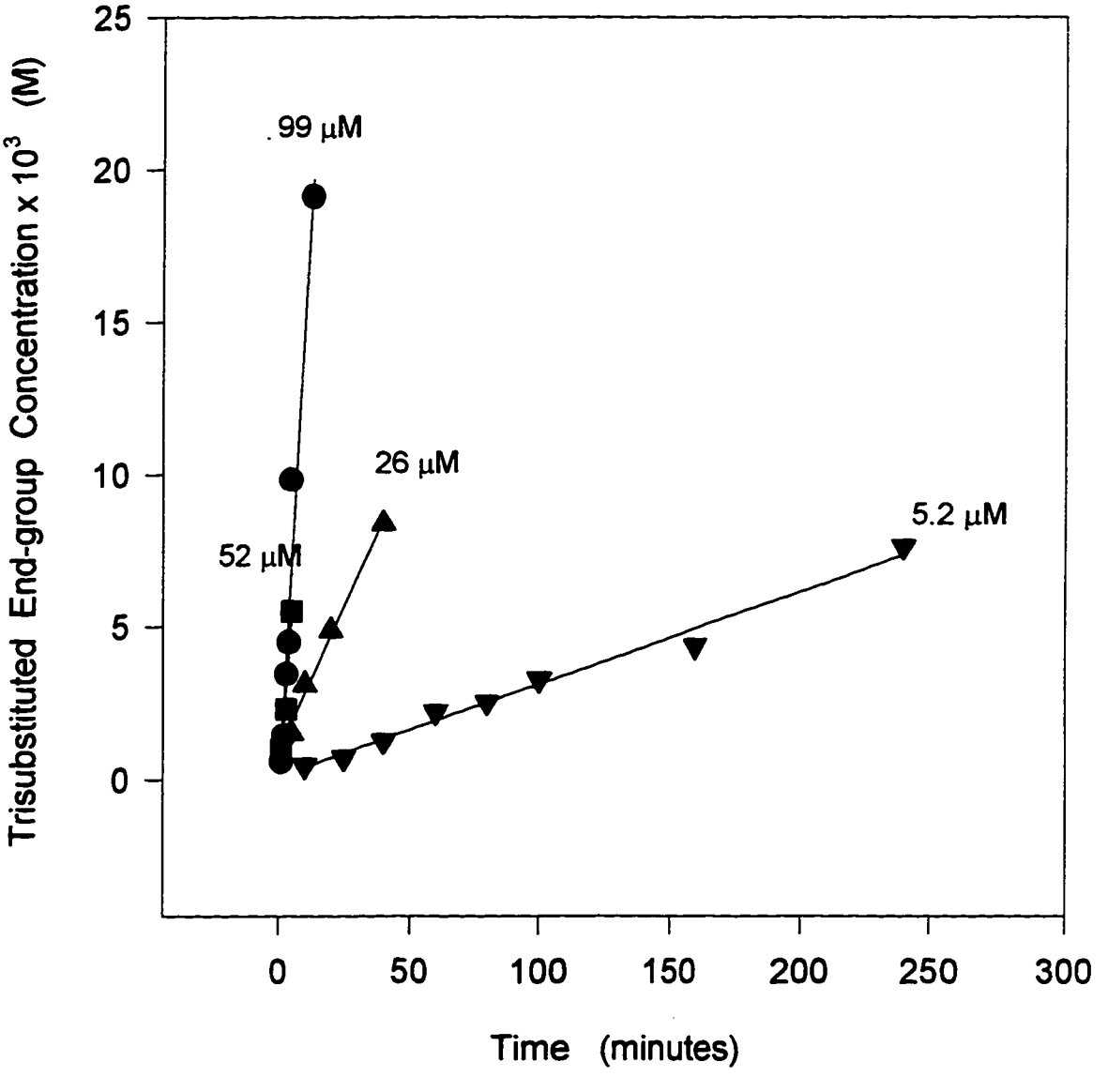

Figure A-28. Trisubstituted end-group concentration as a function of time at 50°C and different catalyst concentrations

Polymerization conditions: [MAO]=62mM, [M]=8.0M and T=50°C
Catalyst concentration is labeled on each curve.

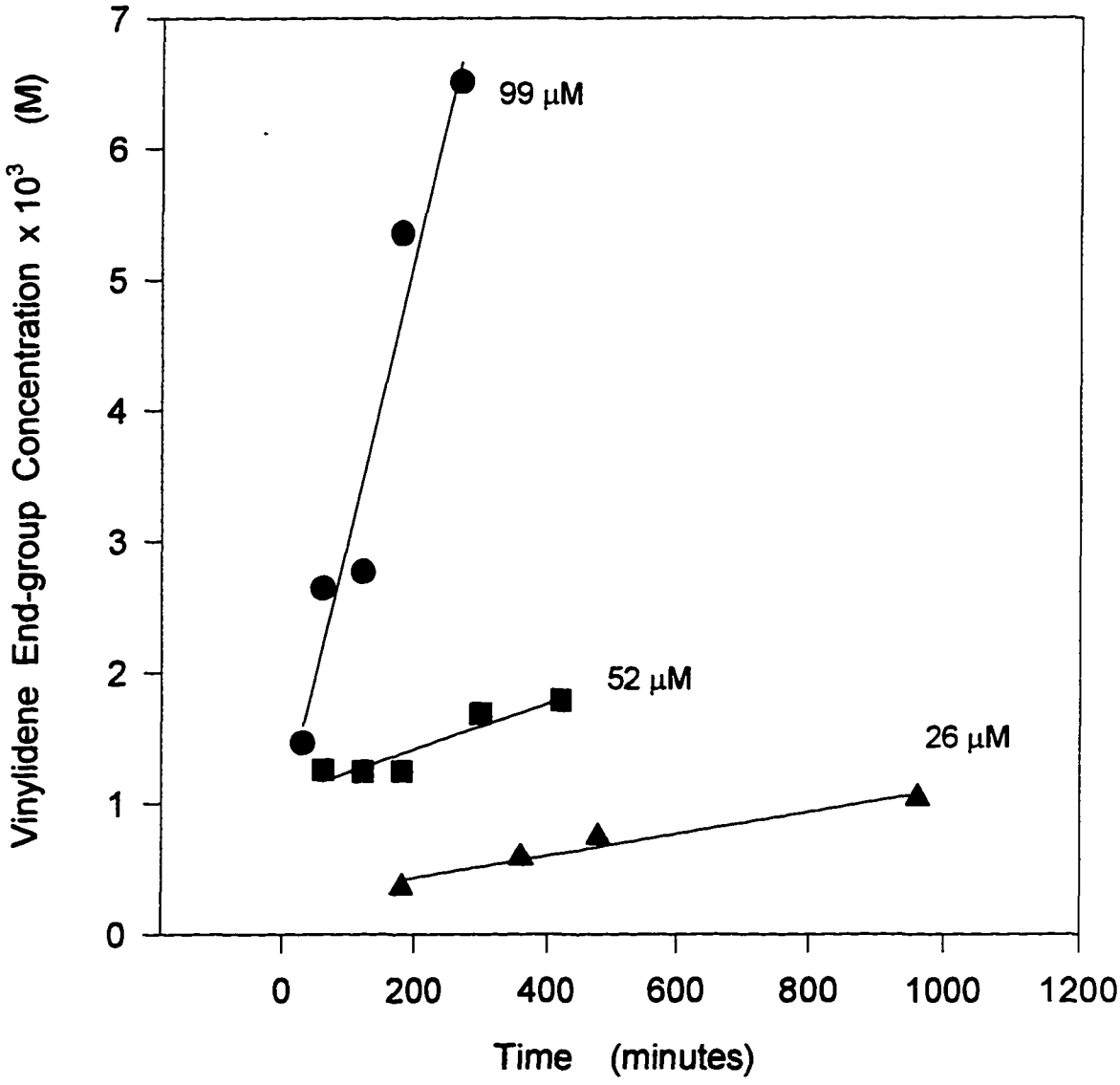

Figure A-29. Vinylidene end-group concentration as a function of time at 0°C and different catalyst concentration

Polymerization conditions: [MAO]=62 mM, [M]=8.0 M, T=0°C
Catalyst concentration is labeled on each curve.

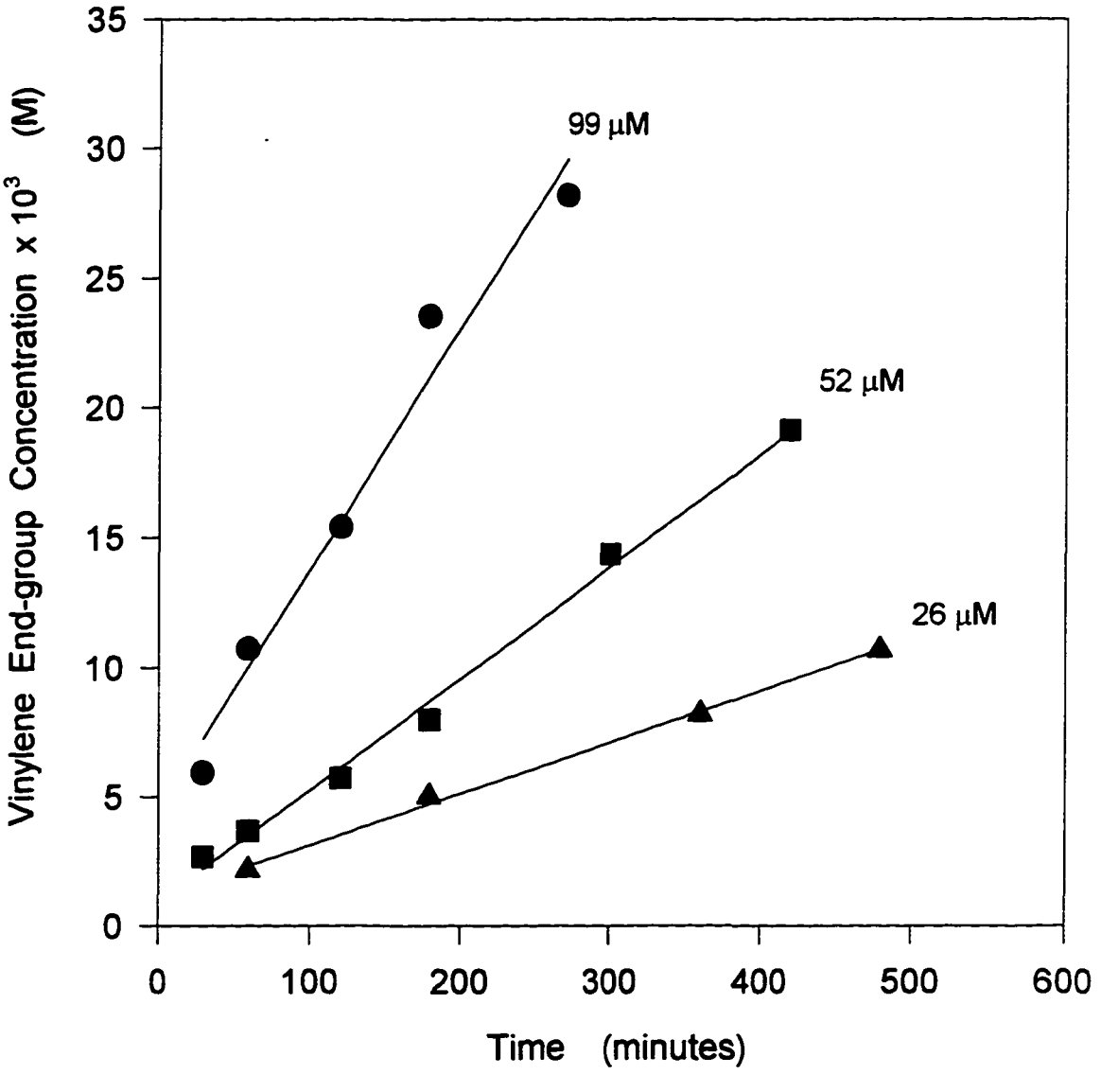

Figure A-30. Vinylene end-group concentration as a function of time at 0°C and different catalyst concentrations

Polymerization conditions: [MAO]=62mM, [M]=8.0M, T=0°C
Catalyst concentration is labeled on each curve.

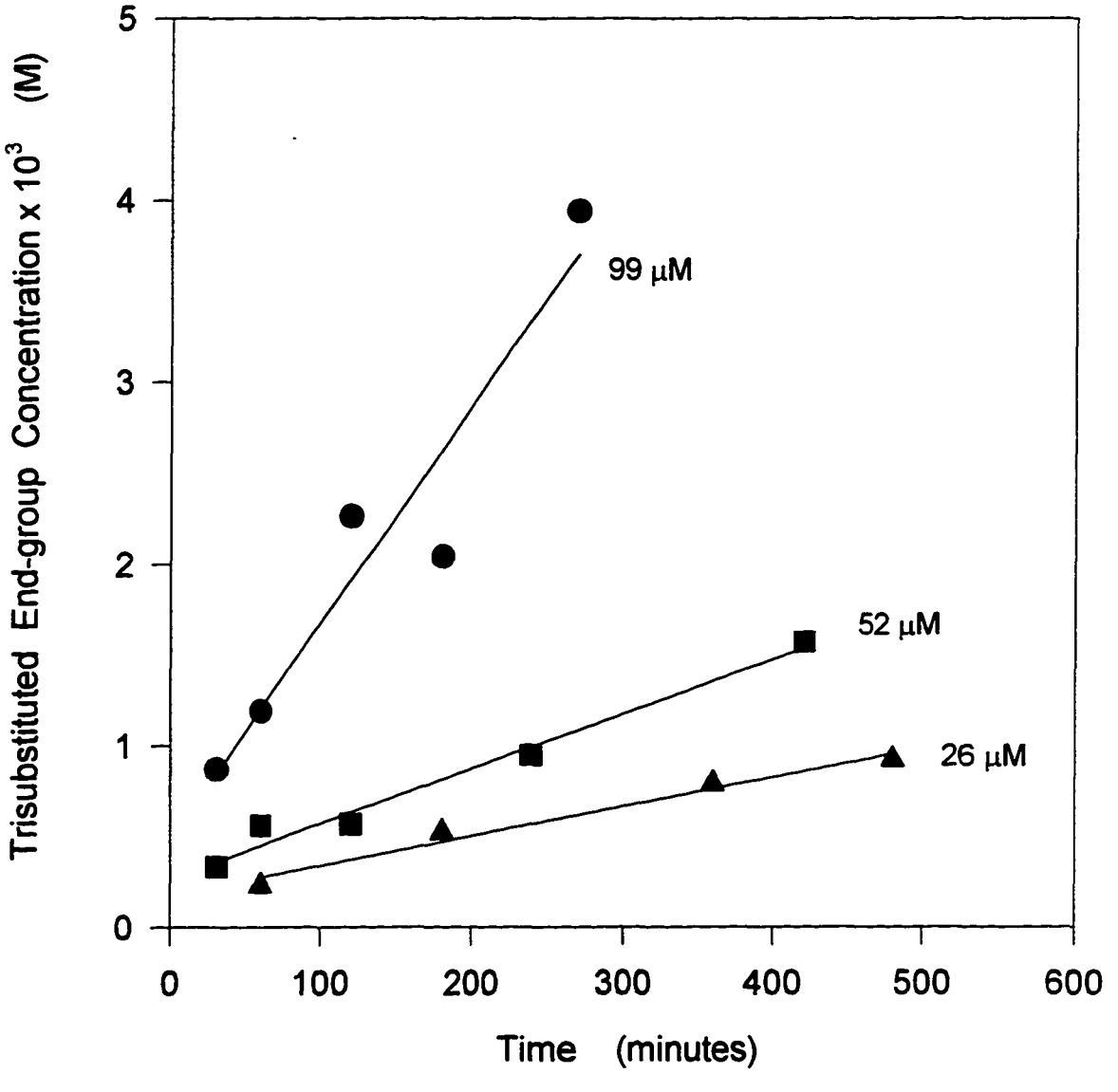

Figure A-31. Trisubstituted end-group concentration as a function of time at 0°C and different catalyst concentrations

Polymerization conditions: [MAO]=62mM, [M]=8.0M and T=0°C
Catalyst concentration is labeled on each curve.

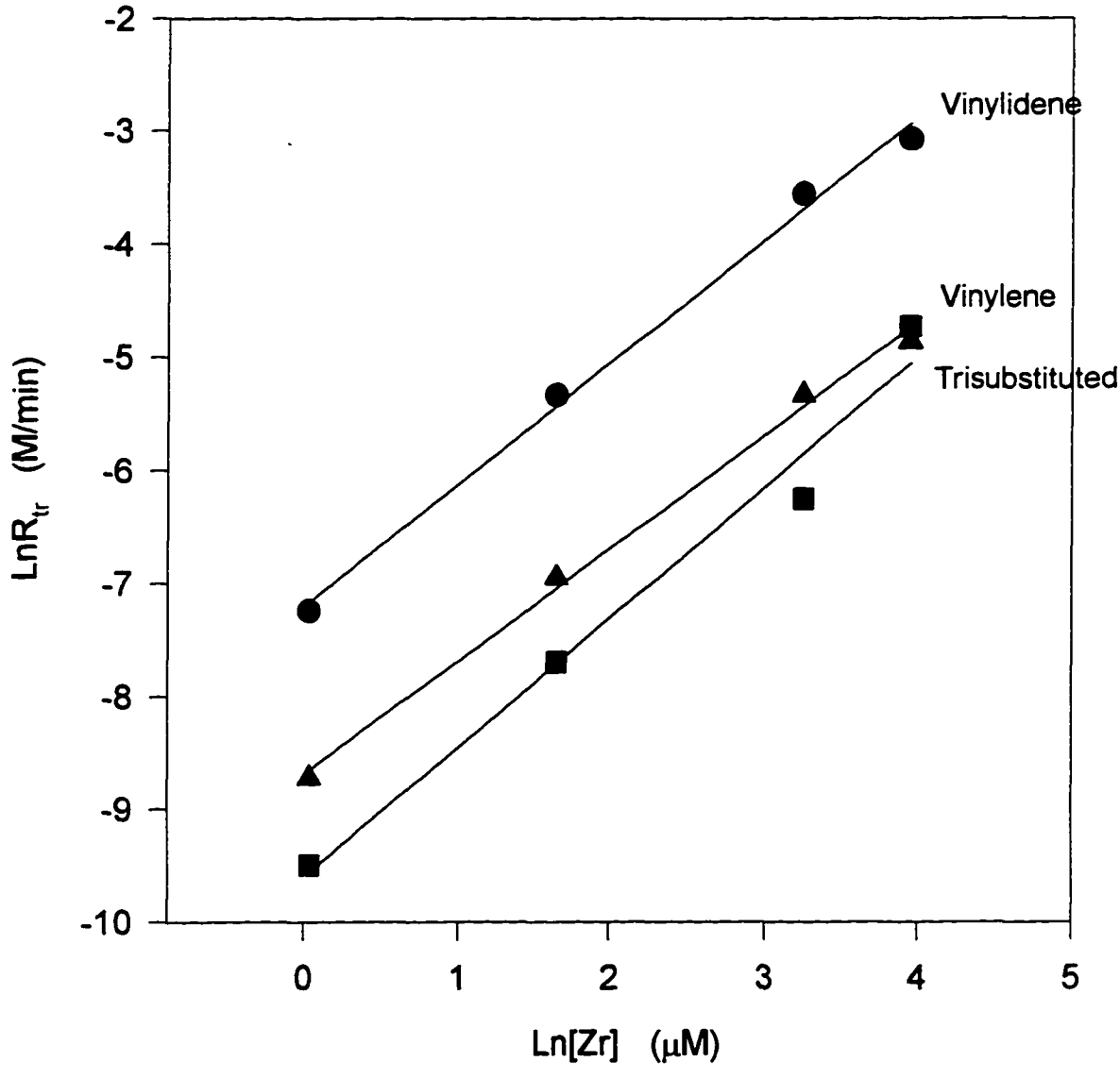

Figure A-32. LnR_{tr} as functions of Ln[Zr] at 100°C

Polymerization conditions: [M]=8.0M, [MAO]=62mM and T=100°C

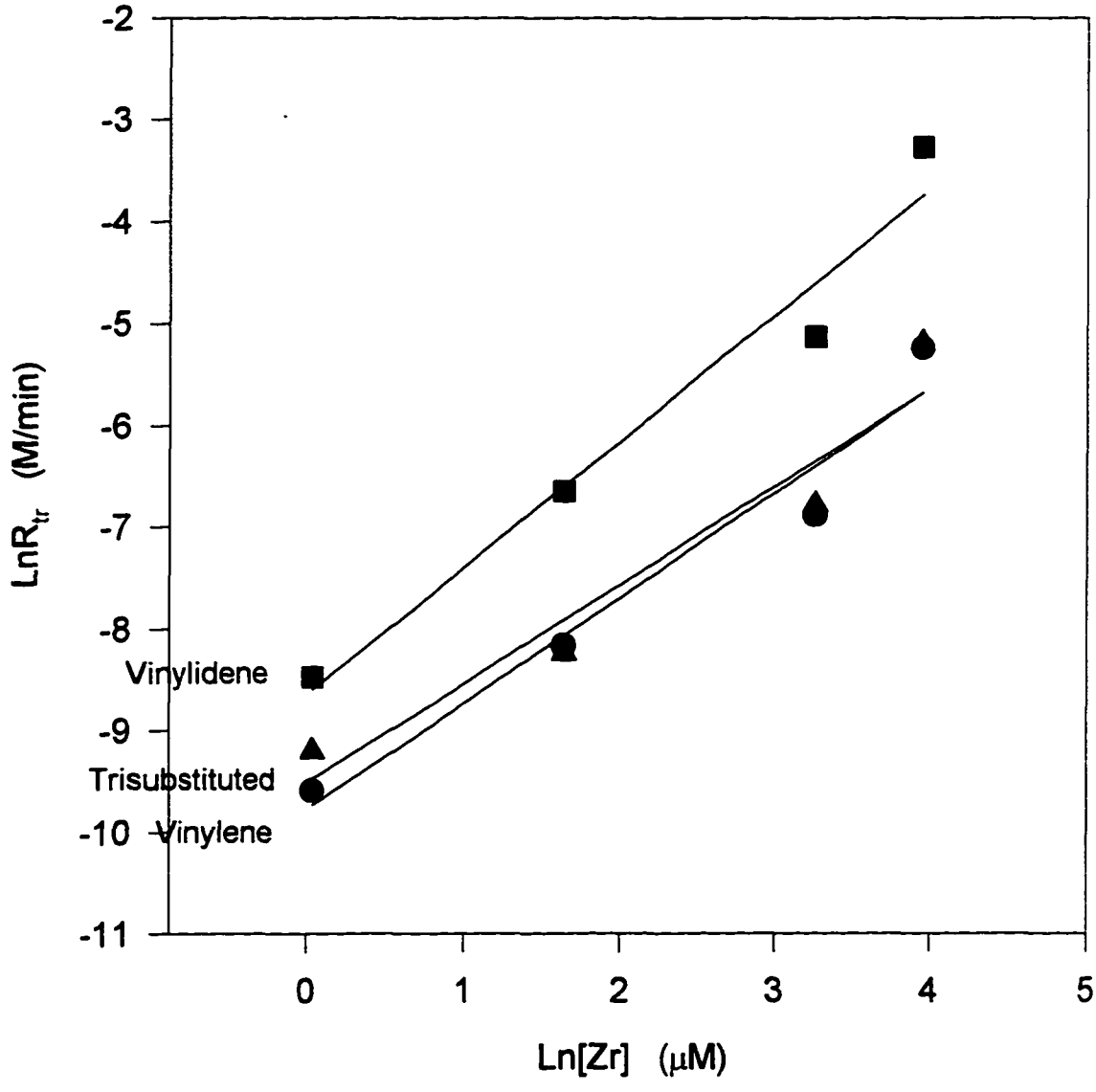

Figure A-33. LnR_{tr} as functions of Ln [Zr] at 80°C

Polymerization conditions: [M]=8.0M, [MAO]=62mM and T=80°C

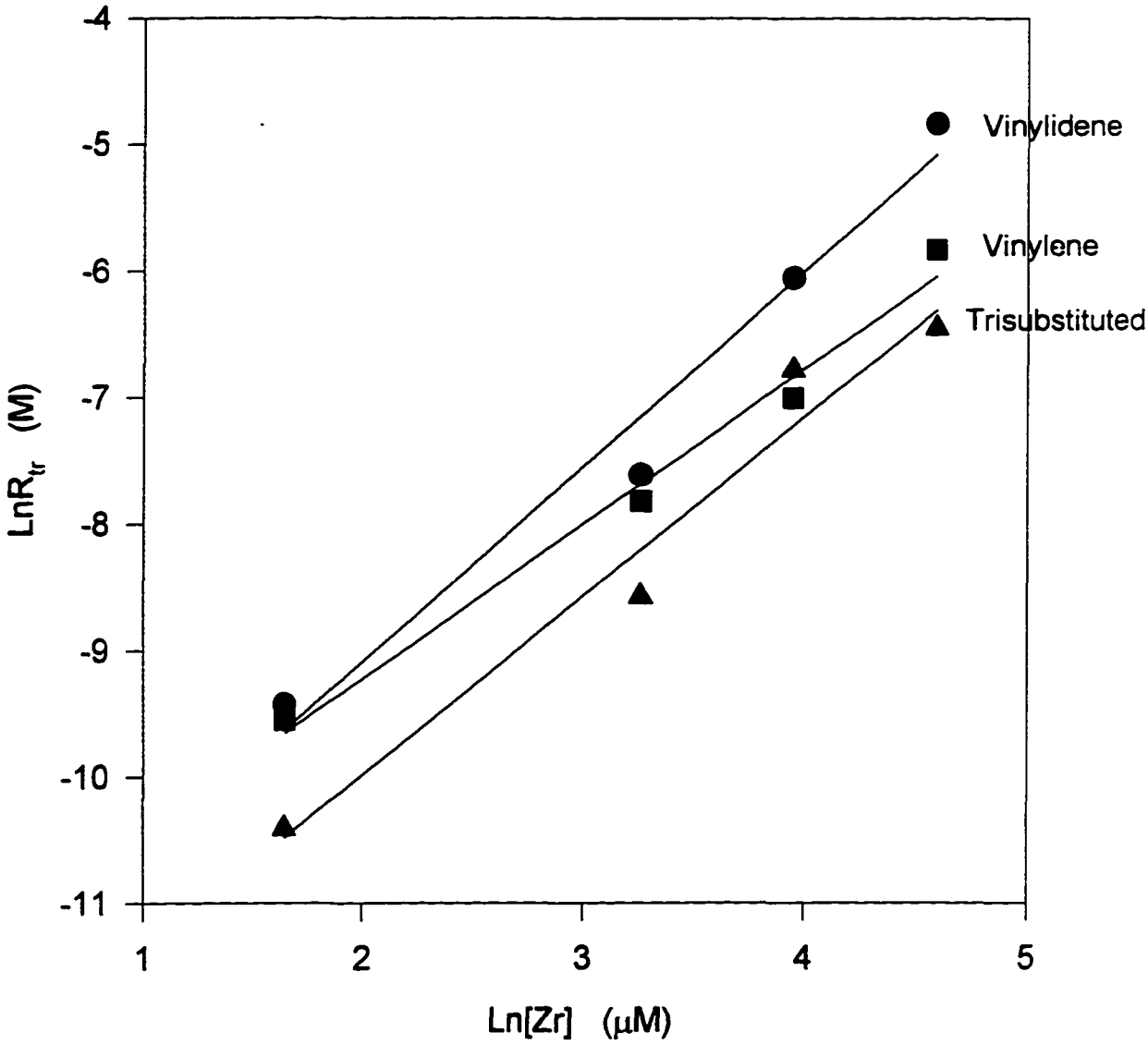

Figure A-34. LnR_{tr} as functions of Ln[Zr] at 50°C

Polymerization conditions: [MAO]=62mM, [M]=8.0M and T=50°C

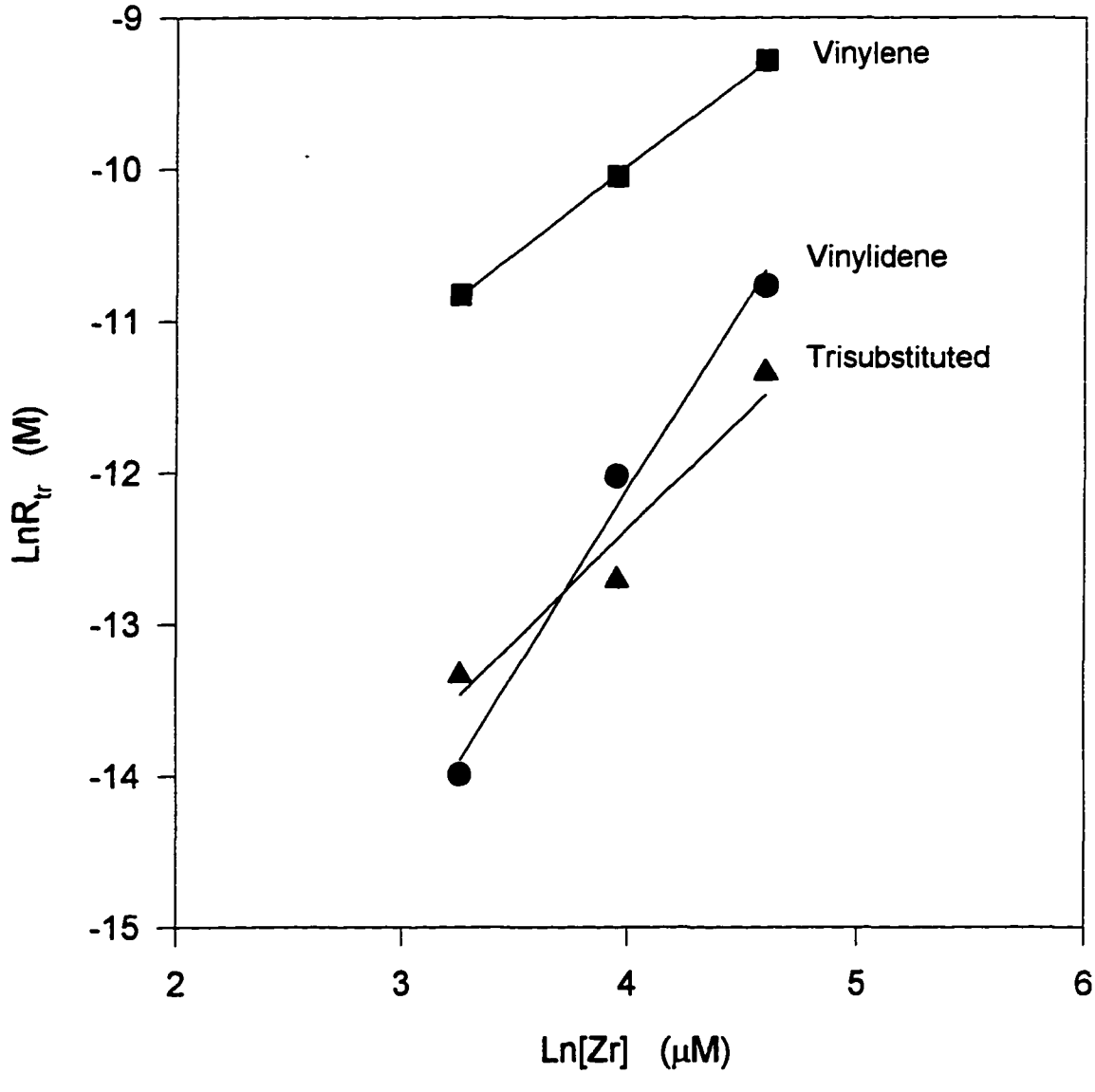

Figure A-35. LnR_{tr} as functions of Ln[Zr] at 0°C

Polymerization conditions: [MAO]=62mM, [M]=8.0M and T=0°C

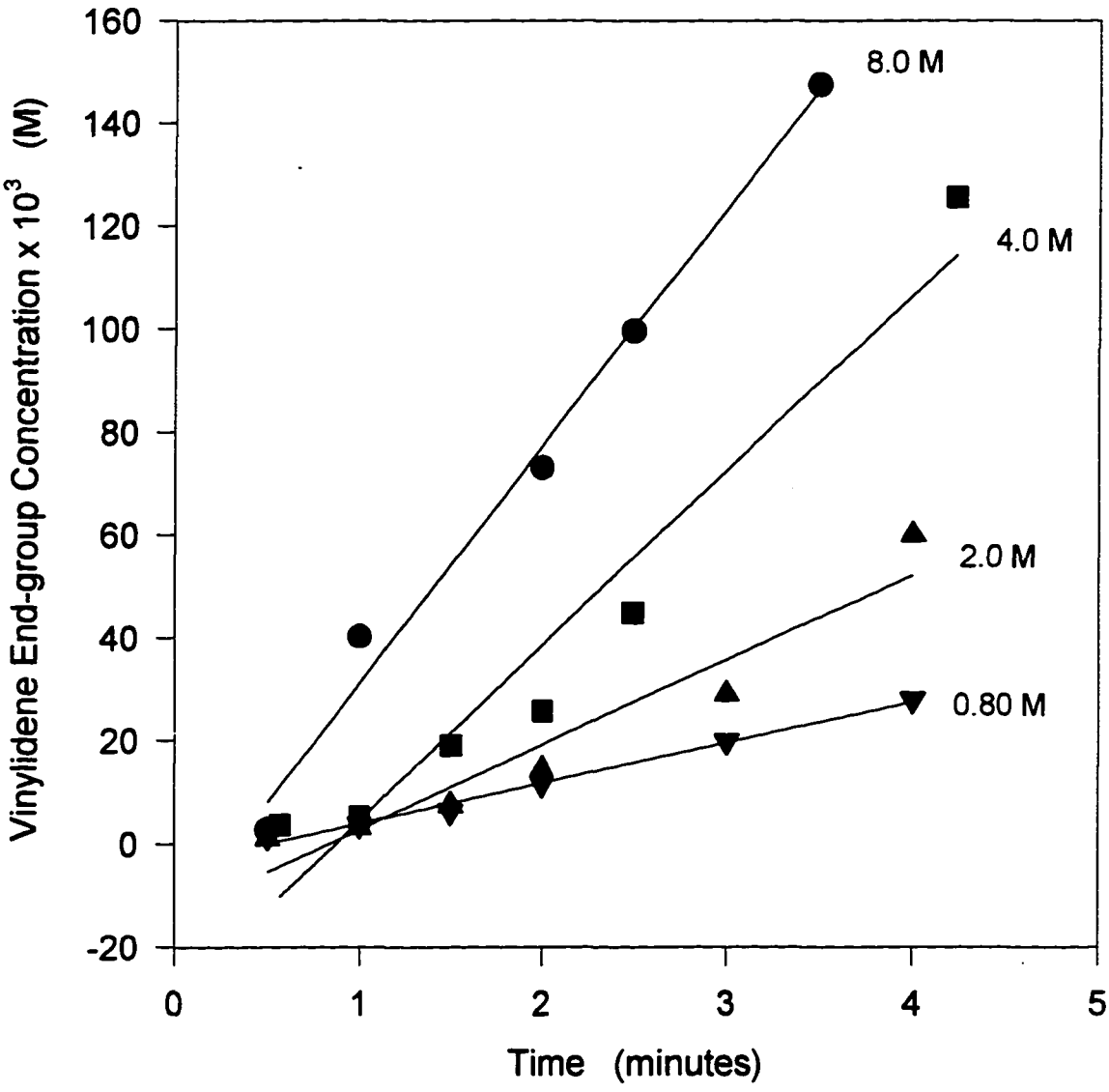

Figure A-36. Vinylidene end-group concentration as a function of time at 100°C and different monomer concentrations

Polymerization conditions: [Zr]=52μM, [MAO]=62mM and T=100°C
Monomer concentration is labeled on each curve.

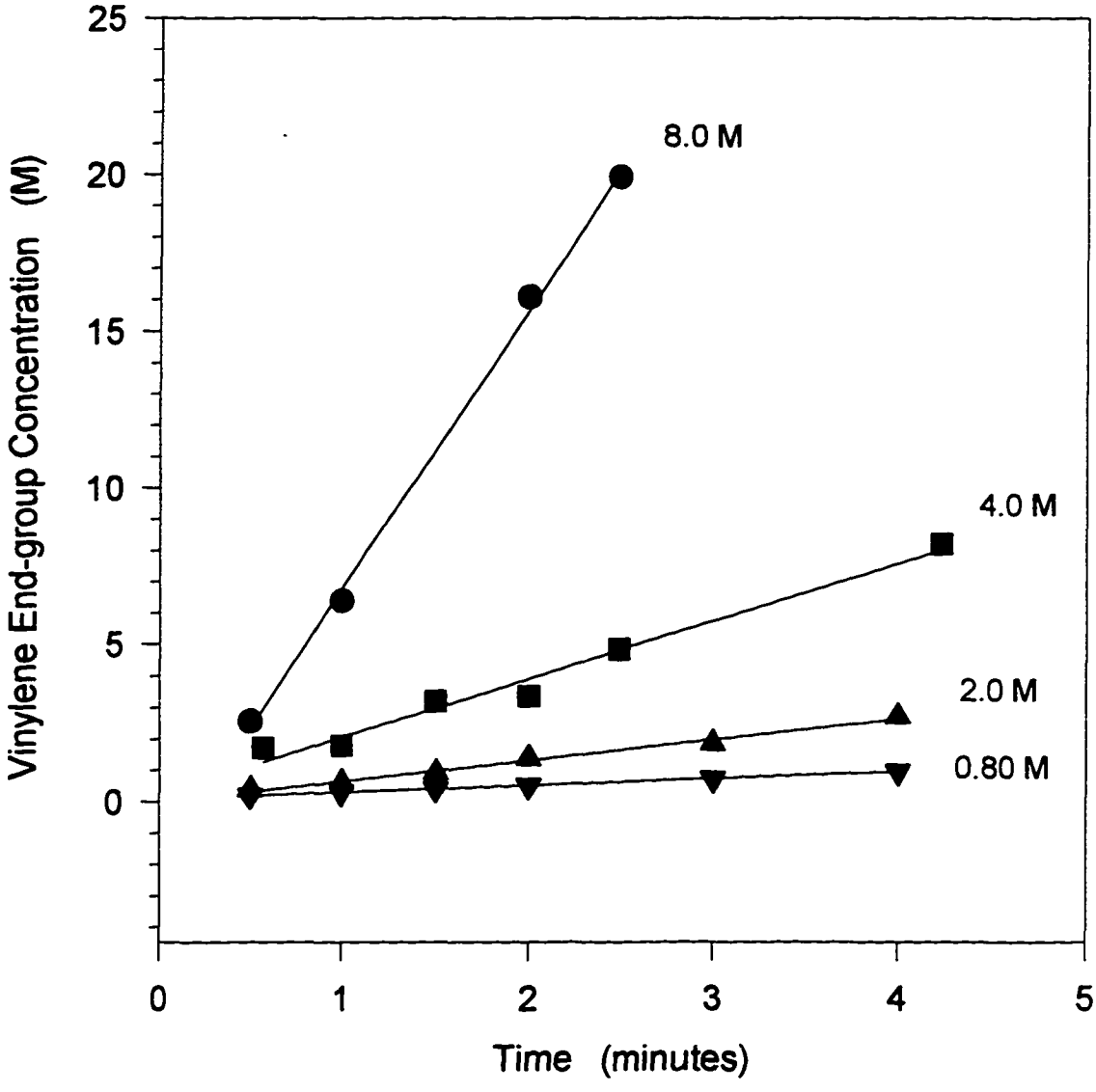

Figure A-37. Vinylene end-group concentration as a function of time at 100°C and different monomer concentrations

Polymerization conditions: [Zr]=52μM, [MAO]=62mM and T=100°C
Monomer concentration is labeled on each curve.

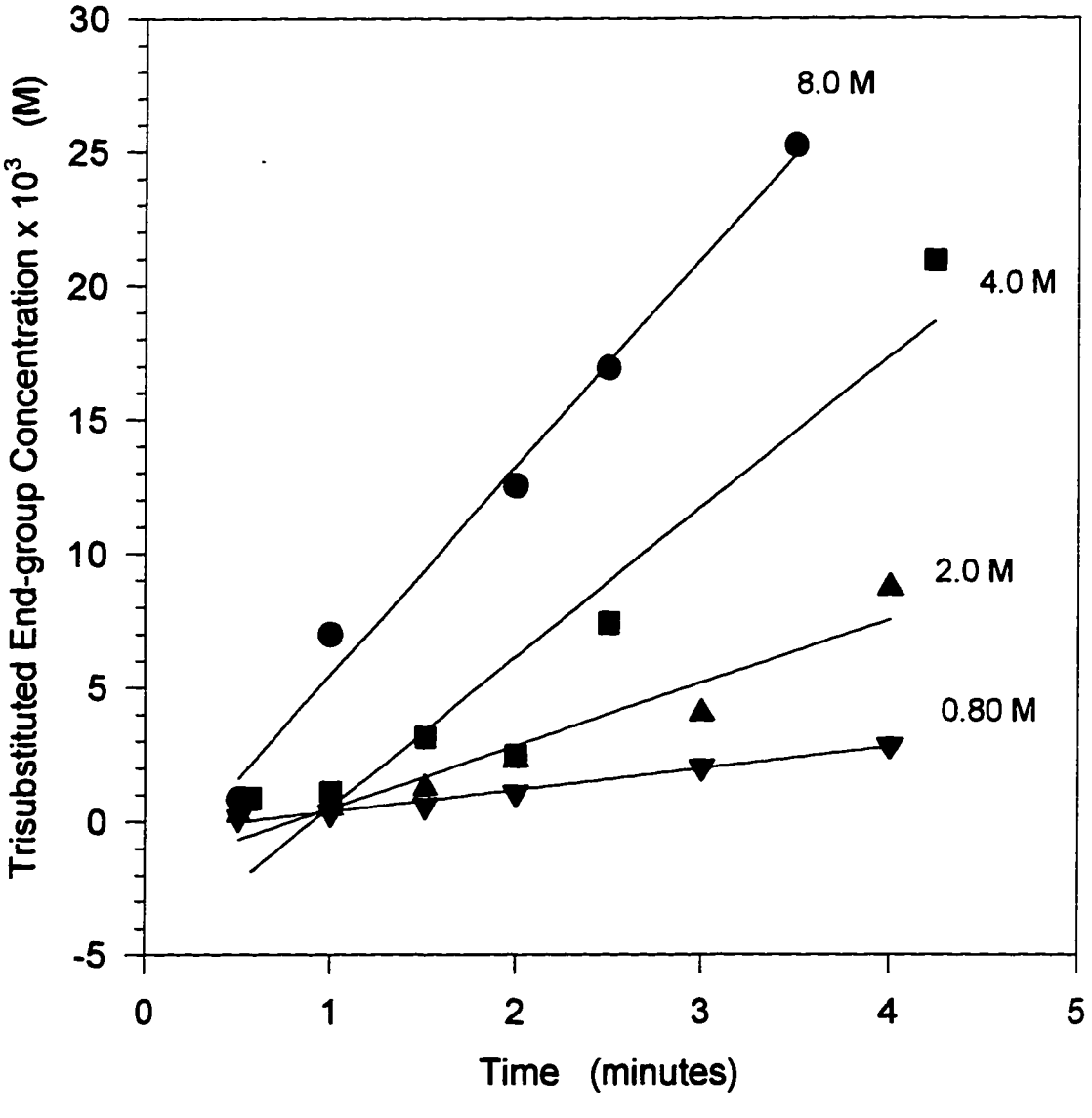

Figure A-38. Trisubstituted end-group concentration as a function of time at 100°C and different monomer concentrations

Polymerization conditions: [Zr]=52μM, [MAO]=62mM and T=100°C
Monomer concentration is labeled on each curve.

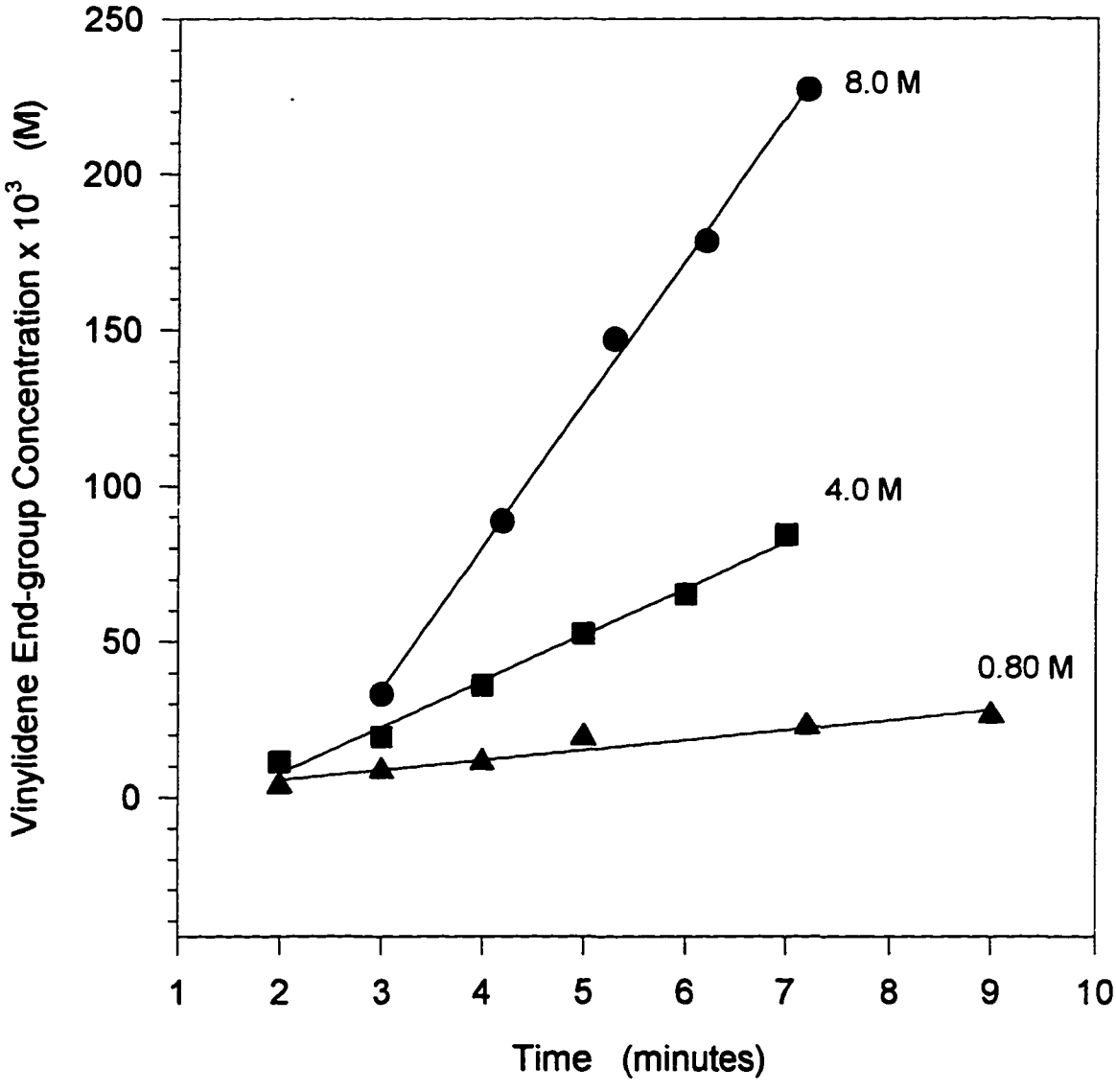

Figure A-39. Vinylidene end-group concentration as a function of time at 80°C and different monomer concentrations

Polymerization conditions: [Zr]=52μM, [MAO]=62mM and T=80°C
Monomer concentration is labeled on each curve.

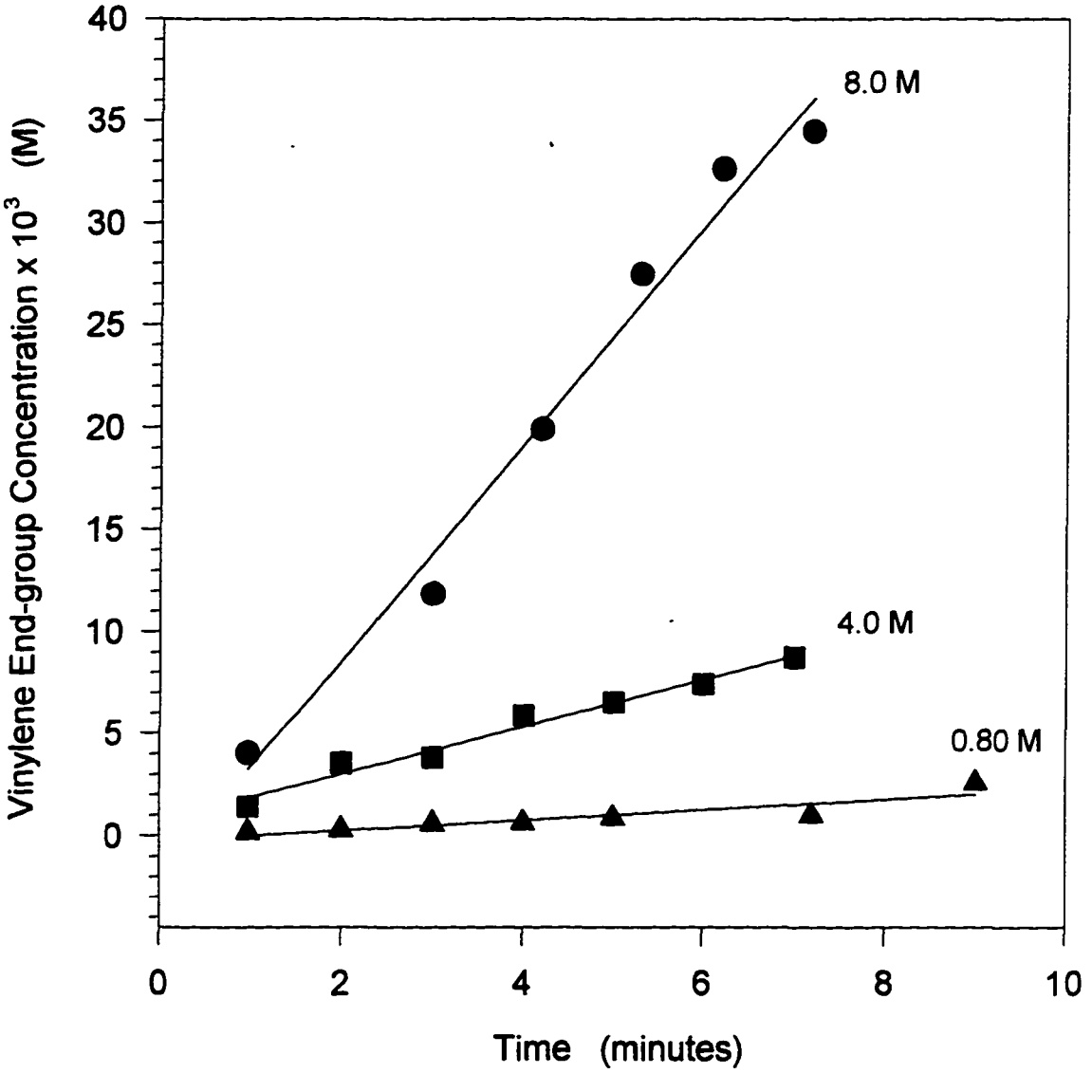

Figure A-40. Vinylene end-group concentration as a function of time at 80°C and different monomer concentrations

Polymerization conditions: [Zr]=52μM, [MAO]=62mM and T=80°C
Monomer concentration is labelled on each curve.

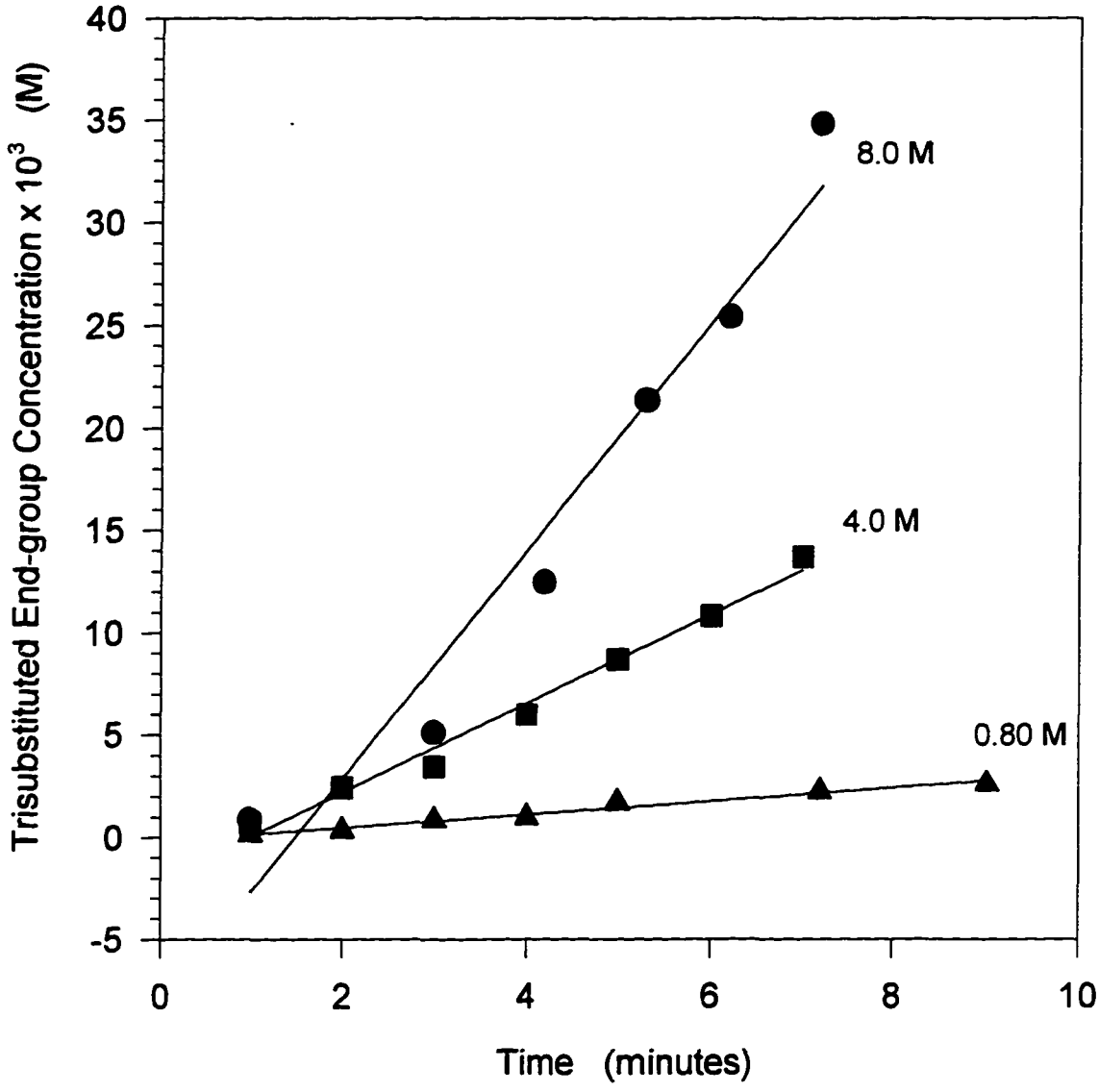

Figure A-41. Trisubstituted end-group concentration as a function of time at 80°C and different monomer concentrations

Polymerization conditions: [Zr]=52μM, [MAO]=62mM and T=80°C
Monomer concentration is labeled on each curve.

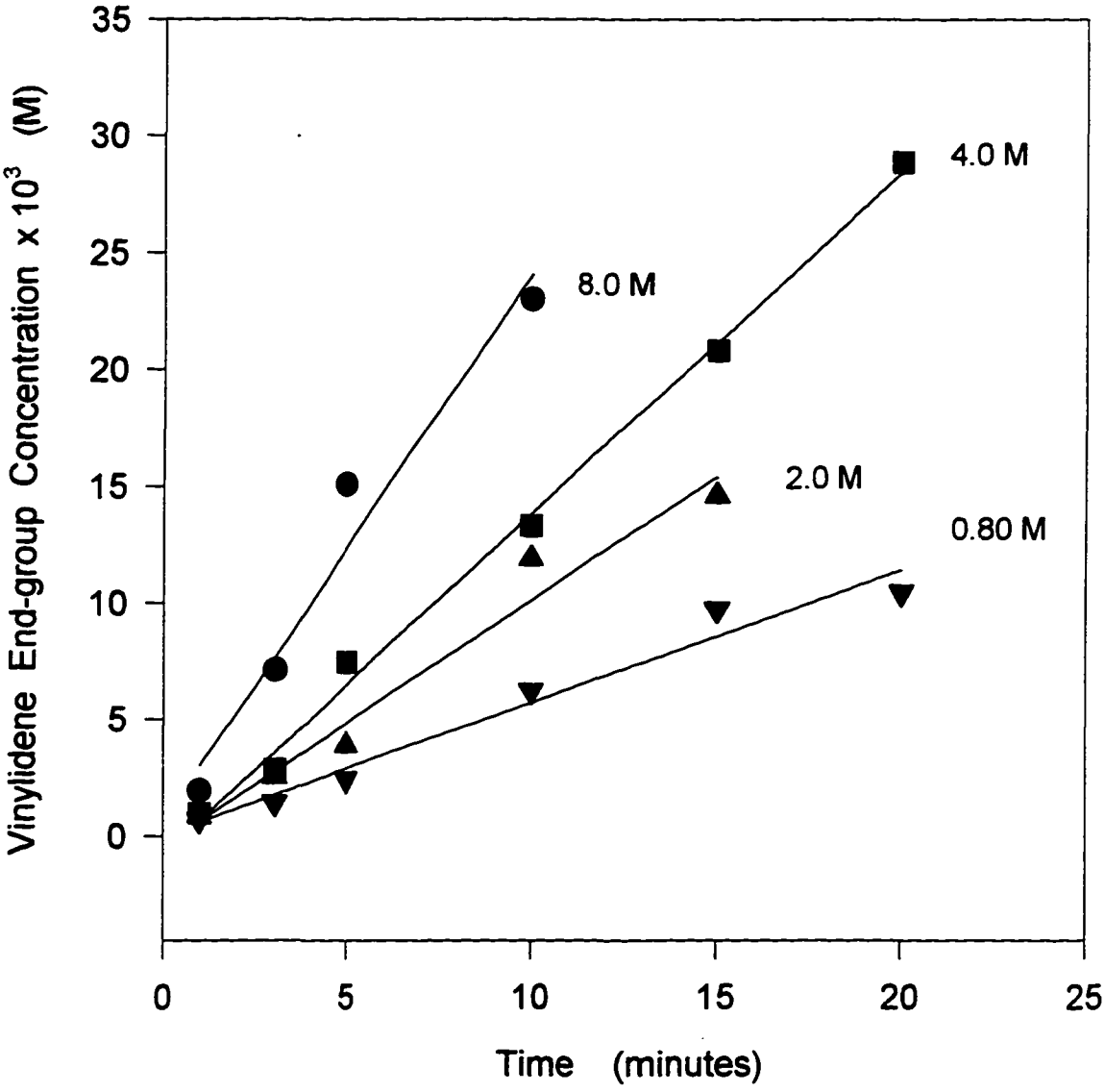

Figure A-42. Vinylidene end-group concentration as a function of time at 50°C and different monomer concentrations

Polymerization conditions: [Zr]=52μM, [MAO]=62mM and T=50°C
Monomer concentration is labeled on each curve.

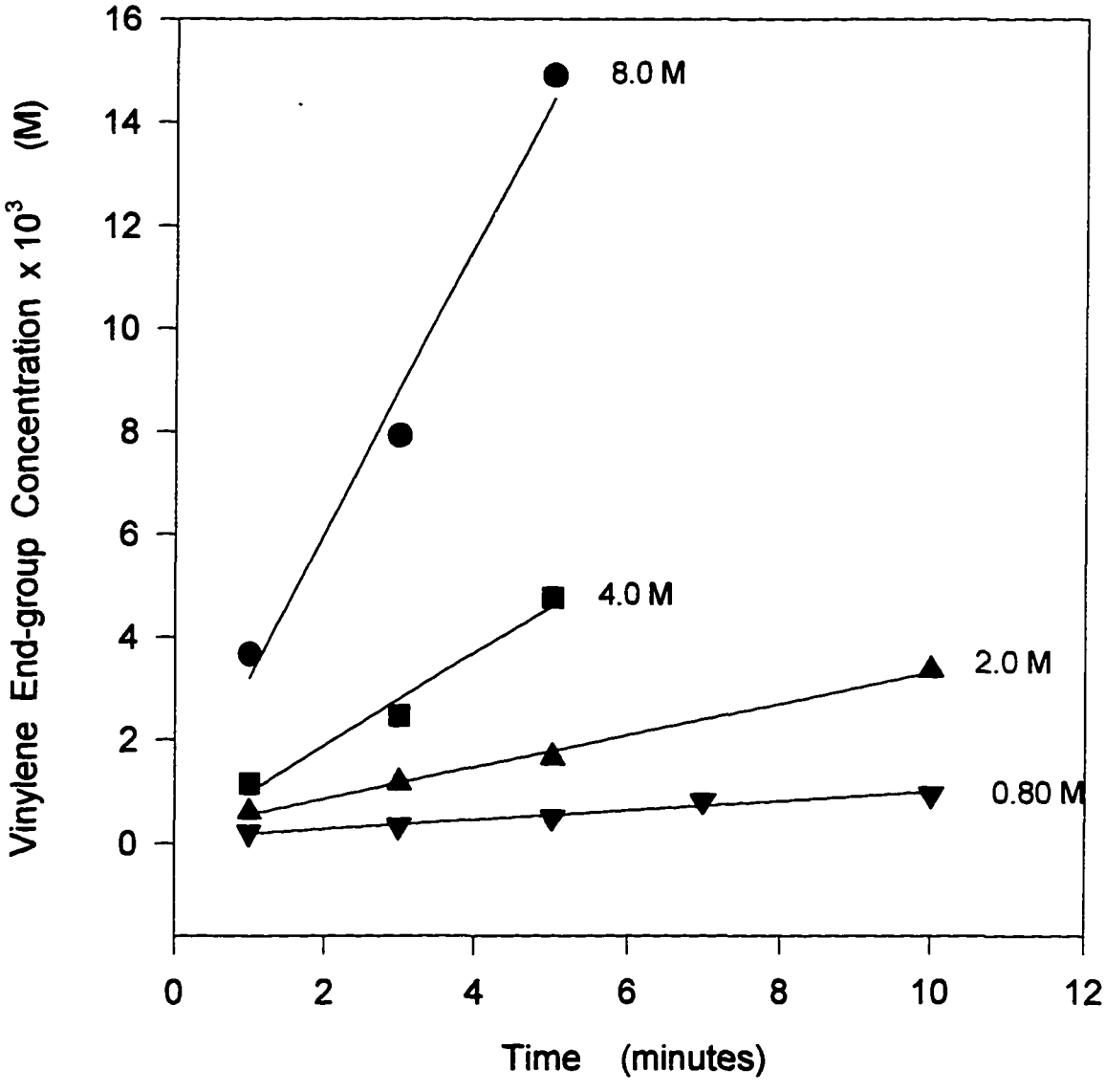

Figure A-43. Vinylene end-group concentration as a function of time at 50°C and different monomer concentrations

Ploymerization conditions: [Zr]=52μM, [MAO]=62mM, T=50°C
Monomer concentration is labeled on each curve.

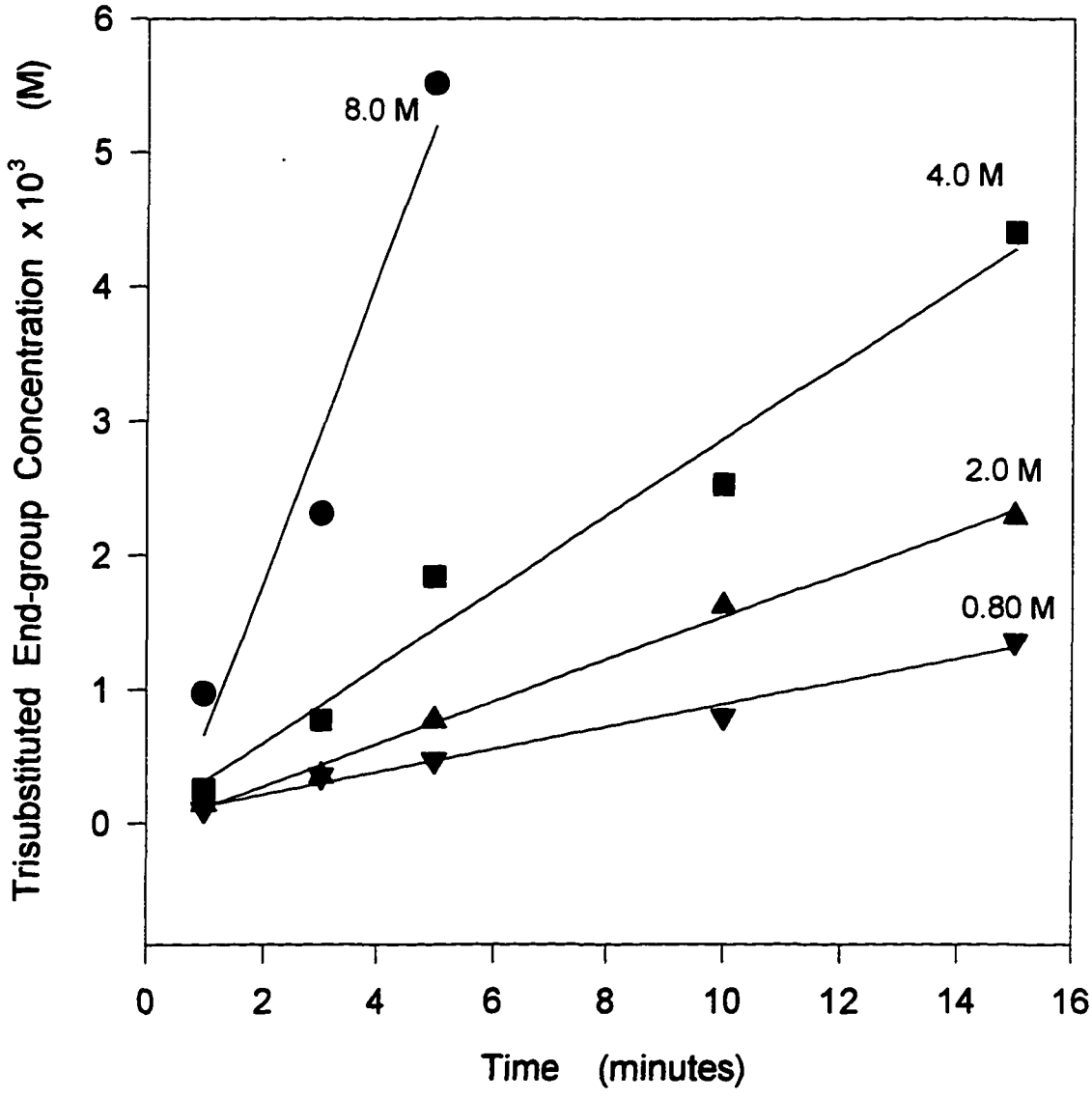

Figure A-44. Trisubstituted end-group conentration as a function of time at 50°C and different monomer concentrations

Polymerization conditions: [Zr]=52μM, [MAO]=62mM and T=50°C
Monomer concentration is labeled on each curve.

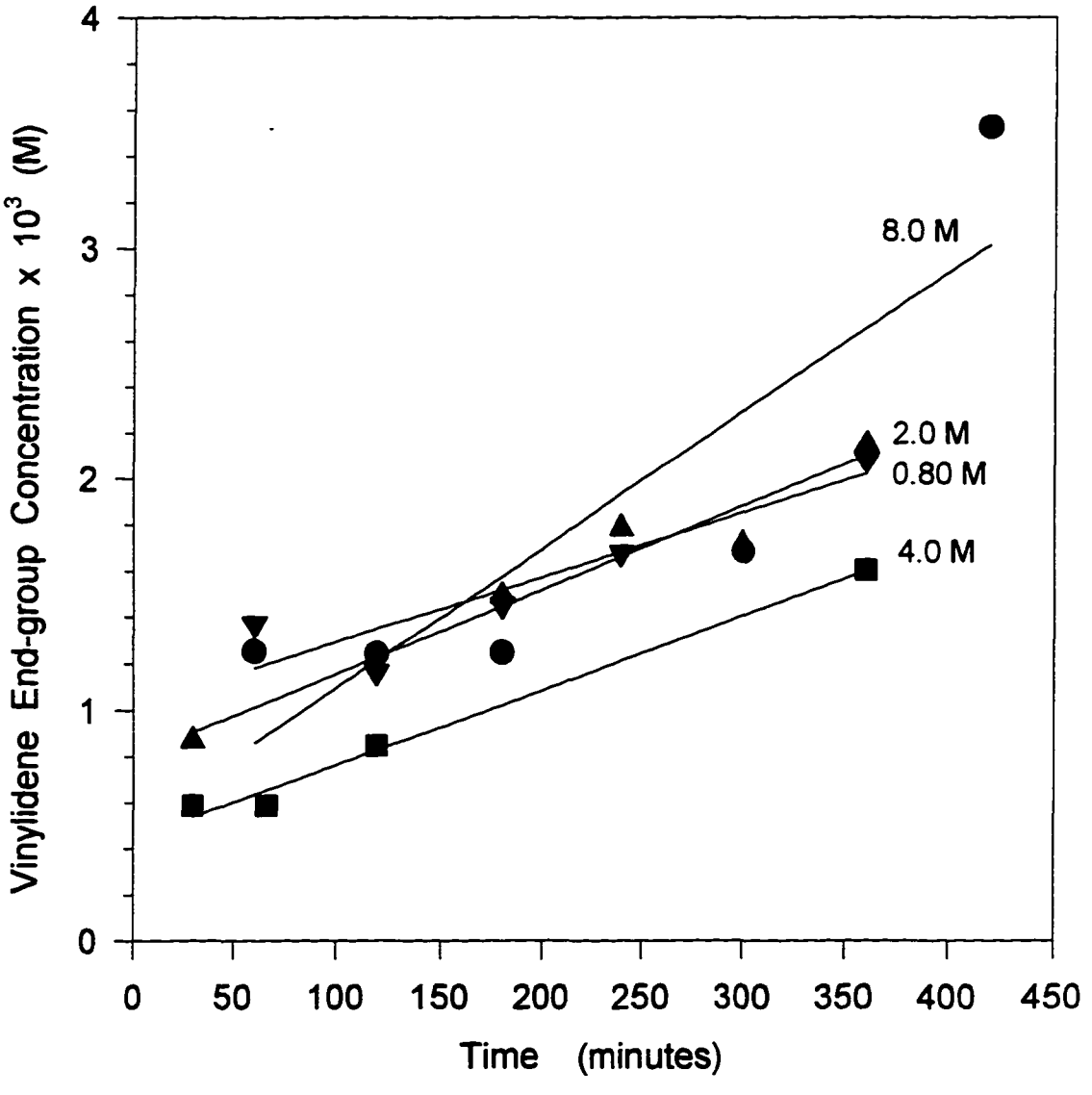

Figure A-45. Vinylidene end-group concentration as a function of time at 0°C and different monomer concentrations

Polymerization conditions: [Zr]=52μM, [MAO]=62mM and T=0°C
Monomer concentration is labeled on each curve.

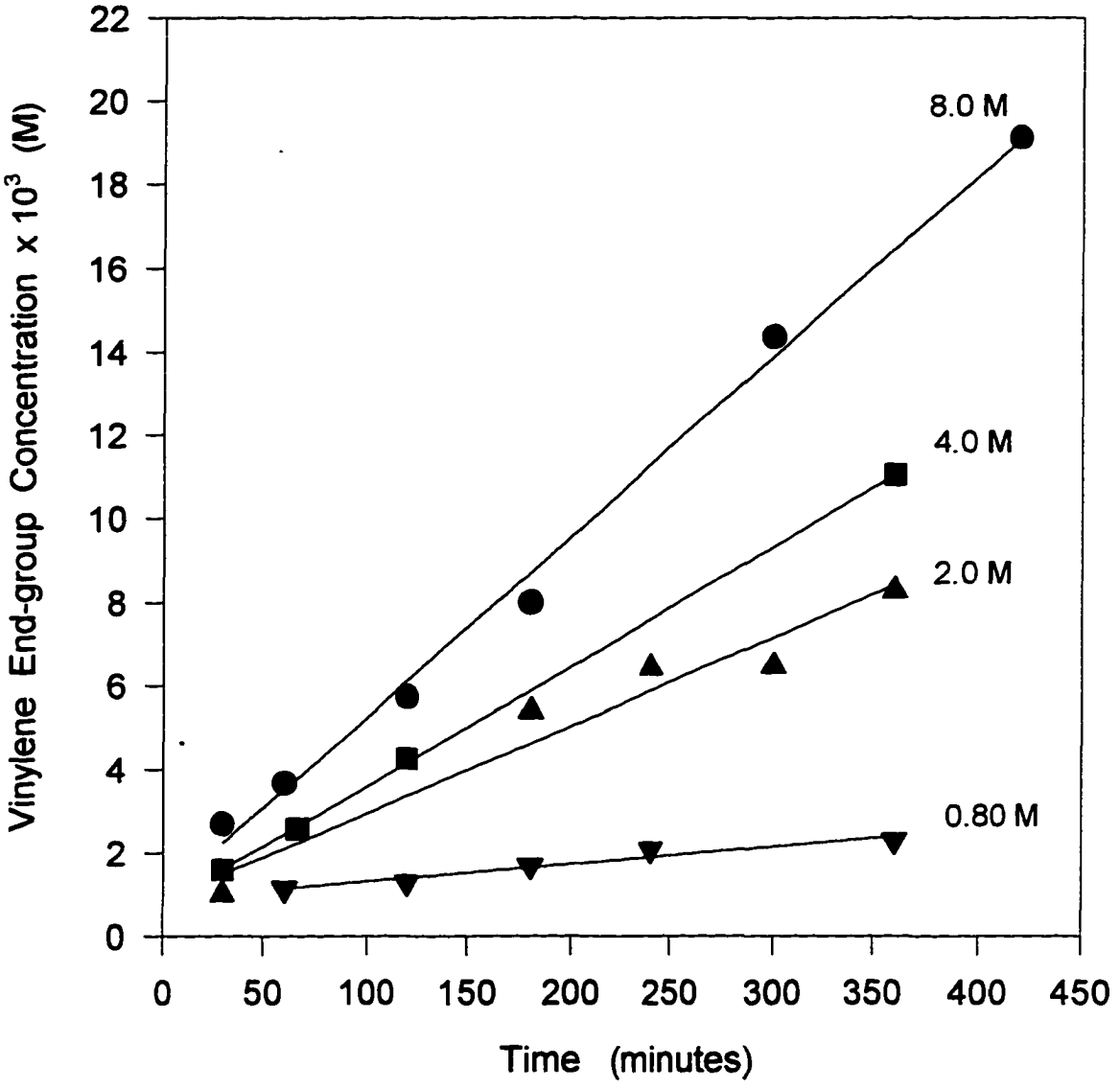

Figure A-46. Vinylene end-group concentration as a function time at 0°C and different monomer concentrations

Polymerization conditions: [Zr]=52μM, [MAO]=62mM and T=0°C
Monomer concentration is labeled on each curve.

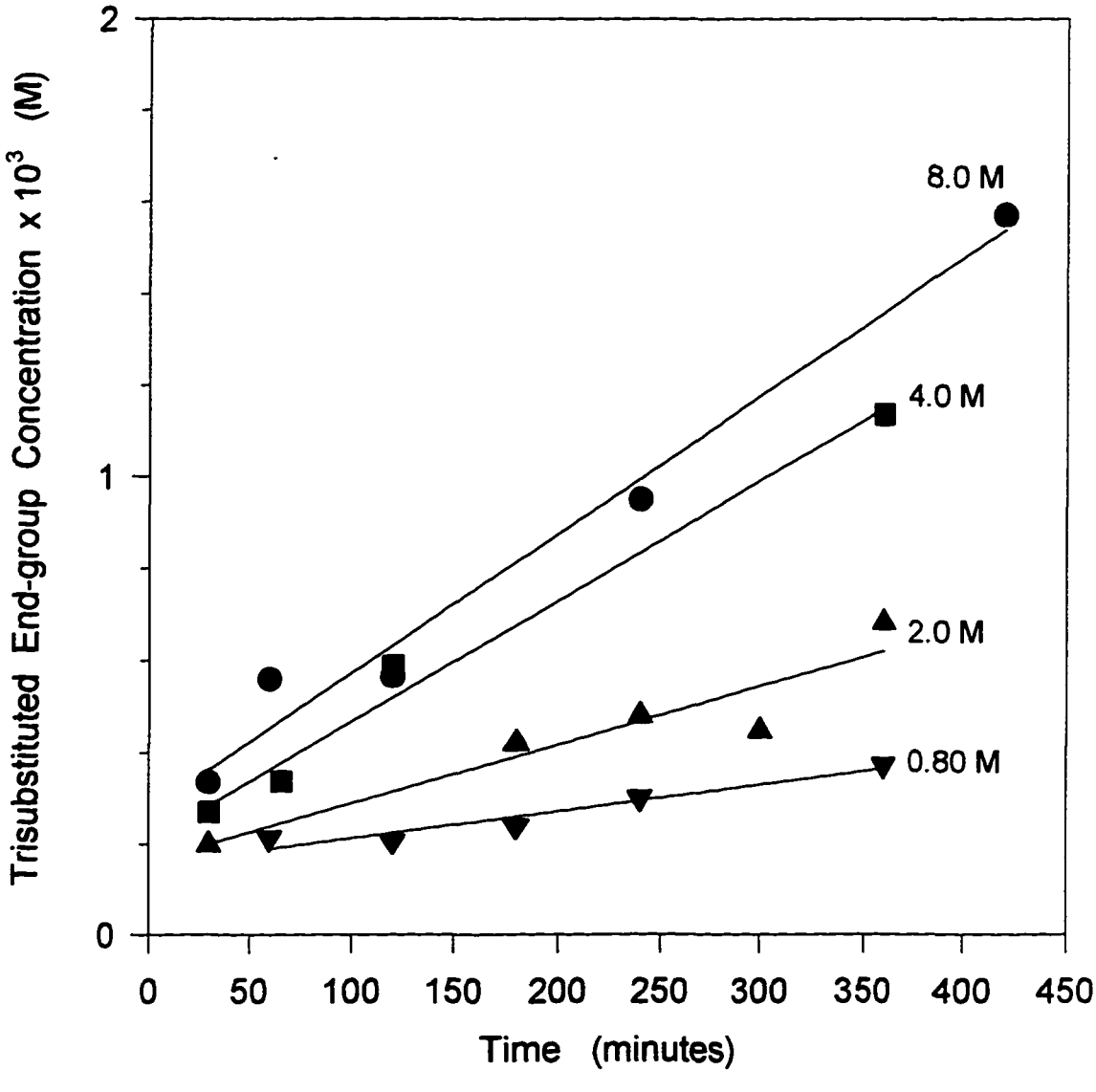

Figure A-47. Trisubstituted end-group concentration as a function of time at 0°C and different monomer concentrations

Polymerization conditions: [Zr]=52μM, [MAO]=62mM and T=0°C
Monomer concentration is labeled on each curve.

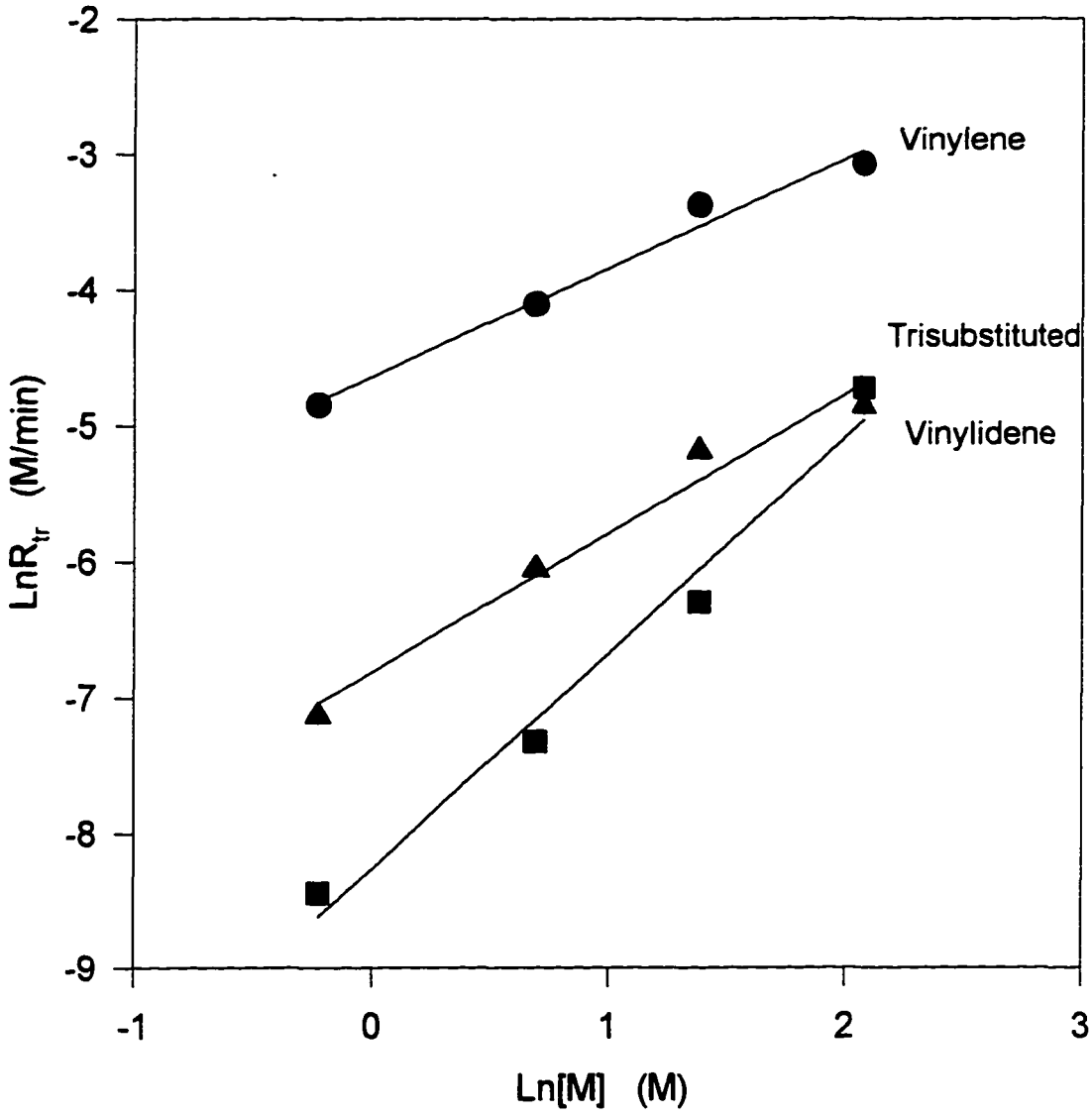

Figure A-48. LnR_{tr} as functions of Ln[M] at 100°C

Polymerization conditions: [Zr]=52μM, [MAO]=62mM and T=100°C

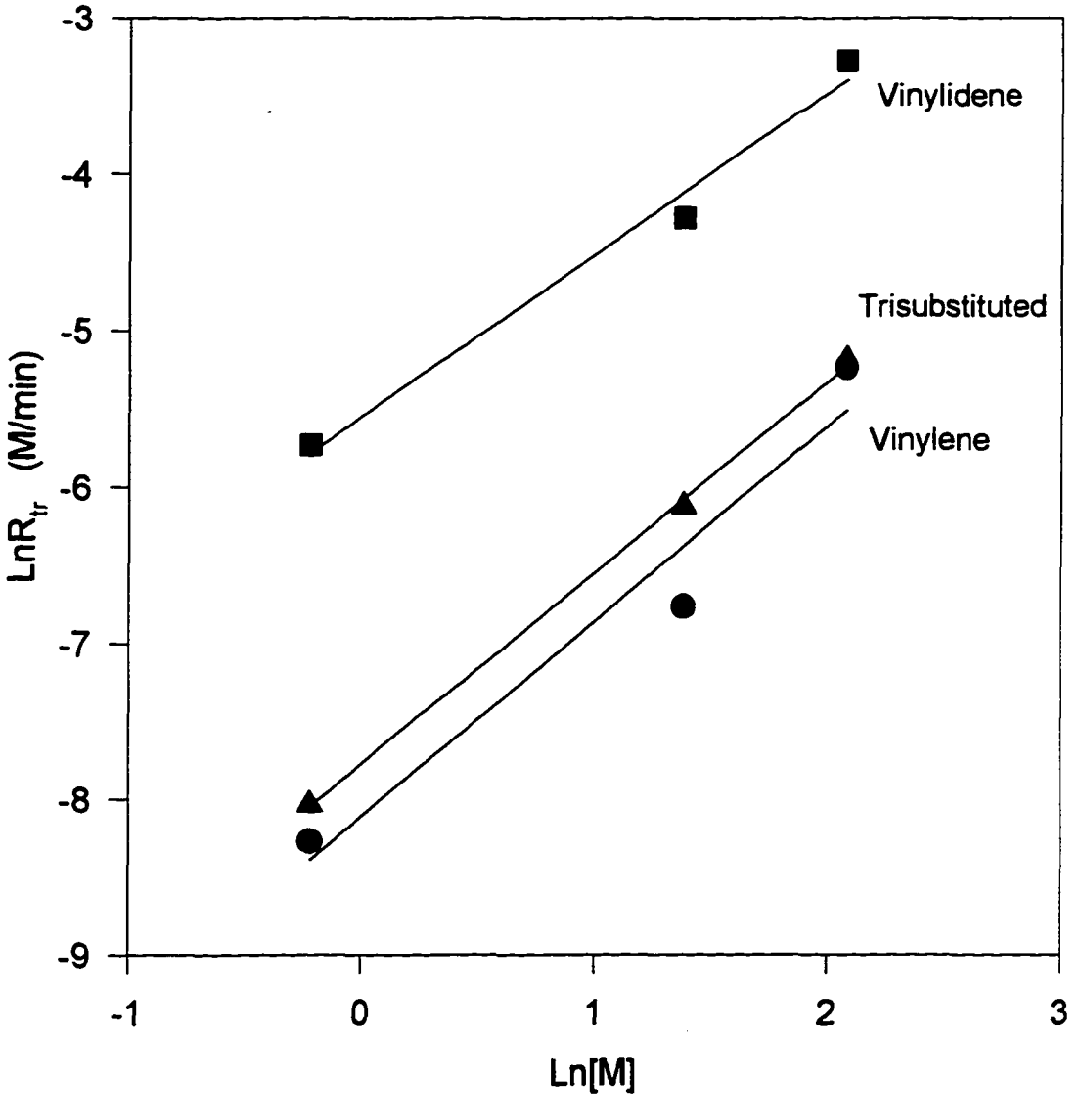

Figure A-49. LnR_{tr} as functions of Ln[M]

Polymerization conditions: [Zr]=52μM, [MAO]=62mM and T=80°C

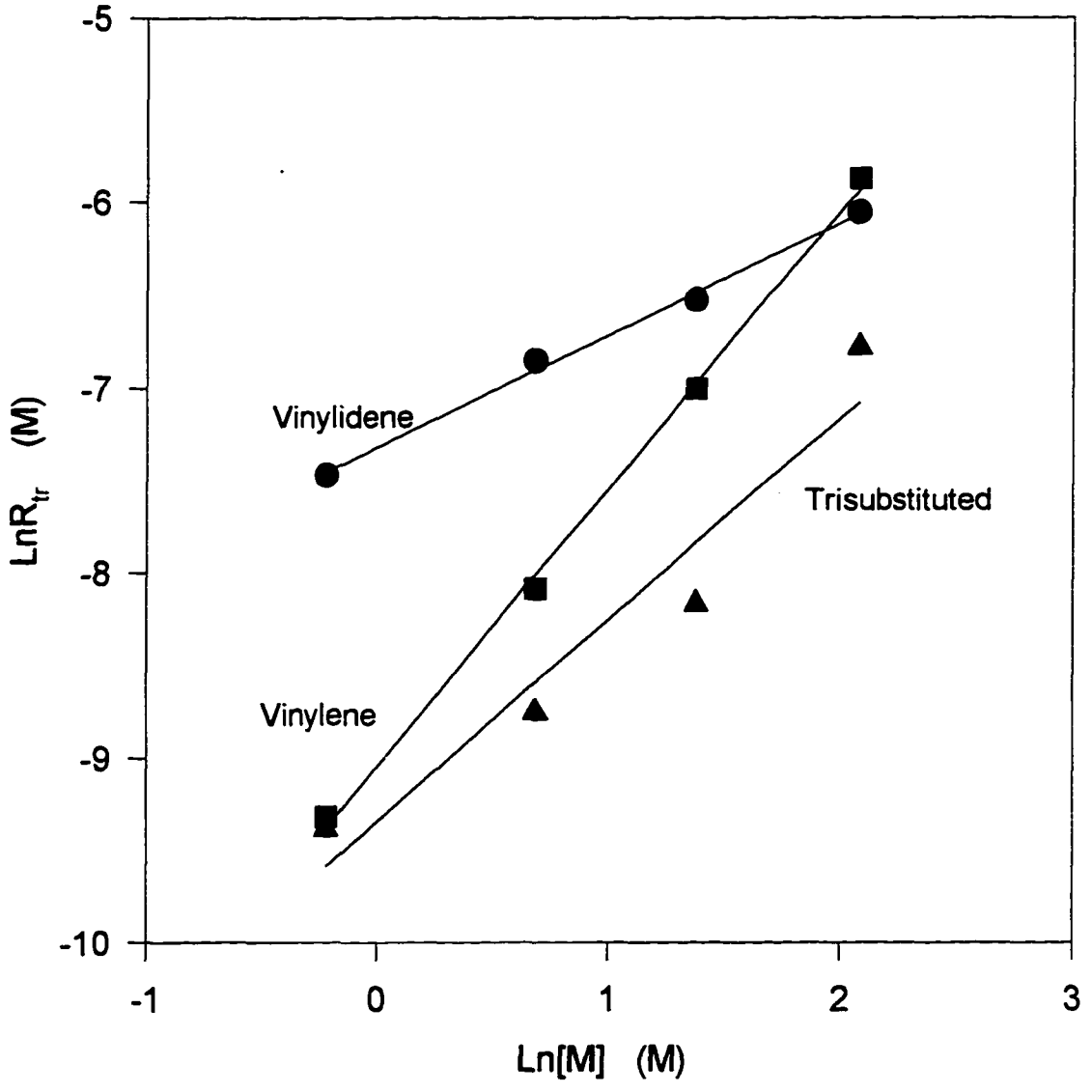

Figure A-50. LnR_{tr} as functions of Ln[M] at 50°C

Polymerization conditions: [Zr]=52M, [MAO]=62mM and T=50°C

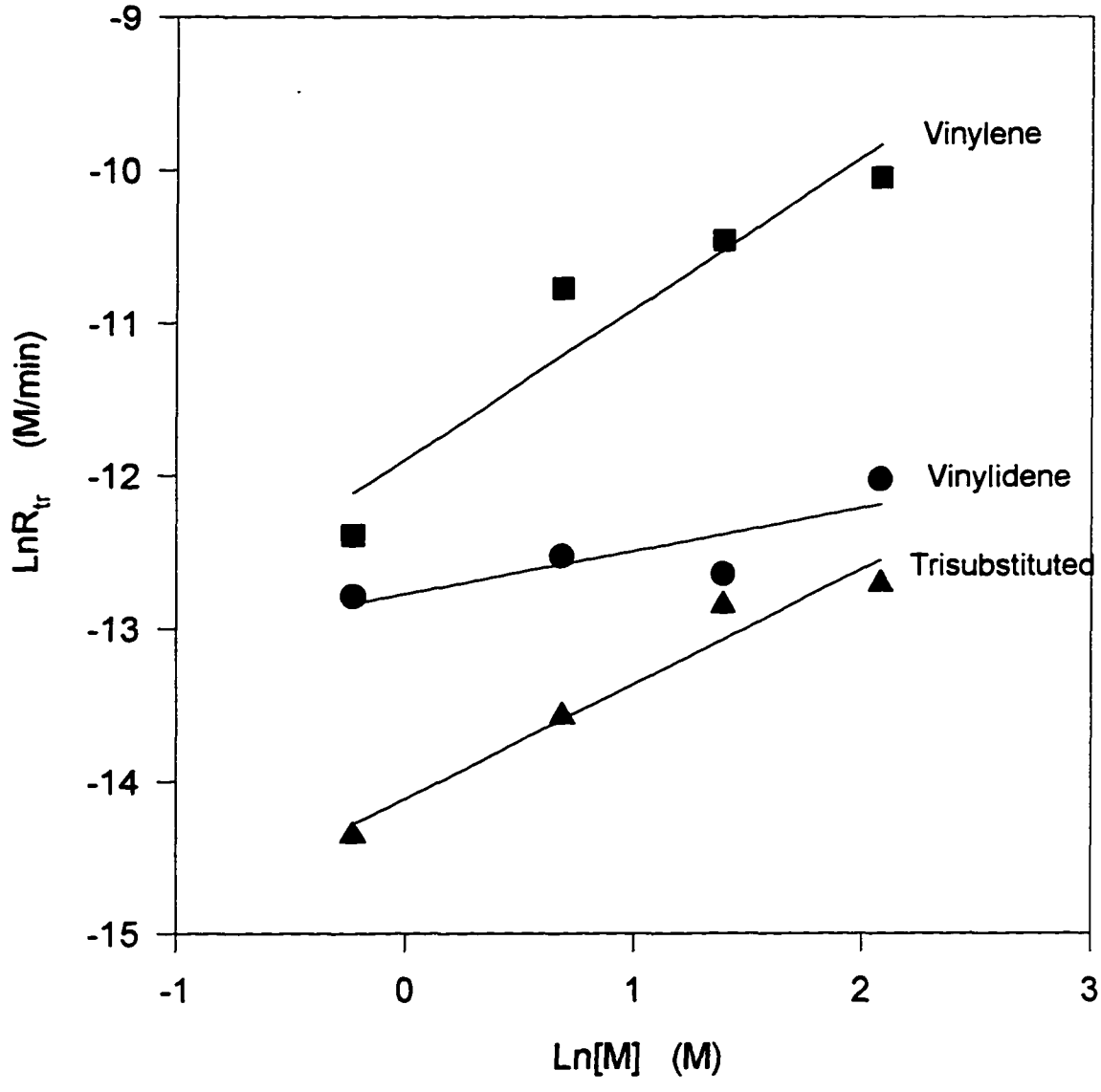

Figure A-51. LnR_{tr} as functions of Ln[M] at 0°C

Polymerization conditions: [Zr]=52μM, [MAO]=62mM and T=0°C

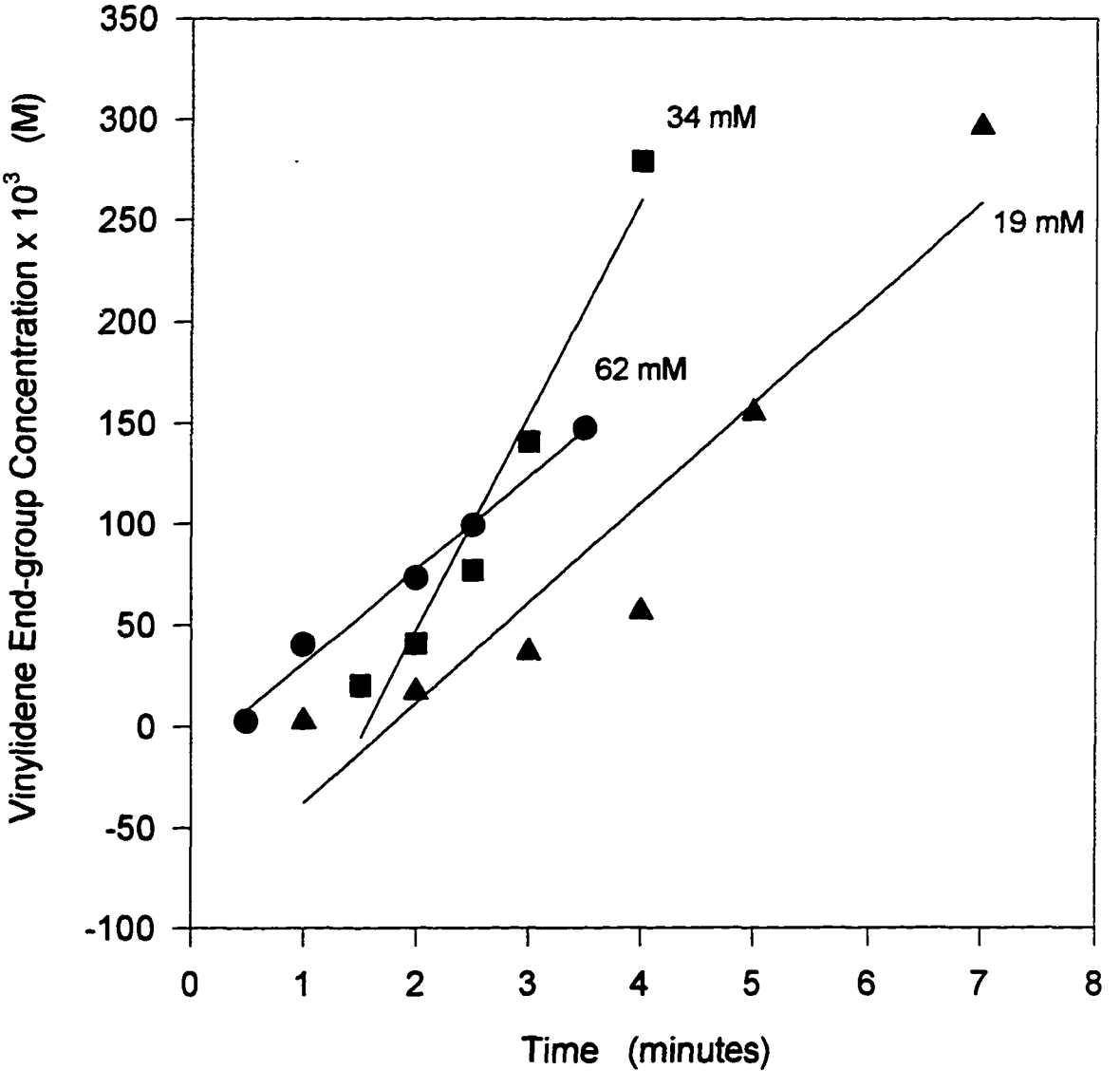

Figure A-52. Vinylidene end-group concentration as a function of time at 100°C and different MAO concentrations

Polymerization conditions: [Zr]=52μM, [M]=8.0M and T=100°C MAO concentration is labeled on each curve.

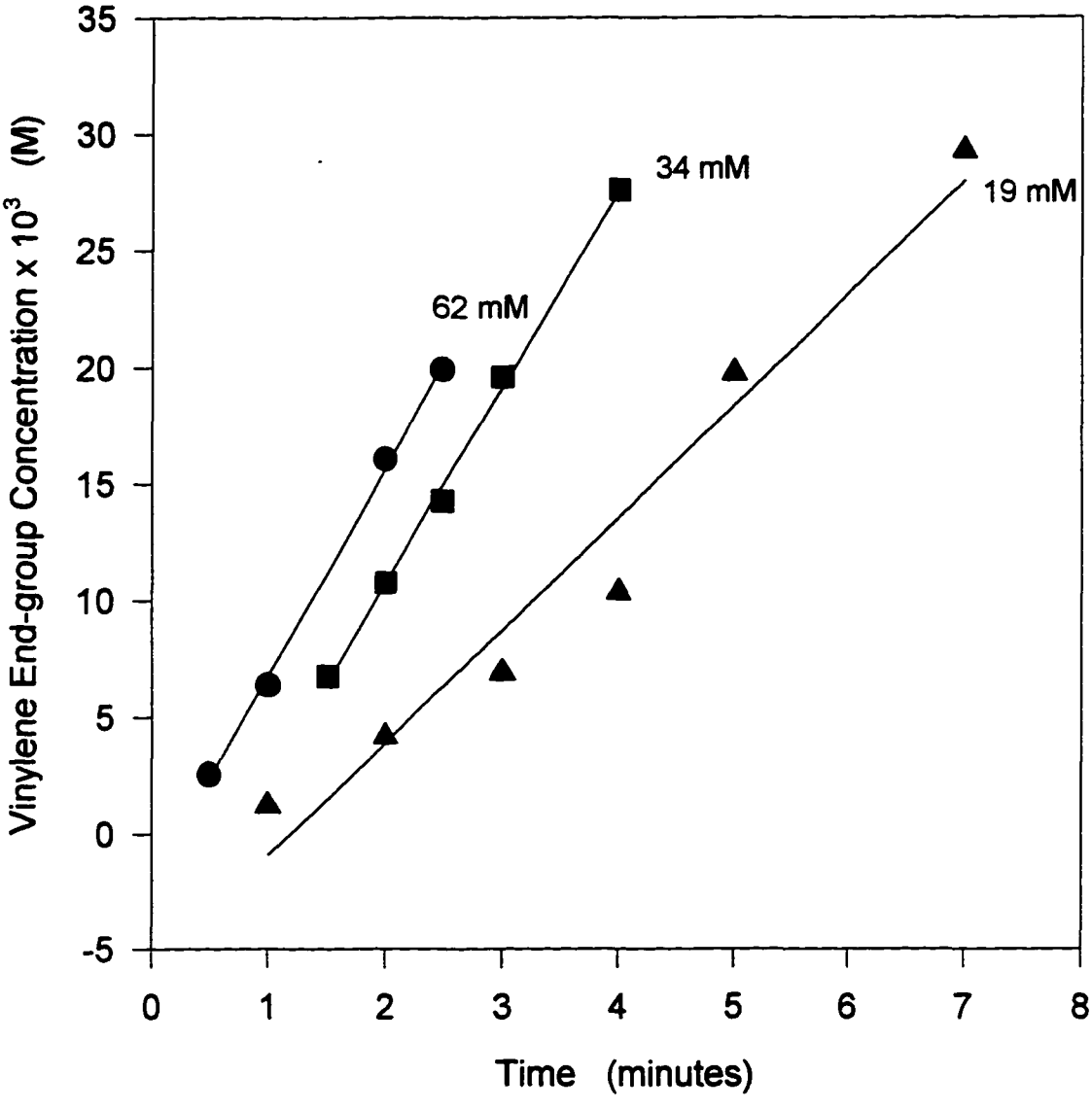

Figure A-53. Vinylene end-group concentration as a function of time at 100°C and different MAO concentrations

Polymerization conditions: [Zr]=52μM, [M]=8.0M and T=100°C
MAO concentration is labeled on each curve.

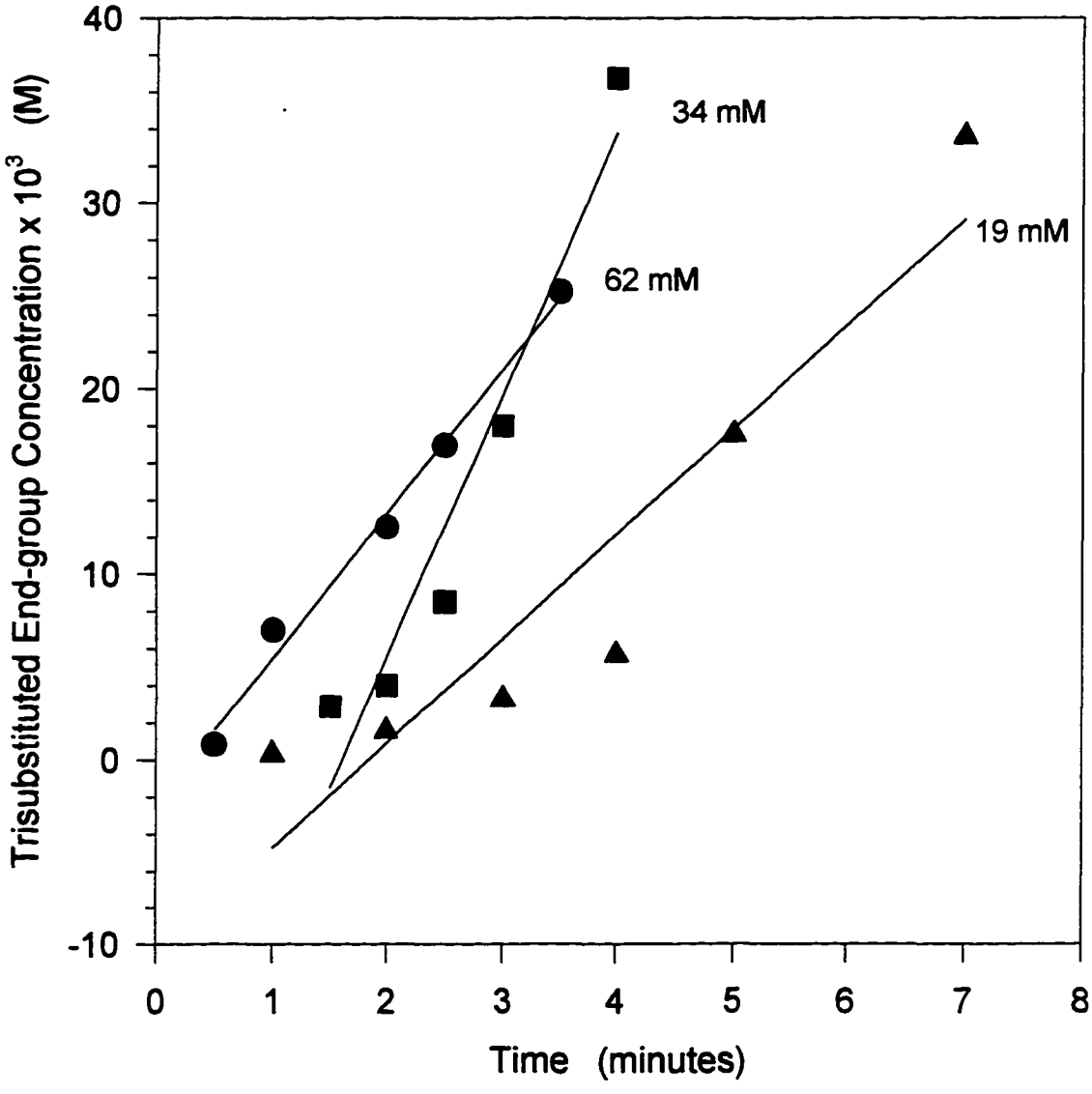

Figure A-54. Trisubstituted end-group concentration as a function of time at 100°C and different MAO concentrations

Polymerization conditions: [Zr]=52μM, [M]=8.0M and T=100°C
MAO concentration is labeled on each curve.

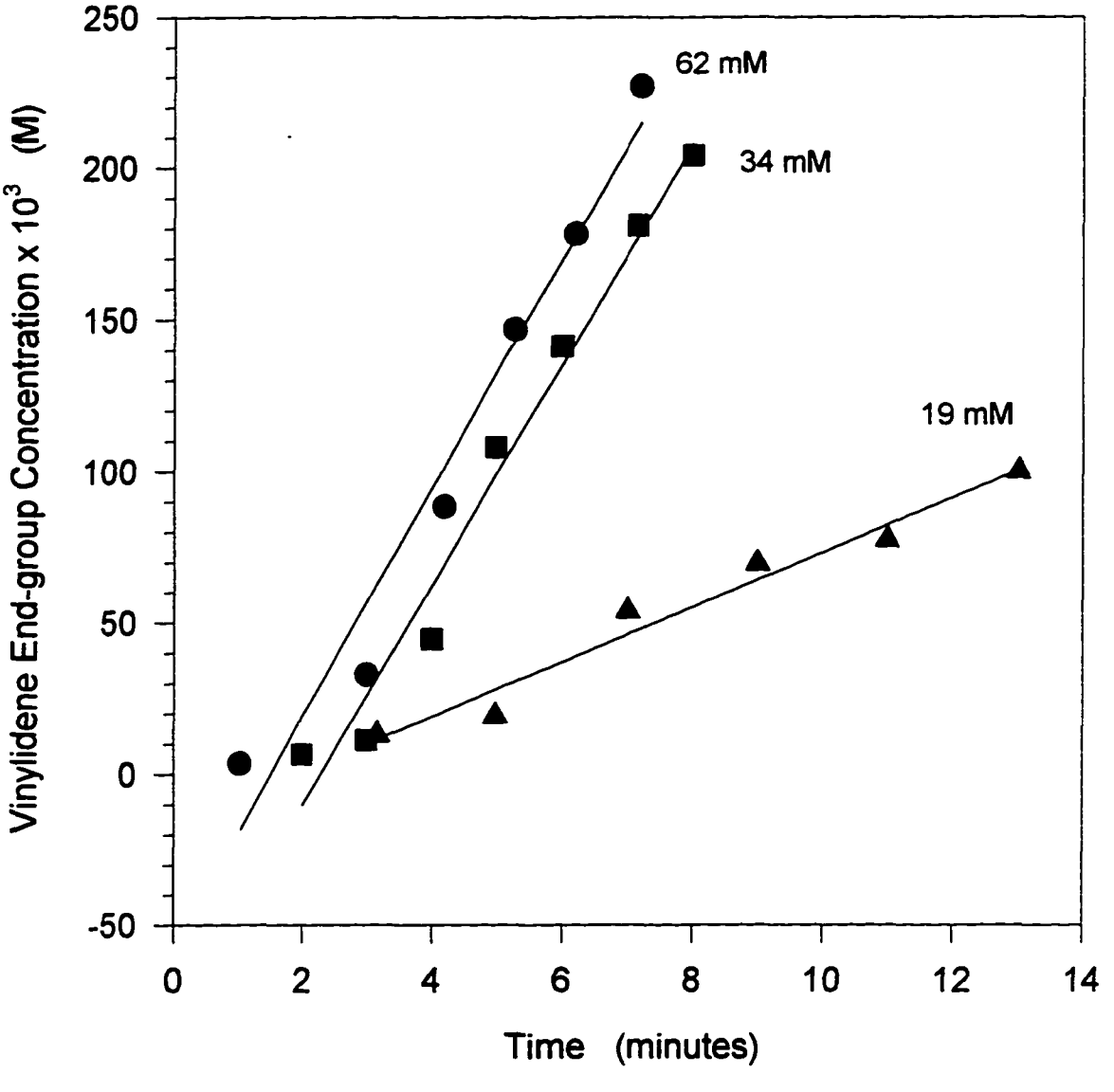

Figure A-55. Vinylidene end-group concentration as a function of time at 80°C and different MAO concentrations

Polymerization conditions: [Zr]=52μM, [M]=8.0M and T=80°C
MAO concentration is labeled on each curve.

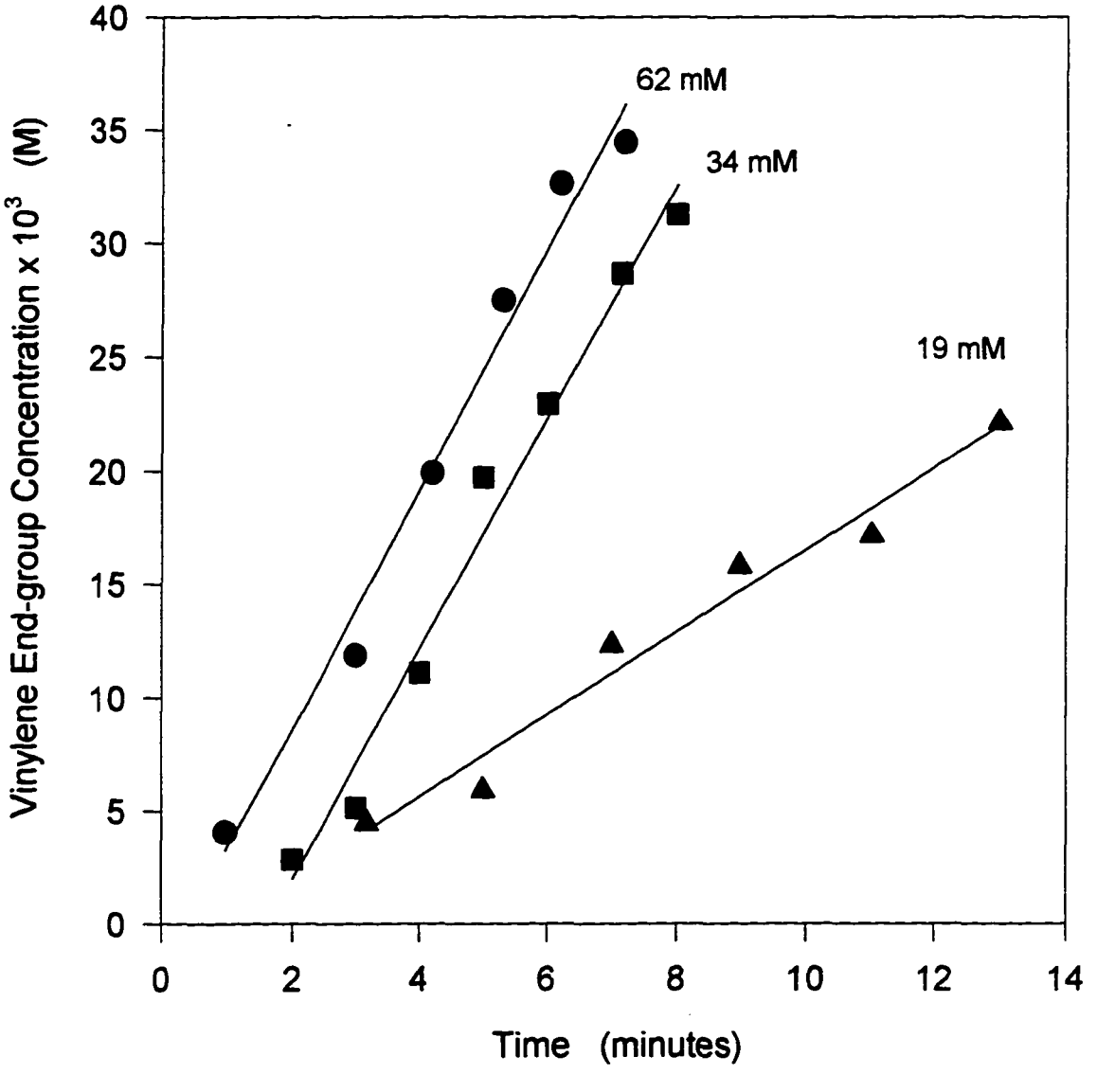

Figure A-56. Vinylene end-group concentration as a function of time at 80°C and different MAO concentrations

Polymerization conditions: [Zr]=52μM, [M]=8.0M and T=80°C
MAO concentration is labeled on each curve.

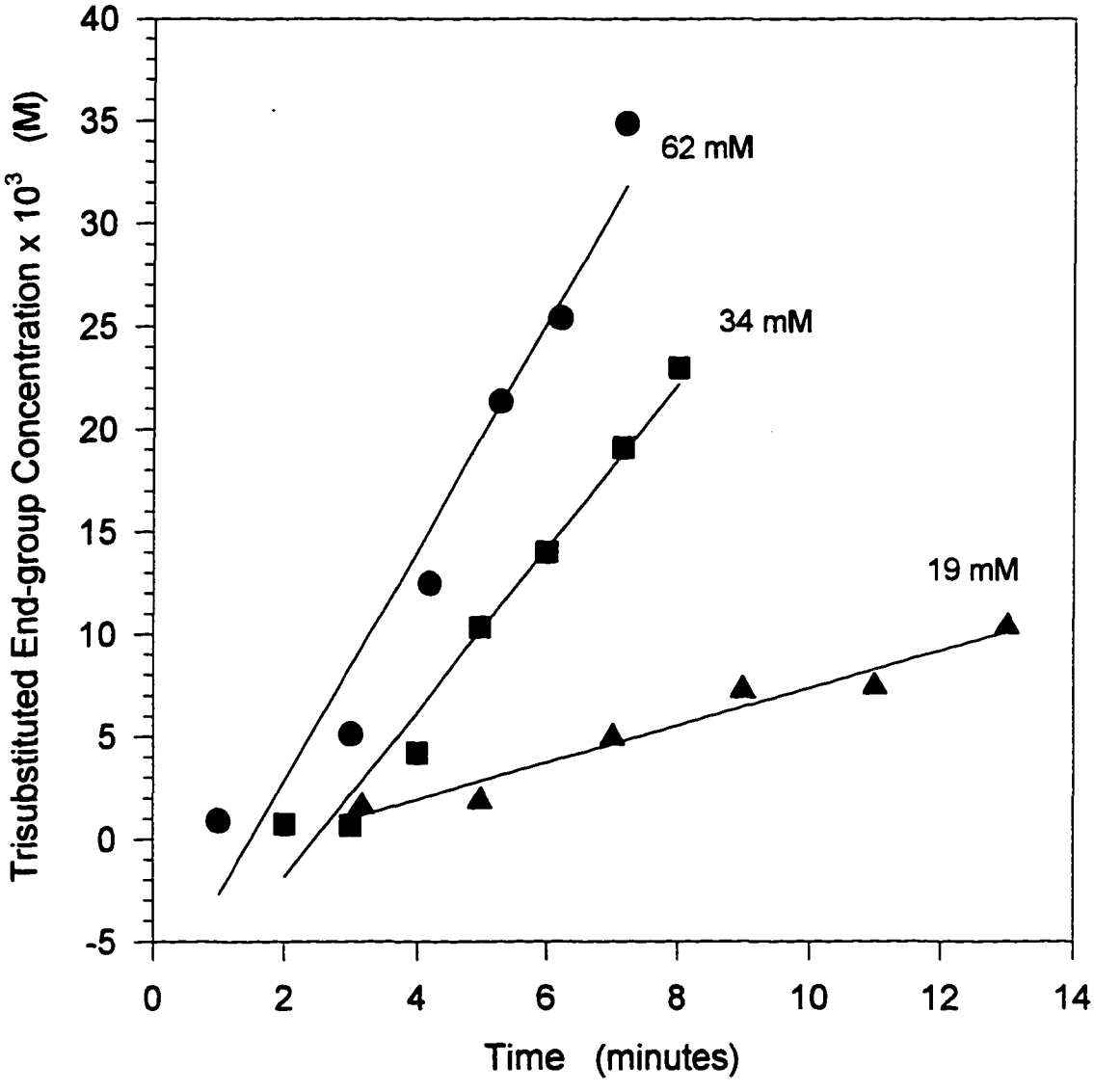

Figure A-57. Trisubstituted end-group concentration as a function of time at 80°C and different MAO concentrations

Polymerization conditions: [Zr]=52μM, [M]=8.0M and T=80°C
MAO concentration is labeled on each curve.

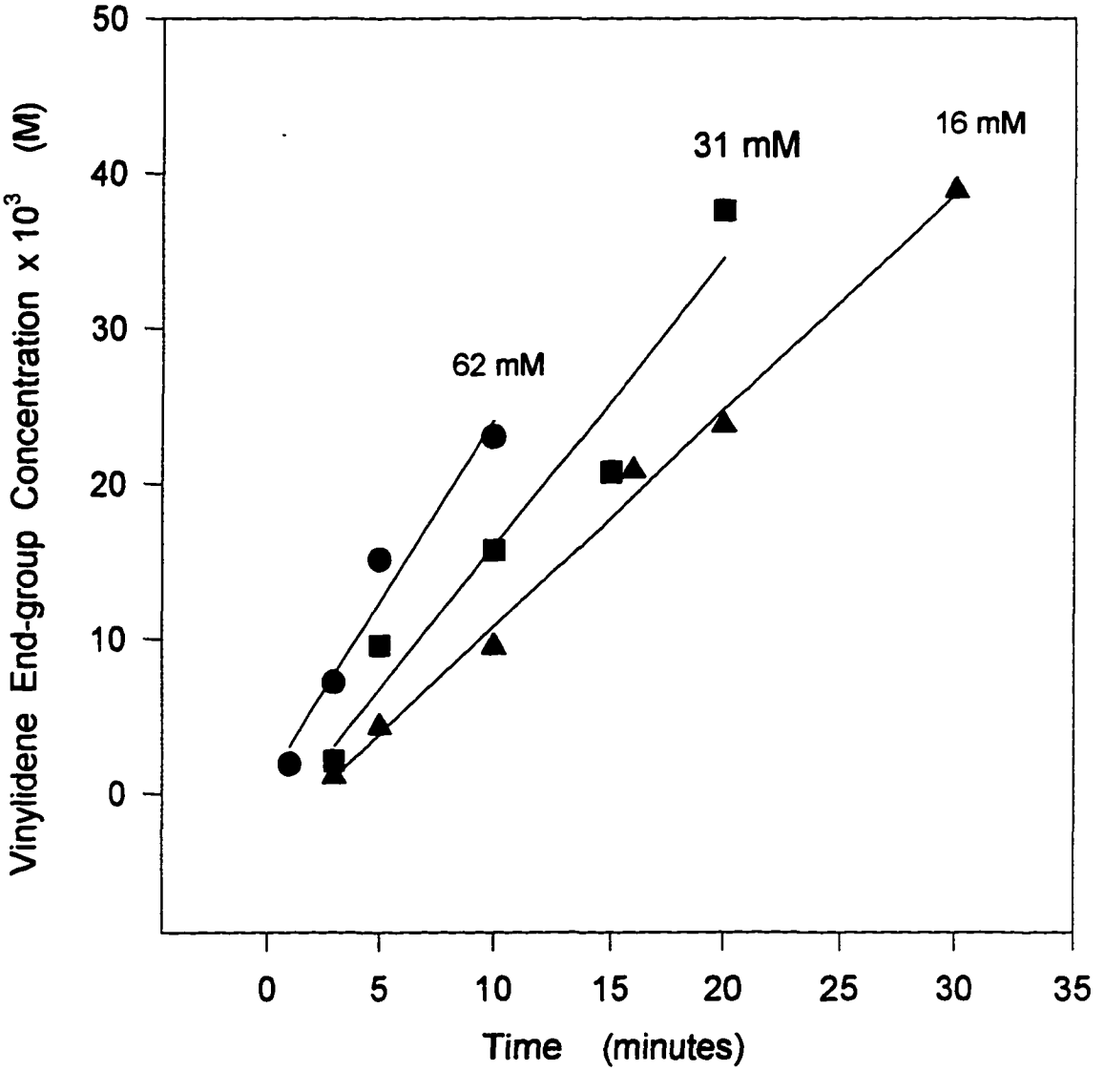

Figure A-58. Vinylidene end-group concentration as a function of time at 50°C and different MAO concentrations

Polymerization conditions: [M]=8.0M, [Zr]=52μM and T=50°C [MAO] is labeled on each curve.

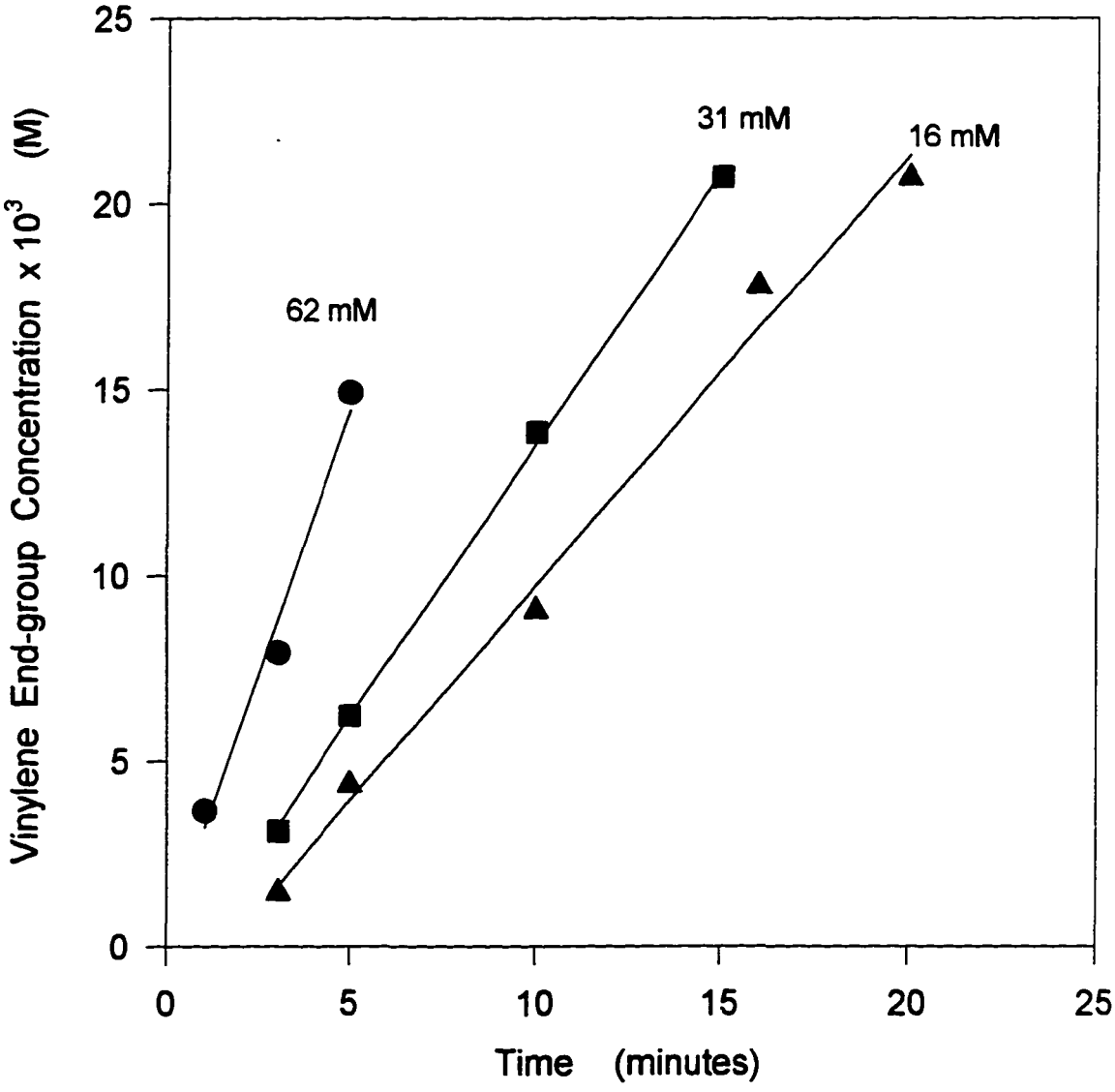

Figure A-59. Vinylene end-group concentration as a function of time at 50°C and different MAO concentration

Polymerization conditions: [M]=8.0M, [Zr]=52μM and T=50°C [MAO] is labeled on each curve.

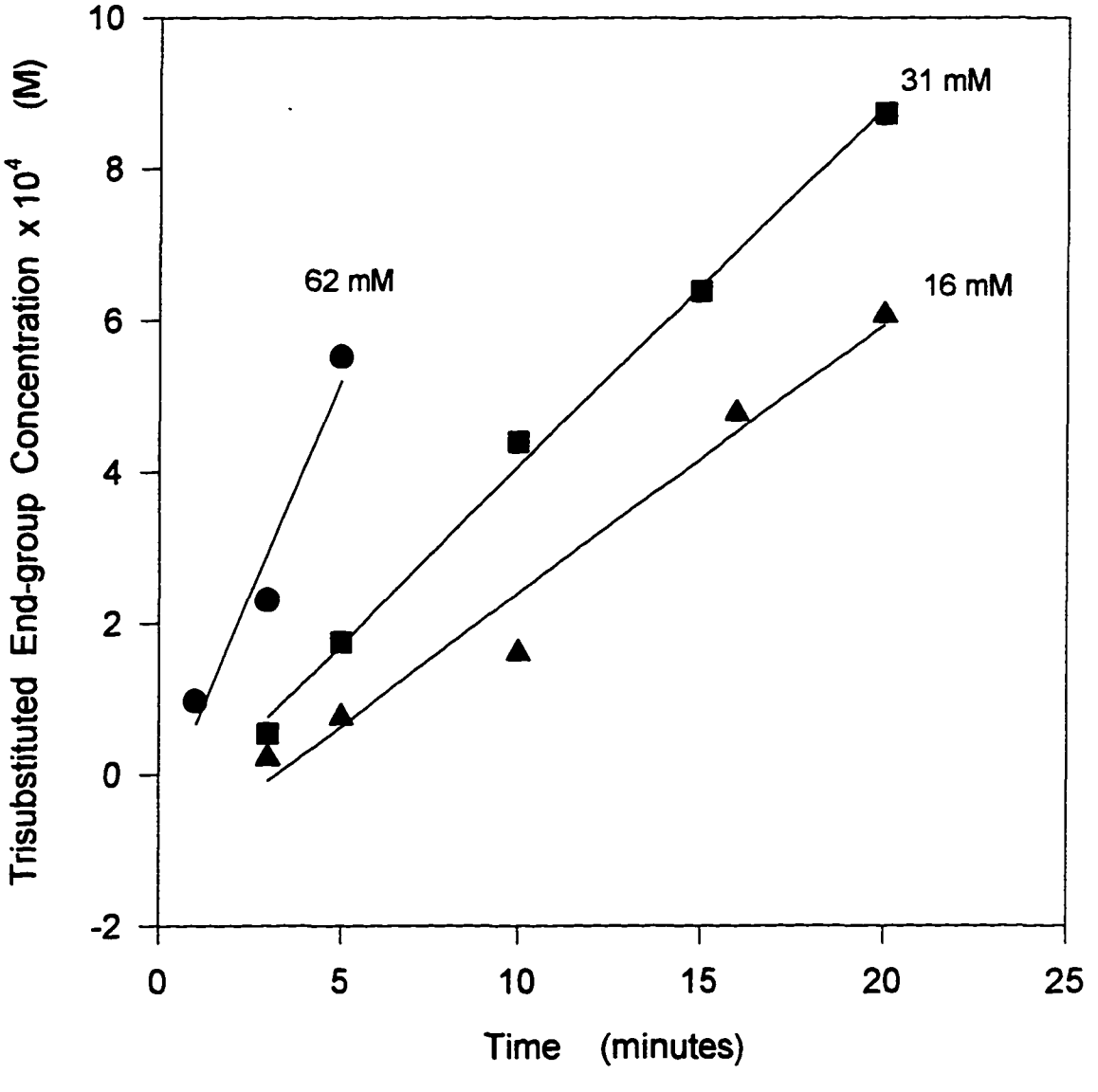

Figure A-60. Trisubstituted end-group concentration as a function of time at 50°C and different MAO concentrations

Polymerization conditions: [M]=8.0M, [Zr]=52μM and T=50°C
[MAO] is labeled on each curve.

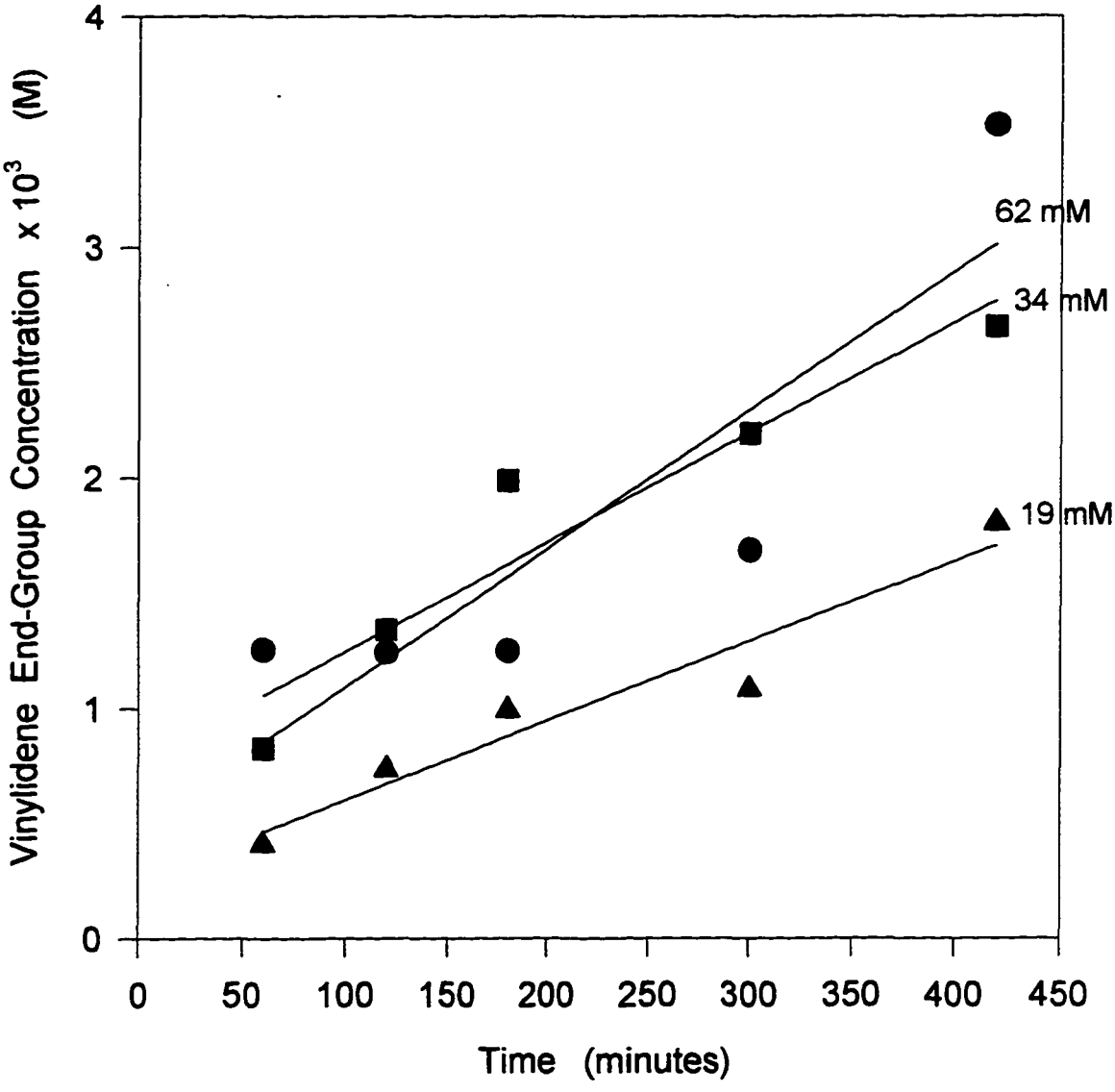

Figure A-61. Vinylidene end-group concentration as a function of time at 0°C and different MAO concentrations

Polymerization conditions: [M]=8.0M, [Zr]=52μM and T=0°C
[MAO] is labeled on each curve.

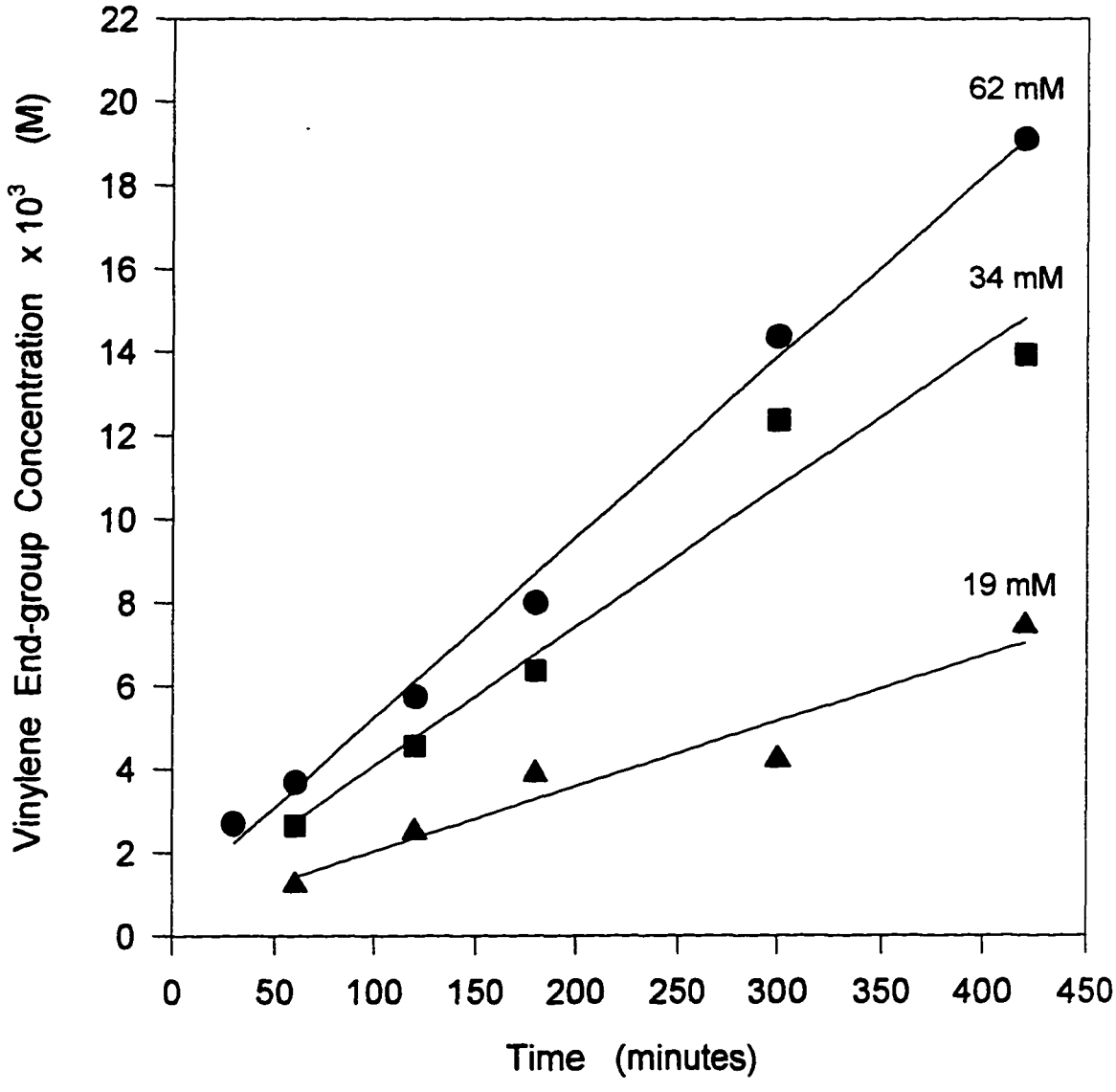

Figure A-62. Vinylene end-group concentration as a function of time at 0°C and different MAO concentrations

Polymerization conditions: [M]=8.0M, [Zr]=52μM and T=0°C [MAO] is labeled on each curve.

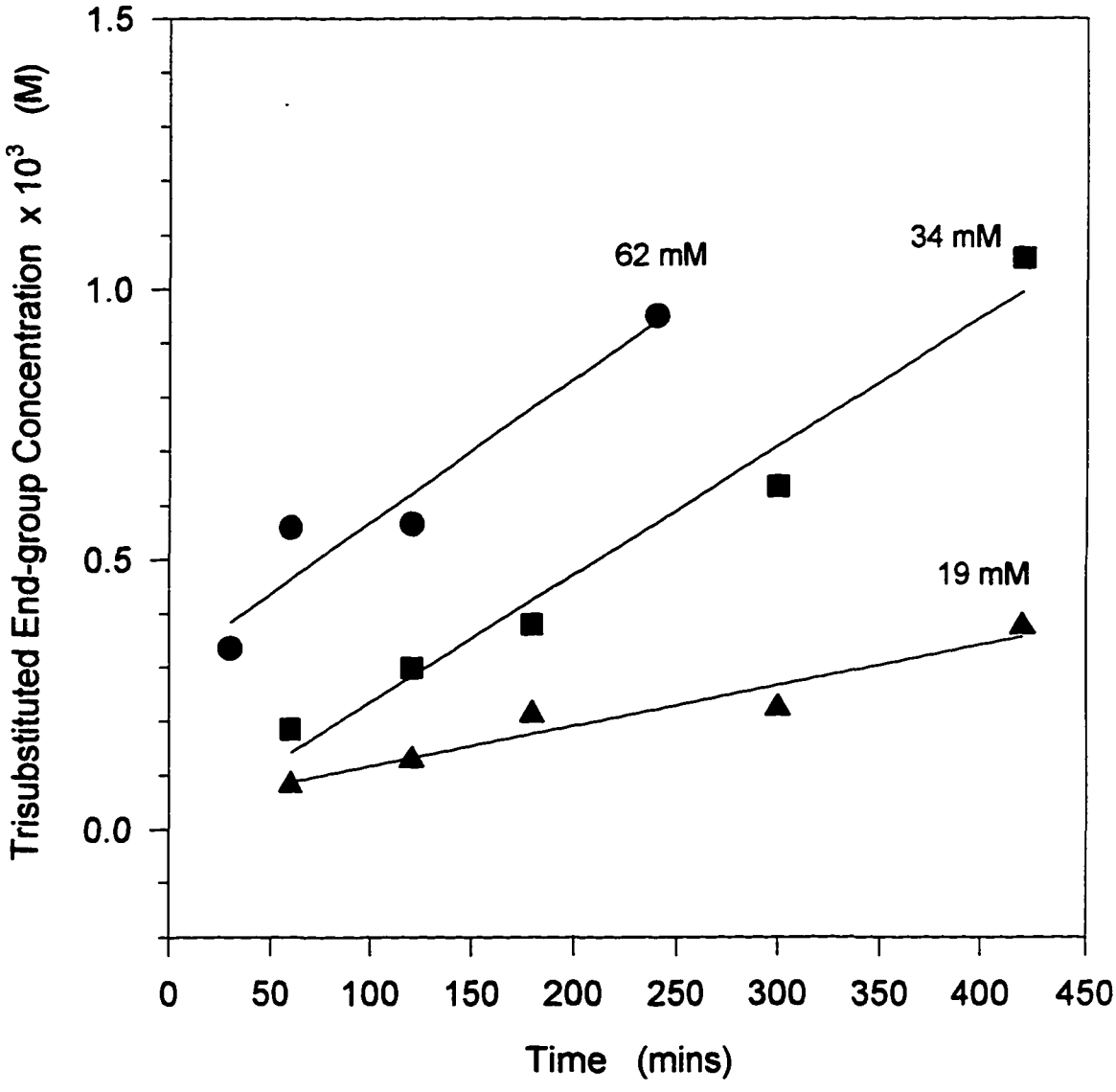

Figure A-63. Trisubstituted end-group concentration as a function of time at 0°C and different MAO concentrations

Polymerization conditions: [M]=8.0M, [Zr]=52μM and T=0°C
[MAO] is labeled on each curve.

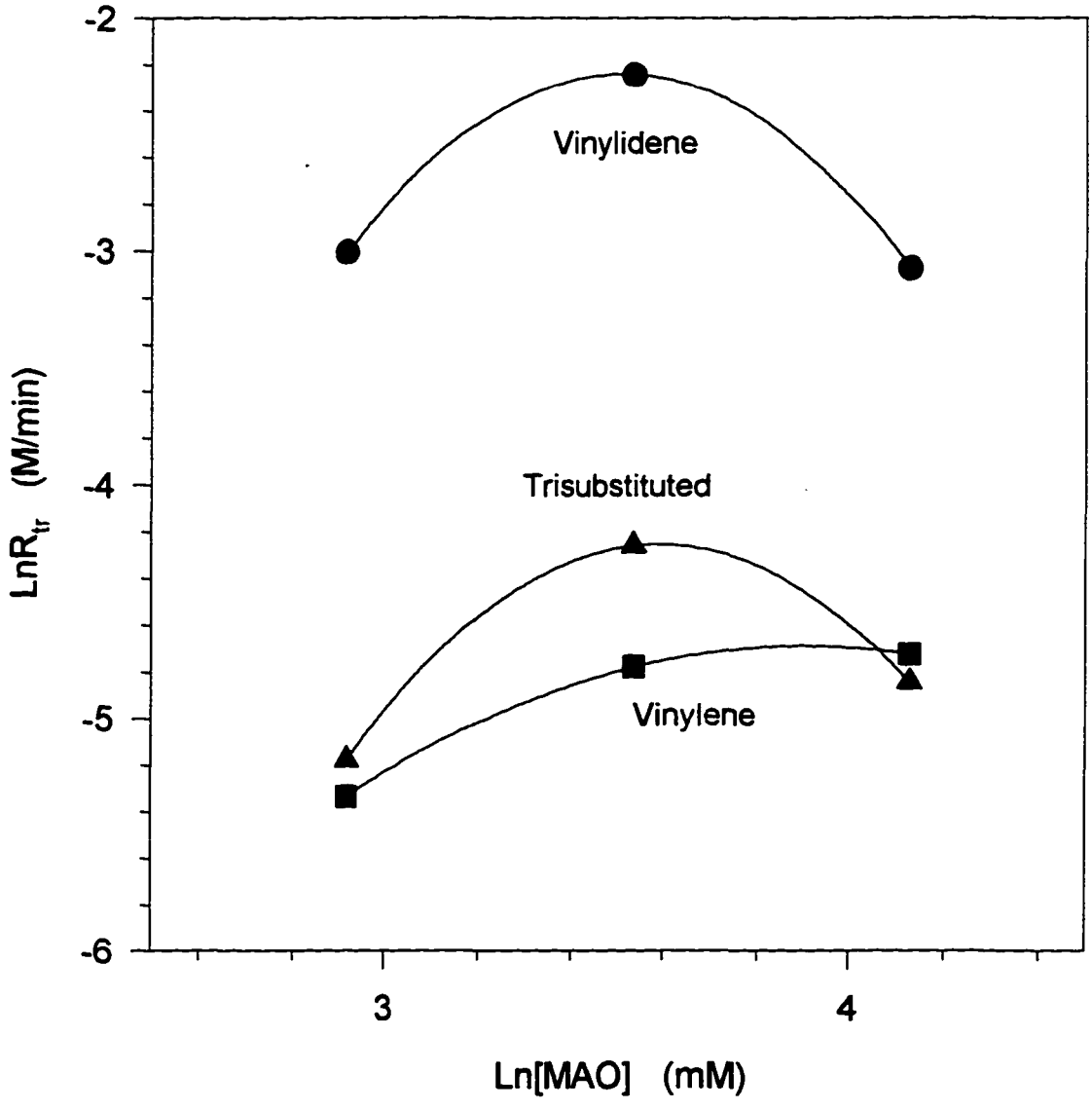

Figure A-64. LnR_{tr} as functions of Ln[MAO] at 100°C

Polymerization conditions: [Zr]=52μM, [M]=8.0M and T=100°C

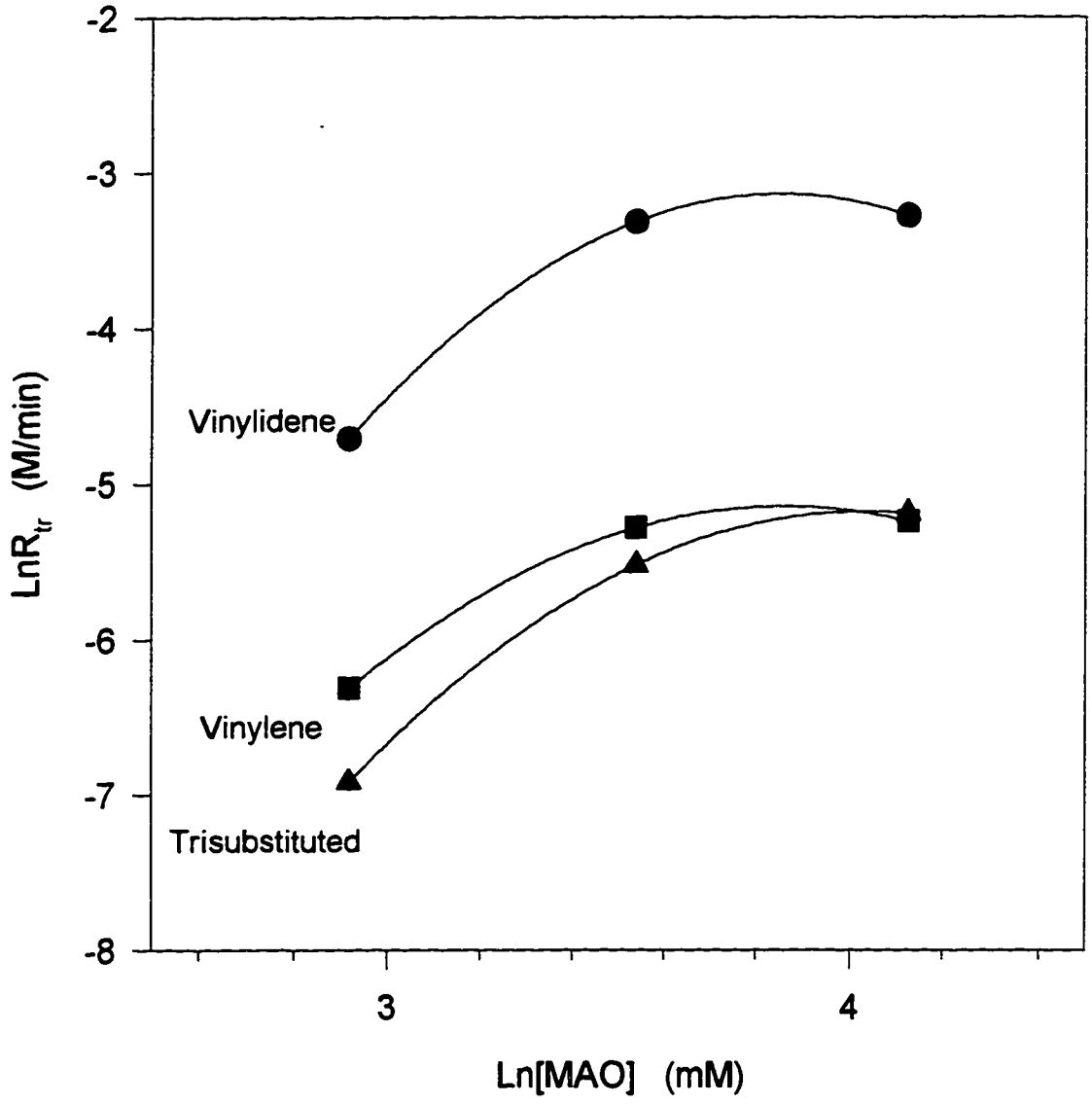

Figure A-65. LnR_{tr} as functions of Ln[MAO] at 80°C

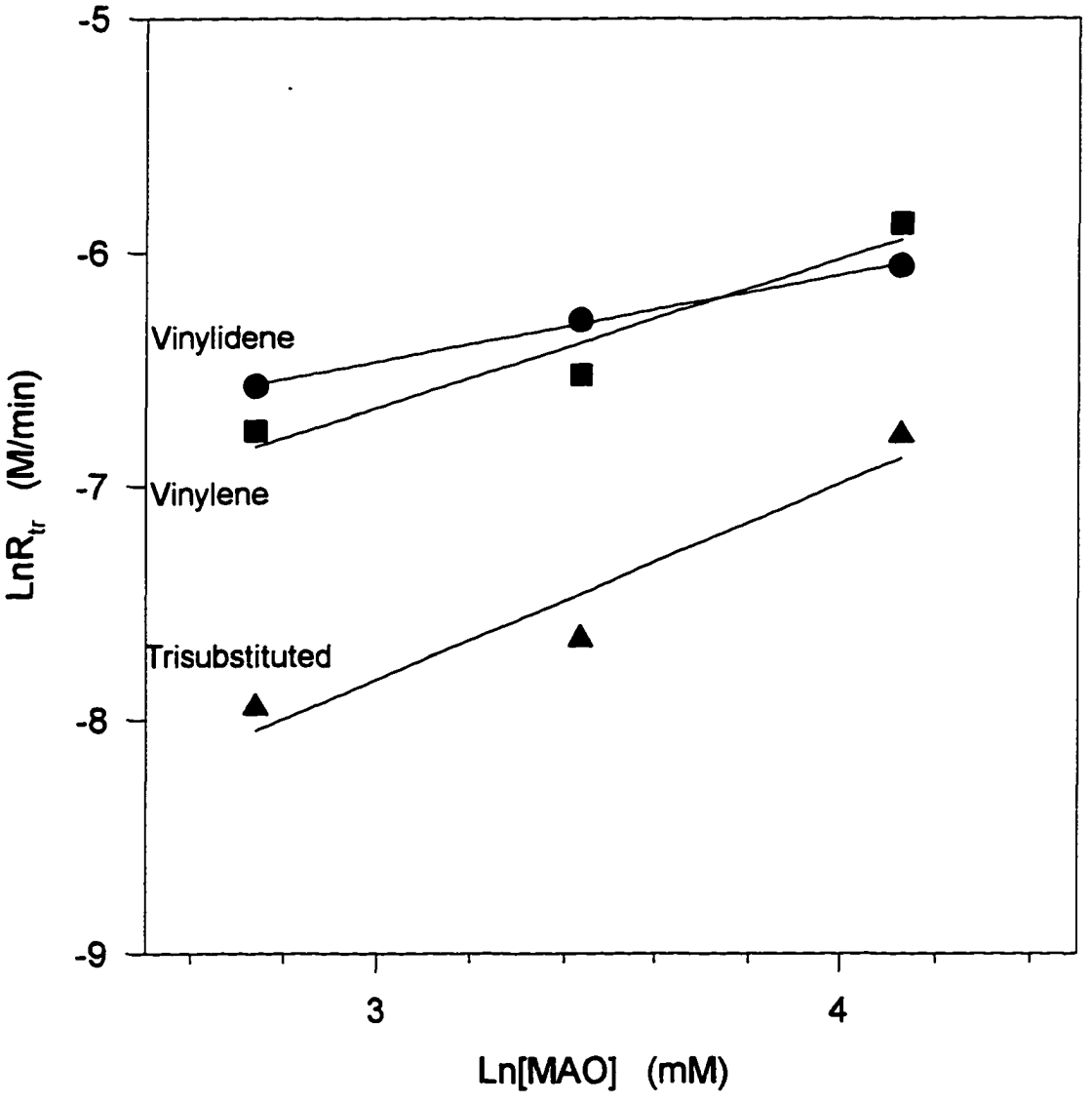

Figure A-66. LnR_{tr} as functions of Ln[MAO] at 50°C

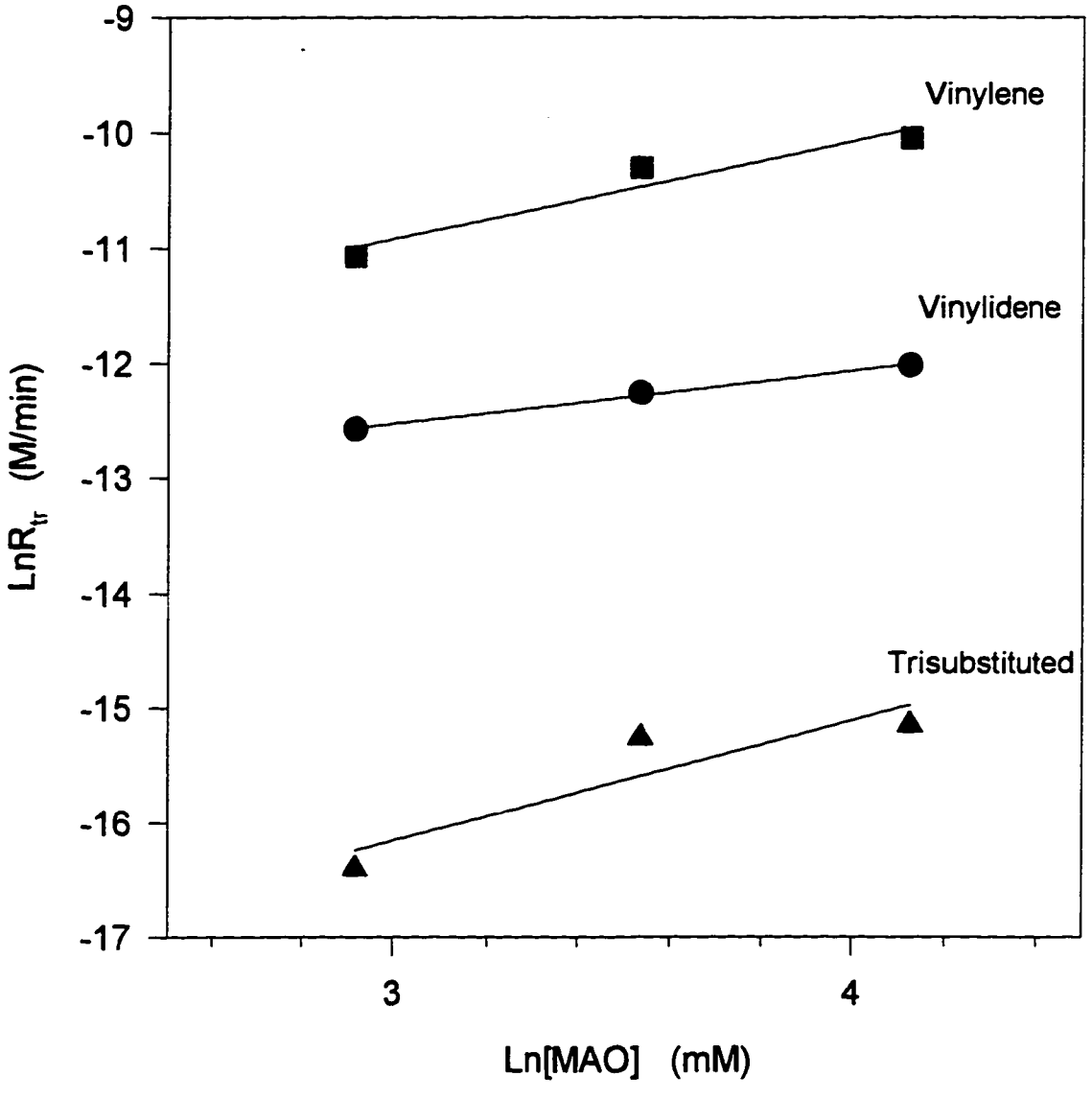

Figure A-67. LnR_{tr} as functions of [MAO] at 0°C

4.0 End-group Investigation

From kinetic studies on the chain transfer reactions, we saw that polymerization conditions such as catalyst concentration, monomer concentration, MAO concentration and temperature, affect chain transfer to form three types of end-groups quite differently. In the following several sections, we will put the data together for three types of end-groups under each change of polymerization conditions so that we can compare them directly instead of separately.

4.1 Temperature Effect on End-group Composition

Figures A-68 - A-70 show the temperature effect on the relative amount of three types of end-groups. It is very obvious that end-group composition changes very significantly with temperature in polymerization of 1-hexene. The composition of vinylidene end-group increases with temperature and the composition of vinylene end-group decreases with temperature, whereas, the composition of trisubstituted end-group only slightly changes with temperature between 10% to 15%. We used the data at medium conversion (~ 50-60%) to draw the curve of end-group compositions versus temperature in Figure A-71.

From the kinetic data of chain transfer rates (see Table A-7), we can see that $R_{tr,vd}$ decreases with the decrease of temperature much faster than $R_{tr,vn}$. For example, when temperature decreases from 100°C to 0°C, $R_{tr,vd}$ decreases about 8,000 times but only $R_{tr,vn}$ decreases about 200 times. This can explain the

reason why the relative ratio of vinylidene end group decreases but that of vinylene increases.

Similar temperature effect on end-group compositions was observed in the polymerization of 1-pentene (see Figures A-72 - A-75). One difference between poly(1-hexene) and poly(1-pentene) is that vinyl end-group (CH_2=CH-) was not shown in ^{1}H NMR spectrum of poly(1-hexene) but was in poly(1-pentene). Vinyl end-group appears at δ5.88ppm (1H) and at δ4.92ppm (2H) The study on poly(1-butene) showed that there is only very small amount of vinylene end group at high temperature whose relative composition increases with the decrease of temperature. However, there is much bigger composition of vinylene end-group in poly(1-hexene) and poly(1-pentene).

4.2 Catalyst Concentration Effect on End-group Composition

Figures A-76 - A-78 show the catalyst concentration effect on three types of end-groups respectively at 100°C, and, Figures A-80 - A-82, A-84 - A-86 and A-88 - A-90 show the same effect at 80°C, 50°C and 0°C, respectively. At medium to low temperature such as 50°C and 0°C, vinylidene end-group composition increases with catalyst concentration increasing. In contrast, vinylene end-group composition decreases with catalyst concentration increasing at these two temperatures. The composition of trisubstituted end-group changes very slightly with catalyst concentration change. However, at higher temperature, end-group compositions almost do not change with catalyst concentration. The above results are consistent with our kinetic model. At high temperature, chain

transfers to monomer are predominating and so, end group compositions almost do not change with catalyst concentration. But at lower temperature, chain transfers to form vinylidene involve in chain transfers to catalyst. This is why at lower temperature vinylidene end group composition increases with catalyst concentration increasing. Trisubstituted end group has the similar situation with vinylidene end group. Although chain transfers to form vinylene are independent of catalyst concentration, its relative composition decreases with vinylidene and trisubstituted end group compositions increasing. We used the end-group compositions at around 60% conversion to show in Figures A-79, A-83, A-87 and A-91 the relationship of end-group composition versus catalyst concentration at 100°C, 80°C, 50°C and 0°C, respectively.

4.3 Monomer Concentration Effect on End-group Composition

Figures A-92 - A-94 show the monomer concentration effect on end-group compositions at 100°C, and, Figures A-96 - A-98, A-100 - A-102 and A-104 - A-106 show the same effect at 80°C, 50°C and 0°C, respectively. We used the end-group composition data at around 60% conversion in Figures A-95, A-99, A-103 and A-107 to show the end-group compositions as functions of monomer concentration at the above four temperatures, respectively. At all temperatures, with monomer concentration increasing, vinylidene composition decreases, vinylene composition increases and trisubstituted end group composition increases slightly. The trends show stronger at low temperature than at high temperature. This can also be explained by our kinetic model. The fractional

order of chain transfer rate with respect to monomer concentration is bigger in formation of vinylene than in formation of vinylidene. Especially at low temperature like 0°C, chain transfer to form vinylidene is almost independent of monomer concentration.

4.4 MAO Concentration Effect on End-group Composition

MAO concentration has little effect on end-group compositions. Figures A-108 - A-110 show that, at 50°C, the compositions of all three kinds of end-groups almost do not change with MAO concentration. The same holds true at 0°C, 80°C and 100°C, which are not shown here. The MAO we used is in greatly excess and the change in its concentration would not bring sensitive changes.

4.5 Equilibrium Study on End-groups

From the results of end-group study, we can see that the end-group compositions depend to a great extent on the polymerization conditions. For example, the composition of vinylidene end-group increases with the increase of temperature, the increase of catalyst concentration and the decrease of monomer concentration. The behavior of the vinylene composition shows the opposite trend. The question arises whether there are equilibria directly between these three types of end-groups during the polymerization active system. To find out, a series of experiments was performed. The experimental detail has been described in Section 2.4. The results are described below.

The first experiment was described in Section 2.4a. The polymerization of 1-hexene was completed at 80°C and 0°C, and the polymerization mixtures were

kept at the same temperature with their polymerization temperature for a certain time (indicated in Table A-12) before termination. The end group compositions of polymers were determined. The results listed in Table A-12 tell us that there is no direct thermodynamic equilibrium between these three end-groups as long as they are formed. Because if there was equilibrium between these three end-groups, the end group compositions should have changed with the sitting time. However, these results showed that the end group compositions do not change with sitting time at all. Certainly, further information is needed to prove there is no equilibrium between these three end groups.

To prove whether there are any direct equilibriums between these three kinds of end groups, further experiments were performed. In Section 2.4b, we completed the polymerization at one temperature (80°C) and without deactivating the catalyst/MAO species, sat the polymerization mixture at another temperature (0°C) for a certain long time. If there was any equilibria between these three kinds of end groups, the temperature change must result in a shift of equilibria and a change of end group compositions would be observed. And in Section 2.4c, we mixed the polymer which was synthesized at one temperature (0°C), catalyst and MAO together, and kept this mixture at another temperature (80°C). If the end group compositions were different before and after the process, there must be some reactions occuring on the polymer at the new temperature. The results from experiment 2.4b and 2.4c are shown in Table A-13. In 2.4b, polymerization was finished at 80°C and the reaction mixture was

brought to 0°C without isolation of polymer. In 2.4c, a polymer, which was polymerized at 0°C for 2 days and isolated from monomer and solvent, was dissolved in toluene followed by additions of catalyst and MAO. The concentrations of catalyst and MAO are the same with those in polymerization. The mixture of polymer, catalyst, MAO and toluene was kept at 80°C for 1 day. The polymer was isolated again. In both of these experiments, there is no significant change in end-group compositions after the polymerization mixtures were sitten at a different temperature. These results show that there is no direct equilibrium between different end-groups as long as they are formed. Even the polymerization at 0°C are under the same conditions in both Table A-12 and A-13, the relative end-group compositions are somehow different because of the limits of accuracy of ^{1}H NMR analysis method.

Table A-14 shows the results of end-group study 2.4d. In this series of experiments, model compounds were used to mix with monomer before polymerization. Catalyst and MAO were added into the mixture to polymerize the monomer. If there was equilibrium during the formation of these three types of end-groups, the addition of model compounds would make the equilibrium shift towards the direction getting less of the end-group which has the same double bond with the added model compound. For example, if we added 2-hexene into the monomer, as a result of equilibrium, the vinylene end-group composition would be decreased, and instead, higher compositions of vinylidene and trisubstituted end-groups would be obtained. However, the experimental results

showed that there was no significant change in the end-group composition. So, from this experiment, we conclude that there is no equilibrium during the formation of three types of end-groups. Meanwhile, Monomer concentration is responsible for different end-group compositions in Table A-14 at 0°C versus in Table A-12.

In summary, the conclusions drawn from the above experiments are: 1) there is no direct equilibrium between these three types of end-groups after they are formed; 2) there is no equilibrium between the intermediates which will result in different end-groups during the formation of end-groups.

Table A-12 Effect of Reaction Time on End-group Composition[a]

T (°C)	Reaction Time	Vinylidene	Vinylene	Trisubstituted
80	30 minutes[b]	79%	10%	11%
	1 week	79%	8%	12%
	2 weeks	81%	7%	12%
	1 month	78%	9%	13%
0	2 days[b]	22%	72%	6%
	1 week	24%	64%	12%
	2 weeks	28%	62%	10%
	1 month	26%	70%	4%

[a] Polymerization conditions: [Zr]=56μM, [M]=8.0M and [MAO]=62mM.
[b] These are the shortest reaction times required for complete conversion.

Table A-13 Polymerization at One Temperature

Followed by Equilibration at Different Temperature[a]

Sample	Time	Vinylidene	Vinylene	Trisubstituted
40 Mins polymn. at 80°C followed by indicated time at 0°C	0	79%	10%	11%
	1 day	78%	10%	12%
	8 days	79%	10%	11%
	2 weeks	81%	9%	11%
	1 month	79%	10%	12%
Isolated polymer after polymned. at 0°C for 2 days		16%	73%	10%
Isolated polymer polymned. at 0°C, dissolved in toluene, added Zr/MAO and kept at 80°C	1 day	18%	72%	9%

[a] Polymerization conditions: [Zr]=56μM, [M]=8.0M and [MAO]=62mM.

Table A-14 End-group Study in Section 2.4d[a]

T & t	Reactant Mixture[b]	Vinylidene	Vinylene	Trisubstituted
80 °C 1 hr	1:3 1-Hex:Tol	85%	3.9%	11%
	1:1:2 1-Hex:2-Hex:Tol	85%	5.6%	9.0%
	1:1:2 1-Hex:2-Me-1-hep:Tol	87%	4.0%	8.9%
	1:1:2 1-Hex:3-Me-2-pen:Tol	85%	5.7%	8.8%
50 °C 2 hrs	1:3 1-Hex:Tol	82%	8.8%	9.4%
	1:1:2 1-Hex:2-Hex:Tol	76%	17%	7.2%
	1:1:2 1-Hex:2-Me-1-hep:Tol	81%	13%	6.5%
	1:1:2 1-Hex:3-Me-2-pen:Tol	83%	9.4%	6.9%
0 °C 1 wk	1:3 1-Hex:Tol	41%	48%	11%
	1:1:2 1-Hex:2-Hex:Tol	44%	51%	5.0%
	1:1:2 1-Hex:2-Me-1-hep:Tol	54%	41%	4.5%
	1:1:2 1-Hex:3-Me-2-pen:Tol	43%	48%	9.9%

[a] Polymerization conditions: [Zr]=56μM and [MAO]=62mM.
[b] 1-Hex: 1-Hexene; Tol: Toluene; 2-Hex: 2-Hexene; 2-Me-1-hep: 2-Methyl-1-heptene; 3-Me-2-pen: 3-Methyl-2-pentene.

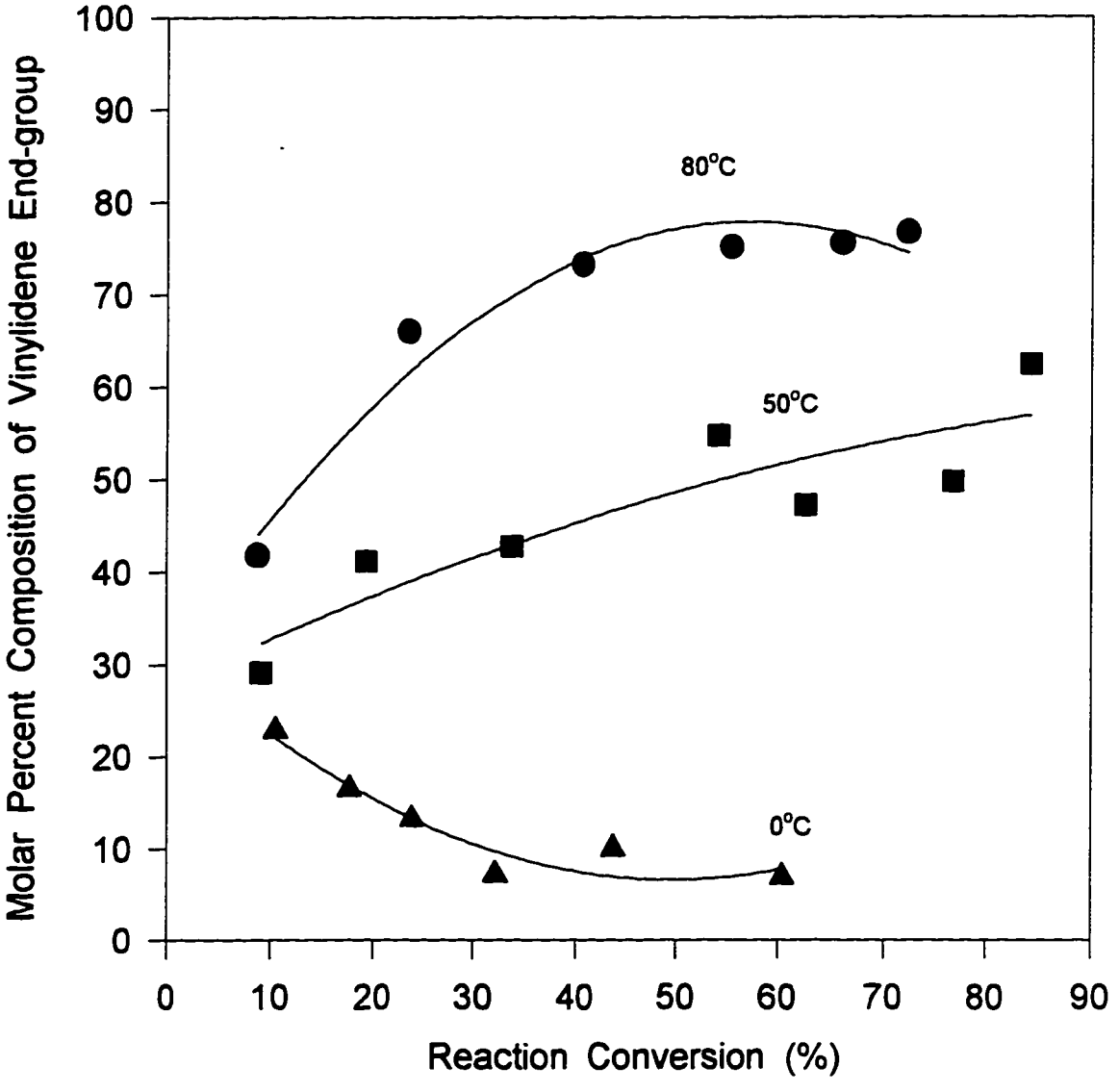

Figure A-68. Molar percent composition of vinylidene end-group versus % coversion at different temperatures

Polymerization conditions: [Zr]=52μM, [M]=8.0M, [MAO]=62mM,

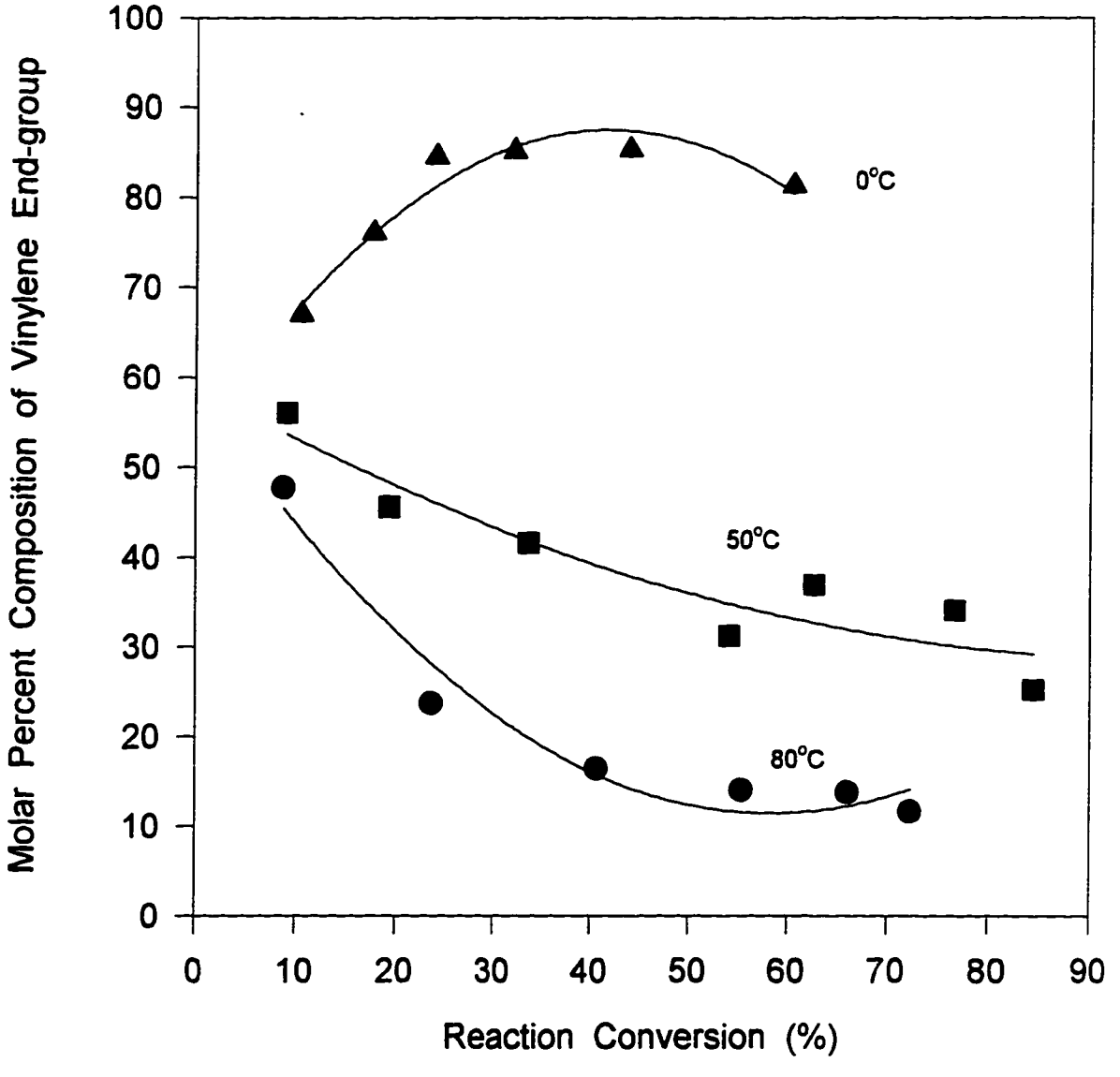

Figure A-69. Molar percent composition of vinylene end-group versus % conversion at different temperatures

Polymerization conditions: [Zr]=52μM, [M]=8.0M and [MAO]=62mM

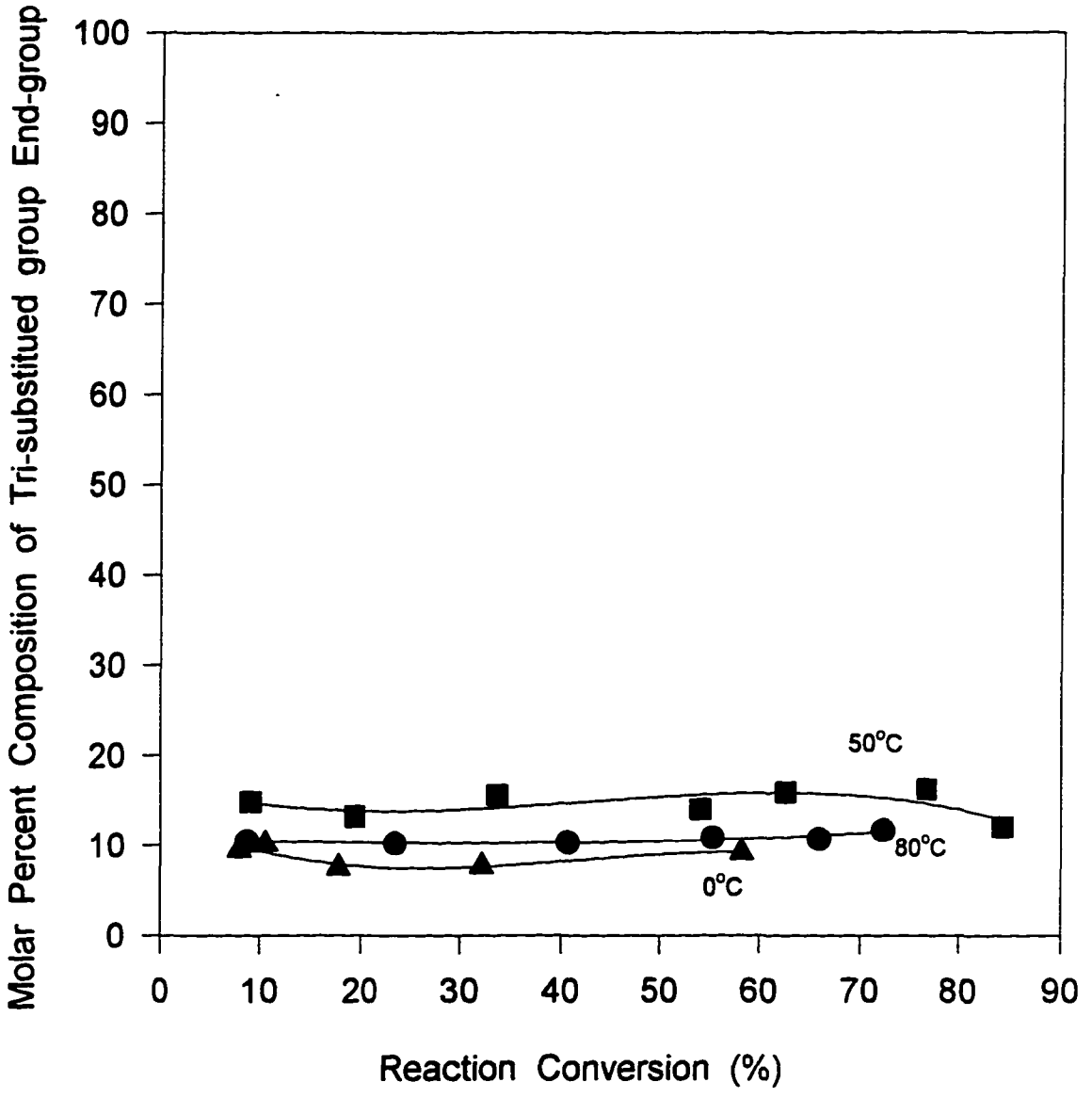

Figure A-70. Molar percent composition of trisubstituted end-group versus % conversion at different temperatures

Polymerization conditions: [Zr]=52M, [M]=8.0M and [MAO]=62mM

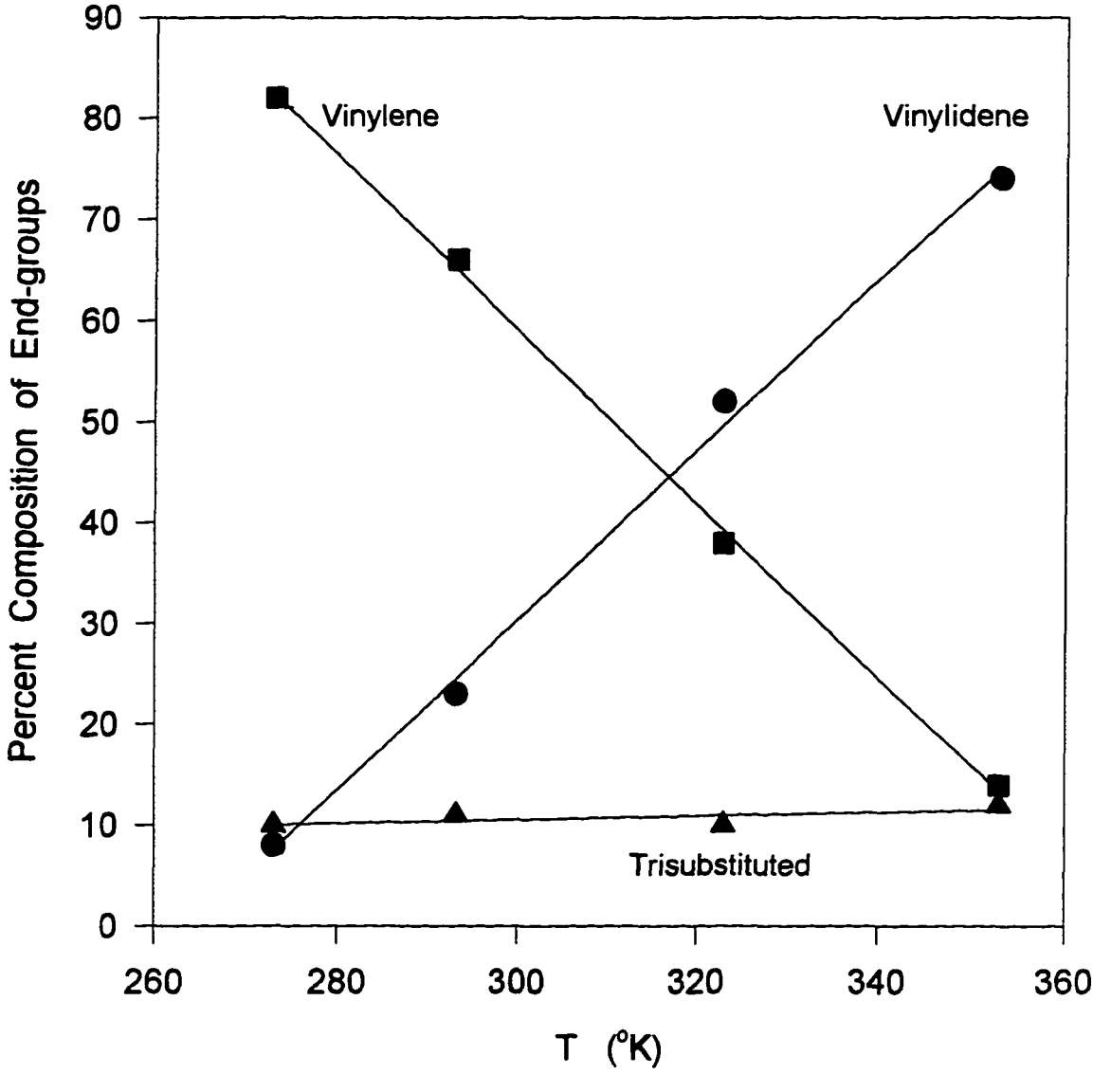

Figure A-71. Percent composition of end-group as function of temperature

Polymerization conditions: [Zr]=52M, [M]=8.0M and [MAO]=62mM

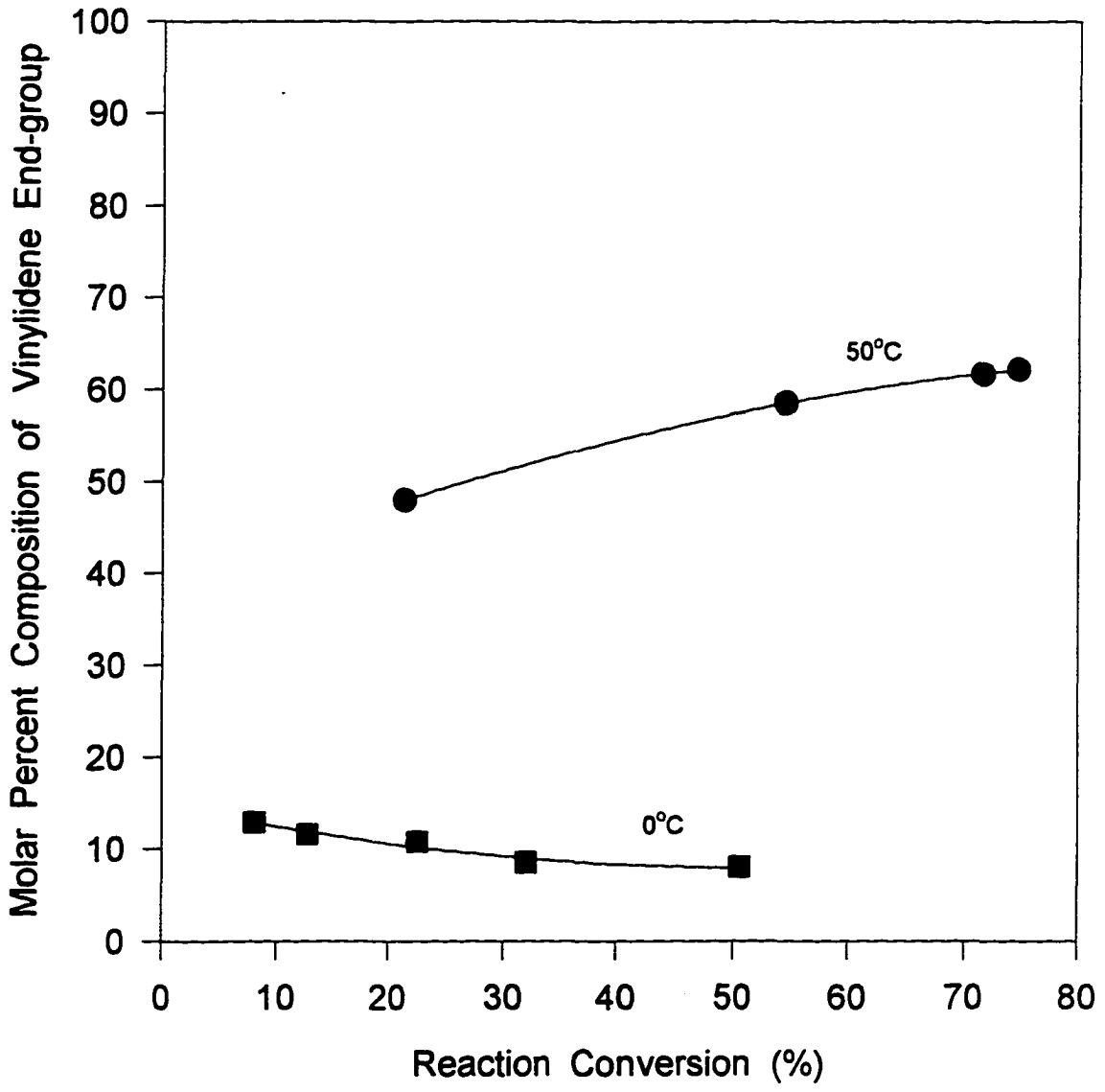

Figure A-72. Molar percent composition of vinylidene end-group versus % conversion at different temperatures in polymerization of 1-pentene

Polymerization conditions: [Zr]=52μM, [M]=9.1M and [MAO]=62mM

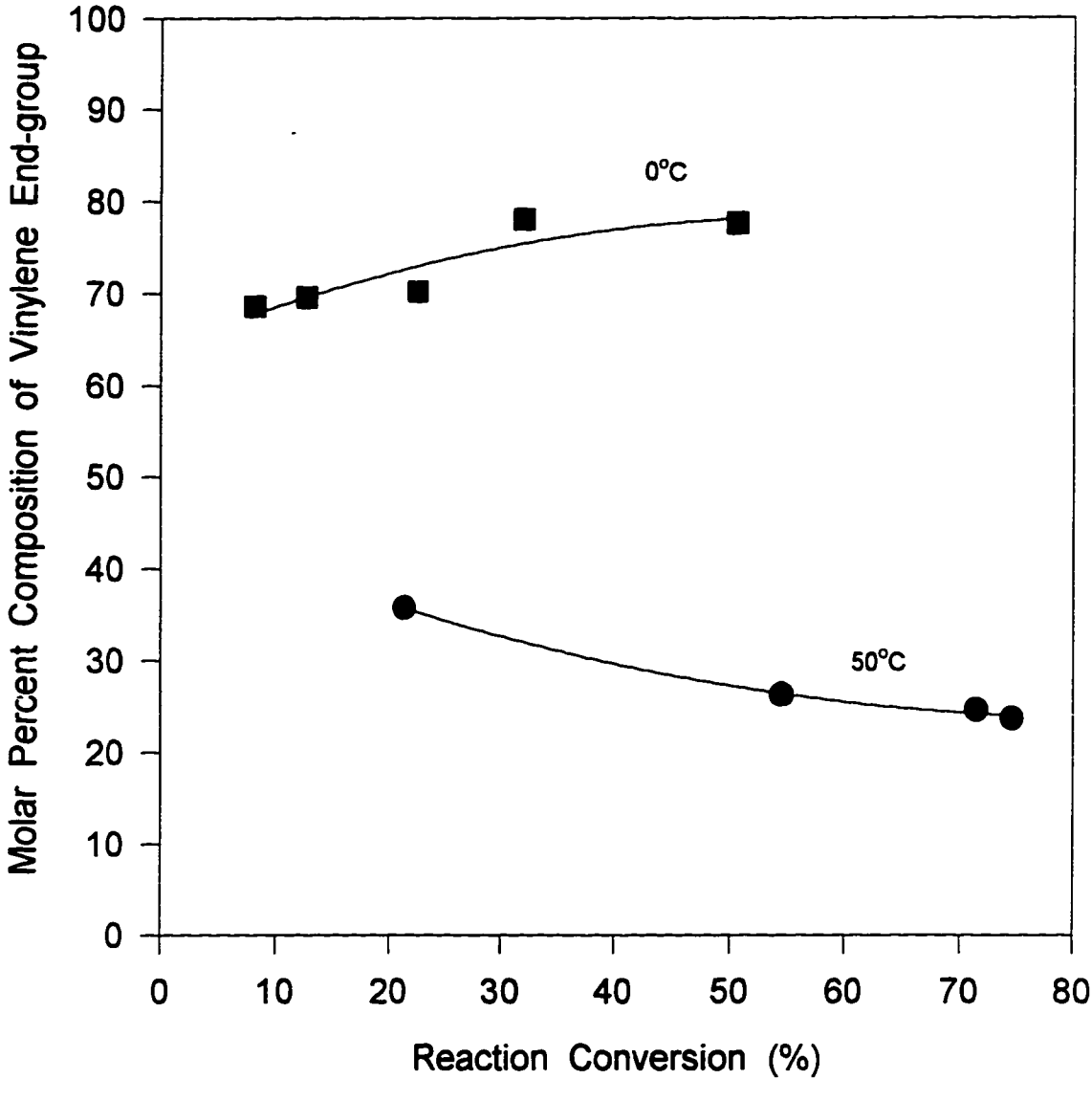

Figure A-73. Molar percent composition of vinylene end-group versus % conversion at different temperature in polymerization of 1-pentene

Polymerization conditions: [Zr]=52μM, [M]=9.1M and [MAO]=62mM,

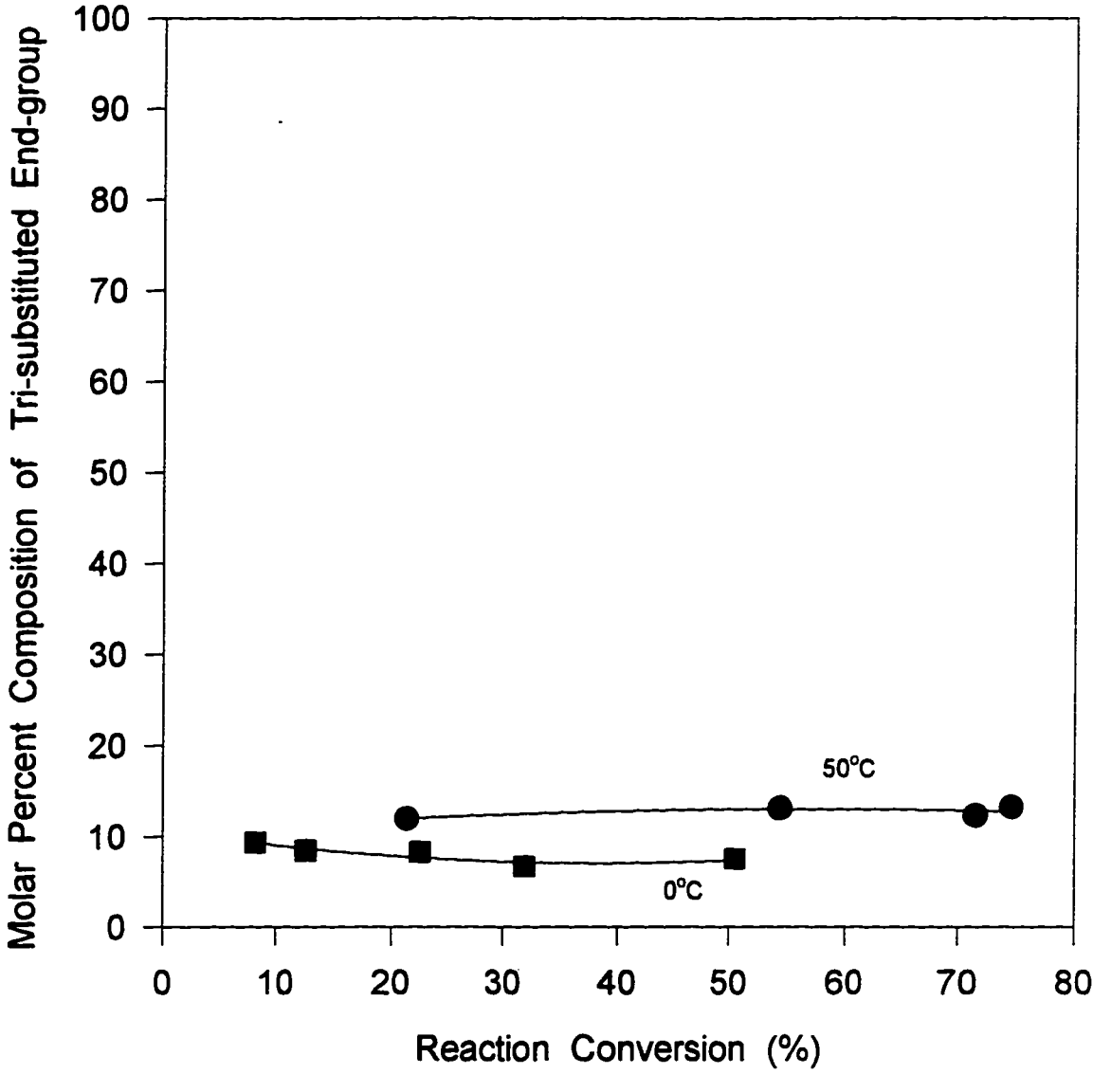

Figure A-74. Molar percent composition of trisubstituted end-group versus % conversion at different temperature in polymerization of 1-pentene

Polymerization conditions: [Zr]=52μM, [M]=9.1M and [MAO]=62mM

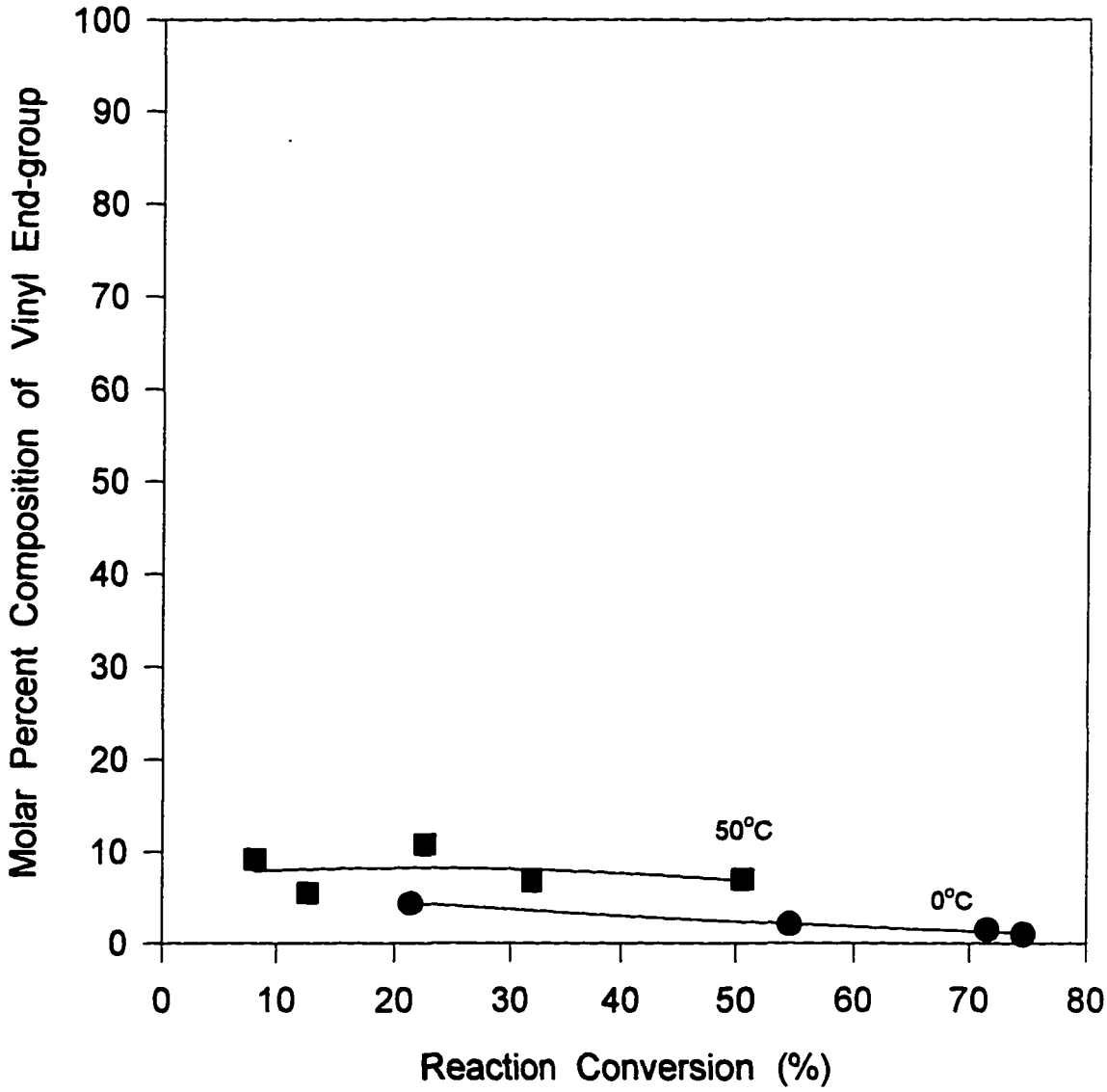

Figure A-75. Molar percent composition of vinyl end-group versus % conversion at different temperatures in polymerization of 1-pentene

Polymerization conditions: [Zr]=52μM, [M]=8.0M and [MAO]=62mM

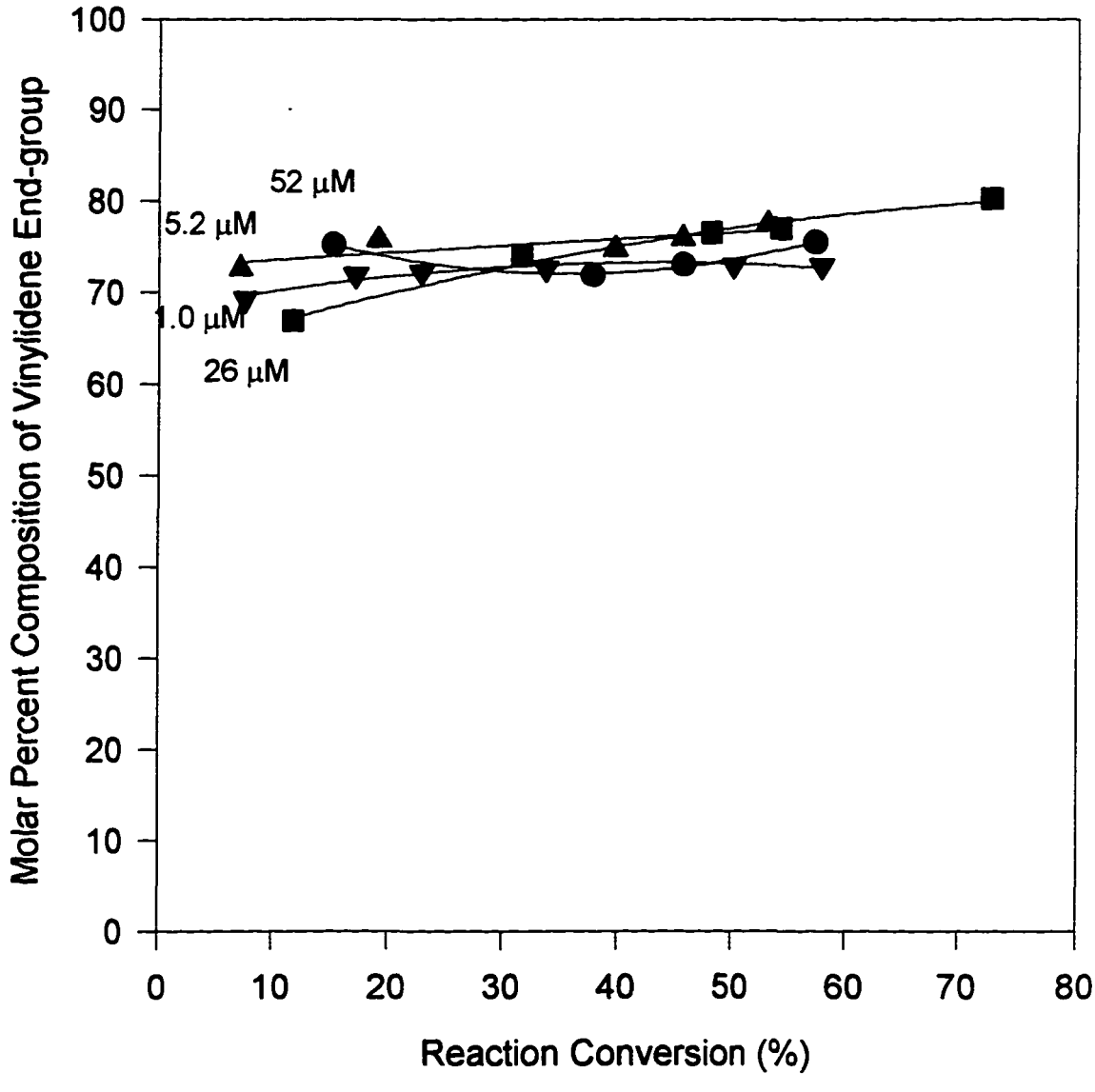

Figure A-76. Molar percent composition of vinylidene end-group versus % conversion at 100°C and different catalyst concentration

Polymerization conditions: [MAO]=62mM, [M]=8.0M and T=100°C
Catalyst concentration is labeled on each curve.

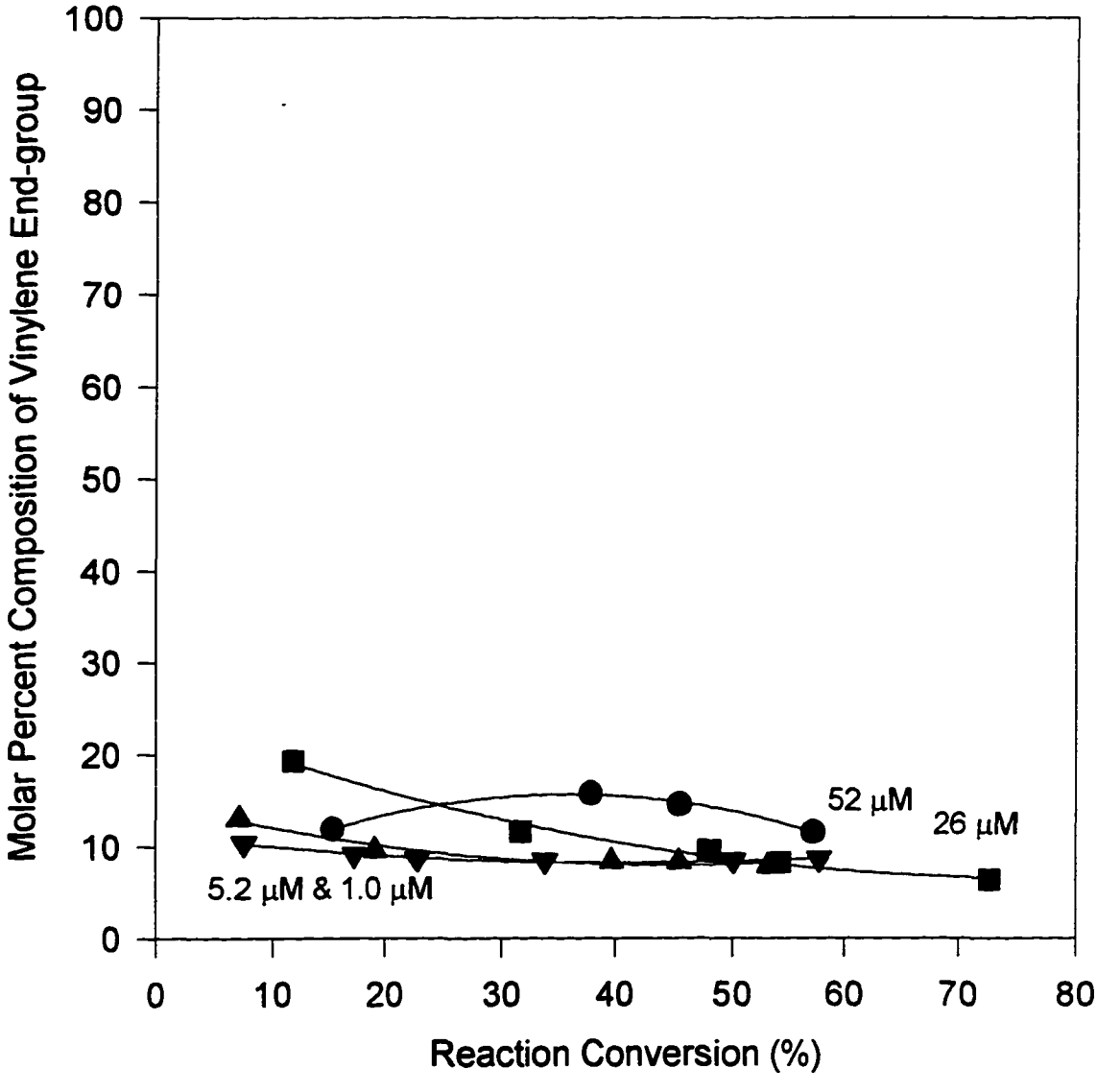

Figure A-77. Molar percent composition of vinylene end-group versus % conversion at 100°C and different catalyst concentration

Polymerization conditions: [MAO]=62mM, [M]=8.0M and T=100°C
Catalyst concentration is labeled on each curve.

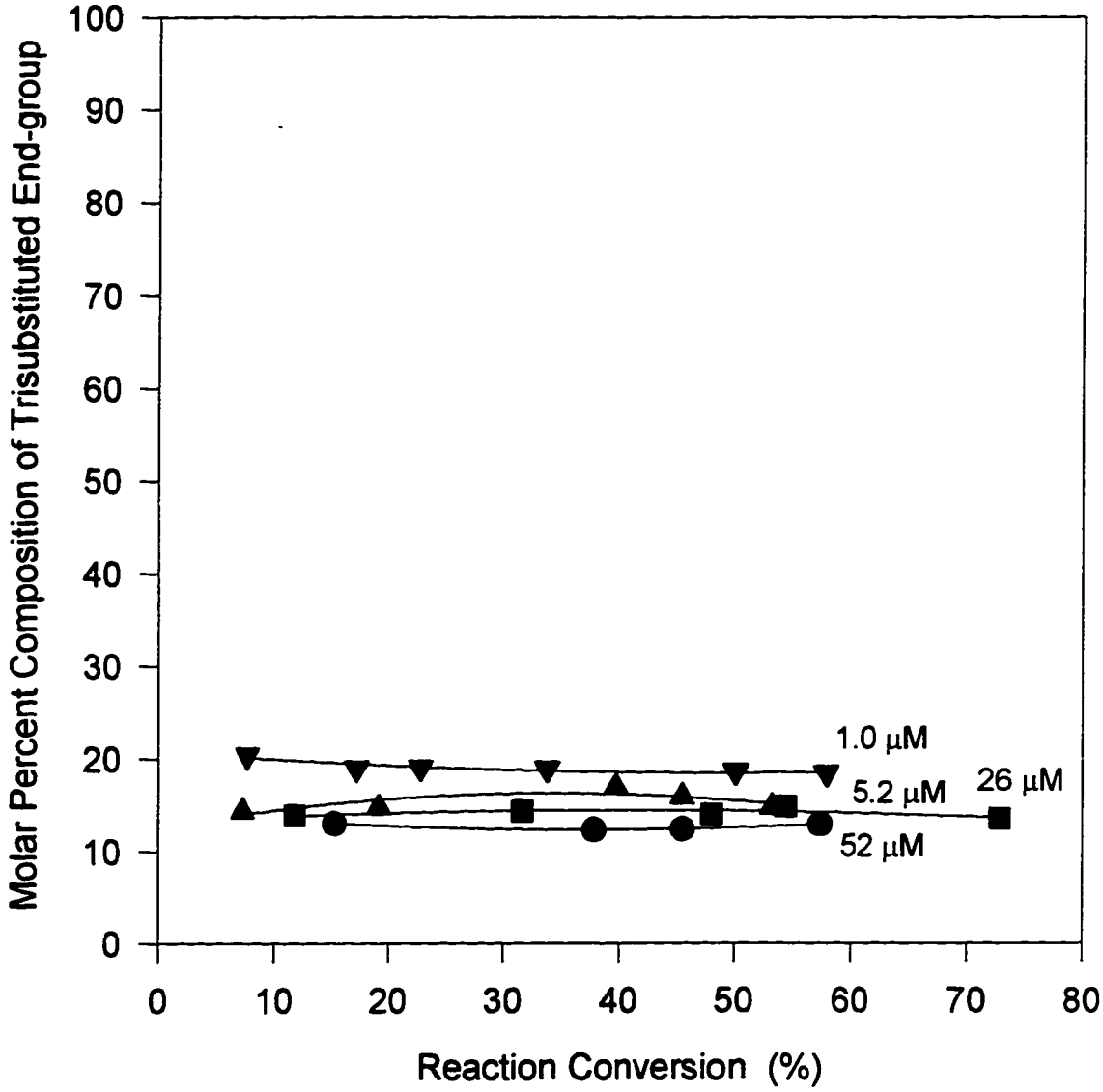

Figure A-78. Molar percent composition of trisubstituted end-group versus % conversion at 100°C and different catalyst concentration

Polymerization conditions: [MAO]=62mM, [M]=8.0M and T=100°C
Catalyst concentration is labeled on each curve.

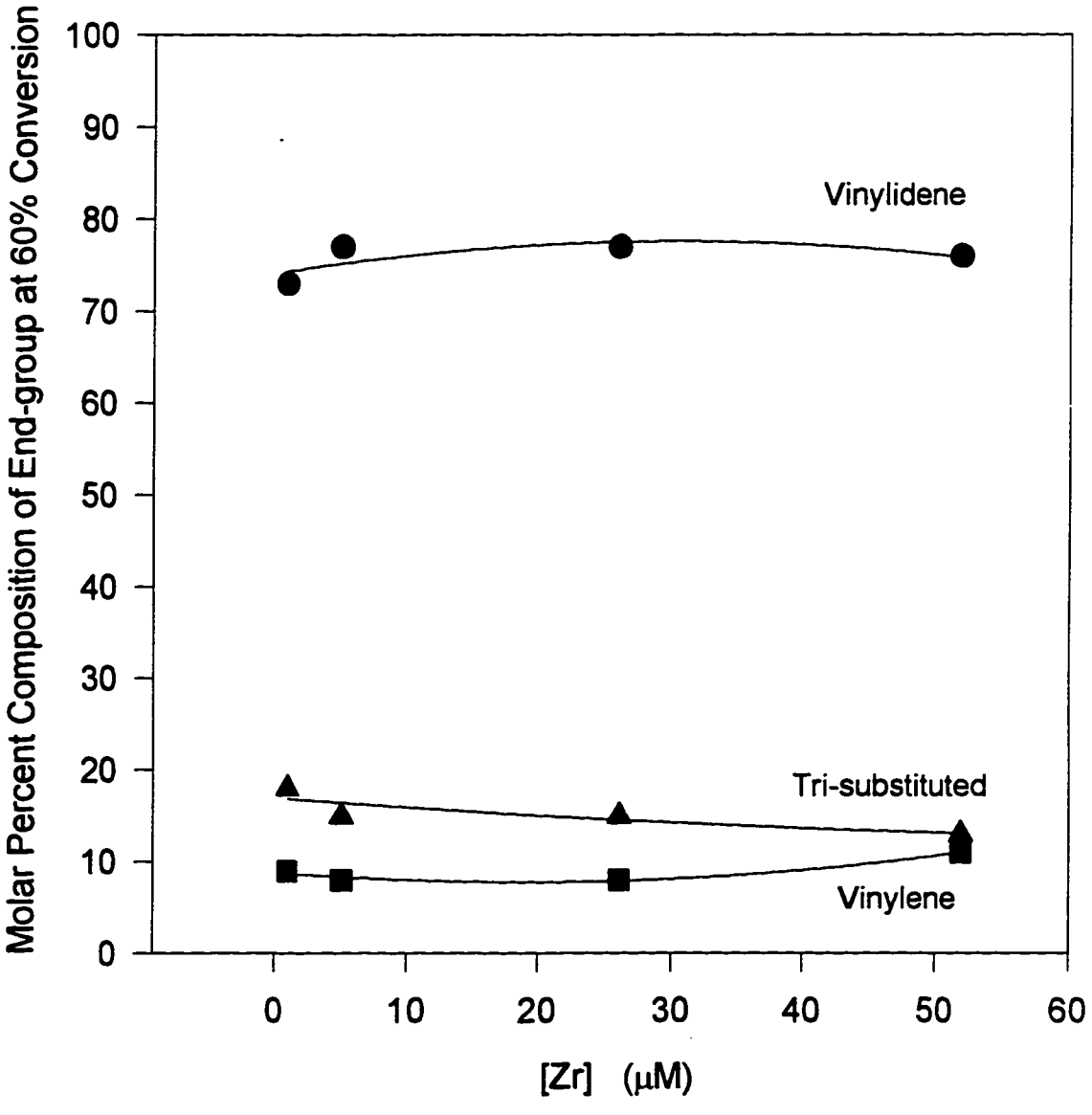

FigureA-79. Molar percent compositions of end-groups as function of catalyst concentration

Polymerization conditions: [MAO]=62mM, [M]=8.0M and T=100°C

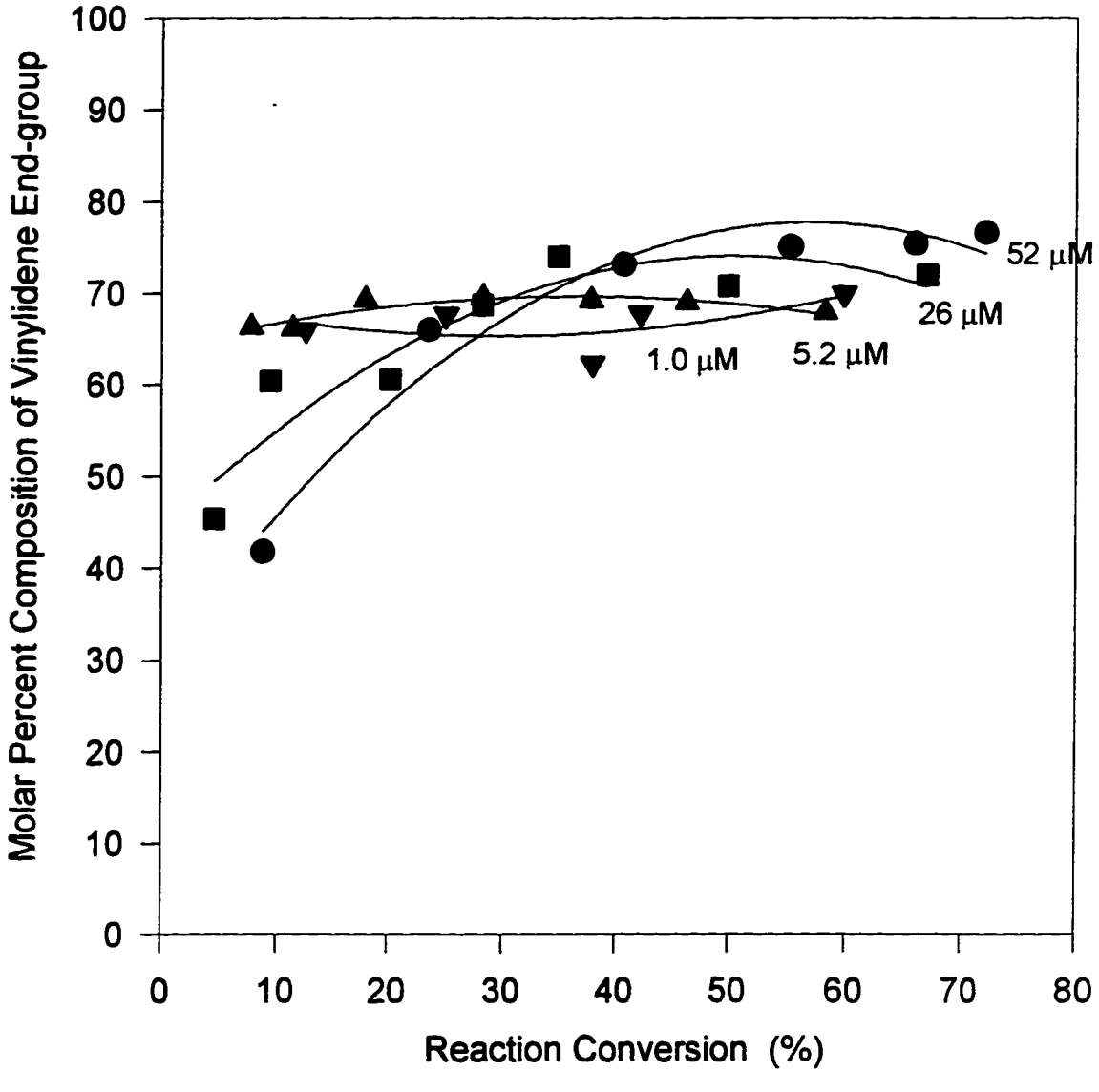

Figure A-80. Molar percent composition of vinylidene end-group versus % conversion at 80°C and different catalyst concentration

Polymerization conditions: [MAO]=62mM, [M]=8.0M and T=80°C
Catalyst concentration is labeled on each curve.

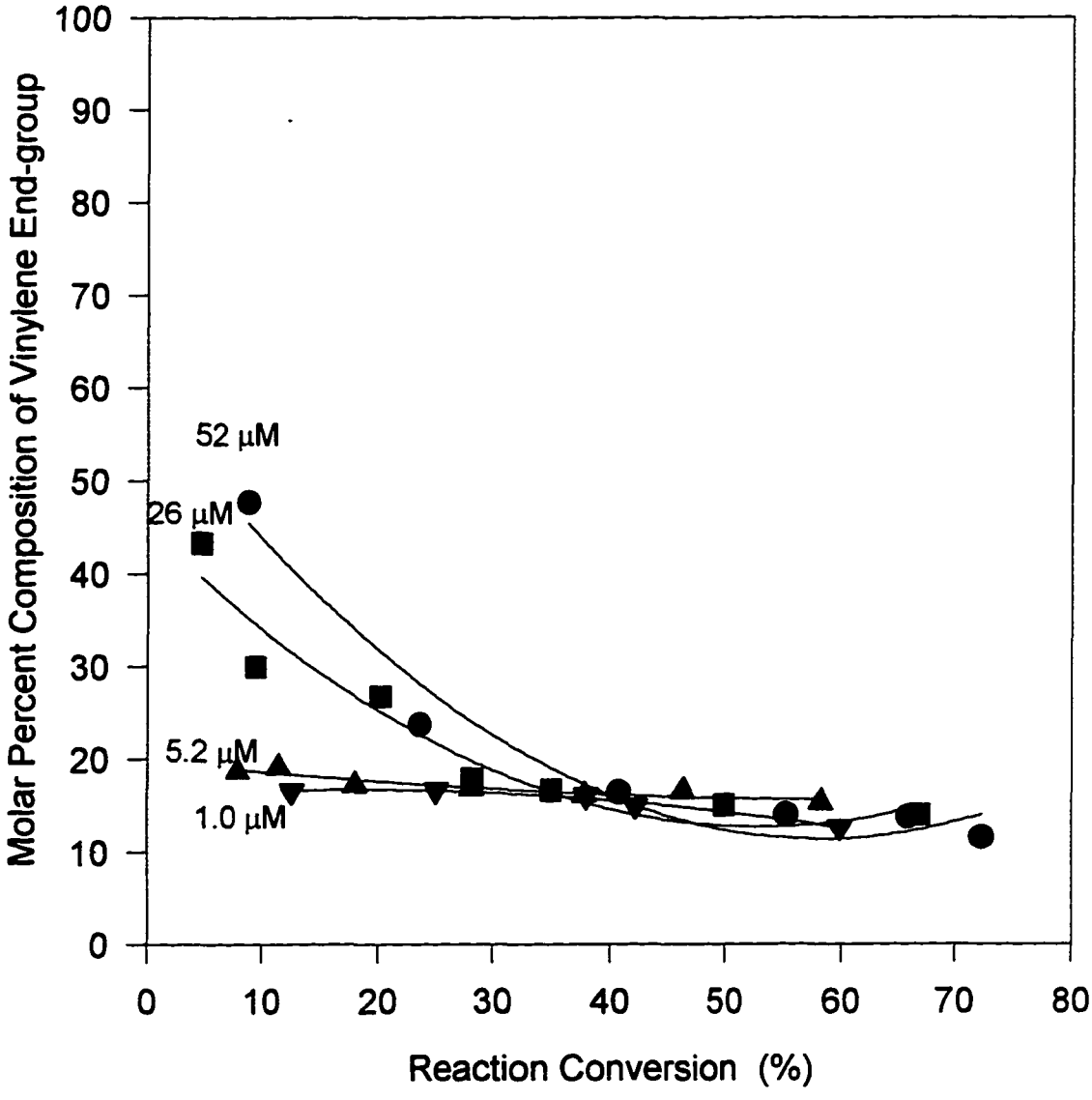

Figure A-81. Molar percent composition of vinylene end-group versus % conversion at 80°C and different catalyst concentration

Polymerization conditions: [MAO]=62mM, [M]=8.0M and T=80°C
Catalyst concentration is labeled on each curve.

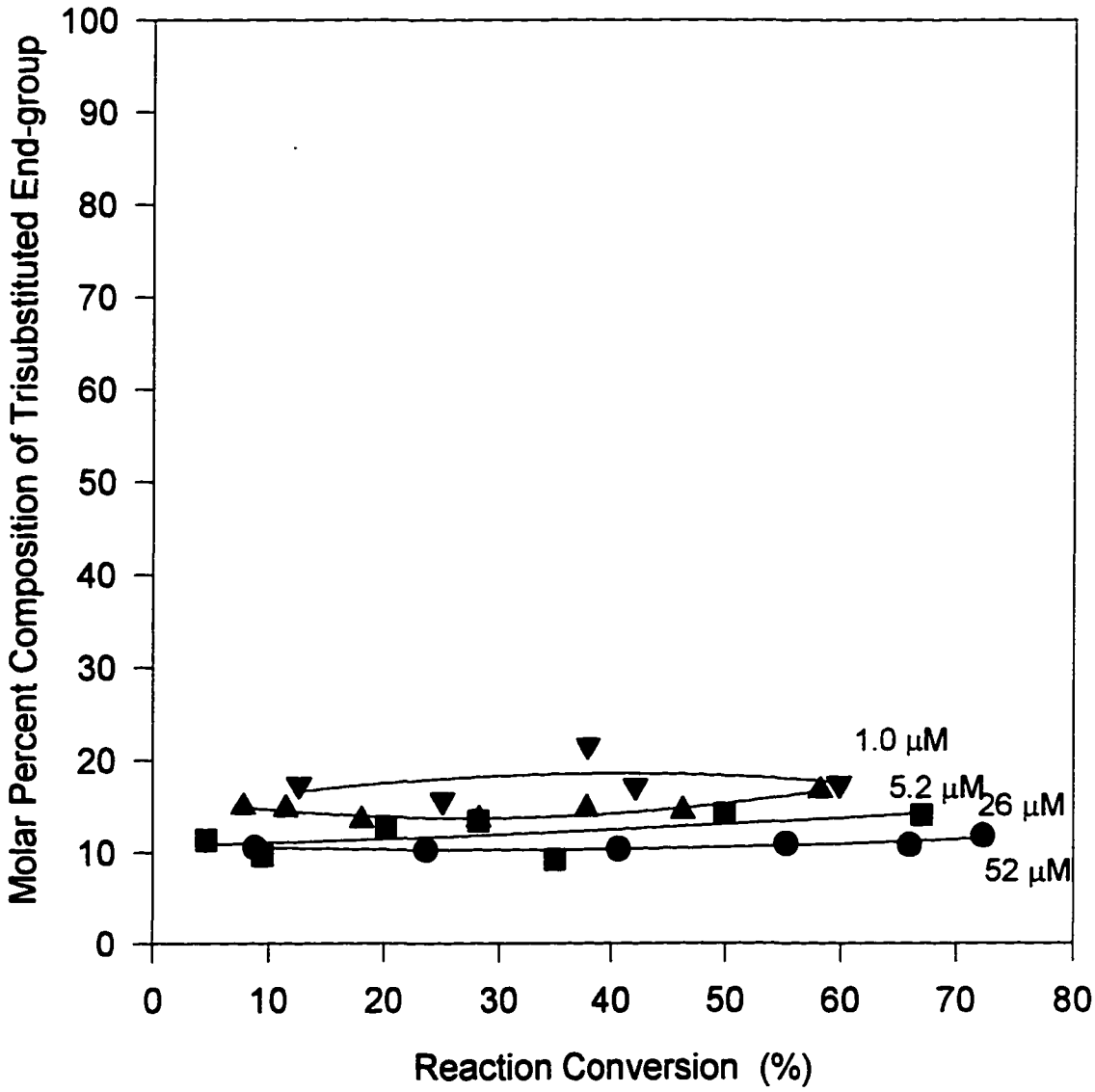

Figure A-82. Molar percent composition of trisubstituted end-group versus % conversion at 80°C and different catalyst concentration

Polymerization conditions: [MAO]=62mM, [M]=8.0M and T=80°C
Catalyst concentration is labeled on each curve.

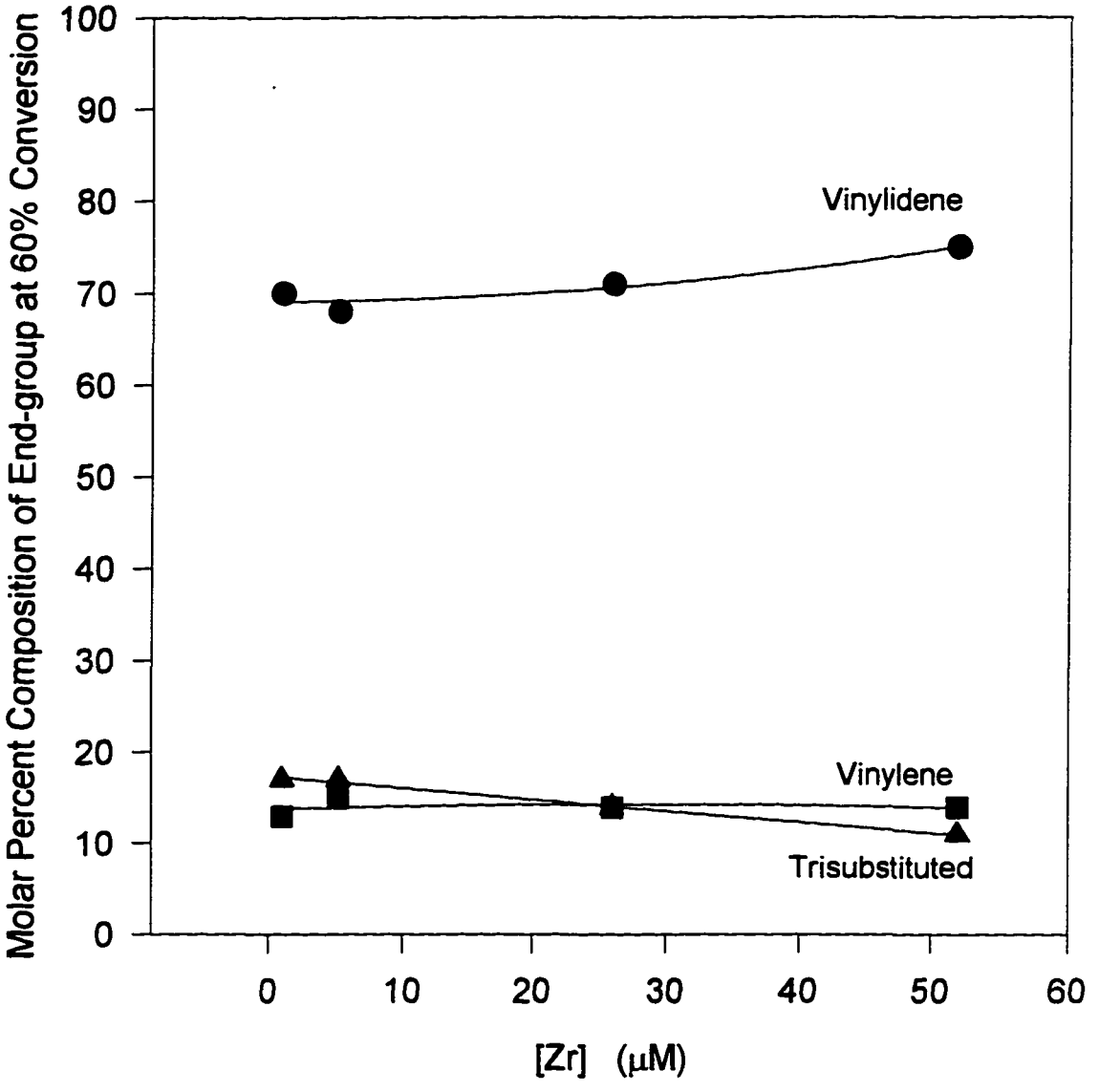

Figure A-83. Molar percent compositions of end-groups as function of catalyst concentration

Polymerization conditions: [MAO]=62mM, [M]=8.0M and T=80°C

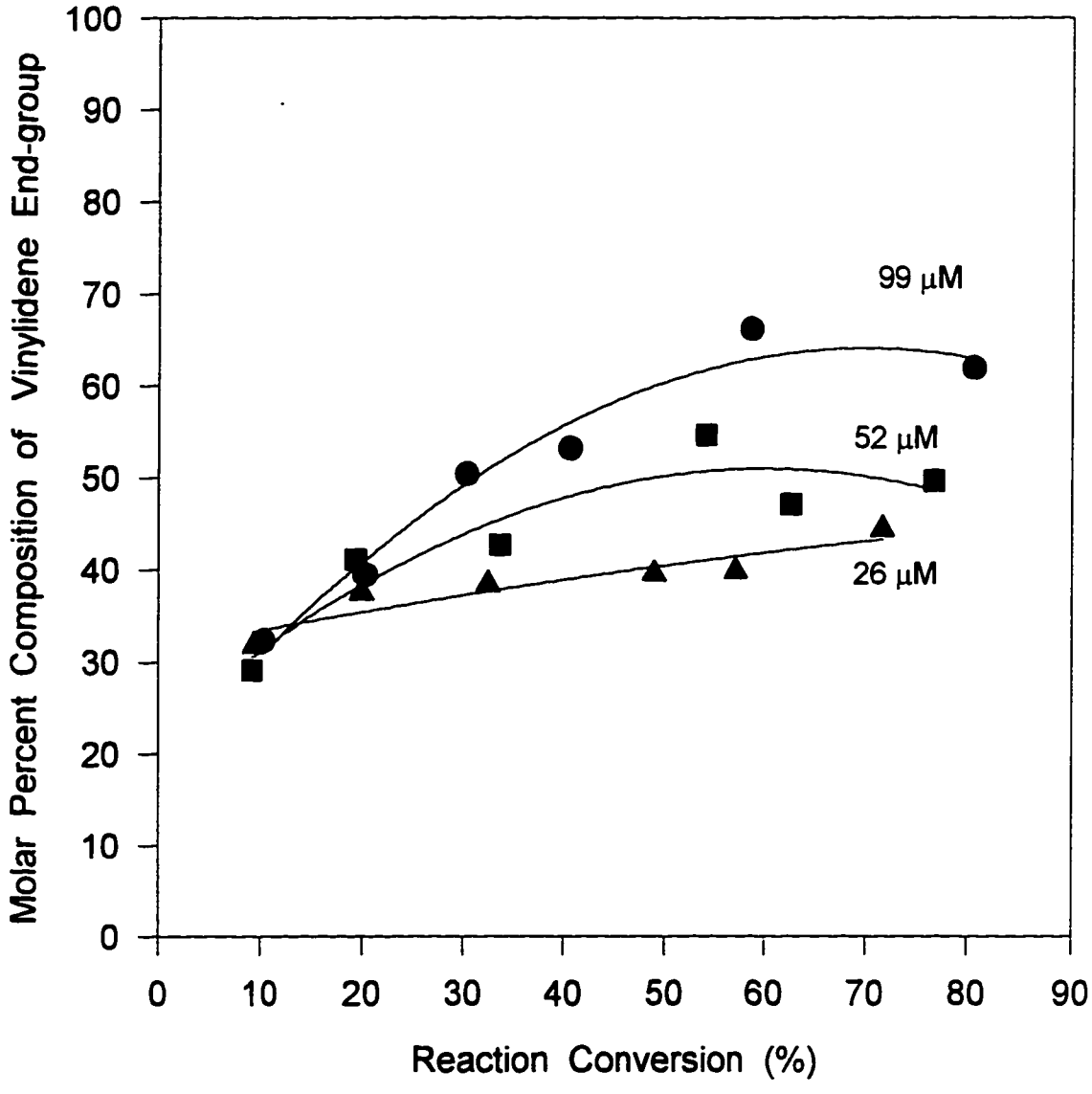

Figure A-84. Molar percent composition of vinylidene end-group versus % conversion at 50°C and different catalyst concentration

Polymerization conditions: [MAO]=62mM, [M]=8.0M and T=50°C
Catalyst concentration is labeled on each curve.

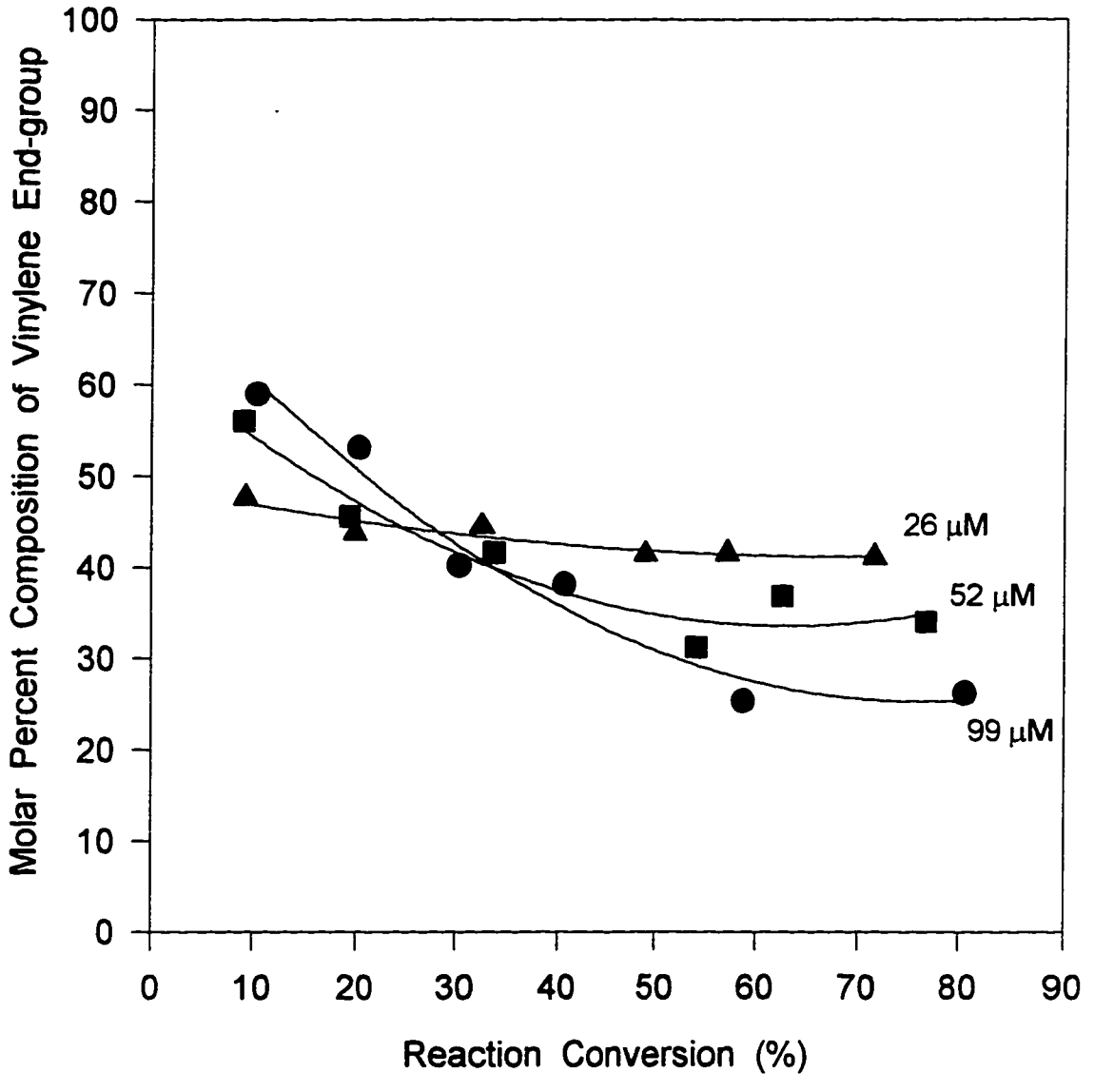

Figure A-85. Molar percent composition of vinylene end-group versus % conversion at 50°C and different catalyst concentrations

Polymerization conditions: [M]=8.0M, [MAO]=62mM and T=50°C

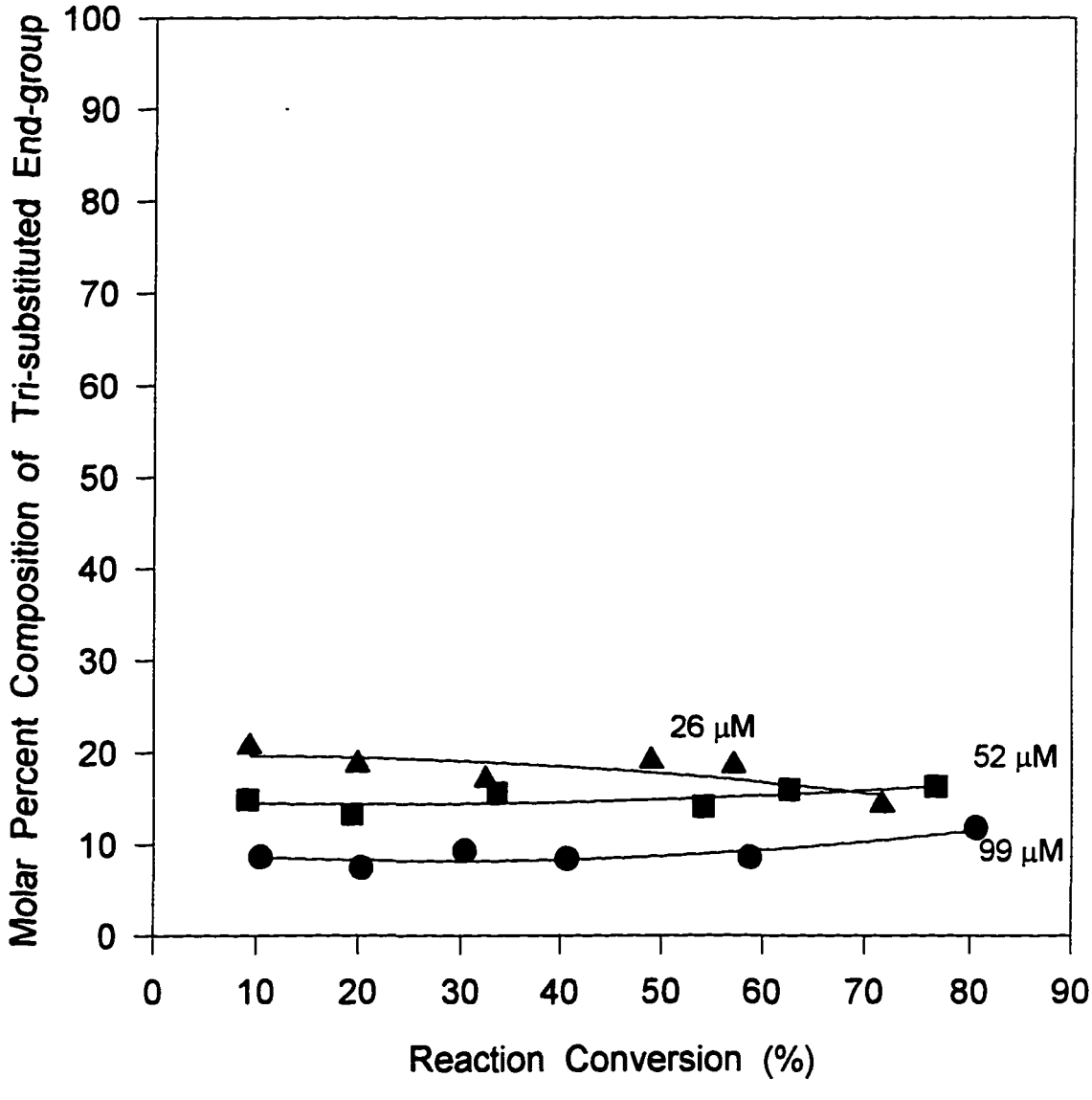

Figure A-86. Molar percent composition of trisubstituted end-group versus % conversion at 50°C and different catalyst concentration

Polymerization conditions: [M]=8.0M, [MAO]=62mM and T=50°C

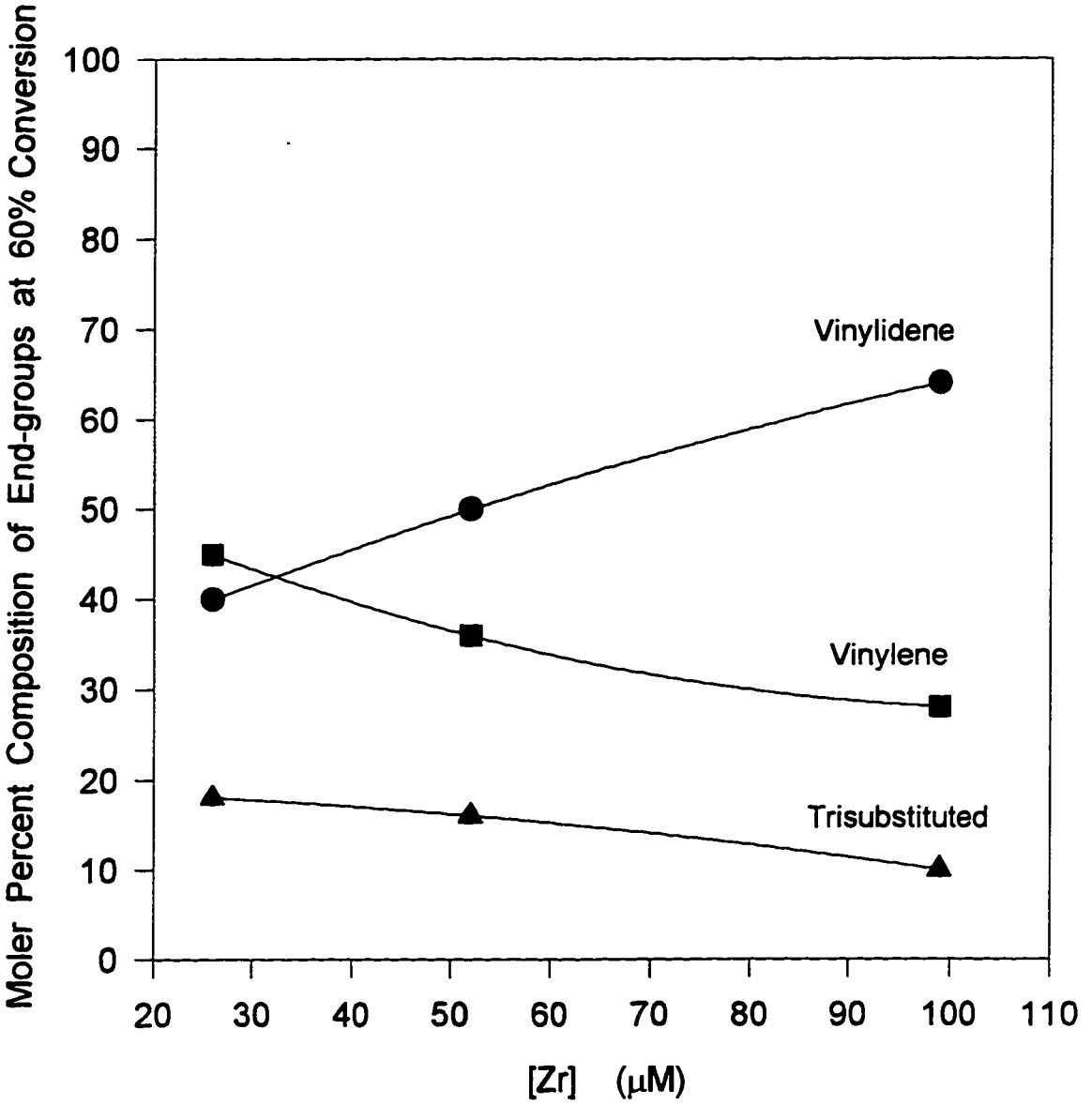

Figure A-87. Molar percent compositions of end-groups as function of catalyst concentration

Polymerization conditions: [M]=8.0M, [MAO]=62mM and T=50°C

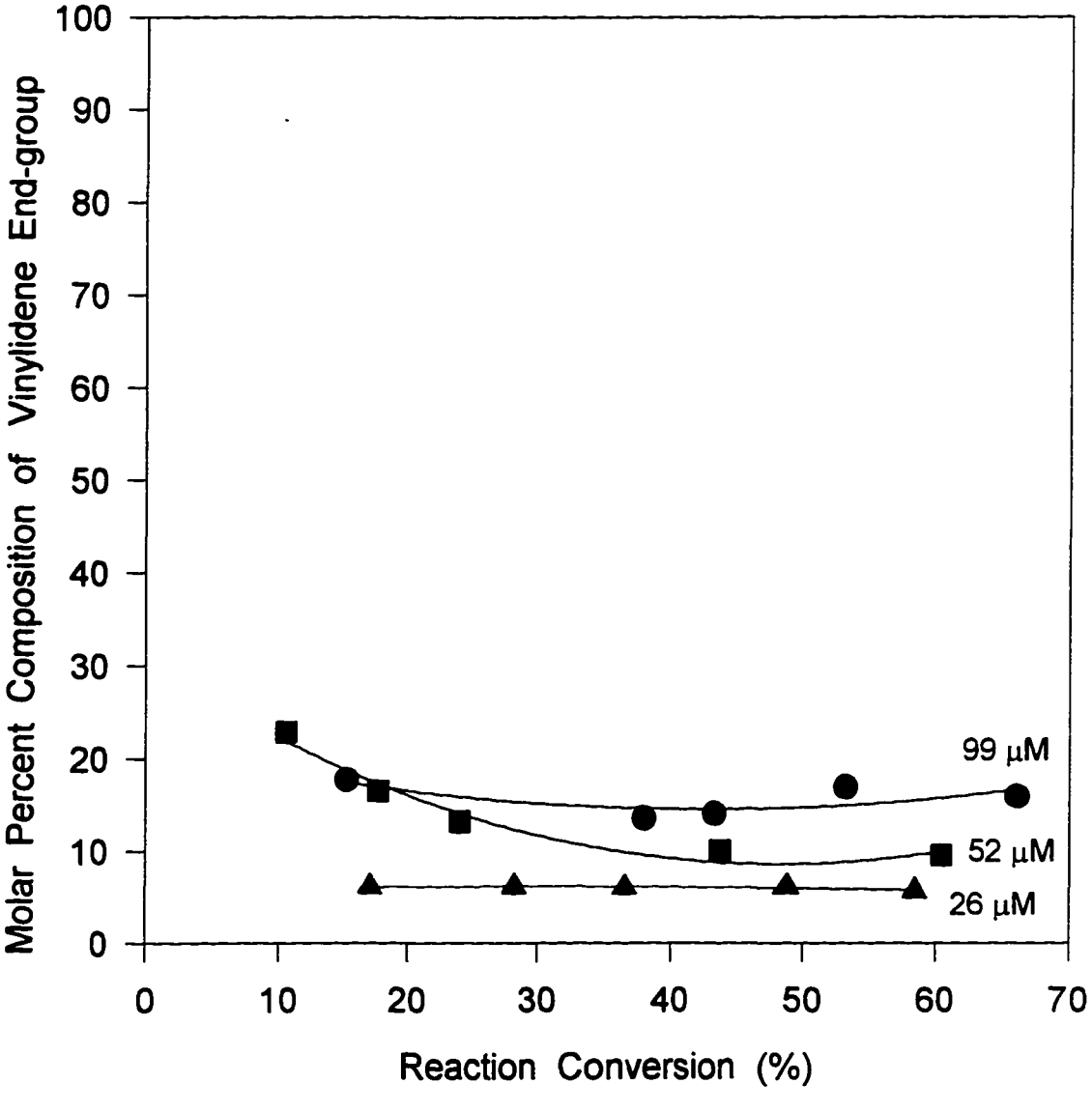

Figure A-88. Molar percent composition of vinylidene end-group versus % conversion at 0°C and different catalyst concentrations

Polymerization conditions: [M]=8.0M, [MAO]=62mM and T=0°C

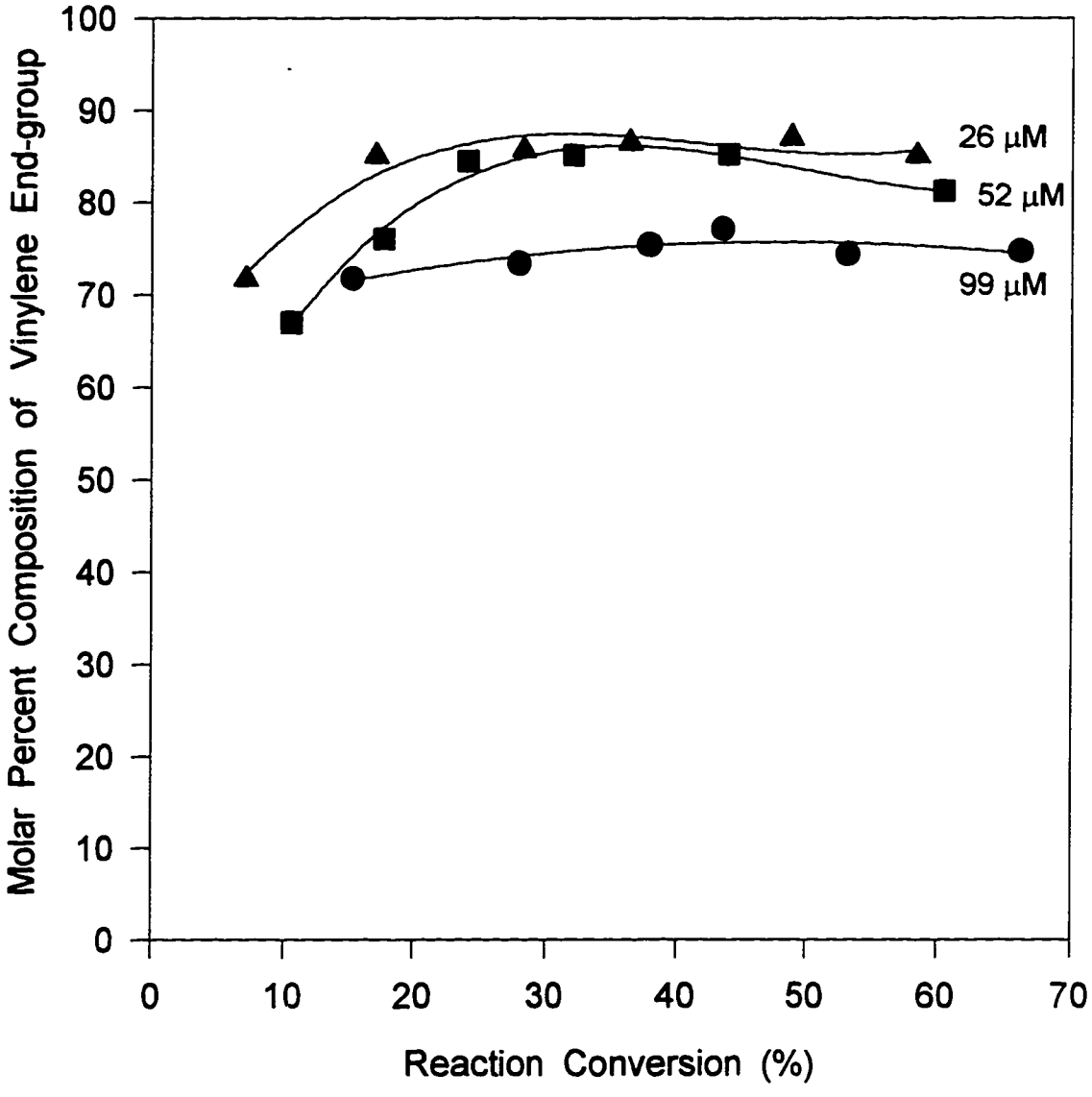

Figure A-89. Molar percent composition of vinylene end-group versus % conversion at 0°C and different catalyst concentrations

Polymerization conditions: [M]=8.0M, [MAO]=62mM and T=0°C

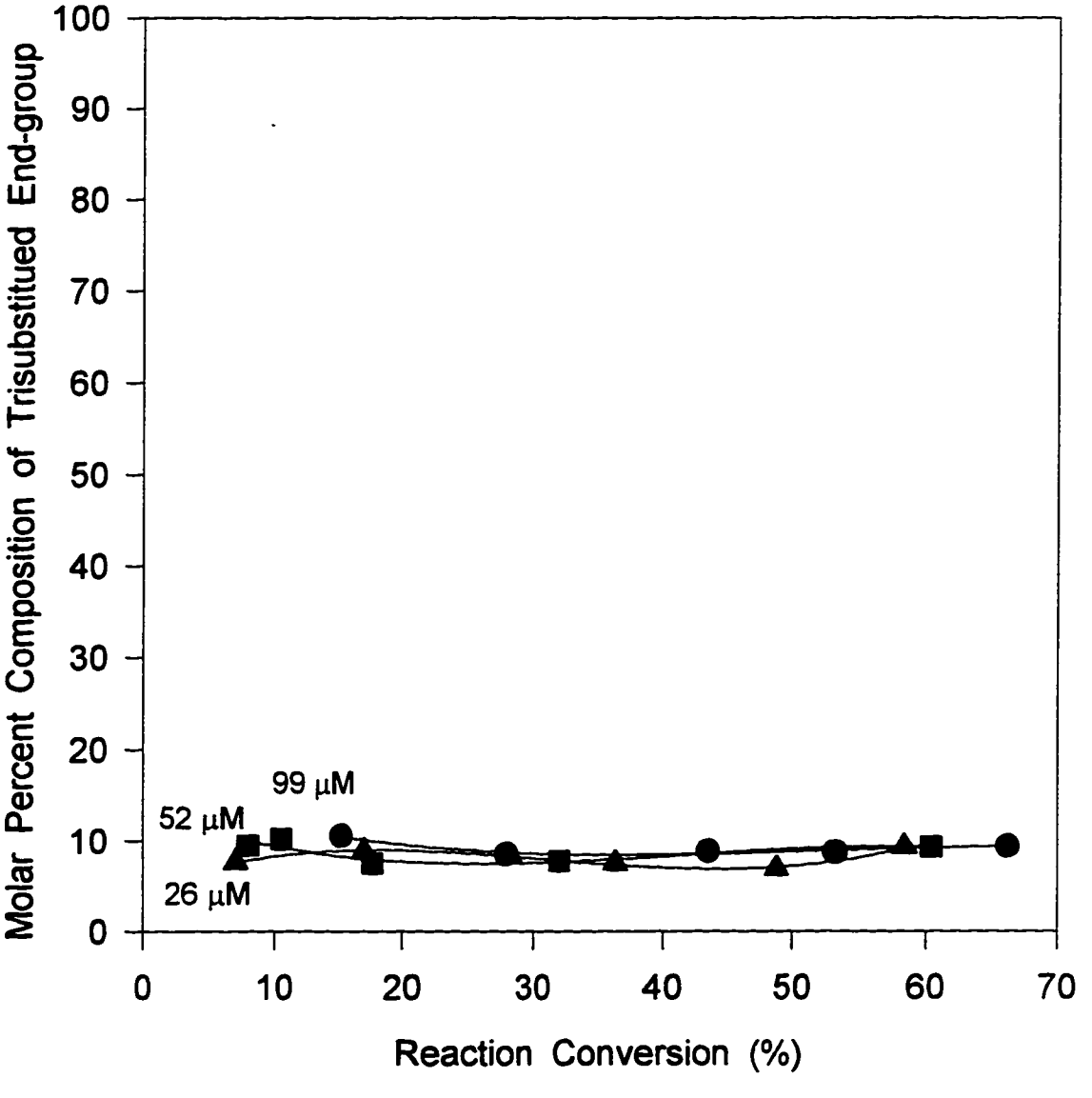

Figure A-90. Molar percent composition of trisubstituted end-group versus % conversion at 0°C and different catalyst concentrations

Polymerization conditions: [M]=8.0M, [MAO]=62mM and T=0°C

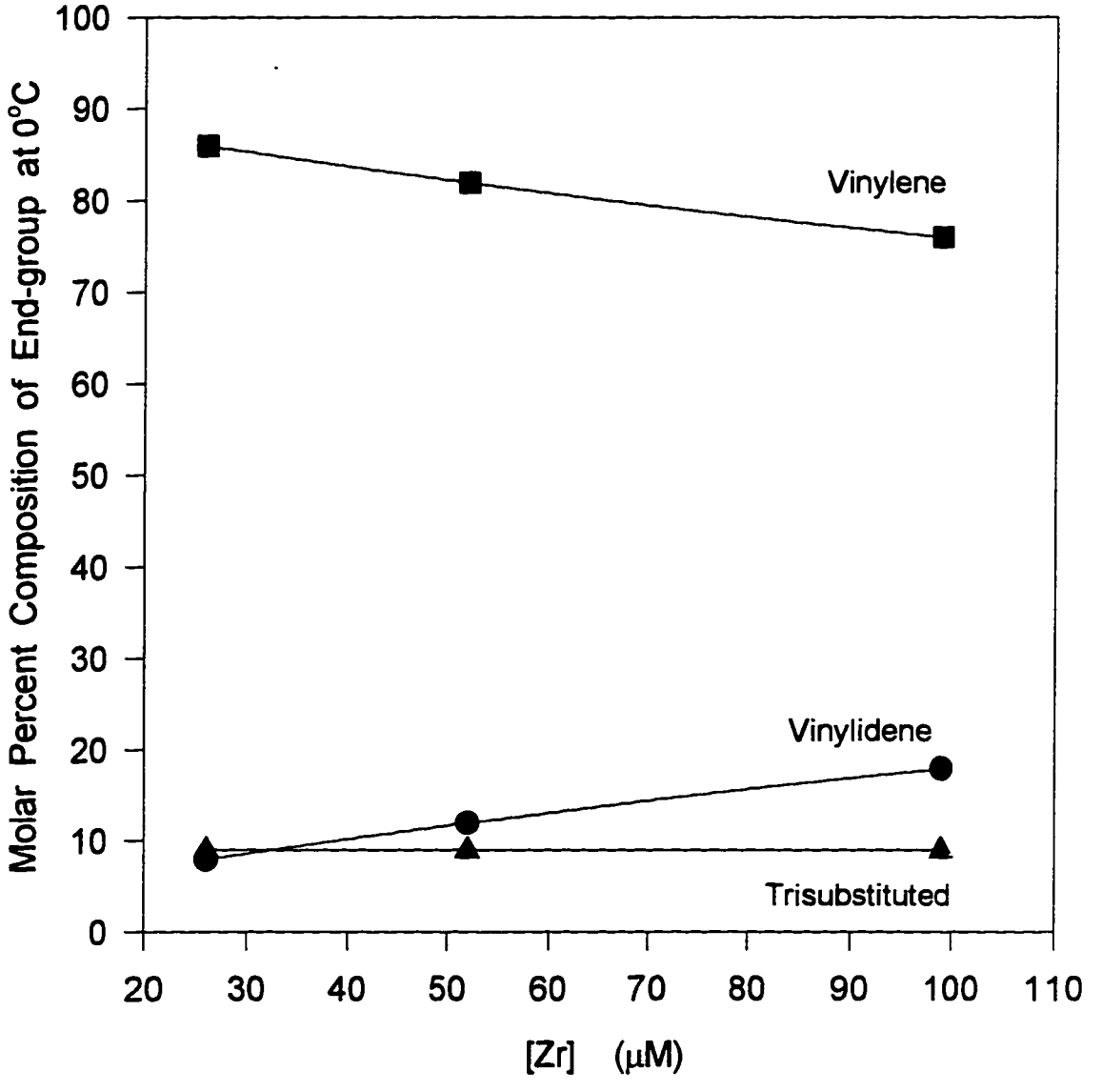

Figure A-91. Molar percent composition of end-groups as function of catalyst concentration at 0°C

Polymerization conditions: [M]=8.0M, [MAO]=62mM and T=0°C

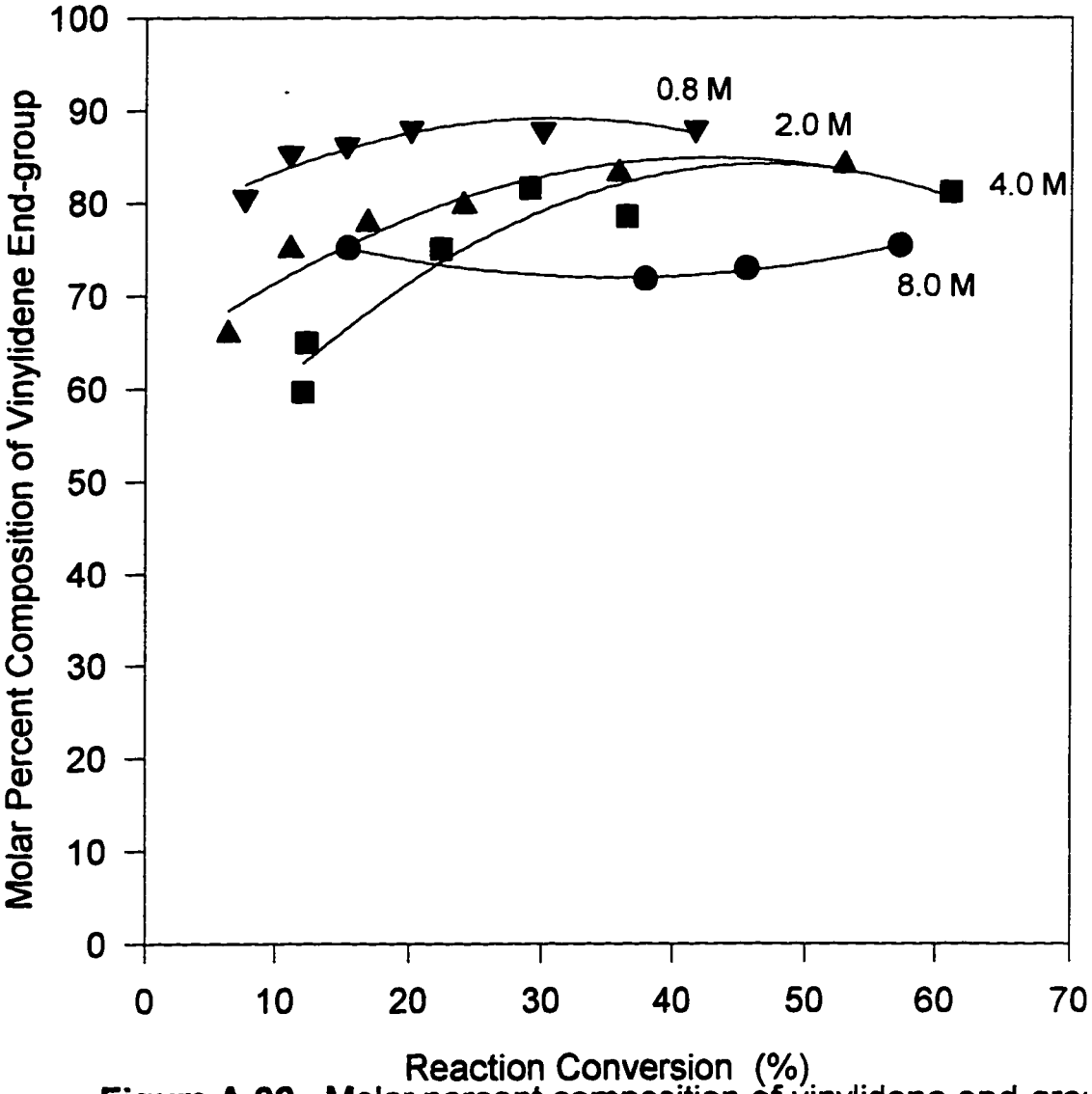

Figure A-92. Molar percent composition of vinylidene end-group versus % conversion at 100°C and different monomer concentration

Polymerization conditions: [Zr]=52μM, [MAO=62mM and T=100°C
Monomer concentration is labeled on each curve.

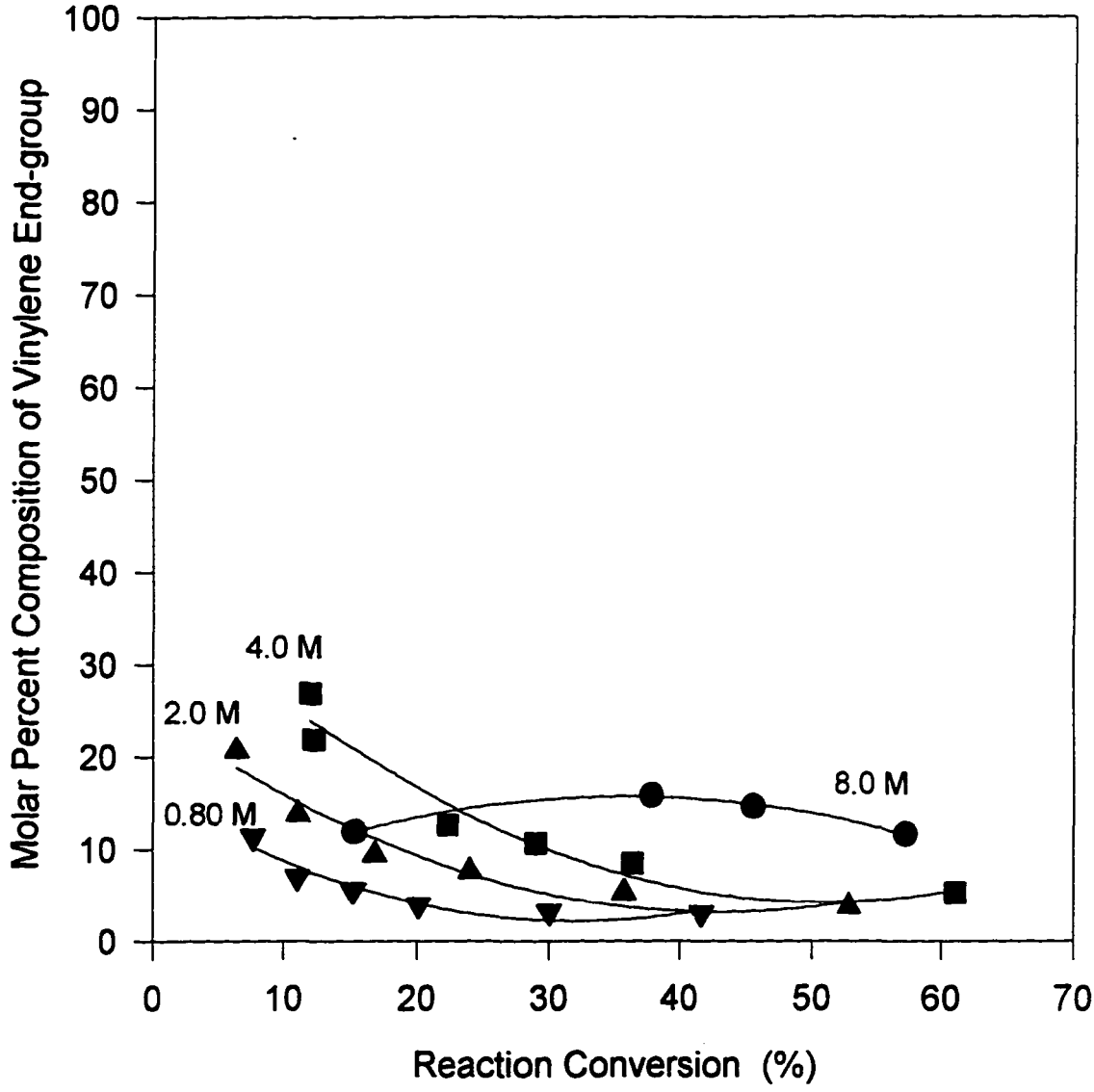

Figure A-93. Molar percent composition of vinylene end-group versus % conversion at 100°C and different monomer concentration

Polymerization conditions: [Zr]=52μM, [MAO]=62mM and T=100°C
Monomer concentration is labeled on each curve.

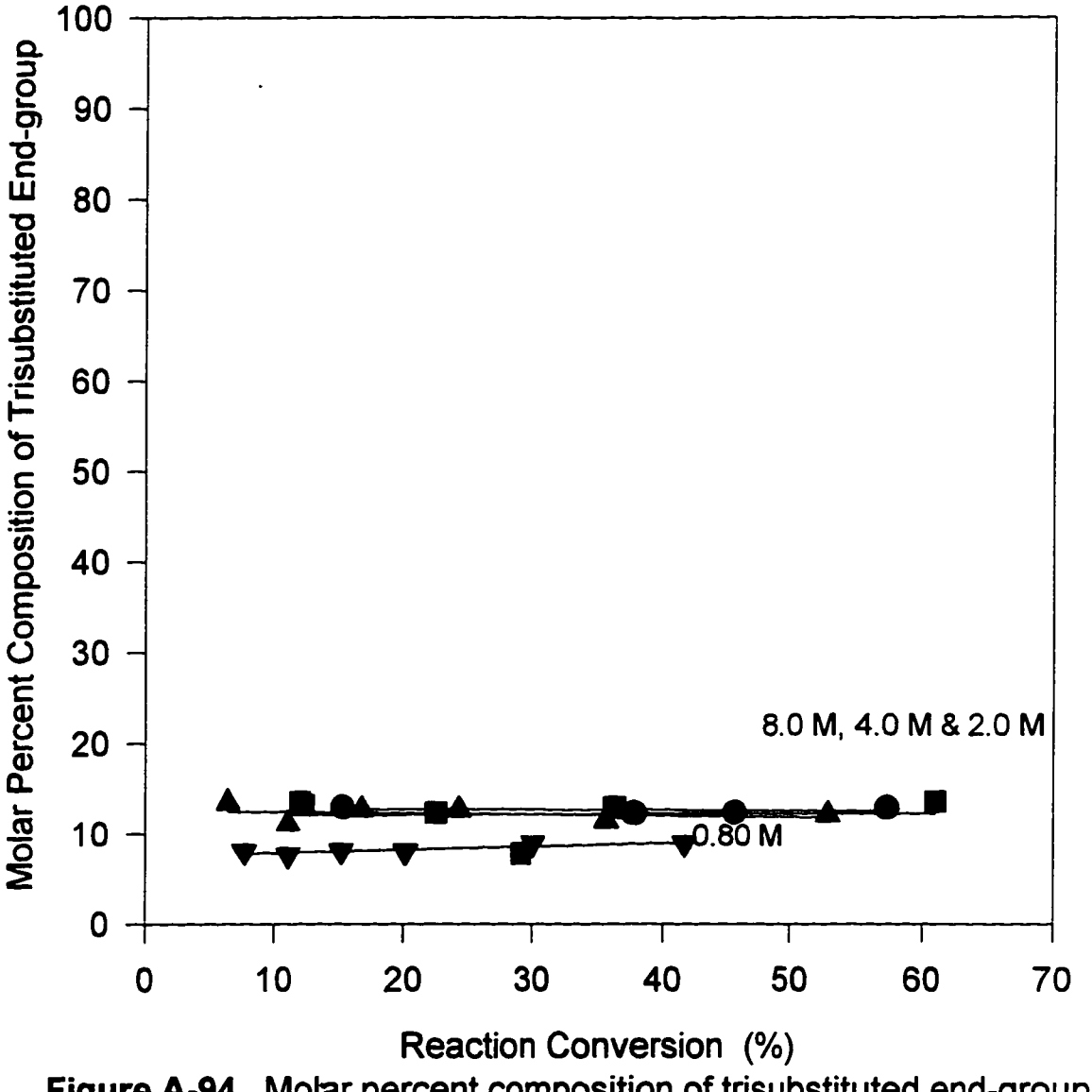

Figure A-94. Molar percent composition of trisubstituted end-group versus % conversion at 100°C and different monomer concentration

Polymerization conditions: [Zr]=52μM, [MAO]=62mM and T=100°C
Monomer concentration is labeled on each curve.

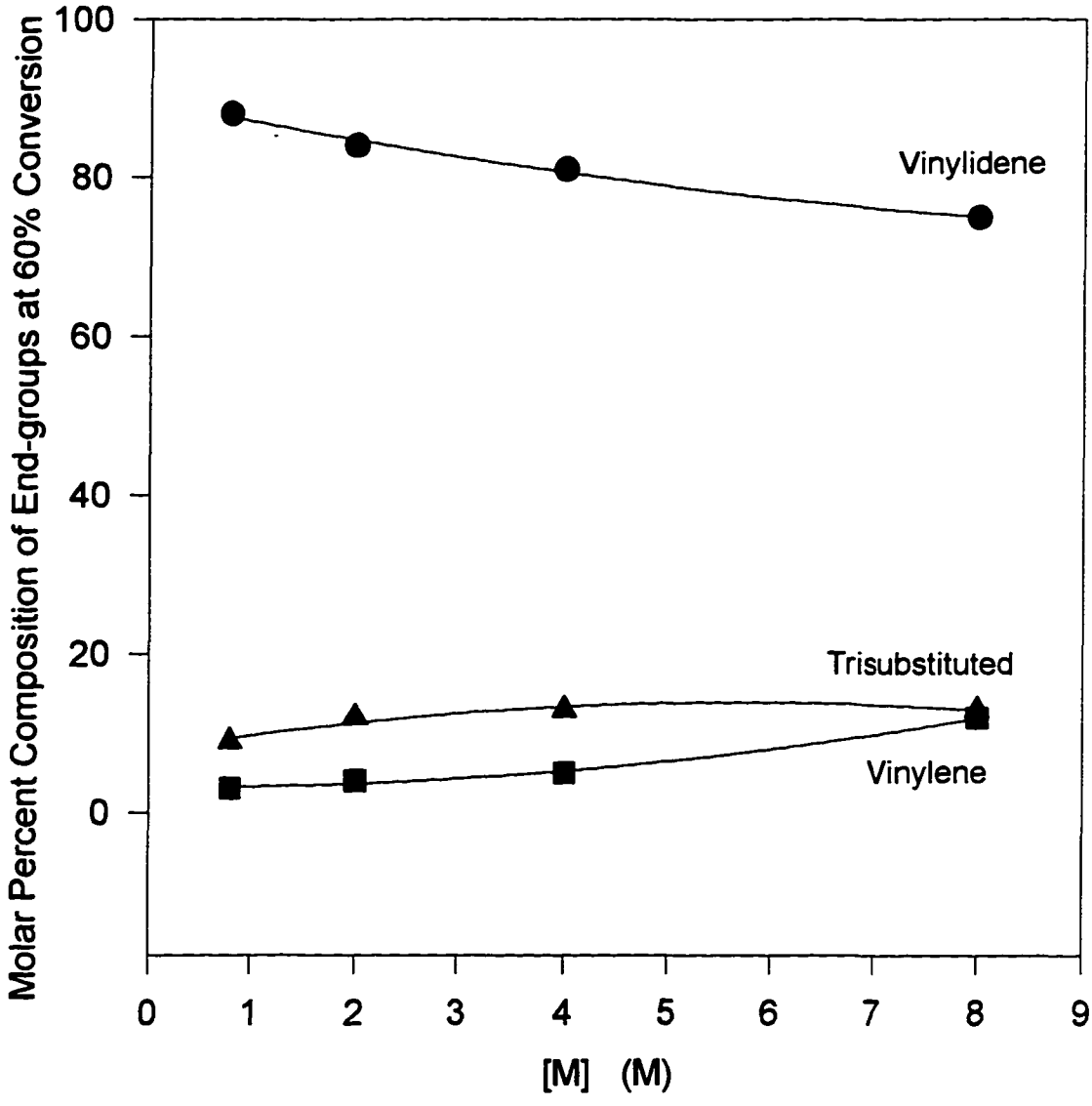

Figure A-95. Molar percent compositions of end-groups as function of monomer concentration

Polymerization conditions: [Zr]=52μM, [MAO]=62mM and T=100°C

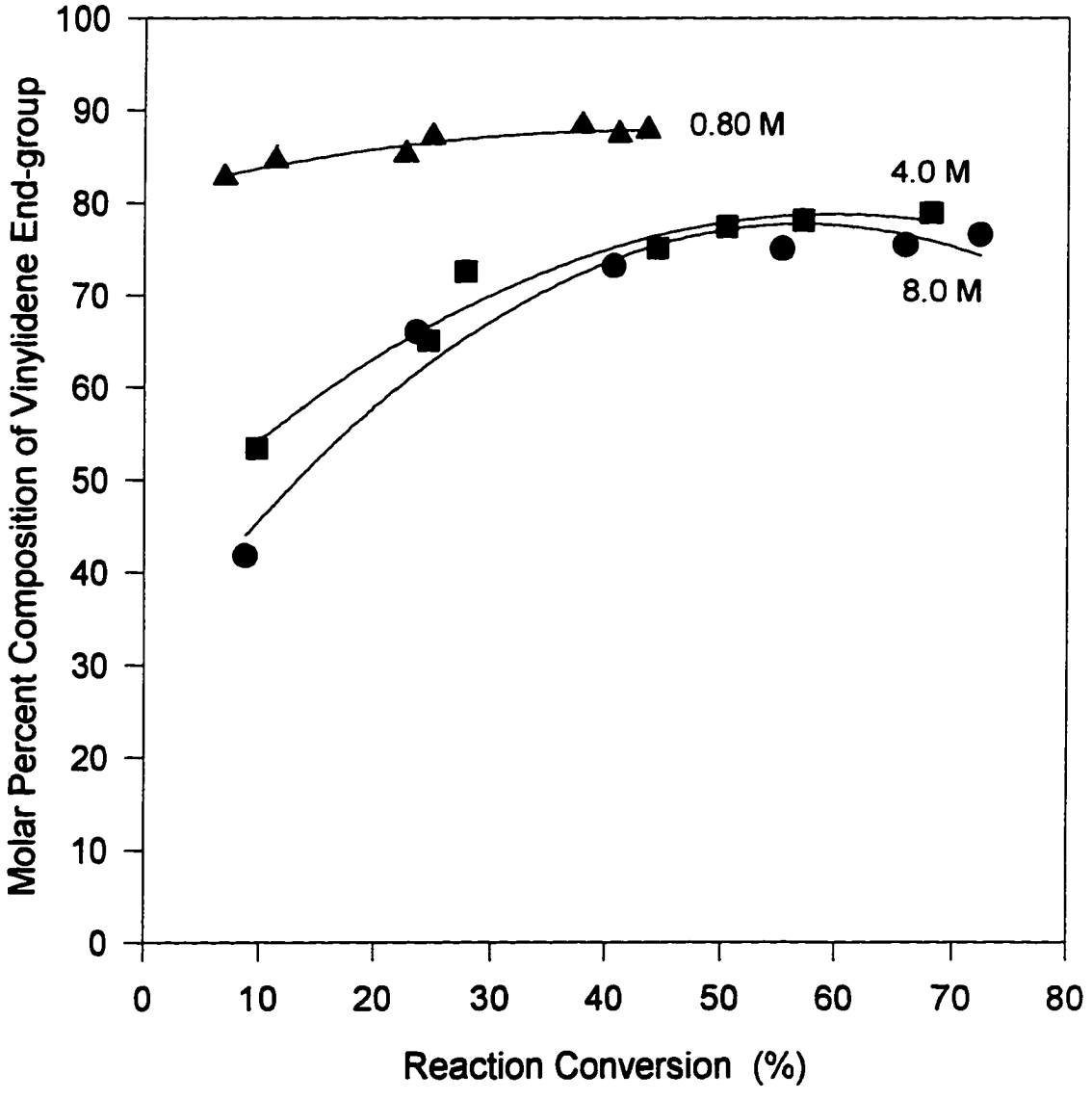

Figure A-96. Molar percent composition of vinylidene end-group versus % conversion at 80°C and different monomer concentration

Polymerization conditions: [Zr]=52μM, [MAO]=62mM and T=80°C
Monomer concentration is labeled on each curve.

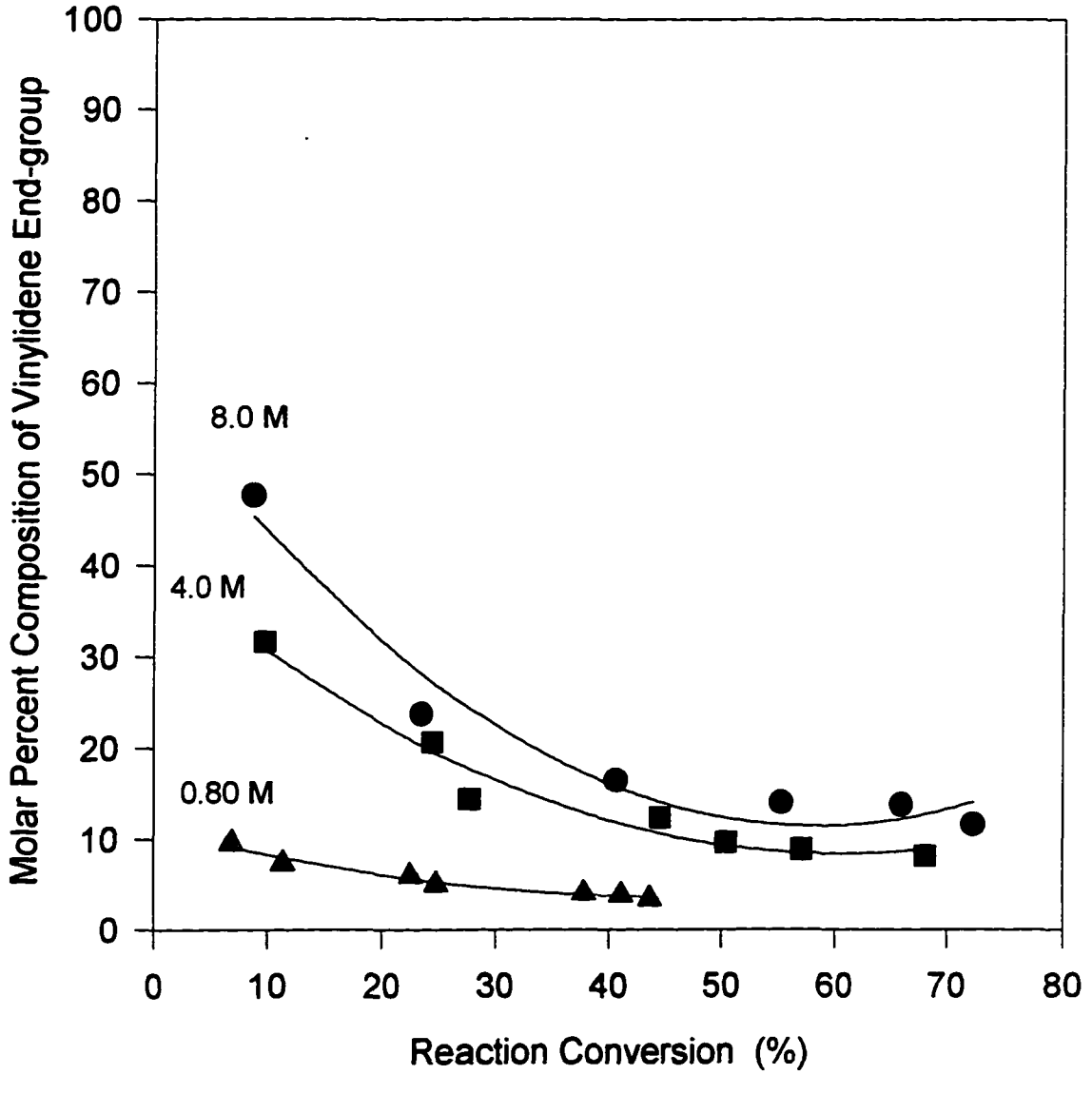

Figure A-97. Molar percent composition of vinylene end-group versus % conversion at 80°C and different monomer concentration

Polymerization conditions: [Zr]=52μM, [MAO]=62mM and T=80°C

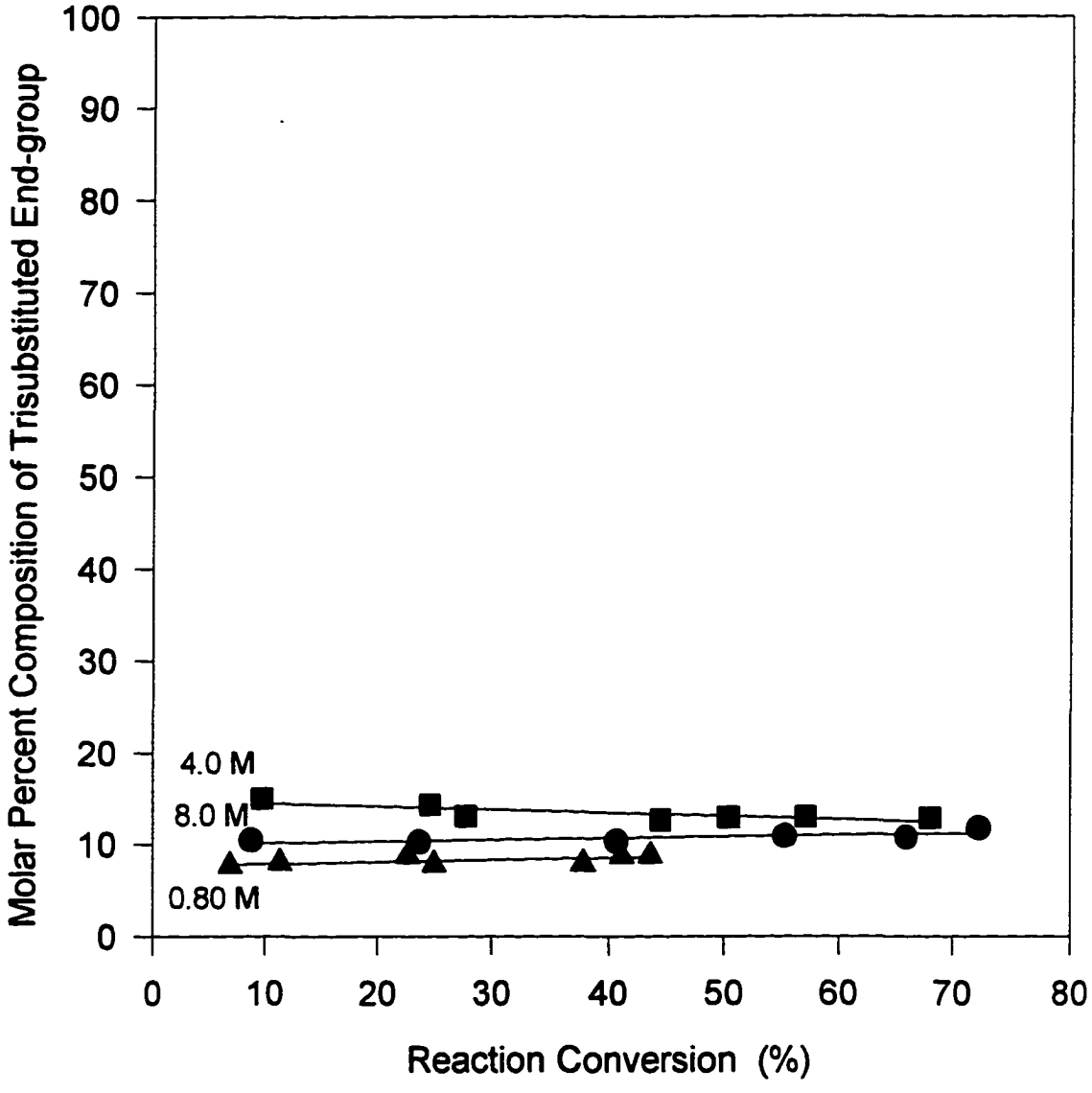

Figure A-98. Molar percent composition of trisubstituted end-group versus % conversion at 80°C and different monomer concentration

Polymerization conditions: [Zr]=52μM, [MAO]=62mM and T=80°C
Monomer concentration is labeled on each curve.

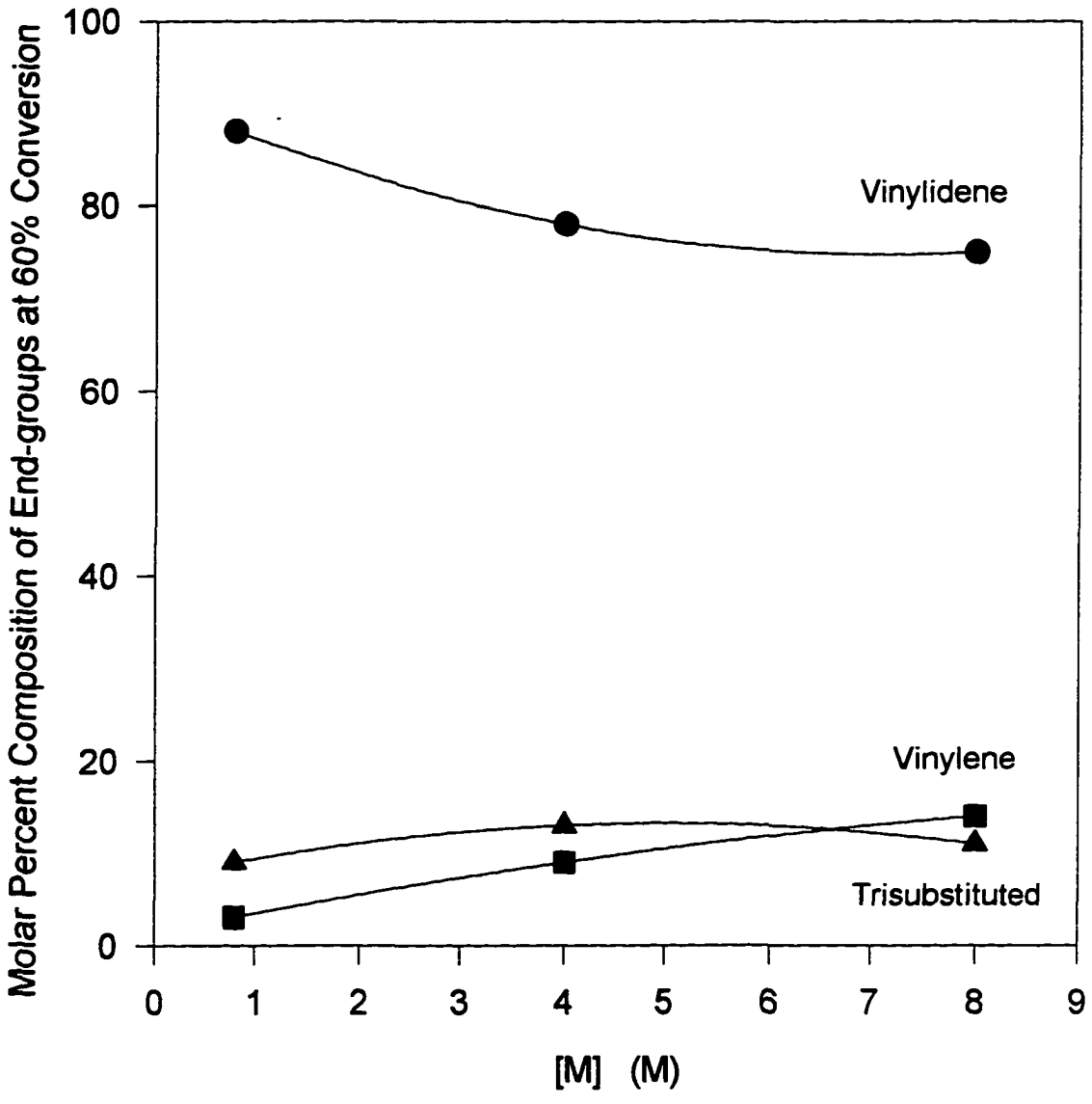

Figure A-99. Molar percent compositions of end-groups as function of monomer concentration

Polymerization conditions: [Zr]=52μM, [MAO]=62mM and T=80°C

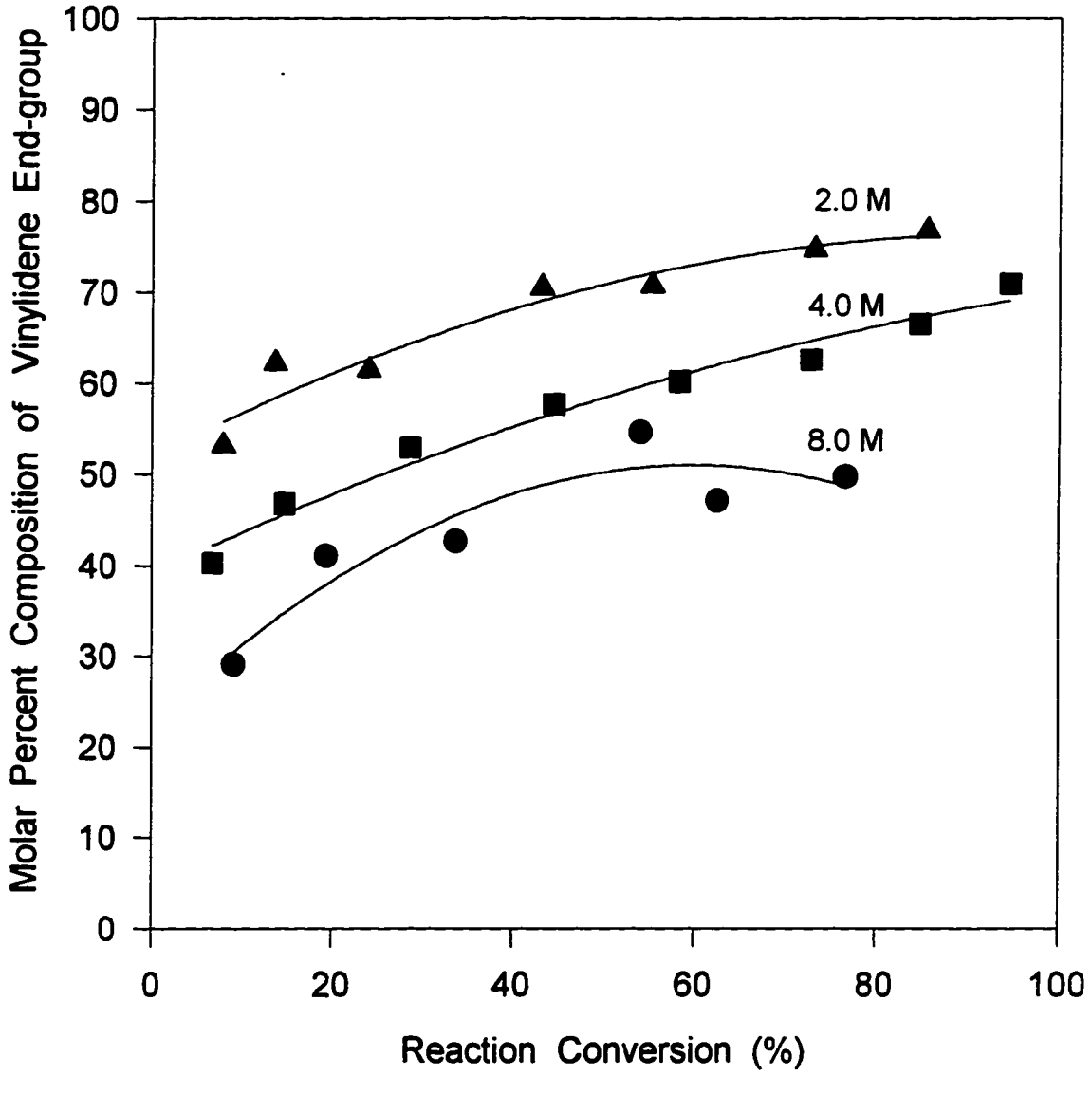

Figure A-100. Molar percent composition of vinylidene end-group versus % conversion at 50°C and different monomer concentrations

Polymerization conditions: [Zr]=52μM, [MAO]=62mM and T=50°C

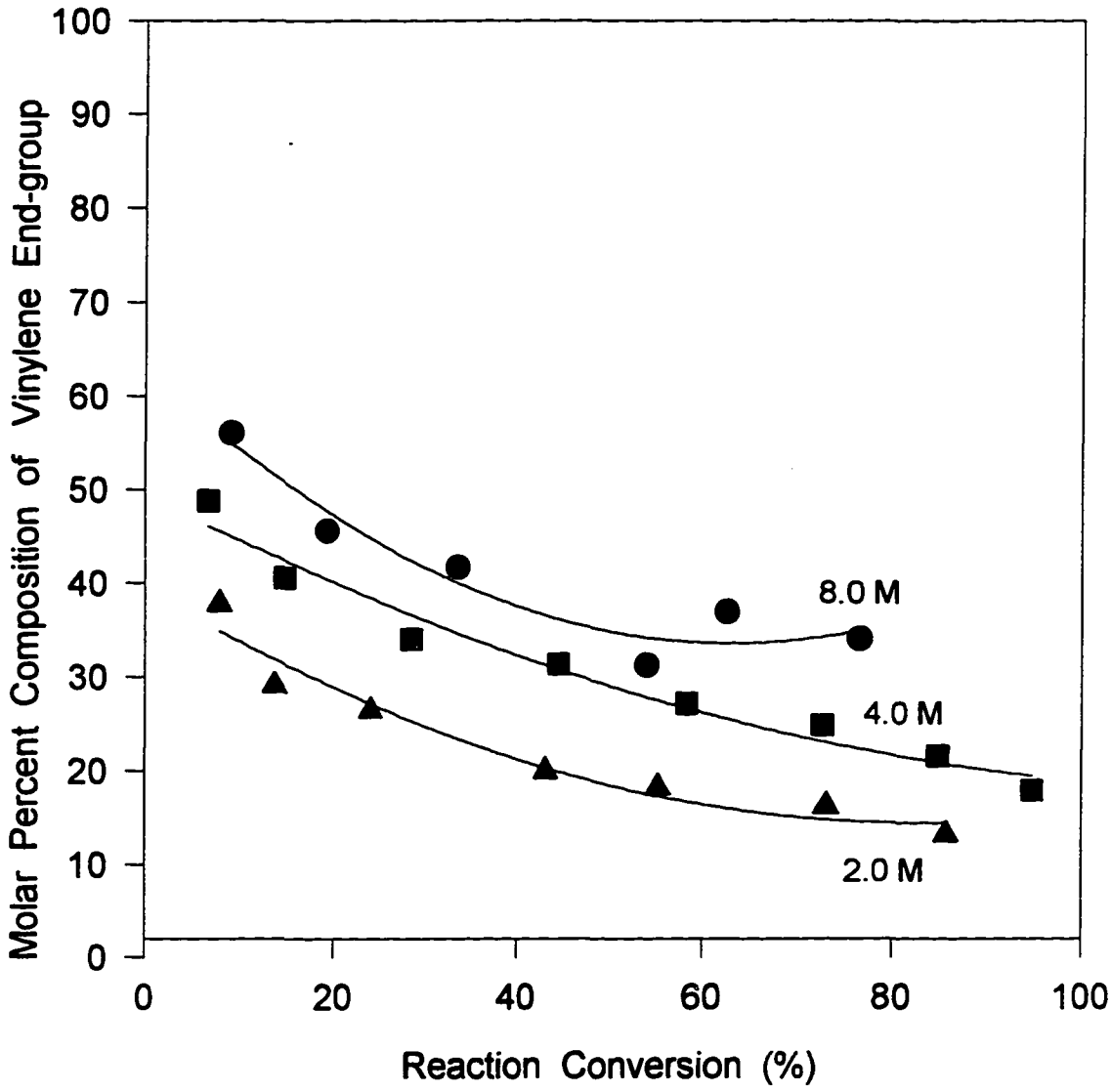

Figure A-101. Molar percent composition of vinylene end-group versus % conversion at 50°C and different [M]

Polymerization conditions: [Zr]=52μM, [MAO]=62mM and T=50°C

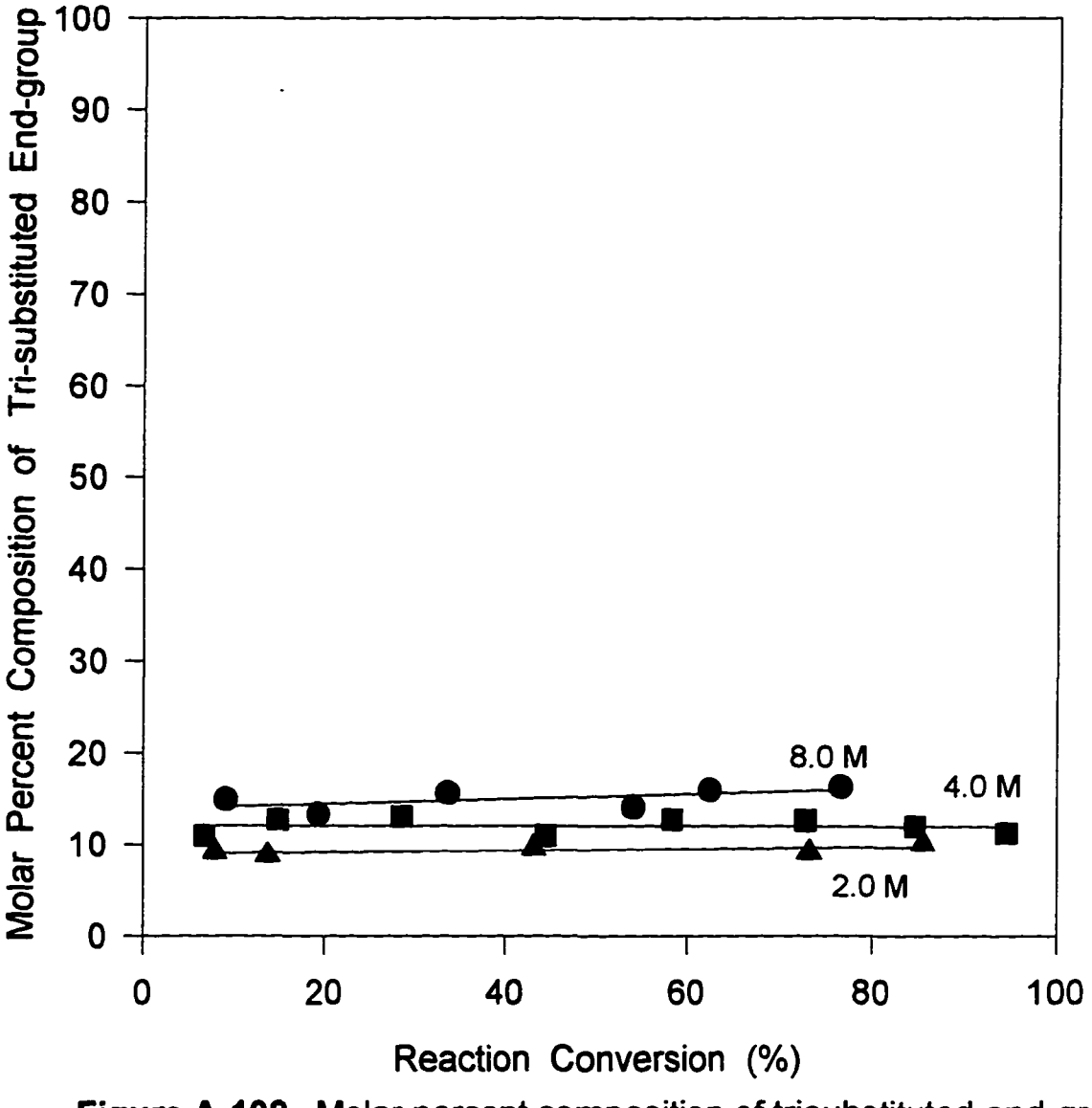

Figure A-102. Molar percent composition of trisubstituted end-group versus % conversion at 50°C and different monomer concentration

Polymerization conditions: [Zr]=52μM, [MAO]=62mM and T=50°C

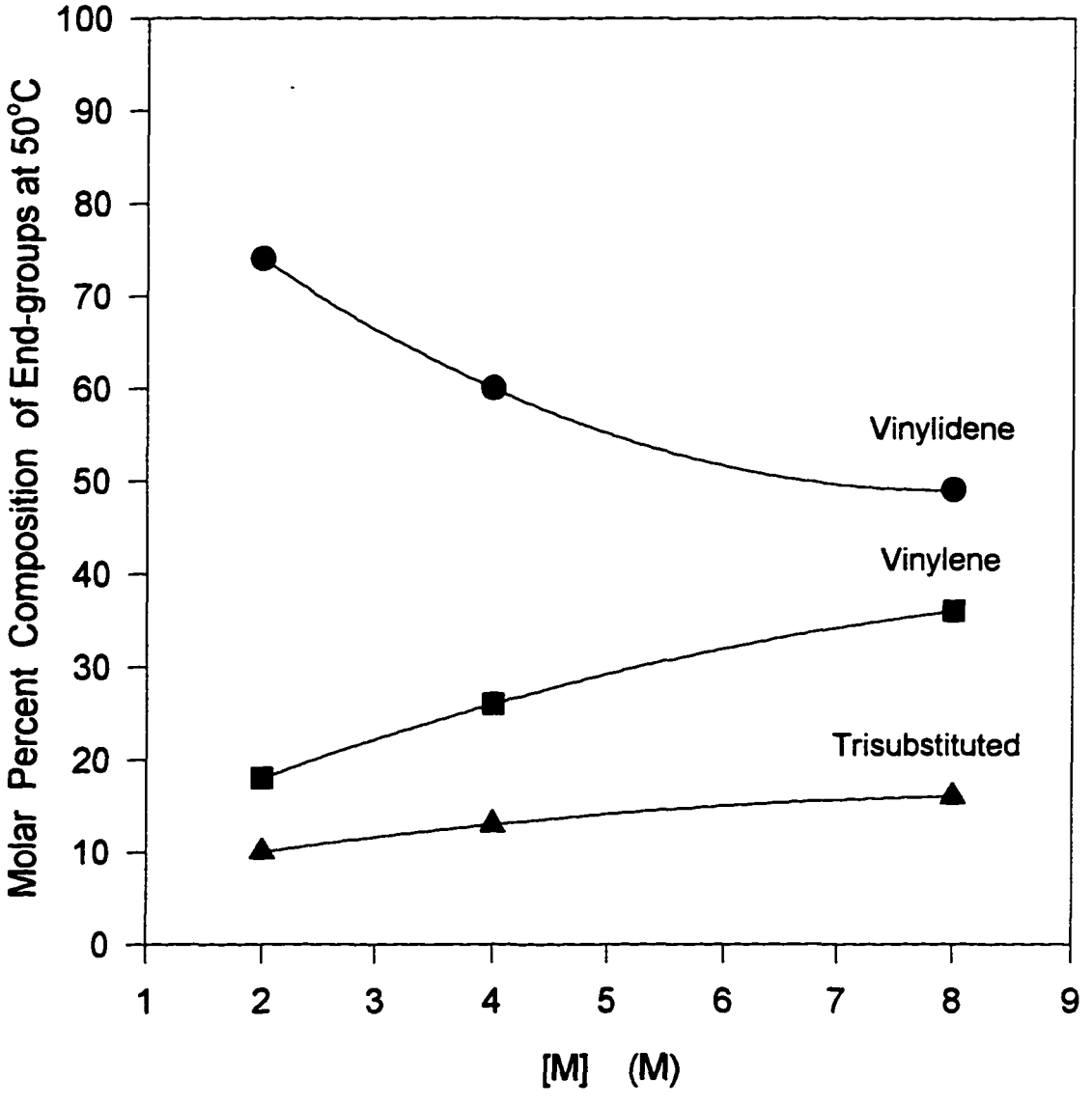

Figure A-103. Molar percent compositions of end-groups as function of [M] at 50°C

Polymerization conditions: [Zr]=52μM, [MAO]=62mM and T=50°C

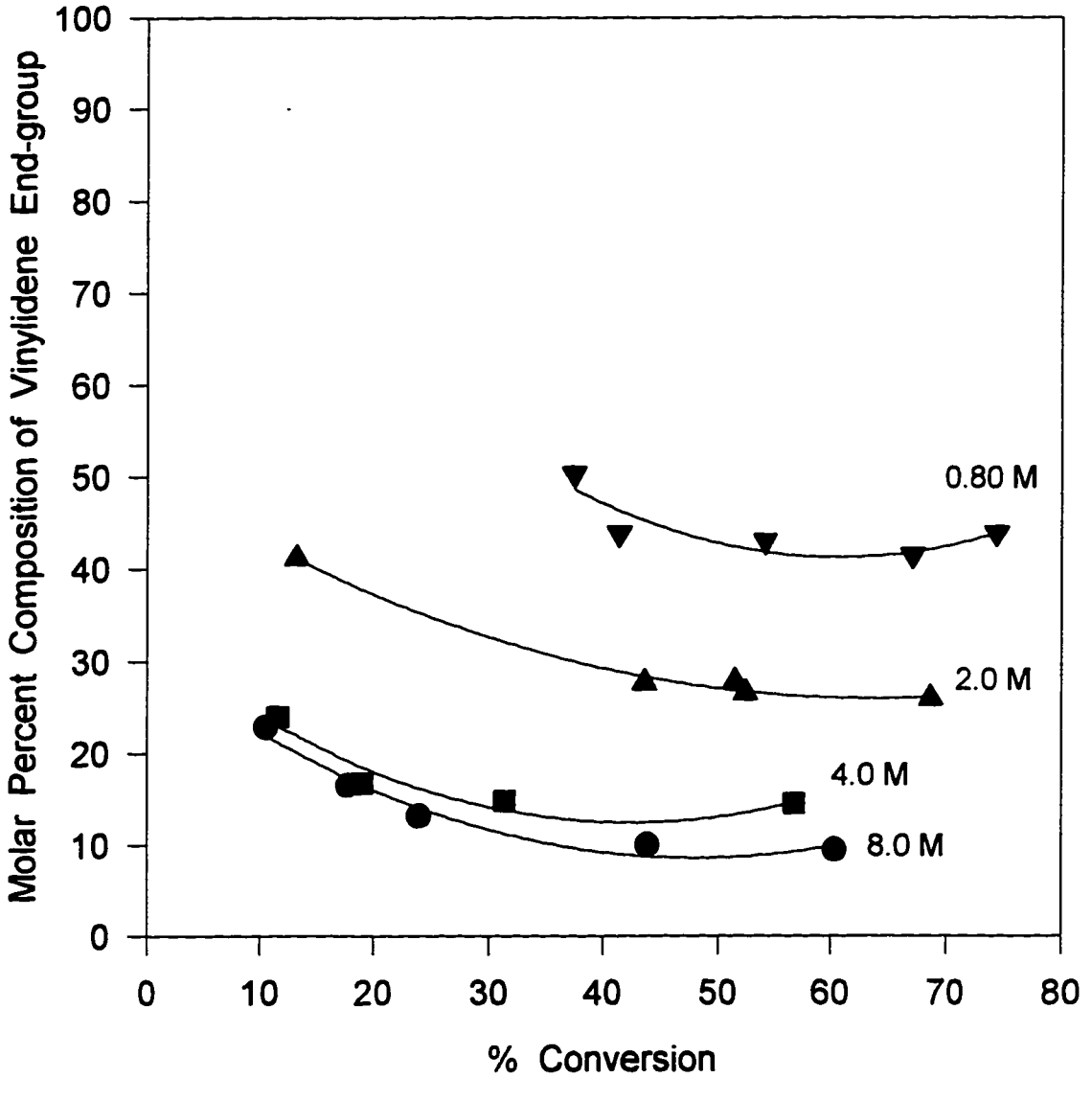

Figure A-104. Molar percent composition of vinylidene end-group versus % conversion at 0°C and different [M]

Polymerization conditions: [Zr]=52μM, [MAO]=62mM and T=0°C

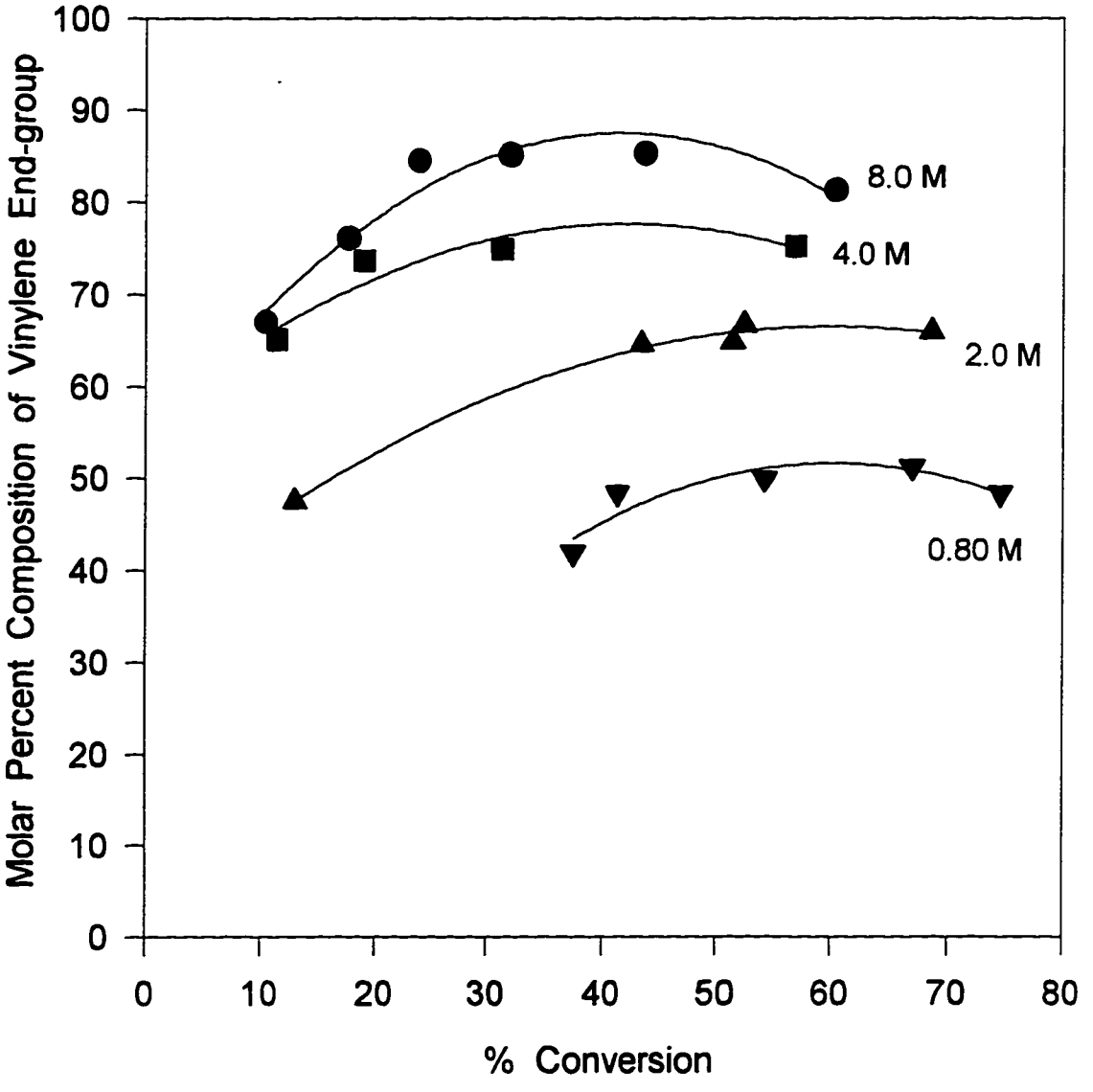

Figure A-105. Molar percent composition of vinylene end-group versus % conversion at 0°C and different [M]

Polymerization conditions: [Zr]=52μM, [MAO]=62mM and T=0°C

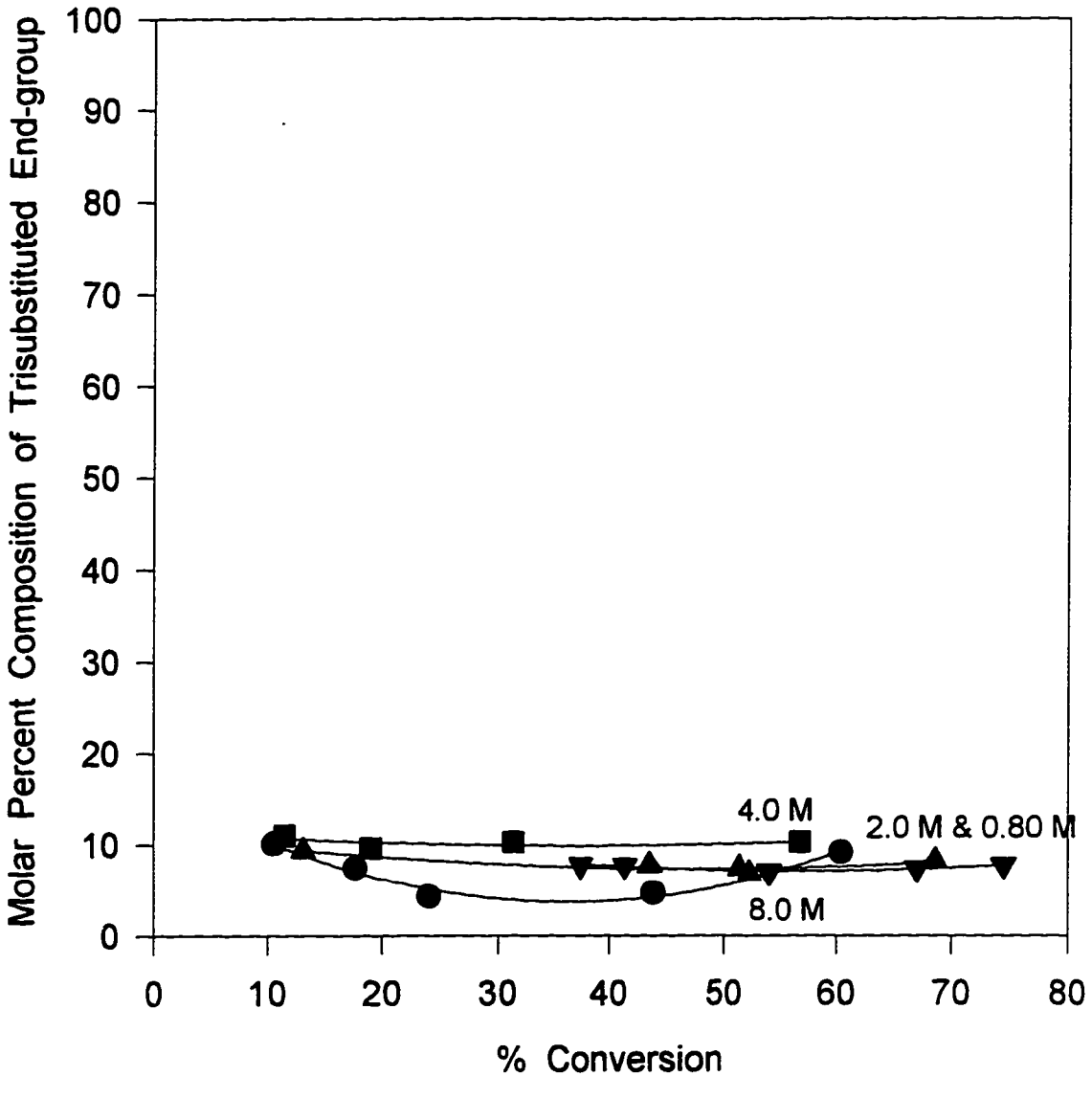

Figure A-106. Molar percent composition of trisubstituted end-group versus % conversion at 0°C and different [M]

Polymerization conditions: [Zr]=52μM, [MAO]=62mm and T=0°C

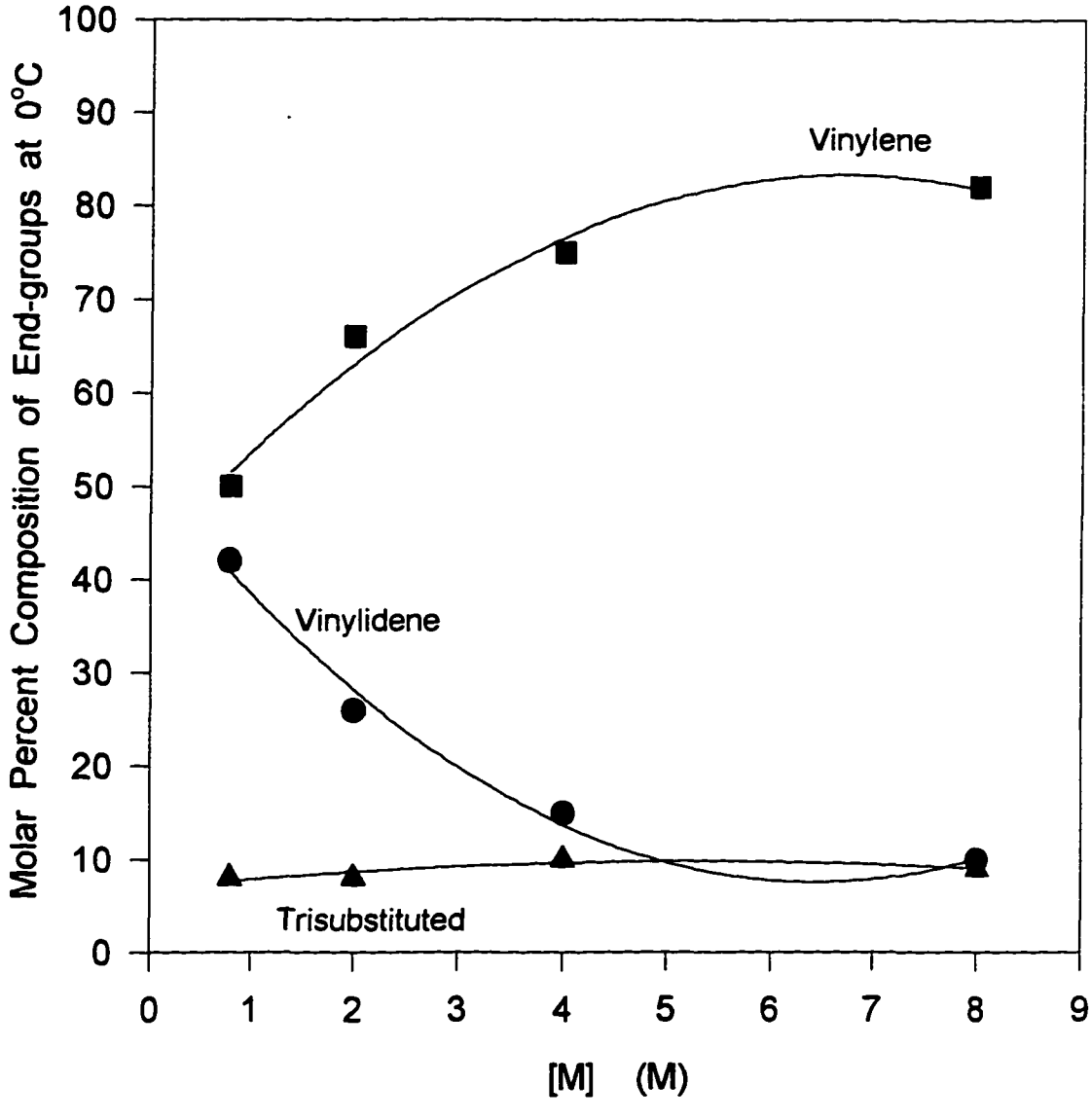

Figure A-107. Molar percent compositions of end-groups as function of monomer concentration at 0°C

Polymerization conditions: [Zr]=52μM, [MAO]=62mM and T=0°C

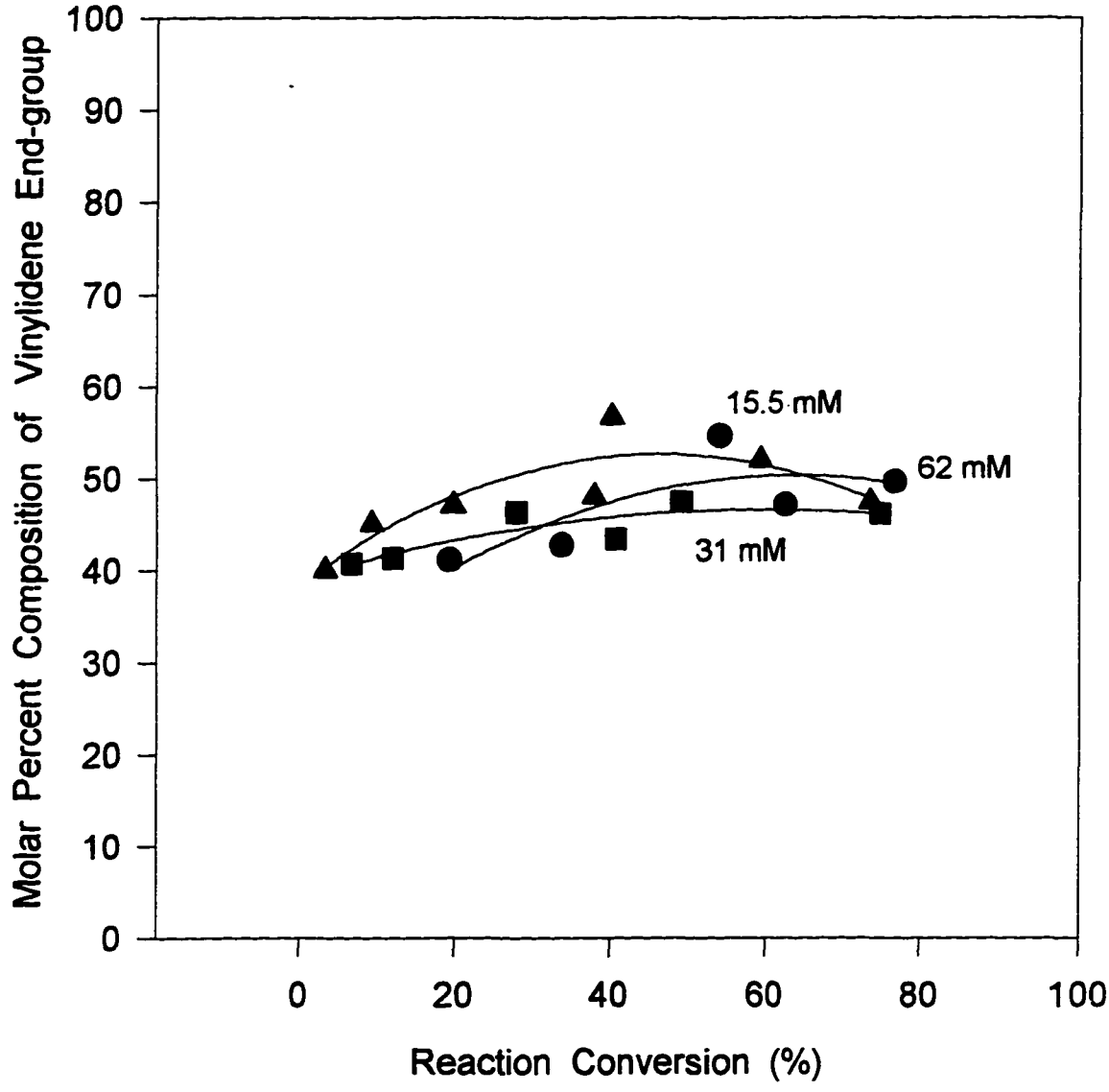

Figure A-108. Molar percent composition of vinylidene end-group versus % conversion at 50°C and different [MAO]

Polymerization conditions: [Zr]=52μM, [M]=8.0M and T=50°C

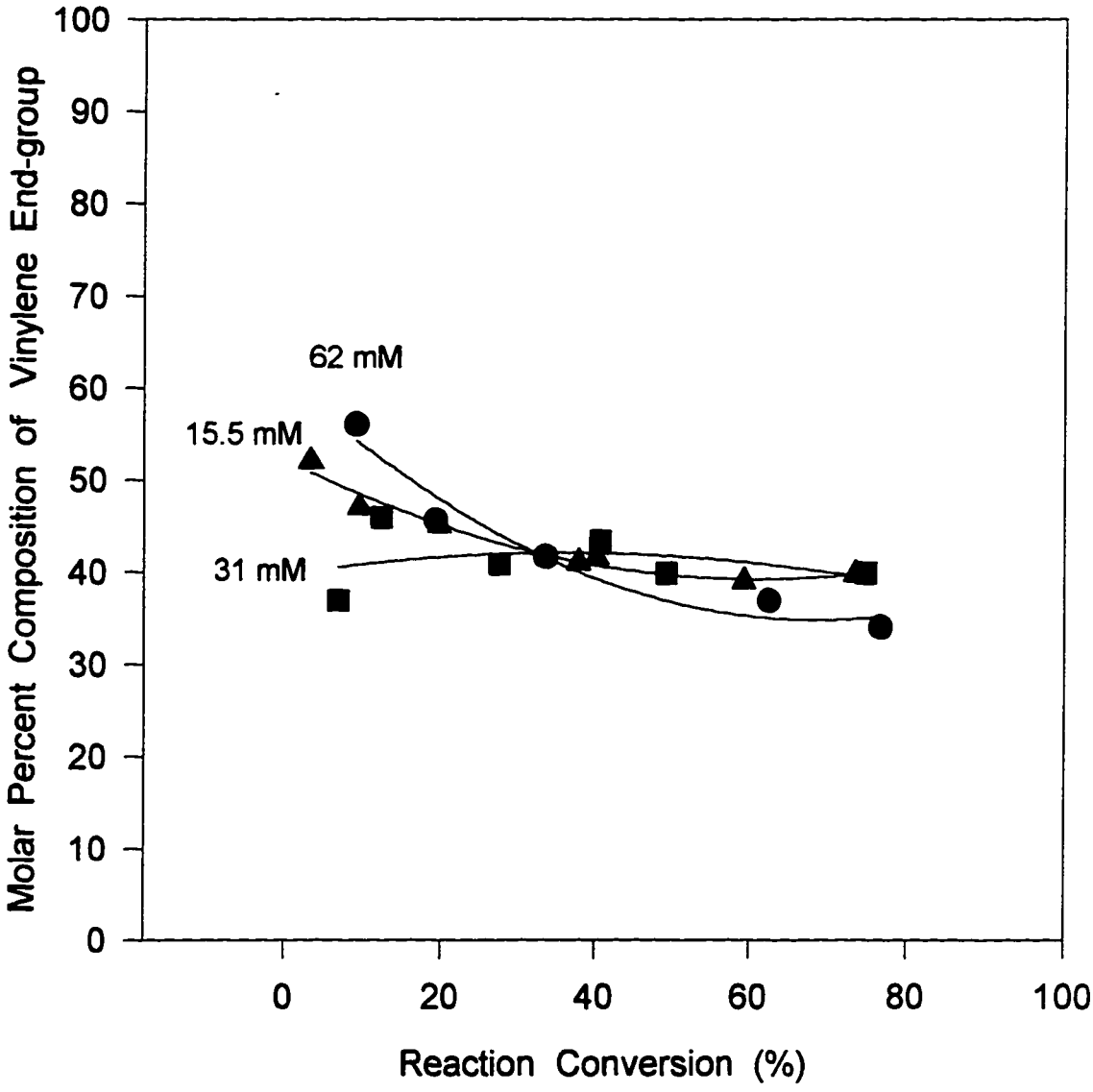

Figure A-109. Molar percent composition of vinylene end-group versus % conversion at 50°C and different [MAO]

Polymerization conditions: [Zr]=52μM, [M]=8.0M and T=50°C

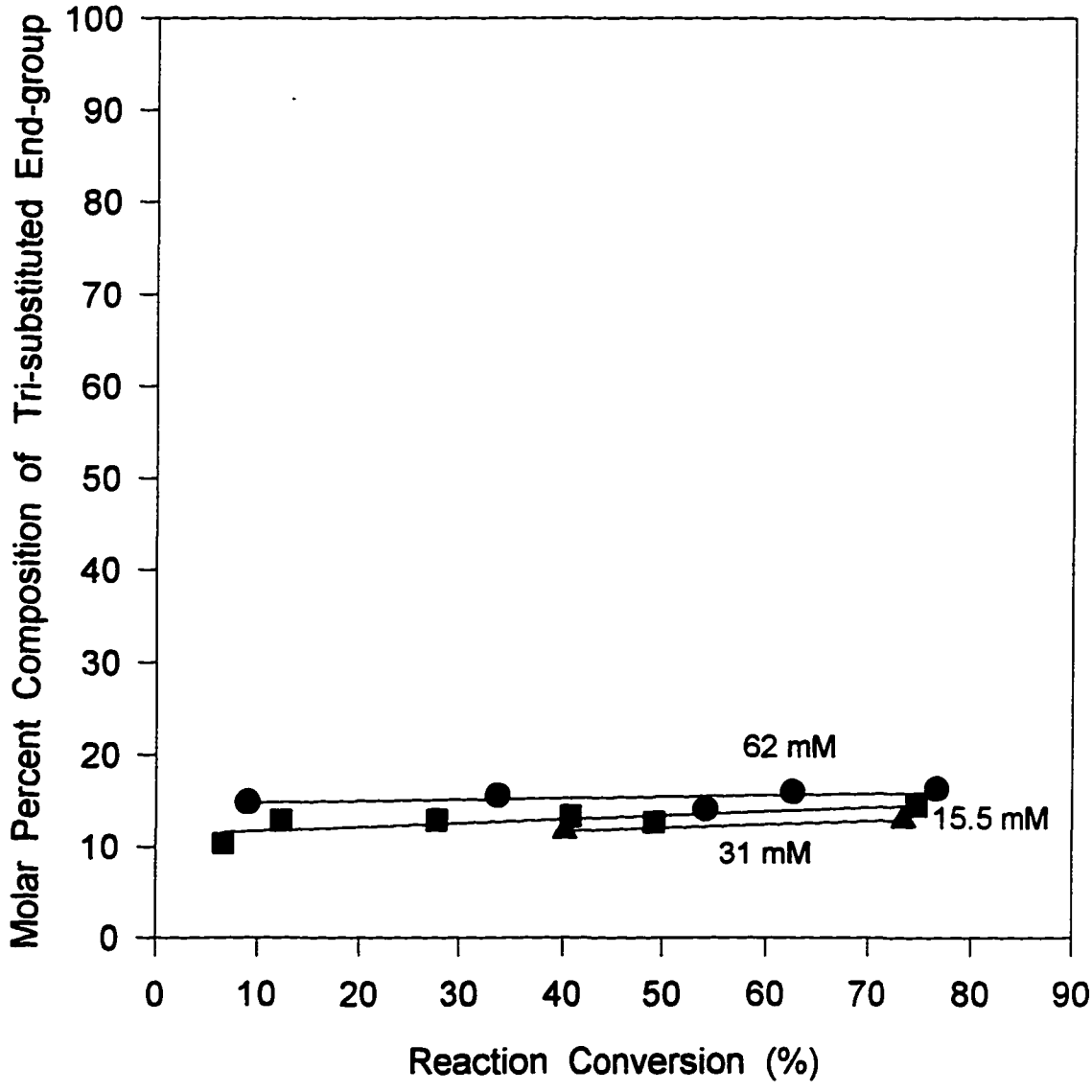

Figure A-110. Molar percent composition of trisubstituted end-group versus % conversion at 50°C and different [MAO]

Polymerization conditions: [Zr]=52μM, [M]=8.0M and t=50°C

5.0 Results and Discussion on Molecular Weight Study

Molecular weight is very important in homogeneous polymerization. The goal is to control the molecular weight, and to adjust it for various purposes. Here, we studied how various polymerization conditions control the molecular weight of poly(1-hexene).

5.1 Comparison of GPC and NMR results in molecular weight

In the calculation of molecular weight from ^{1}H NMR results, we assumed that, on average, every polymer chain contains one double bond end group. This assumption was supported by the ^{13}C NMR results. In the ^{13}C NMR spectra of poly(1-hexene), the amount of saturated end group and the amount of double bond end group were equal, within 10% NMR integral error. Meanwhile, we used GPC to determine the molecular weights of some samples and compare these two methods. It is known that GPC does not accurately measure the molecular weight of poly(1-hexene), because there are no standards of poly(1-hexene) in GPC. Instead, we used polystyrene standards. The hydrodynamic volume of poly(1-hexene) is not exactly the same as that of polystyrene. Table A-15 lists the results from both methods.

From this table, we can see that the difference between the molecular weights obtained from these two methods are in a reasonable range. Either of them can be picked up to measure the polymer molecular weight.

It also can been seen from the GPC method that the poly(1-hexene) obtained from homogeneous polymerization has very narrow molecular weight

distribution. The MWD is only very slightly affected by the reaction conversion. This is one of the greatest advantages of homogeneous polymerization besides high polymer tacticity and high activity because metallocene catalysts have well-defined single catalytic sites.

5.2 Temperature Effect on Molecular Weight

As in most polymerizations, in homogeneous polymerization the molecular weight of the polymer decreases with the increase of temperature. Figure A-111 shows the relationship between M_n and T. Since molecular weight increases with the increase of %conversion because of the decrease of monomer concentration, molecular weight data are picked up within three different ranges of %conversion. There is no simple relationship between M_n and T. When the temperature decreases 20°C from 100°C to 80°C, molecular weight almost does not change; However, when temperature drops another 30°C from 80°C to 50°C, molecular weight almost doubles. The same holds true when the temperature continues to drop from 50°C to 0°C. The molecular weight almost triples. The big temperature effect here is due to the double effects of temperature on chain transfer reactions. These are the effect on rate constants and the effect on the kinetic orders of chain transfer rates with respect to catalyst concentration, monomer concentration and MAO concentration. As in any polymerization, the number-average degree of polymerization is obtained as the propagation rate divided by the sum of chain termination rates.

$$X_n = R_p/\Sigma R_{tr} \qquad (25)$$

Molecular weight of the polymer can be obtained as X_n multiplied by the molecular weight of monomer

$$M_n = (R_p / R_{tr,\ overall}) \times MW_{monomer\ unit} \qquad (26)$$

Since there are three kinds of chain transfers here, M_n can be expressed by

$$M_n = (k_p[Zr]^A[MAO]^B[M]^C / k_{tr1}[Zr]^{X1}[MAO]^{Y1}[M]^{Z1} + k_{tr2}[Zr]^{X2}[MAO]^{Y2}[M]^{Z2} + k_{tr3}[Zr]^{X3}[MAO]^{Y3}[M]^{Z3}) \times MW_{monomer\ unit} \qquad (27)$$

From our results, temperature effects not only on k_p and k_{tr} but also X, Y and Z values, which makes the temperature effect much more complicated.

Kaminsky[19,61] once reported that the mean molecular weights are strongly dependent on reaction temperature in the propylene polymerization using rac-$C_2H_4[Ind]_2ZrCl_2$ and rac-$C_2H_4[H_4Ind]_2ZrCl_2$ as catalysts. The relationship between molecular weight and polymerization temperature was pretty similar with what we got. With the elevation of temperature, molecular weight decreases quickly in the beginning, then slows down, and finally almost levels off. Polypropylene was yielded with molecular weights ranging from Mw ≈ 50,000 g/mol at ambient polymerization temperatures down to Mw ≈ 10,000 g/mol at 60-70 °C. These molecular weights are almost two orders of magnitude higher than those of the atactic polypropylene obtained under otherwise identical conditions with Cp_2ZrCl_2. This effect is probably due, at least in part, to an increased rate of chain propagation R_p for *ansa*-metallocene catalysts.[34] In addition to an increased R_p, β-substituents in these complexes might also cause a decreased rate of chain transfer R_{tr}, for example by sterically hindering the tertiary β-CH

group of the growing chain in its approach to the Zr Center. Bulky β-*tert*-butyl substituents as in $Me_2Si[2\text{-}Me\text{-}4\text{-}t\text{Bu}\text{-}C_5H_2]_2ZrCl_2$ lead to rather low molecular weights at elevated temperature.[30a]

5.3 Catalyst Concentration Effect on Molecular Weight

Figure A-112 shows the relationship of M_n versus [Zr] at 100°C, 50°C and 0°C, respectively. It can be seen that the catalyst concentration effect is temperature dependent, which means that X values in (27) vary with temperature. At 100°C, M_n is proportional to $[Zr]^{-0.1}$, at 50°C, M_n is proportional to $[Zr]^{-0.5}$ and at 0°C, M_n is proportional to $[Zr]^{-0.3}$. Generally, with catalyst concentration increasing, catalytic activity decreases and molecular weight decreases too. However, this cannot explain why at different temperatures, the molecular weight decreases with catalyst concentration increasing at different rates. At these temperatures, the order of the propagation with respect to the catalyst concentration is smaller than the overall order of chain transfers with respect to catalyst concentration. Temperature effects the dependency of chain transfer rates on catalyst concentration differently though its effect on propagation is almost the same at different temperature. Because X values are temperature dependent, no better analysis can be done.

Catalyst concentration effect on molecular weights of atactic polypropylene only was studied by Kaminsky[61] with Cp_2ZrCl_2. It parallel that on catalytic activities: molecular weights increased substantially as catalyst concentration

were decreased. Our situation is more complicated because the fractional order of catalyst concentration in chain transfer rate is not one.

5.4 Monomer Concentration Effect on Molecular Weight

Figure A-113 shows the relationship versus monomer concentration at 100, 50 and 0 °C. It seems that there is no simple relationship between M_n and [M]. M_n is proportional to $[M]^{0.4}$ at 100°C, to $[M]^{0.3}$ at 50°C and to $[M]^{0.2}$ at 0°C. It is because of change in temperature effects chain transfer reactions in such a complicated way that Z values in Equation (27) vary with temperature. In addition, Z1, Z2 and Z3 are different from each other. In Equation (27), C is 1-2 (Table A-2) and Z1, Z2 and Z3 are 0-2 (Table A-8).

Resconi et al[62b] derived the overall for X_n form

$$X_n = (k'_{p1}[M] + k'_{p2}[M]^2)/(k'_{tMet} + k'_{t1}[M] + k'_{t2}[M]^2) \qquad \textbf{(28)}$$

The results we obtained are consistent with Equation (28). Different catalysts were found to result in different relationship between monomer concentration and molecular weight because of the different chain transfer mechanisms. Stehling et al[63] reported that in *ansa*-zirconocene catalysts without α-methyl substituents, direct β-H transfer from the growing polymer chain to a coordinated olefin did indeed appear to predominate, as indicated by a near-constancy of molecular weights with increasing olefin concentration. But for *ansa*-metallocene catalysts with α-methyl substituents, a strong increase of molecular weight almost proportional to olefin concentration indicated that the remaining chain termination arose almost exclusively from β-H transfer to the metal. α-Methyl

substituents thus appeared to block a relatively large fraction of chain termination that would otherwise arose from β-H transfer directly to a coordinated olefin.

5.5 MAO Concentration Effect on Molecular weight

Figure A-114 shows the relationship between M_n and MAO concentration. At 50 and 0 °C, M_n almost does not change with MAO concentration. At 100°C, M_n is proportional to $[MAO]^{0.2}$. At the first two temperatures, [MAO] effects on both propagation and overall chain transfer are the same and cancel each other in the calculation of M_n according to Equation (27). But at 100°C, they can not cancel each other any more.

Kaminsky[61] reported that molecular weight of polypropylene obtained with MAO activated Cp_2ZrCl_2 system increased with the concentration of the MAO concentration. He changed MAO : Zr from 1,000 to 100 and then to 10. However the ratio of MAO : Zr we used changed pretty small, which resulted in no significant change in molecular weight.

5.6 Summary from the Molecular Weight Studies

From the above results and the discussion based on these results, we find that temperature effects molecular weight in two ways instead of one way: first, the change of temperature results in the change of rate constants, which is the same with other polymerizations; second, the change of temperature also changes the kinetic orders of rates with respect to catalyst concentration, cocatalyst concentration and monomer concentration, which is not normal in

other polymerizations. These two effects of temperature make the temperature effect on homogeneous polymerization much more complicated.

Since the temperature effect is complicated, the concentration effects will become more complicated too. The concentration effects will depend on temperature to a great extent.

Table A-15 Experimental Molecular Weight Values

Sample		M_n	GPC Results		
Conditions	% Conv.	(^{1}H NMR)	M_n	M_w	MWD
50°C [Zr]=99μM [M]=8.0M [MAO]=62 mM	10.4%	1.0×10^4	1.2×10^4	2.7×10^4	2.2
	20.3%	7.0×10^3	8.3×10^3	1.9×10^4	2.4
	30.3%	5.4×10^3	6.6×10^3	1.5×10^4	2.2
	40.6%	5.1×10^3	5.8×10^3	1.4×10^4	2.4
	58.7%	3.4×10^3	4.2×10^3	1.1×10^4	2.6
	80.6%	3.4×10^3	4.2×10^3	9.6×10^3	2.3
	86.2%	2.1×10^3	3.0×10^3	8.6×10^3	2.9
0°C [Zr]=99μM [M]=8.0M [MAO]=62 mM	15.3%	1.2×10^4	1.2×10^4	4.2×10^4	3.5
	27.9%	1.3×10^4	1.8×10^4	4.1×10^4	2.3
	38.0%	1.3×10^4	1.8×10^4	4.2×10^4	2.3
	44.5%	1.3×10^4	1.9×10^4	4.5×10^4	2.4
	53.2%	1.1×10^4	1.7×10^4	3.9×10^4	2.4
	65.5%	1.3×10^4	1.5×10^4	3.7×10^4	2.4

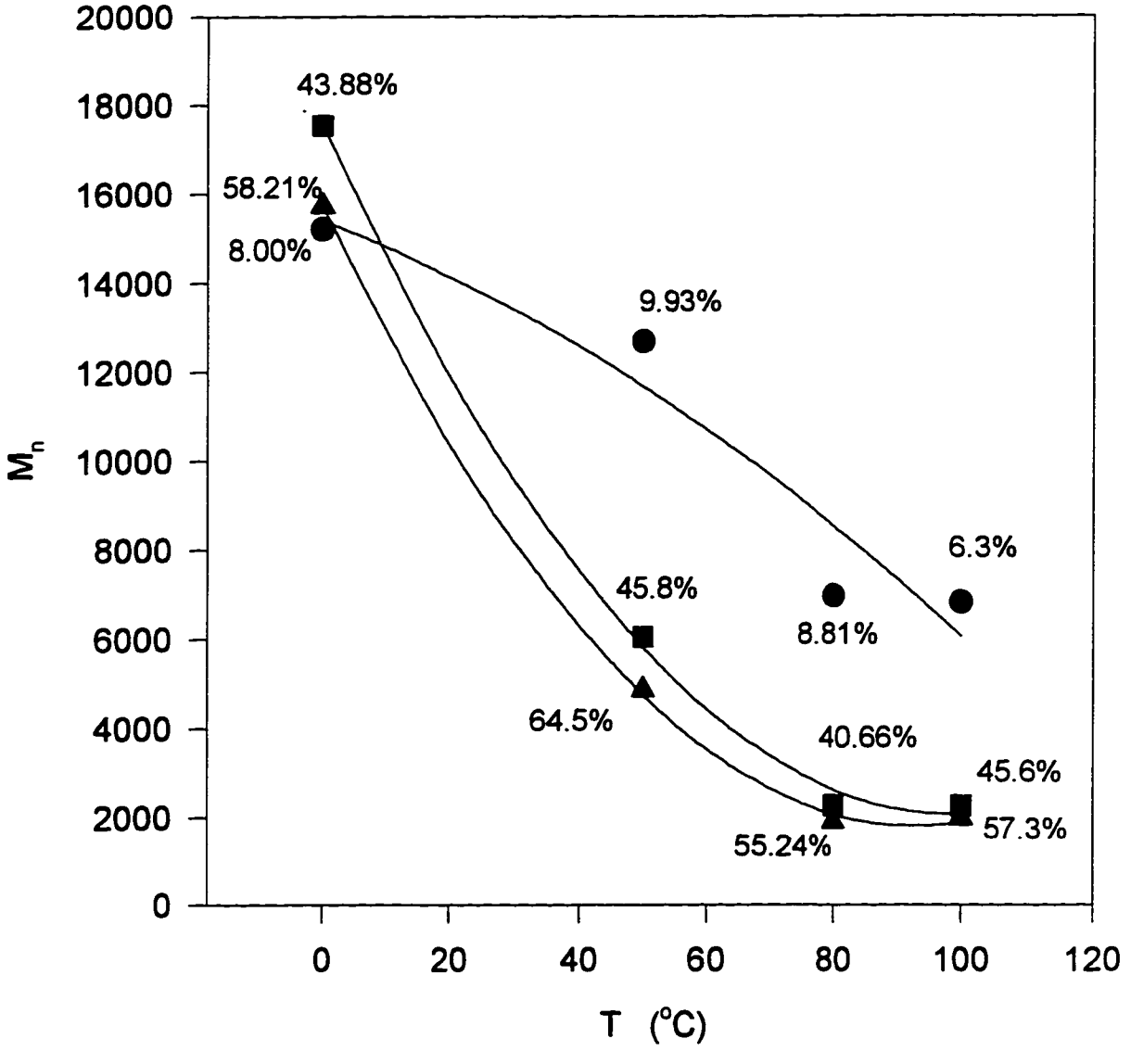

Figure A-111. M_n as a function of temperature
% Conversion is labeled on each point.

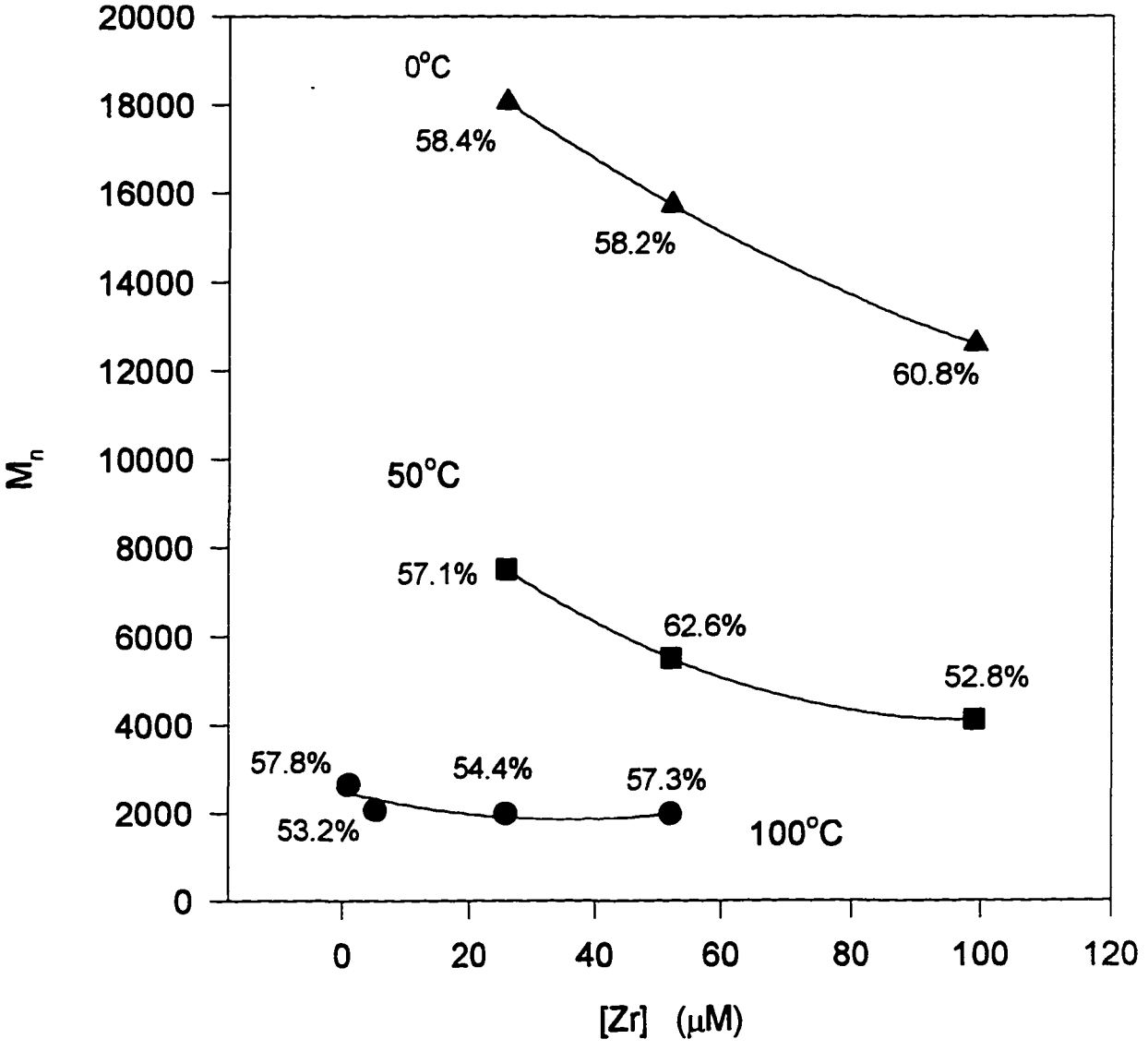

Figure A-112. M_n as a function of catalyst concentration

Note: % Conversion is labeled on each point.

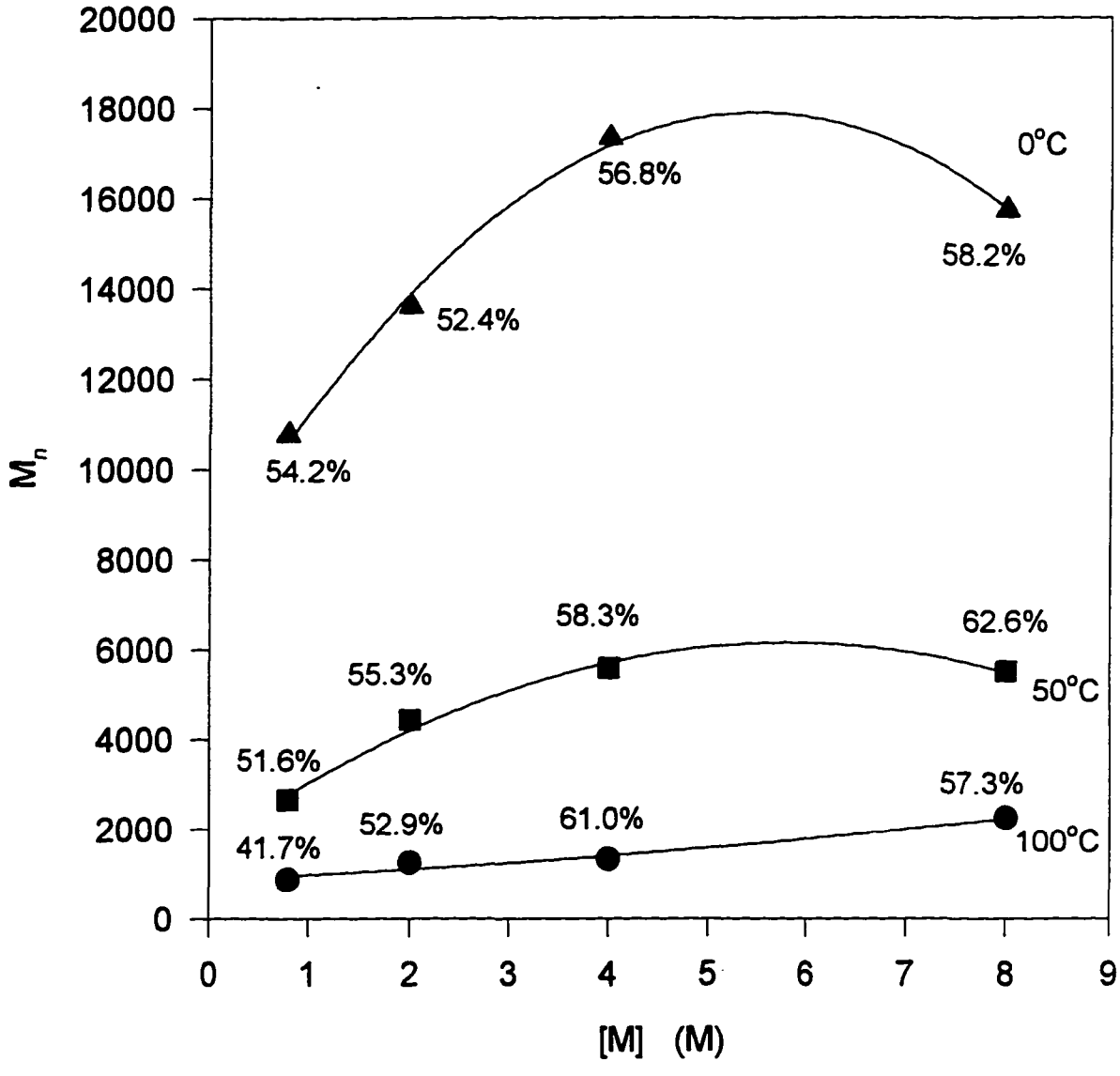

Figure A-113. M_n as a function of Monomer concentration

% Conversion is labeled on each point.

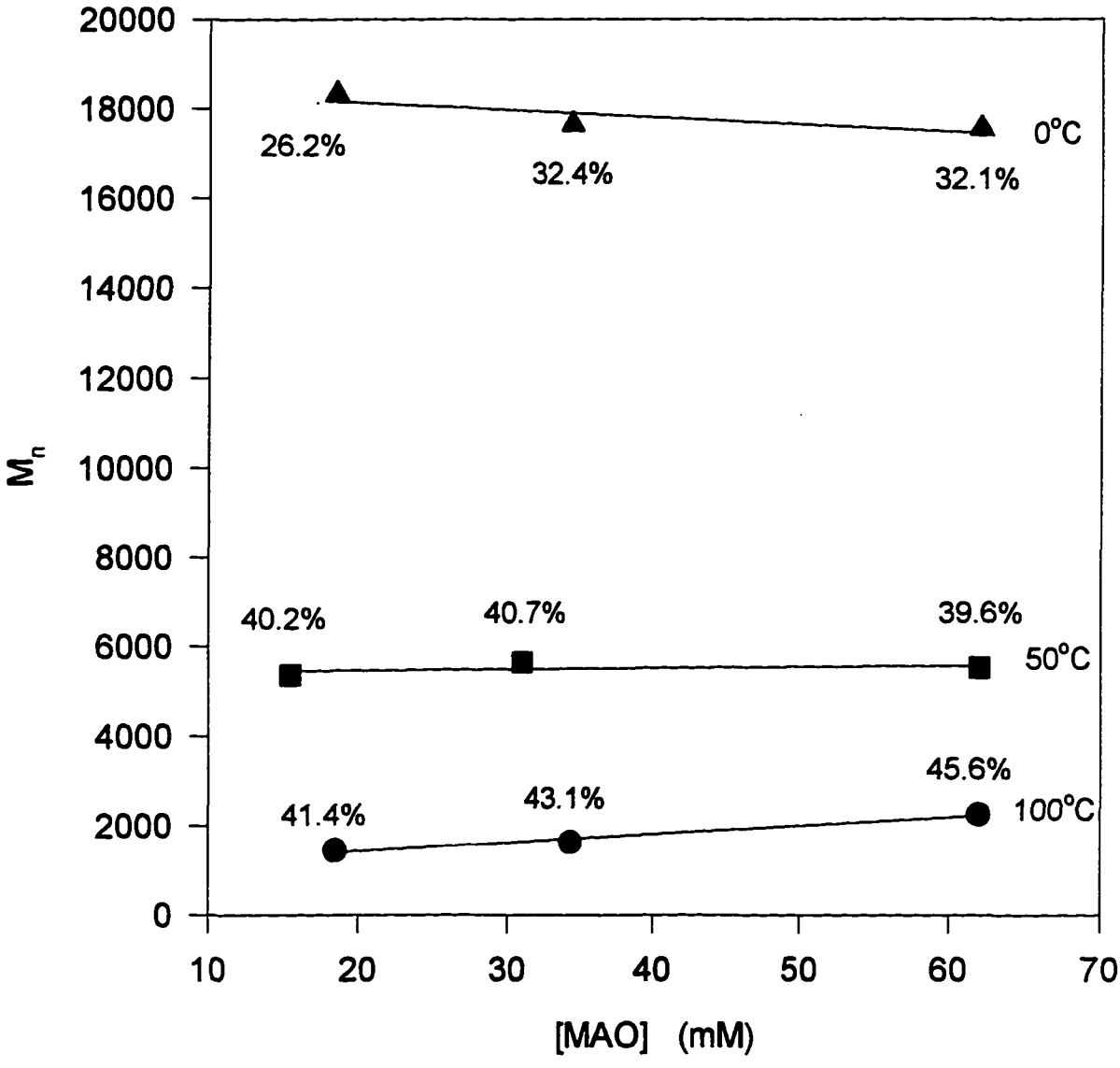

Figure A-114. M_n as a function of MAO concentration

% Conversion is labeled on each point.

6.0 Results and Discussion on Microstructure of Poly(1-hexene)

^{13}C NMR was used to study the microstructure of poly(1-hexene). Our attention here is on how the polymerization conditions effect isotacticity stereochemistry. To this end, we focus on the saturated carbon region.

6.1 ^{13}C NMR Chemical Shift of Saturated Carbon

The saturated carbon atoms in alkanes show absorption in the range of around 0-50ppm downfield from TMS.

For polypropylene, poly(1-butene) and other poly(α-olefins), the ^{13}C NMR tacticity assignments of all carbons have been reported in detail previousely[64], and thus only brief assignments for poly(1-hexene) are shown here. Chemical shifts of the six major resonances have been estimated using two different methods[49]. Calculated values using the CSPEC program[65] are based on the Grant and Paul[66] additivity rules for hydrocarbon substituents. The second set of calculated shifts is from the spectral estimation feature of the SPECINFO database[67]. This program calculates chemical shifts based on a comparison of the given structure to carbons in the database which have the most similar substituents on α, β, γ, and δ carbons attached to the carbon of interest.

Comparison of the calculated and observed values shows the empirical values from the SPECINFO database are better for some carbons, while the calculated values based on additivity effects fare better for others. The estimated

	$[CH_2-CH-(CH_2-CH_2-CH_2-CH_3)]_n$					
	1	2	3	4	5	6
CSPEC calc	40.4	31.3	35.1	30.1	23 .0	13.6
SPECINFO calc	43.4	33.8	33.9	29.2	23.0	14.1
obsd	40.4	32.4	34.7	28.6	23.2	14.1

errors for the SPECINFO calculation are mostly under 1 ppm, except for the C1 of the backbone, for which the error is 3 ppm. The failure of SPECINFO to give better values indicates the absence of carbons with almost identical substituents in the database. Actually the observed chemical shift values are slight different. For example, the chemical shift of the C3 was 34.4 ppm reported by Chien[49], was 34.9 ppm reported by Asakura[64] and is 34.7 ppm obtained here.

The ^{13}C NMR spectrum of an isotactic poly(1-hexene) is shown in Figure A-115. Since C3 is the carbon on the substituent group which is directly attached on the chiral center C2 on the polymer chain, its resonance tells the most detailed information about the tacticity of poly(α-olefins). We will focus on this resonance to compare the tacticity. The chemical shift intensity of the C3 at 34.7 ppm indicates that this polymer is highly isotactic; the C3 in atactic and syndiotactic triads occurs between 0.4 and 1.0 ppm upfield from 34.7 ppm[64]. Therefore, small peaks are observed at upfield of C3, indicating the tacticity of the polymer chain. Asakura et al[64] reported the tacticity assignment of ^{13}C NMR spectra of poly(α-olefins). They calculated the ^{13}C NMR chemical shifts at the heptad level and pentad level on the basis of the ^{13}C NMR γ-shielding effect and the RIS model. Table A-20 summarizes chemical shifts relative to the chemical

shift of mmmmmm calculated for C3 of poly(α-olefins) and the observed C3 chemical shifts of poly(1-hexene)

6.2 Temperature Effect on Isotacticity

Isotacticity of poly(1-hexene) decreases with the increase of temperature (see figure A-116). From Figure A-116, we see not only that stereochemistry decreases at the pentad level but also at the heptad level. With the increase of temperature from 0°C to 100°C, a resonance splits from the main resonance which is at 34.7 ppm. The chemical shift of the split resonance is -0.06 relative to the main isotactic (mmmmmm+mmmmmr) resonance, indicating the decrease of isotacticity. The split signal is possibly due to rmmmmr. Table A-21 summarizes the quantitative integral results of isotacticity from Figure A-116 to A-119 at both pentad level and heptad level.

Busico et al[68b] and Resconi et al[62a] investigated the effect of polymerization temperature on the structural details of isotactic polypropylene produced with two C_2 symmetric zirconocenes (rac-C_2H_4[Ind]$_2ZrCl_2$ and rac-C_2H_4[3-Me-Ind]$_2ZrCl_2$). The results were similar with our result in the polymerization of 1-hexene that the %mmmm decreased with the increase of temperature. It was reported that in the polymerization of propylene, increasing polymerization temperature from 20 to 70 °C, rac-C_2H_4[Ind]$_2ZrCl_2$ yielded polypropylenes with %mmmm from 92% to 82%, and increasing polymerization temperature from 0 to 70 °C, rac-C_2H_4[3-Me-Ind]$_2ZrCl_2$ yielded polypropylenes with %mmmm from 36% to 14%. In our polymerization of 1-hexene, increasing polymerization

temperature from 0 to 100 °C, rac-$Me_2Si[Ind]_2ZrCl_2$ yields poly(1-hexene) with %mmmm from 97% to 47%. In addition, %mmmmmm + %mmmmmr decreases from 97% to 21%.

The increase of temperature causes the increase of propagation rate and also results in the increase of error in stereochemistry. The possible explanation for the above results is that there are two steps involved in this kind of coordination polymerization: The first step is that the catalyst connecting with a propagating chain will coordinate a monomer molecule; The second step is that the monomer molecule coordinated with the catalyst will be added to the propagating chain to finish the propagation process. The stereochemistry selection by the catalyst could either occur in the first step or in the second one. If this selection occurs in the first step, it takes a certain time for the catalyst to choose one side, instead of the other, of the monomer when it approaches the monomer molecules. When the temperature increases, the rate of the second step increases and the catalyst can not get enough time to make the selection because of the increased desire of monomer molecules. Stereochemical error occurs very easily. The higher the temperature, the faster the propagating rate, the more the stereochemical errors. If the stereochemical selection is made in the second step, the monomer molecules are added onto the propagating chain from their one side instead the other. The selectivity decreases due to the faster addition of monomer onto the propagating chain when temperature increases.

Besides, the explanation from Busico et al[68b] was that the possible reason for the strong temperature effect on the stereospecificity of homogeneous catalysts was the competition between the chain propagation and the epimerization of the last-inserted monomeric unit. If the active energy of epimerization is much higher than that of chain propagation, increase of temperature will greatly favor the epimerization.

6.3 Monomer Concentration Effect on Isotacticity

The influence of monomer concentration on the stereospecificity of propylene polymerization with C_2 symmetric ansa- or rac-metallocene catalysts have been studied[64,65b]. It was found that isotacticity (%m and %mmmm) decreased by decreasing the monomer concentration. In our study on the 1-hexene polymerization with catalyst/MAO, isotacticity of poly(1-hexene) also decreases with the decrease of monomer concentration (see Figure A-117 and Table A-21). At 50°C, isotacticity of poly(1-hexene) increases greatly at both pentad and heptad levels with the increase of monomer concentration when monomer concentration is under a certain level. Then mmmm% levels off after monomer concentration reaches a certain level and mmmmm% increases slightly with monomer concentration. Overall, the monomer concentration effect on the stereospecificity in our polymerization system is not as great as that shown in the previous reported polymerization system.

To explain the loss of stereospecificity with the decrease of monomer concentration, Resconi et al[62b] postulated an equilibrium between an isospecific

site C_i*M having a coordinated monomer and an aspecific one C_a* without a coordinated monomer:

$$C_a^* + M \Leftrightarrow C_iM^*$$

$$K_{eq} = [C_iM^*]/[C_a^*][M] \qquad [C_iM^*] = K_{eq}[C_a^*][M] \qquad \textbf{(29)}$$

C_a* was experimentally proven to be an epimerization catalyst[62b] which is able to racemize the chiral carbon of the last inserted unit. From his experimental results, Resconi concluded that the active center needs a coordinated monomer molecule in order to retain its stereospecificity.

Another possible explanation from Busico et al[68a] is that a slow reaction of epimerization of the last-inserted monomeric unit competes with that of chain propagation. It should be admitted that the reaction order with respect to monomer concentration, which is almost 1 for chain propagation, is 0 for epimerization. Therefore, between the compitition of propagation and epimerization, increasing monomer concentration favors propagation.

6.4 Catalyst Concentration Effect on Isotacticity

The isotacticity of poly(1-hexene) increases with the decrease of catalyst concentration. Figure A-118 and Table A-21 shows the increase of %mmmm and %mmmmmm+%mmmmmr with the decrease of catalyst concentration. However, Busico et al[68] and Resconi et al[62] once reported that the stereospecificity of polypropylene was independent of catalyst concentration in the normal range of 1×10^{-4} to 1×10^{-6} mol/L. The catalyst they used included the catalyst we used. The only difference between our experiment and his was that we used 1-hexene

as the monomer and he used propylene as the monomer. If there exists the competition of epimerization and propagation at the end of the active growing chain, the higher ratio of [M] : [active species] should favor propagation. The [active species] is proportional to [Zr]. Thus in another word, high [M] : [Zr] favors propagation and results in higher isotacticity.

6.5 MAO concentration Effect on Isotacticity

Figure A-119 and Table A-21 show that the isotacticity increases with the decrease of MAO concentration only at heptad level but not at pentad level. This effect has not been reported that much so far, but is very small. The higher the concentration of MAO, the higher the concentration of activated catalyst species, the lower the ratio of [M] : [active species]. Therefore high [MAO] favors epimerization.

6.6 Regiospecificity

Regiospecificity of Poly(1-hexene) was determined by ^{13}C NMR. If inverse insertion (or 2,1-addition) occurs, the chemical shift of the C1 (methylene carbon) and C2 (methine carbon) of the 2,1-inserted repeat units should be different from those on 1,2-inserted repeat units. The calculation[64] of carbon chemical shifts for the 2,1-inserted repeat units gives δ30.8ppm for C1 and δ37.58ppm for C2. The chemical shifts for C1 and C2 of 1,2-inserted repeat units are δ40.4ppm and δ31.1ppm, respectively, which were shown in Section 6.1. The experimental chemical shift value of C2 on 2,1-inserted unit was δ35.6ppm. The ratio of signal integral at δ35.6ppm (HHHHH) to signal integral of repeat unit

C2 represents the percentage of reverse repeat units. Table A-22 and Figure A-120 summarize the polymerization temperature effect on the percentage of reverse repeat units. Overall, the regiospecificity of poly(1-hexene) here is very high, even at high temperature. It slightly decreases with the elevation of temperature. At polymerization temperature of 100°C, the reverse repeat unit comprises of about 4.1% of entire repeat units. With the decreasing of polymerization temperature, the percentage of reverse repeat units decreases. When the polymerization temperature drops to 0°C, the percentage of reverse repeat units becomes only 0.32%. Our observation was consistent with the general trend for the polymerization temperature effect on regiospecificity, which is that the lower the polymerization temperature, the higher the regiospesificity in terms of monomer 1,2-insersion because less mistakes will make when the reaction rate is slower.

Literature regiospecificity studies of α-olefin polymerization with metallocene catalysis revealed that the polymerization effect on regiospecificity depended on catalysis system. Resconi et al.[62a] reported the similar trend of polymerization temperature effect on the regiospecificity of propylene polymerization by using catalysis systems of rac-C_2H_4[Indenyl]$_2ZrCl_2$/MAO and rac-C_2H_4[3-Me-Indenyl]$_2ZrCl_2$/MAO. They reported that in their polymerization of propylene,with the polymerization temperature increasing from 20 to 70 °C, the overall fraction of regioirregularities increased from 0.3% to 0.7% when rac-C_2H_4[Indenyl]$_2ZrCl_2$/MAO was used, but no regioirregularities could be detected

when rac-C_2H_4[3-Me-Indenyl]$_2ZrCl_2$/MAO was used. But so far, no literature studied the effect of polymerization temperature on regiospecificity in homogeneous 1-hexene polymerization.

Table A-23 and Figure A-121 show the catalyst concentration effect on the regiospecificity of poly(1-hexene) at polymerization temperature of 50°C. With the decrease of catalyst concentration, regiospecificity increases. There are no literature reports on the effect of catalyst concentration on regiospecificity in α-olefin polymerization.

Table A-24 and Figure A-122 summarize the monomer concentration effect on the regiospecificity of poly(1-hexene) at polymerization temperature of 50°C. When the monomer concentration decreases from 8.0M to 4.0M, the 2,1-insersion percentage almost does not change. But with the further decrease of the monomer concentration to 2.0M, the 2,1-insersion percentage increases to 1.7%. And when the monomer concentration continuely decreases to 0.80M, the 2,1-insersion percentage increases to 3%. The overall trend of monomer concentration effect on regiospecificity is: the lower the monomer concentration, the lower the regiospecificity.

There are literatures reported on the monomer concentration effect on the regiospecificity in propylene polymerization using metallocene catalysts. Reconi et al[62b] reported that regiospecificity is independent from monomer concentration in propylene polymerization using rac-C_2H_4[Indenyl]$ZrCl_2$. They also reported that these 2,1-inserted units were gradually converted into 1,3 propylene units

as the monomer concentration is lowered. Acually it was Busico et al[67] who first reported the transformation of 2,1-inserted units into 1.3 propylene unit in propylene polymerization with rac-C_2H_4[Indenyl]$ZrCl_2$ and rac-Me_2Si[Indenyl]-$ZrCl_2$ catalysts.

Table A-25 and Figure A-123 summarize MAO concentration effect on the regiospecificity of poly(1-hexene) at polymerization temperature of 50°C. When the MAO concentration decreases, regiospecificity of poly(1-hexene) increases slowly. This result is consistant with the catalyst concentration effect because the higher the catalyst concentration or/and the higher the MAO concentration, the higher the concentration of catalyst/MAO complex, the lower the ratio of catalyst active species concentration to monomer concentration.

6.7 Conclusions From the Microstructure Studies

From the above sections, we can get the following conclusions:

1. Isotacticity of the polymer decreases with the increase of temperature;
2. Isotacticity of the polymer increases with the increase of monomer concentration;
3. Isotacticity of the polymer slightly increases with the decrease of zirconocene catalyst concentration;
4. Isotacticity of the polymer slightly increases with the decrease of MAO concentration;
5. The lower the polymerization temperature, the higher the regiospecificity of poly(1-hexene);

6. The lower the catalyst concentration, the higher the regiospecificity of poly(1-hexene);

7. The lower the monomer concentration, the lower the regiospecificity of poly(1-hexene);

8. The lower the MAO concentration, the higher the regiospecificity of poly(1-hexene).

Table A-16 ^{13}C NMR Chemical Shifts of the C3 Carbon of Poly(α-olefins) (in ppm Relative to the Chemical Shift of mmmmmm)[a]

	Heptad	Pentad	PHEX obsd
m(mmmm)m	0.000	0.000	0.00
m(mmmm)r	0.000		
r(mmmm)r	-0.116		
m(mmmr)m	-0.135	-0.192	-0.18
m(mmmr)r	-0.135		
r(mmmr)m	-0.248		
r(mmmr)r	-0.250		
m(rmmr)m	-0.382	-0.348	-0.18
m(rmmr)r	-0.382		
r(rmmr)r	-0.280		
m(mmrr)m	-0.328	-0.383	-0.21
m(mmrr)r	-0.328		
r(mmrr)m	-0.443		
r(mmrr)r	-0.431		
m(mmrm)m	-0.438	-0.469	-0.42
m(mmrm)r	-0.438		
r(mmrm)m	-0.546		
r(mmrm)r	-0.455		
m(rmrr)m	-0.576	-0.545	-0.58
m(rmrr)r	-0.566		
r(rmrr)m	-0.472		
r(rmrr)r	-0.566		

Table A-16 (continued)

m(rmrm)m	-0.684	-0.660	-0.65
m(rmrm)r	-0.689		
r(rmrm)m	-0.684		
r(rmrm)r	-0.584		
m(rrrr)m	-0.671	-0.733	-0.71
m(rrrr)r	-0.763		
r(rrrr)r	-0.763		
m(mrrr)m	-0.887	-0.860	-0.78
m(mrrr)r	-0.882		
r(mrrr)m	-0.789		
r(mrrr)r	-0.882		
m(mrrm)m	-1.011	-0.943	-0.82
m(mrrm)r	-0.909		
r(mrrm)r	-0.909		

[a] The pentad chemical shifts were obtained by averaging over the heptad

Table A-17 Effects of Polymerization Conditions on the Isotacticity

Temp. (°C)	[M] (M)	[Zr] (μM)	[MAO] (mM)	mmmm (%)	mmmmmm + mmmmmr (%)
100	8.0	52	62	47	21
	8.0	1.0	62	54	27
	8.0	52	7.4	58	27
80	8.0	52	62	58	43
	8.0	1.0	62	74	52
50	8.0	104	62	76	55
	8.0	52	62	84	67
	8.0	26	62	88	76
	8.0	5.2	62	90	83
	4.0	52	62	84	65
	2.0	52	62	82	59
	0.8	52	62	69	42
	8.0	52	18	92	83
	8.0	52	4.0	92	92
0	8.0	52	62	97	97
	2.0	52	62	89	89

Table A-18 Polymerization Temperature Effect

on the Regiospecificity of Poly(1-hexene)*

Polymerization Temperature (°C)	Percentage of Reverse Repeat Units
100	4.1
80	3.9
50	1.4
0	0.32

*Polymerization conditions: [Zr] = 52 μM, [MAO] = 62 mM and [M] = 8.0 M.

Table A-19 Catalyst Concentration Effect

on the Regiospecificity of Poly(1-hexene)

Catalyst Concentration (μM)	Percentage of Reverse Repeat Units
99	1.6
52	1.4
26	1.0
5.2	0.94

*Polymerization conditions: T=50°C, [MAO] = 62 mM and [M] = 8.0 M.

Table A-20 Monomer Concentration Effect

on the Regiospecificity of Poly(1-hexene)

Monomer Concentration (M)	Percentage of Reverse Repeat Units
8.0	1.4
4.0	1.4
2.0	1.7
0.80	3.0

*Polymerization conditions: T=50°C, [Zr] = 52 μM, and [MAO] = 62 mM.

Table A-21 MAO Concentration Effect

on the Regiospecificity of Poly(1-hexene)

MAO Concentration (mM)	Percentage of Reverse Repeat Units
62	1.4
16	1.1
3.7	0.85

*Polymerization conditions: T=50°C, [Zr] = 52 μM, and [M] = 8.0 mM.

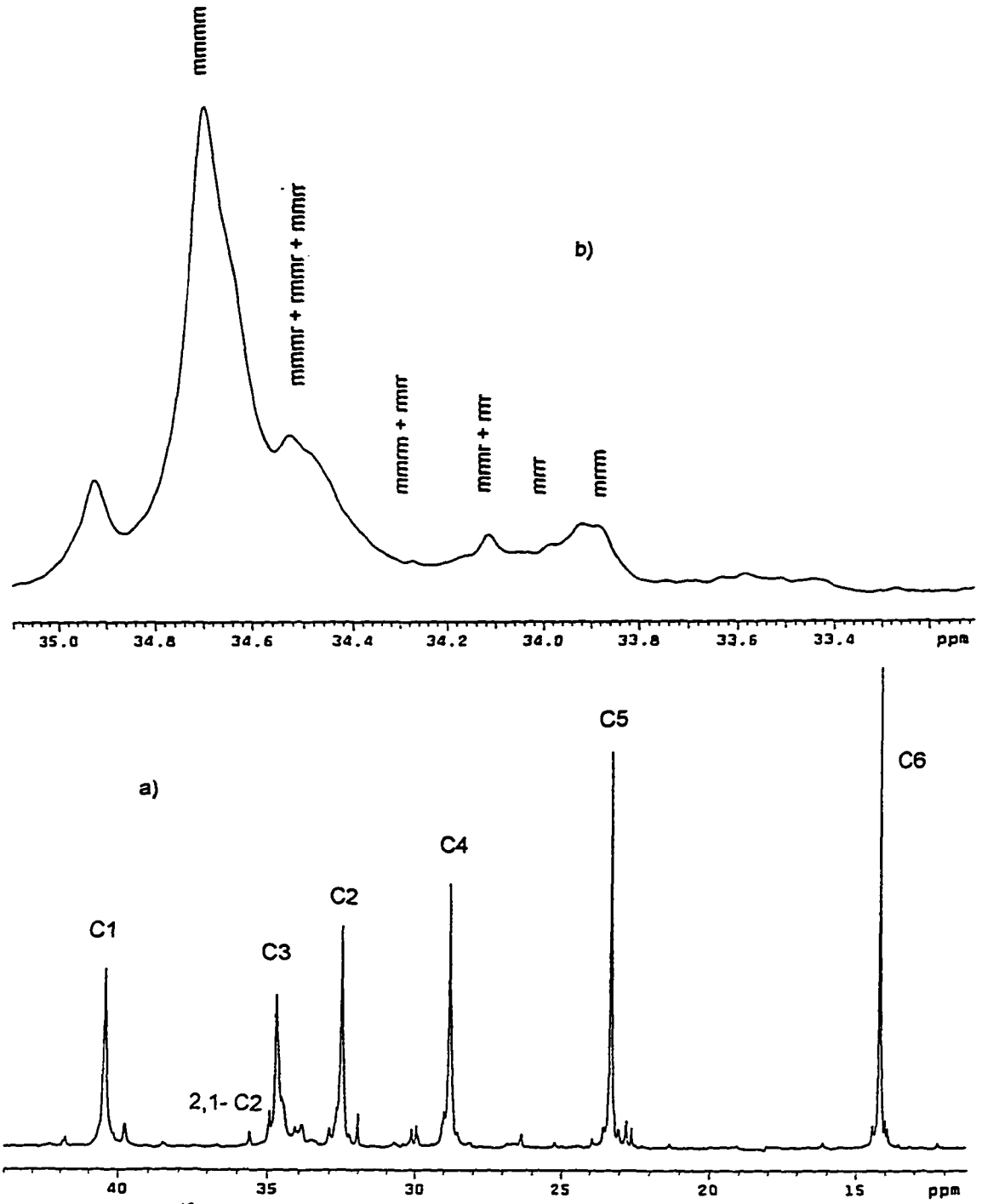

Figure A-115 ^{13}C NMR of an isotactic poly(1-hexene)
Polymerization conditions: [Zr]=52μM, [M]=8.0M, [MAO]=62mM and T=80oC.
a) six saturated carbons; b) C3 expended spectrum.

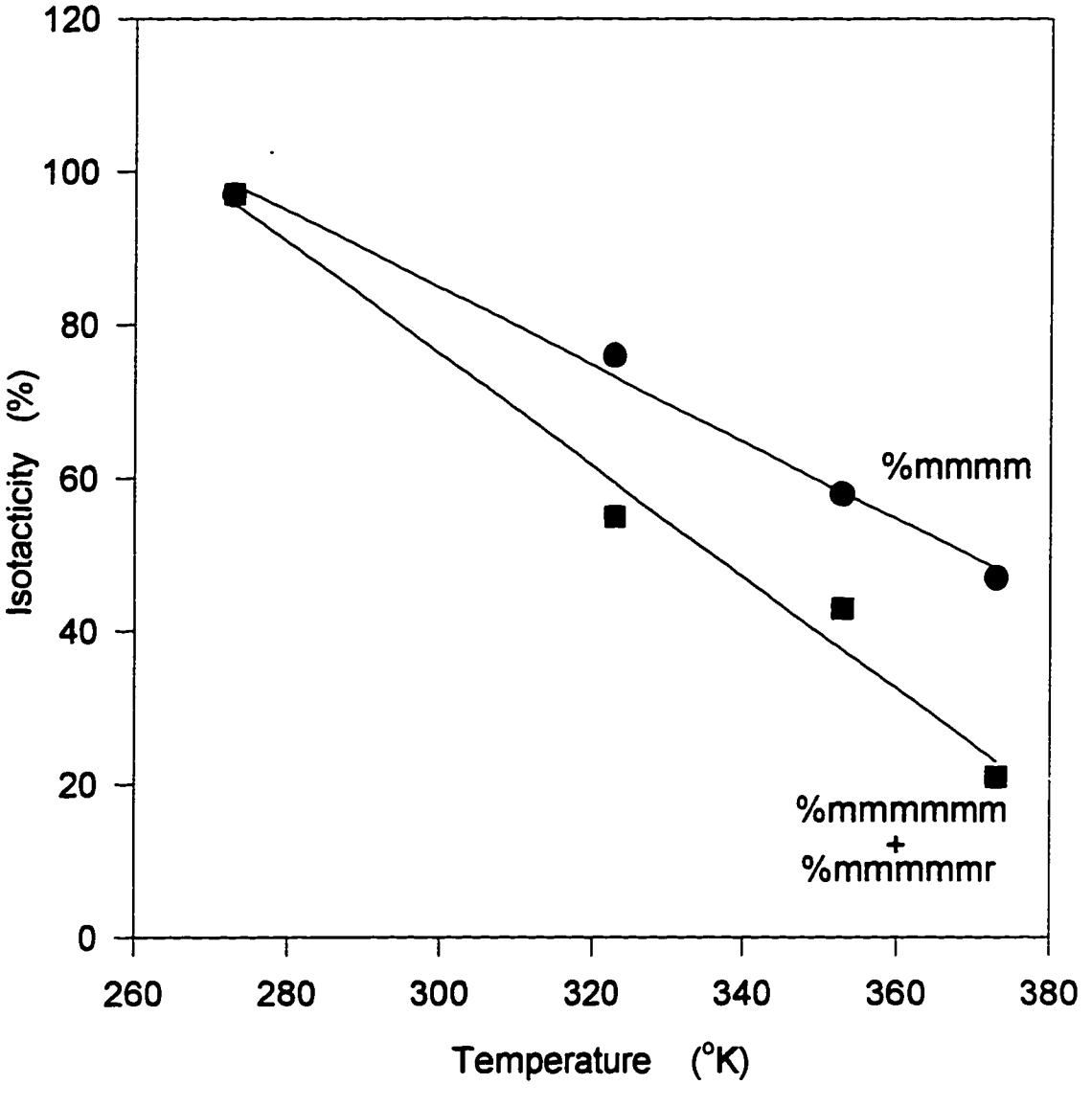

Figure A-116 Isotacticity of poly(1-hexene) as a function of temperature

Polymerization conditions: [Zr]=52μM, [MAO]=62mM and [M]=8.0M

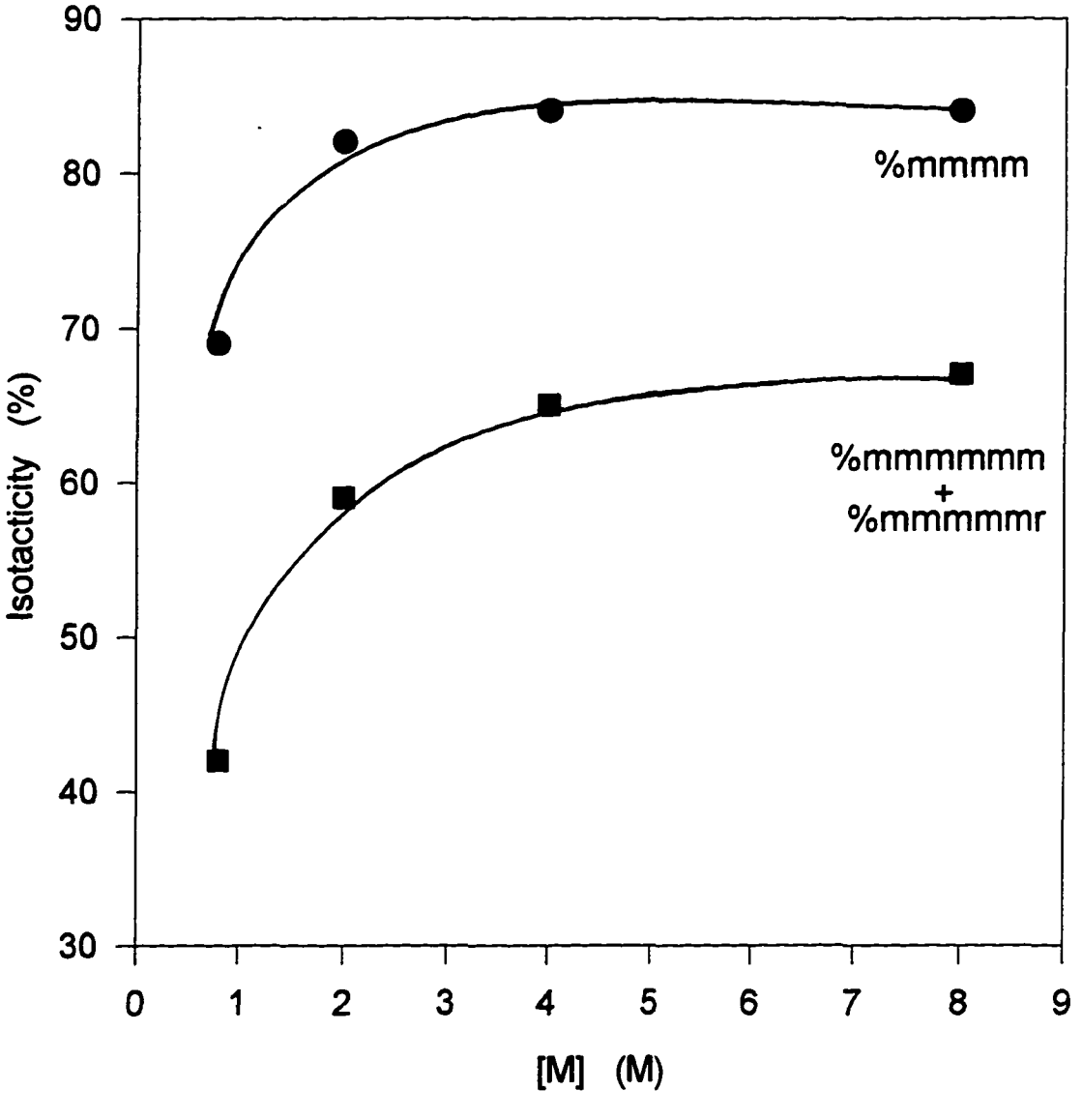

Figure A-117 Isotacticity of poly(1-hexene) as a function of monomer concentration

Polymerization conditions: T=50°C, [Zr]=52μM and [MAO]≈62mM

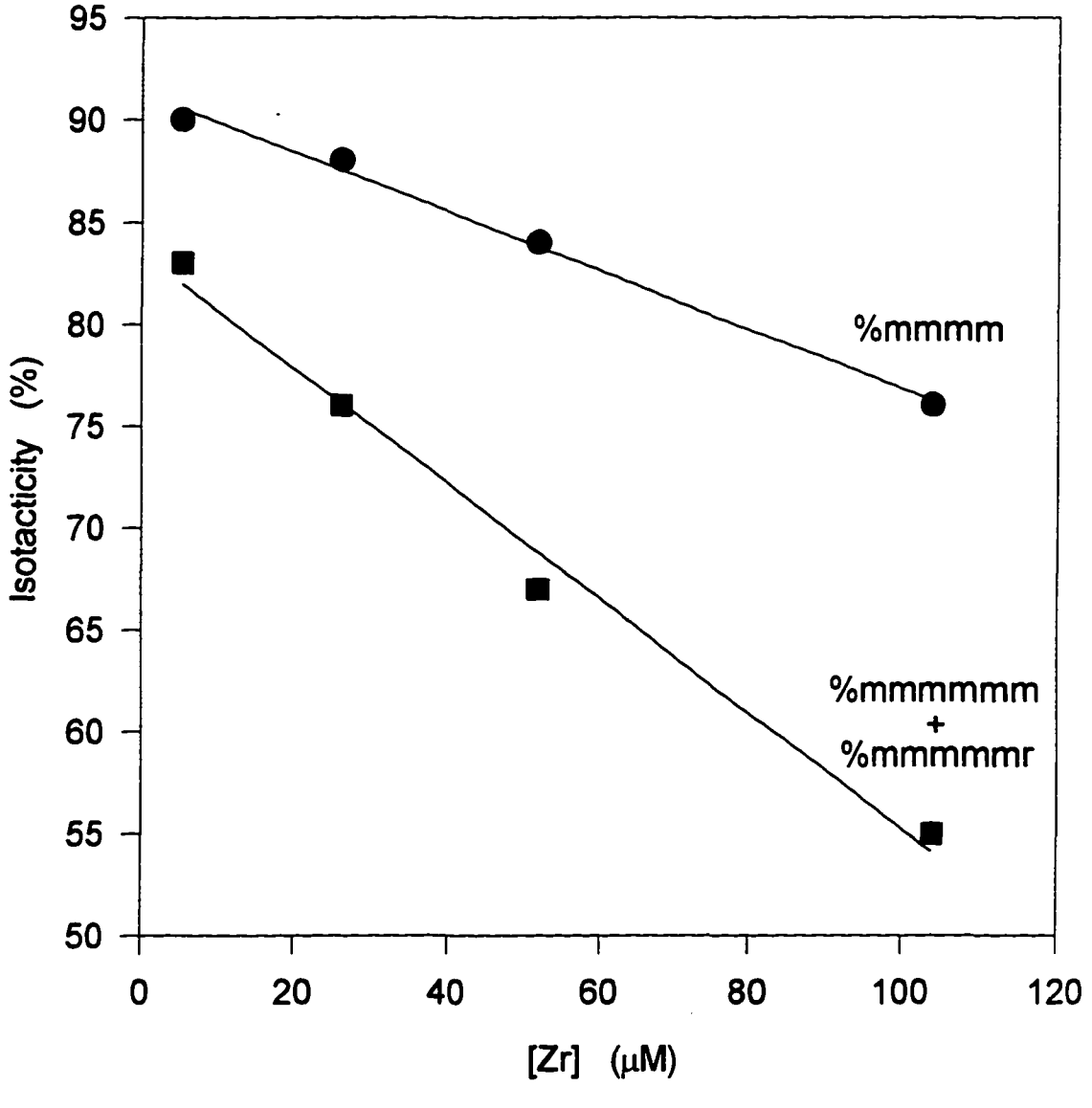

Figure A-118 Isotacticity of poly(1-hexene) as a function of catalyst concentration

Polymerization conditions: T=50°C, [MAO]=62mM and [M]=8.0M

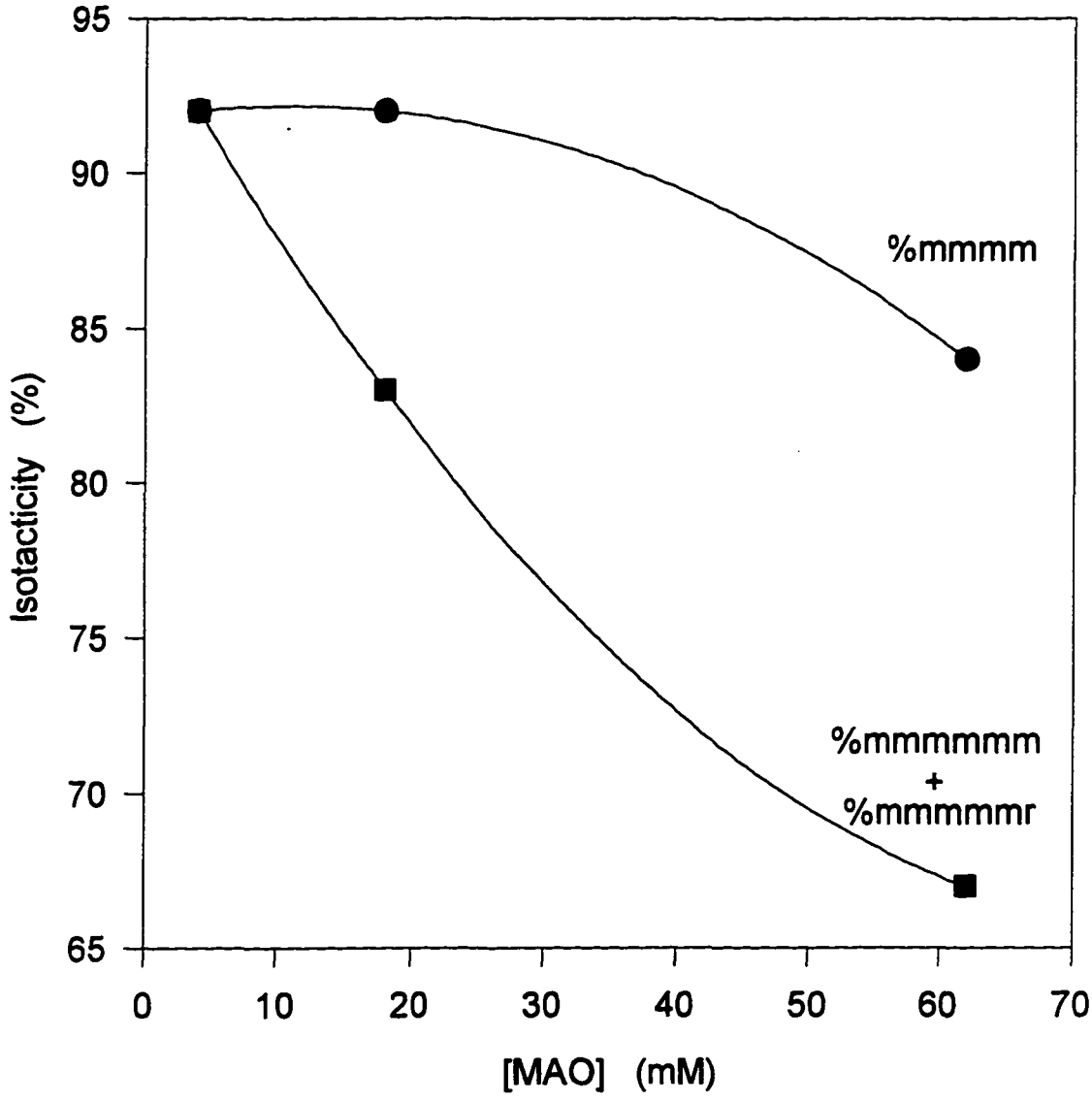

Figure A-119 Isotacticity of poly(1-hexene) as a function of MAO concentration

Polymerization conditions: T=50°C, [Zr]=52μM and [M]=8.0M

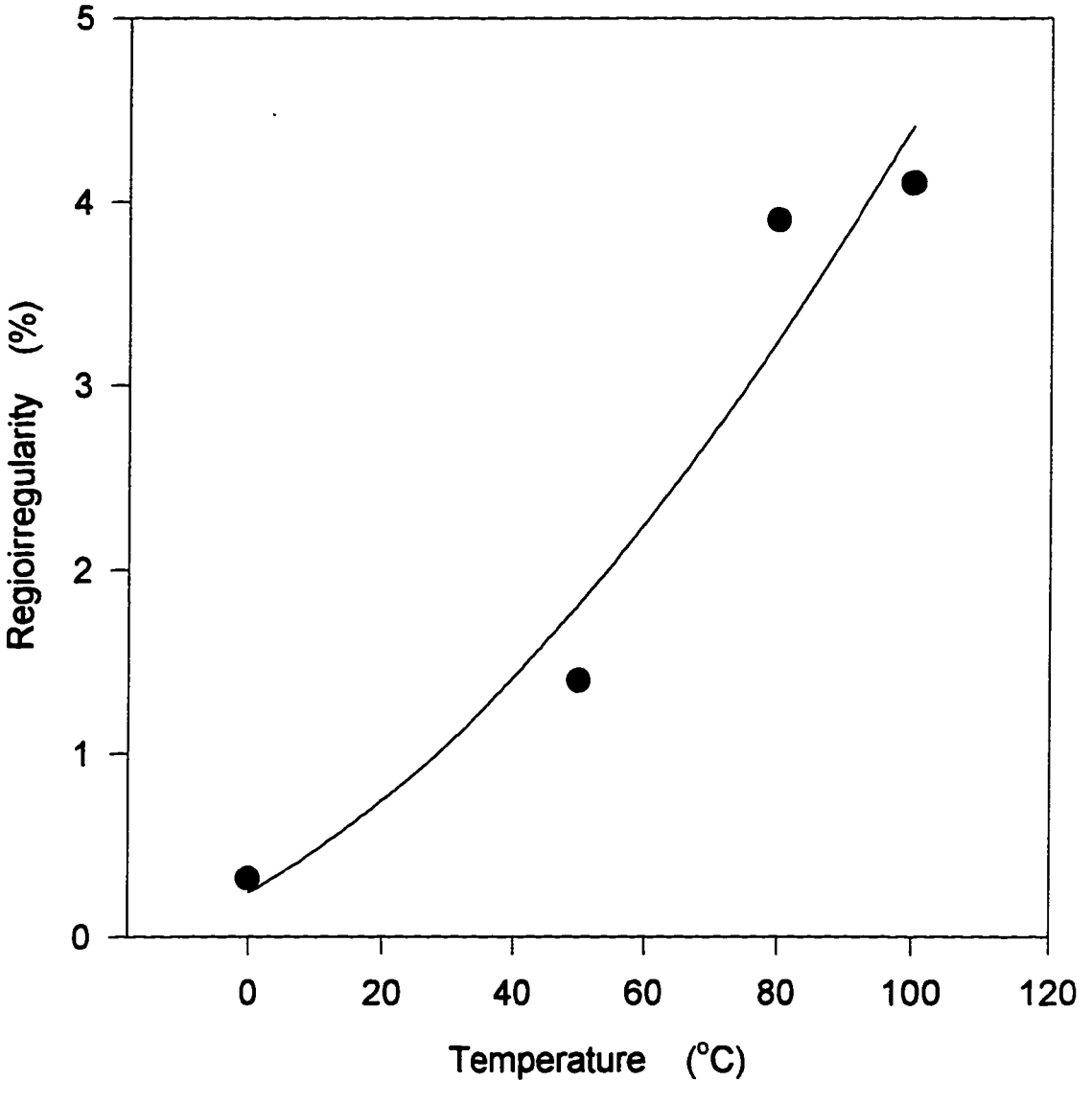

Figure A-120 Temperature effect on regiospecificity

Polymerization conditions: [Zr]=52μM, [MAO]=62mM and [M]=8.0M

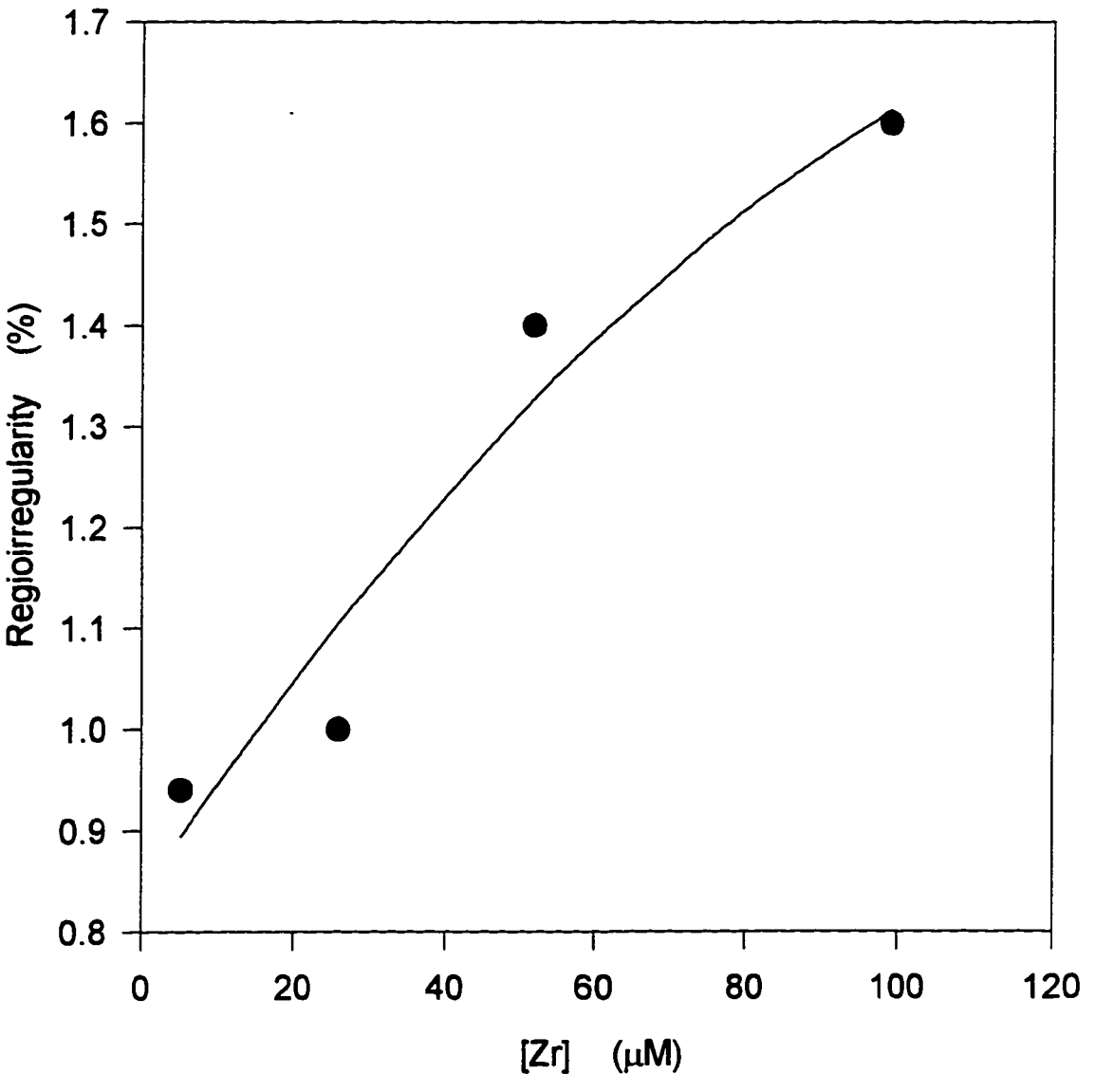

Figure A-121 Catalyst concentration effect on regiospecificity

Polymerization conditions: T=50°C, [MAO]=62mM and [M]=8.0M

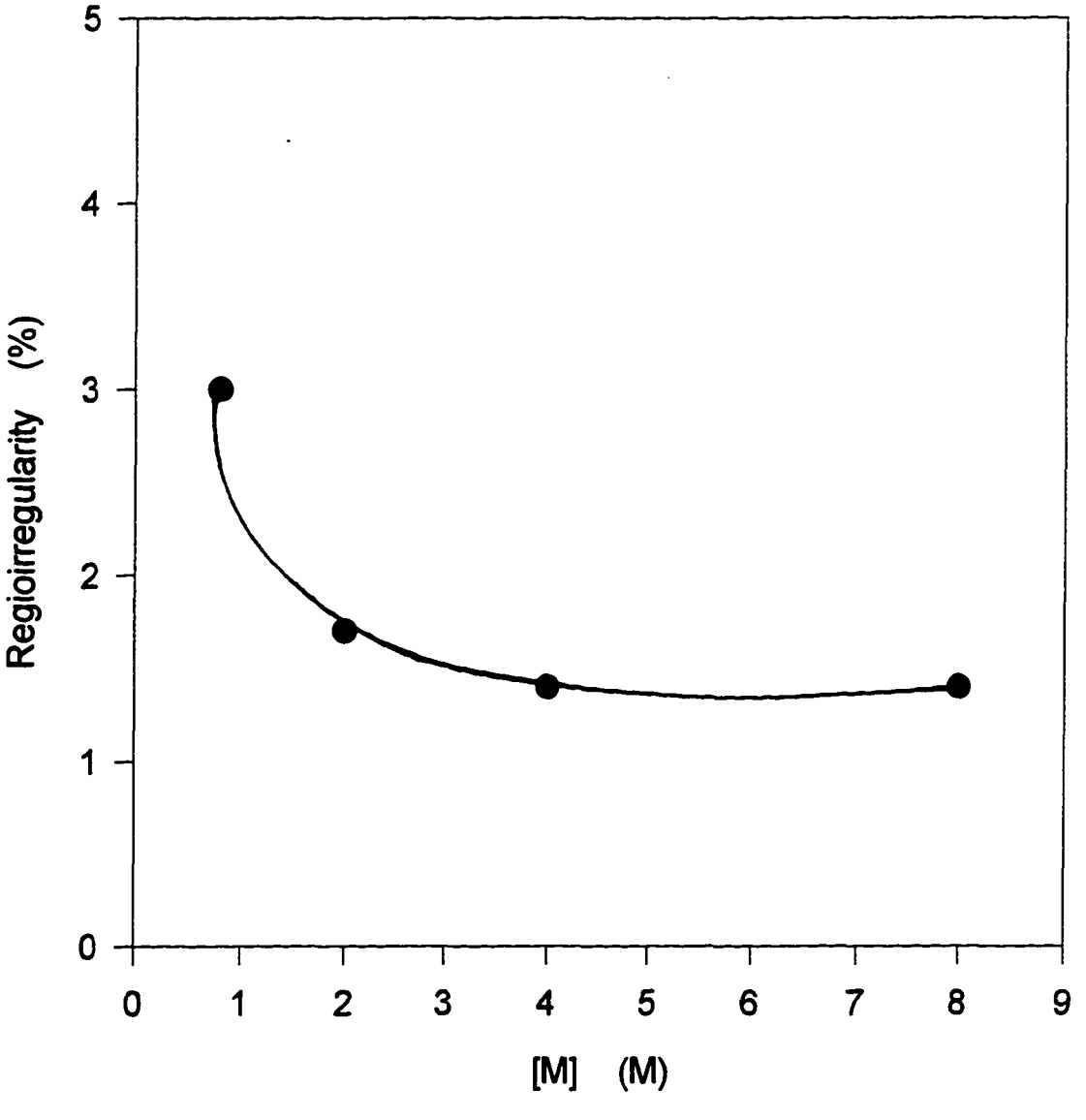

Figure A-122 Monomer concentration effect on regiospecificity

Polymerization conditions: T=50°C, [Zr]=52μM and [MAO]=62mM

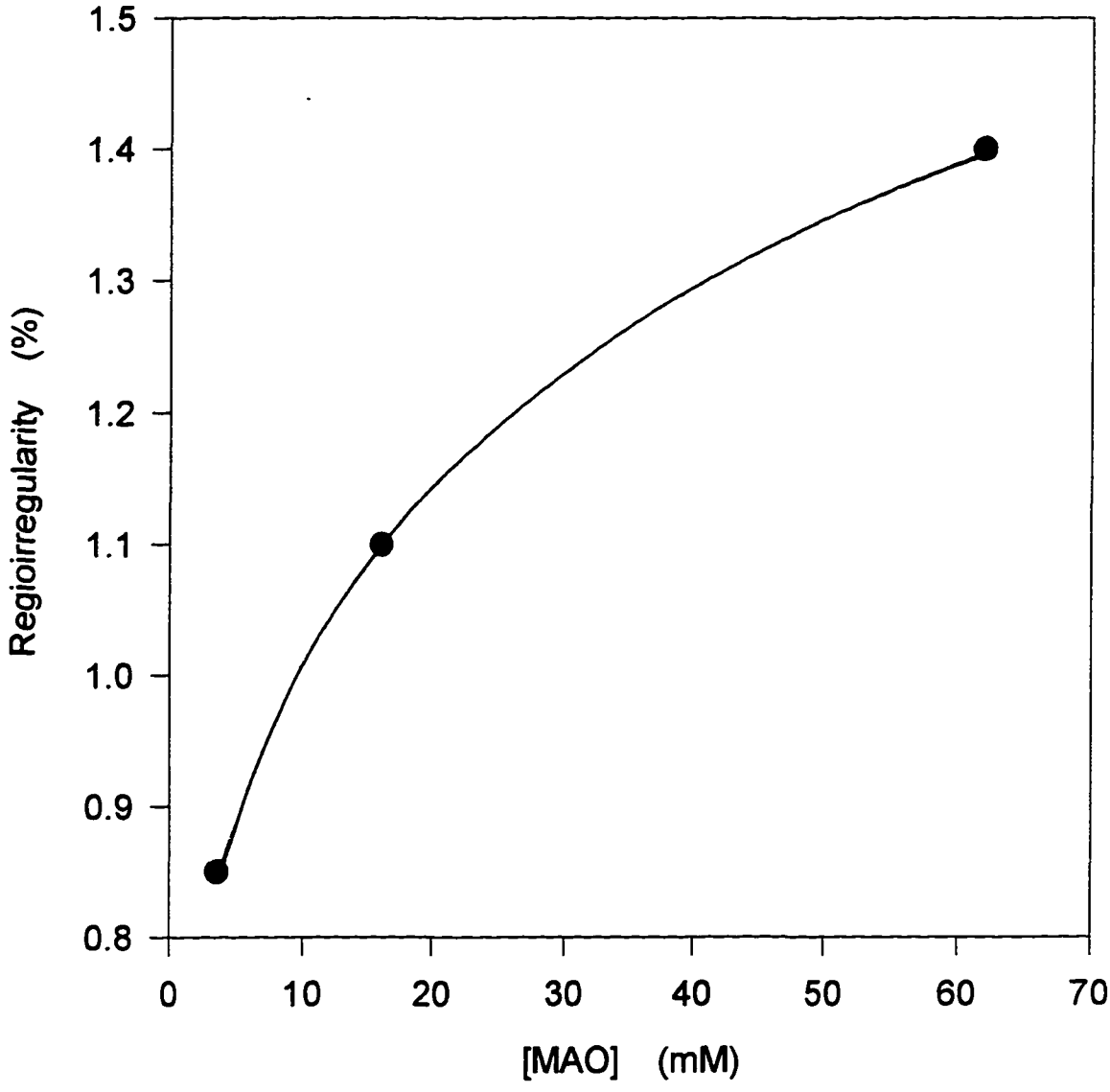

Figure A-123 MAO concentration effect on regiospecificiity

Polymerization conditions: T=50°C, [Zr]=52μM and [M]=8.0M

7.0 References

1. K. Ziegler, E. Holzkamp, H. Breil and H. Martin, *Angew . Chem.*, 1955, **426**, 541.

2. K. Ziegler, *Angew. Chem.*, 1964, **76**, 545.

3. G. Natta, *Makromol. Chem.*, 1955, **16**, 213.

4. G. Natta, *J. Polym. Sci.*, 1955, **16**, 143.

5. G. Natta, *J. Polym. Sci.*, 1960, **48**, 219.

6. G. Natta, *Science*, 1965, **147**, 261.

7. K. Y. Choi and W. H. Ray, *J. Macromol. Sci., Rev. Macromol. Chem Phys.*, 1985, **C25**, 1, 57.

8. P. Pino, U. Giannini and L. Porri, *"Insertion Polymerization,"* pp147, in "Encyclopedia of Polymer Science and Engineering," Vol. 8, 2nd ed., H. F. Mark, N. M. Bikales, C. G. Overberger and G. Imenges, Eds., Wiley-Interscience, New York, 1987.

9. I. Pasquon, L. Porri and U. Giannini, *"Stereo Polymers,"* pp632, in "Encyclopedia of Polymer Science and Engineering," Vol. 15, 2nd ed., H. F. Mark, N. M. Bikales, C. G. Overberger and G. Imenges, Eds., Wiley-Interscience, New York, 1989.

10. A. M. Thayer, *C&E News*, 1995, Sep. 11, 15.

11. G. Natta, P.Pino, G. Mazzanti and V. Giannini, *J. Am. Chem. Soc.*, 1957, **79**, 2975.

12. W. Kaminsky, M. Miri, H. Sinn and R. Woldt, *Makromol. Chem. Rapid Commun.*, 1983, **4**, 417.

13. D. Cam, E. Albizzati and P. Cinquina, *Makromol. Chem.*, 1990, **191**, 1641.

14. J. A. Ewen, *J. Am. Chem. Soc.*, 1984, **106**, 6355.

15. L. Oliva, P. Longo and C. Pellecchia, *Makromol. Chem. Rapid Commun.*, 1988, **9**, 51.

16. A. Zambelli, P. Ammendola, Allegra, A. Grassi, P. Longo and A. Proto, *Makromol.*, 1988, **19**, 2703.

17. F. R. W. P. Wild, M. Wasiacionek, G. Huttner and H. H Brintzinger, *J. Organomet. Chem.*, 1985, **288**, 63.

18. J. A. Ewen, *"Catalytic Polymerization of Olefins,"* T. Keii, and K. Soga, Eds., Kodansha Elsevier, Tokly, 1986, 271.

19. W. Kaminsky, K. Külper, H. H. Brintzinger and F. R. W. P. Wild, *Angew. Chem. Int. Ed. Engl.*, 1985, **24**, 507.

20. W. Kaminsky, *Angew. Makromol. Chem.*, 1986, **145/146**, 149.

21.a) N. Kashiwa and J. Yoshitake, *Makromol. Chem.*, 1984, **185**, 1133;

b) P. Galli, P. C. Barbe and L. Noristi, *Angew. Makromol. Chem.*, 1984, **120**, 73;

c) P. Galli and J. C. Haylock, *Makromol. Chem., Macromol. Symp.*, 1992, **63**, 19.

22. T. Tsutsui, N. Ishimaru, A. Mizuno, A. Toyota and N. Kashiwa, *Polymer*, 1989, **30**, 1350.

23. D. Seebach, *Angew. Chem.*1990, 102, 1363; *Angew. Chem. Int. Ed. Engl.*, 1990, **29**, 1320.

24. B. Rieger, X. Mu, D. T. Mallin, M. D. Rausch and J. C. W. Chien, *Macromolecules*, 1990, **23**, 3559.

25. H. N. Cheng, G. N. Babu, R. A. Newmark and J. C. W. Chien, *Macromolecules*, 1992, **25**, 6980.

26. a) J. A. Ewen, R. L. Jones, A. Razaui and J. D. Ferrara, *J. Am. Chem. Soc.*, 1988, **110**, 6255;

b) J. A. Ewen, M. J. Elder, R. L. Jones, L. Haspeslagh, J. L. Atwood, S. G. Bott and K. Robinson, *Makromol. Chem., Macromol. Symp.*, 1991, **48/49**, 253.

27. a) W. A. Herrmann, J. Rohrmann, E. Herdweck, W. Spaleck and A. Winter, *Angew. Chem.*1989, 101, 1536; *Angew. Chem. Int. Ed. Engl.*, 1989, **28**, 1511;

b) W. Spaleck, M. Antberg, J. Rohrmann, A. Winter, B. Bachmann, P. Kiprof, J. Behm and W. A. Herrmann, *Angew. Chem.*1992, 104, 1373; *Angew. Chem. Int. Ed. Engl.*, 1992, **31**, 1347;

c) W. Spaleck, F. Küber, A. Winter, J. Rohrmann, B. Bachmann, M. Antberg, V. Dolle and E. F. Paulus, *Organometallics*, 1994, **13**, 954.

28. T. Mise, S. Miy and H. Yamzaki, *Chem. Lett.*, 1989, 1853.

29. S. Collins, W. J. Gauthier, D. A. Holden, B. A. Kuntz, N.J. Taylor and D. G. Ward, *Organometallics*, 1991, **10**, 2061.

30. a) W. Röll, H. H. Brintzinger, B. Rieger and R. Zolk, *Angew. Chem.*, 1990, **102**, 339; *Angew. Chem. Int. Ed. Engl.*, 1990, **29**, 279;

b) U. Stehling, J. Diebold, R. Kirsten, W. Röll, H. H. Brintzinger, S. Jüngling, R. Mülhaupt and F. Langhauser, *Organometallics*, 1994, **13**, 964.

31. B. Rieger, *J. Organomet. Chem.*, 1992, **428**, 33.

32. Y. X. Chen, M. D. Rausch and J. C. W. Chien, *Organometallics*, 1994, **13**, 748.

33. J. A. Ewen, L. Haspeslagh, M. J. Elder, J. L. Atwood, H. Zhang and H. N. Cheng, *"Transition Metals and Organometallics as Catalysts for Olefin Polymerization,"* W. Kaminsky and H. Sinn, Ed., Springer, Berlin, 1988, pp281.

34. W. Kaminsky, R. Engehausen, K. Zoumis, W. Spaleck and J. Rohrmann, *Makromol. Chem.*, 1992, **193**, 1643;

35. E. B. Coughin and J. E. Bereaw, *J. Am. Chem. Soc.*, 1992, **114**, 7606.

36. a) P. Longo, A. Grassi, C. Pellecchia and A. Zambelli, *Macromol.*, 1987, **20**, 1015.

b) A. Zambelli, C. Pellecchia and L. Oliva, *Makromol. Chem., Macromol. Symp.*, 1991, **48/49**, 297.

37. a) L. Cavallo, G. Guerra, L. Oliva, M. Vacatello and P. Corradini, *Polym. Commun.*, 1989, **30**, 16;

b) V. Venditto, G. Guerra, P. Corradini and R. Fnsso, *Polymer*, 1990, **31**, 530;

c) L. Cavallo, P. Corradini, G. Guerra and M. Vacatello, *Macromol*ecules, 1991, **24**, 1784;

d) G. Guerra, L. Cavallo, V. Venditto, M. Vacatello and P. Corradini, *Makromol. Chem., Macromol. Symp.*, 1993, **69**, 237;

e) G. Guerra, L. Cavallo, G. Moscardi, M. Vacatello and P. Corradini, *J. Am. Chem. Soc.*, 1994, **116**, 2988.

38. a) P. Corradini, V. Barone, R. Fusco and G. Guerra, *Eur. Polym. J.*, 1979, **15**, 1133;

b) P. Corradini, G. Guerra, R. Fusco and V. Barone, *ibid.*, 1980, **16**, 835;

c) P. Corradini, V. Barone and G. Guerra, *Macromolecules.*, 1982, **15**, 1282.

39. P. Pino, P. Cioni and J. Wei, *J. Am. Chem. Soc.*, 1987, **109**, 6189.

40. E. B. Coughlin and J. E. Bercaw, *J. Am. Chem. Soc.* 1992, **114**, 7606.

41. M. Leclere and H. H. Brintzinger, *J. Am. Chem. Soc.*, 1995, **117**, 1651.

42. W. Röll, L. Zsolnai, G. Huttner and H. H. Brintzinger, *J. Organomet. Chem.*, 1987, **322**, 65.

43. P. Burger, K. Hortmann and H. H. Brinzinger, *Makromol. Chem., Macromol. Symp.*, 1993, **66**, 127;

44. a) D. T. Mallin, M. D. Rausch and J. C. W. Chien, *Polym. Bull.*, 1988, **20**, 421;

b) J. C. W. Chien and A. Razavi, J. *Polym. Sci., Part A*, 1988, **26**, 2369.

45. B. W. S. Kolthammer, D. J. Mangold and D. R. Gifford, J. *Polym. Sci., Part A*, 1992, **30**, 1017.

46. a) D. Fischer and R. Mülhaupt, *J. Organomet. Chem.*, 1991, ?;

b) D. Fischer and R. Mülhaupt, *Makromol. Chem.*, 1994, **195**, 1433.

c) S. Jüngling, R. Mülhaupt, U. Stehling, H. Brintzinger, D. Fischer and F. Langhauser, J. *Polym. Sci., Part A*, 1995, **33**, 1305.

47. D. E. James, *"Ethylene Polymers: Linear Low Density Polyethylene,"* in "Encyclopedia of Polymer Science and Engineering," 2nd ed., H. F. Mark, N. M. Bikales, C. G. Overberger and G. Imenges, Eds., Wiley-Interscience, New York, 1986, **Vol. 6**, pp429.

48. A. Rossi, G. Odian and J. B. Zhang, *Macromolecules*, 1995,

49. G. N. Babu, R. A. Newmark and J. C. W. Chien, *Macromolecules*, 1994, **27**, 3383;

50. a) N. Herfert and G. Fink, *Makromol. Chem.*, 1992, **193**, 1959;

b) N. Herfert and G. Fink, *Makromol. Chem., Macromol. Symp.*, 1993, **66**, 157.

51. A. R. Siedle, W. M. Lamanna, J. M. Olofson, B. A. Nerad and R. A. Newmark, "*Selectivity in Catalysis,*" in "ACS Symposium Series. 517," M. E. Davis, S. L. Suib, Eds., Washington, DC, 1993, pp156.

52. A. R. Anderson, "*Aluminum Compounds*", in "Encyclopedia of Chemical Technolygy," 1st ed., M. Grayson, D. Eckroth, G. J. Bashey, A. Klingsberg and I. V. Nes, Eds., 1964, **Vol. 2**, pp33.

53. J. C. W. Chien and R. Sugimoto, *J. Polym. Sci., Part A*, 1991, **29**, 459.

54. D. Cam and E. Albizzati, *Makromol. Chem.*, 1990, **191**, 1641.

55. M. S. Howie, Presentation at MetCon '93, unpublished.

56. L. Resconi, S. Bossi and L. Abis, *Macromolecules*, 1990, **23**, 4489.

57. D. Cam and U. Giannini, *Makromol. Chem.*,1992, **193**, 1049.

58. W. Kaminsky, M. Schlobohm, *Makromol. Chem., Macromol. Symp.*, 1986, **4**, 103.

59. G. Odian, "*Principles of Polymerization*," 3rd ed., John Wiley & Son, Inc., 1991, a) pp275; b) pp650.

60. "*Non-Aromatic Hydrocarbons: 3) Unsaturated Straight Chain; 4) Unsaturated Branched Chain*" in "The Aldrich Library of ^{13}C and ^{1}H FT-NMR Spectra", 1st ed., C. J. Pouchert and J. Behnke, **Vol. 1**, 17C-35B.

61. W. Kaminsky, K. Külper, S. Niedoba, *Makromol. Chem., Macromol. Symp.*, 1986, **4**, 103.

62. a) L. Resconi, F. Piemontesi, I Camurati, H. Rychlicki, M. Colonnesi and D. Balboni, *PSME Symposium*, 1995, **73**, 516.

b) L. Resconi, A. Fait, F. Piemontesi, M. Colonnesi, H. Rychlicki and R. Zeigler, *J. Am. Chem. Soc.*, 1995, **117**, 6667.

63. U. Stehling, J. Diebold, R. Kirsten, W. Röll, H. H. Brintzinger, S. Jüngling, R. Mülhaupt and F. Langhauser, *Organometallics*, 1994, **13**, 964.

64. T. Asakura, M. Demura and Y. Nishiyama, *Macromolecules*, 1991, **24**, 2334.

65. H. N. Cheng and M. A. Bennet, *Anal. Chim. Acta.*, 1991, **242**, 43.

66. E. G. Paul and D. M. Grant, *J. Am. Chem. Soc.*, 1964, **86**, 2984.

67. SPECINFO database in STN, available from Chemical Abstracts Service, Columbus, OH.

68. a) V. Busico and R. Cipullo, *J. Am. Chem. Soc.*, 1994, **116**, 9329.

b) V. Busico and R. Cipullo, *Makromol. Chem., Macromol. Symp.*, 1995, **87**, 277.

c) V. Busico, R. Cipullo, J. Chadwick, J. F. Modder and O. Sudmeijer, *Macromolecules*, 1994, **27**, 7538.

69. U. W. Suter and P. Neuenschwander, *Macromolecules*, 1981, **14**, 528.

Part. B Synthesis of Oscillating Metallocene Catalysts

1.0 Introduction

1.1 Stereochemistry of Poly(α-olefin) and Their Influences on Polymer Properties

The stereochemistry of poly(α-olefin) is critical for their application. In 1963, Ziegler and Natta won the Nobel Prize for their work in stereoregular polypropylene[1] and opened a gate for commercial use of polypropylene. There are three kinds of stereochemistry for poly(α-olefin), isotactic, syndiotactic and atactic polymer, distinguished by the overall order (tacticity) of the polymer chain[2]. Here, we use polypropylene, which is the simplest poly(α-olefin), as an example. The structure A is termed atactic if the Me groups on successive stereocenters are randomly distributed on the two sides of the planer zigzag polymer chain and the polymer does not have order. Two types of stereoregular or tactic structures can be distinguished. The structure B is termed Isotactic structure because the stereocenter in each repeating unit in the polymer chain has the same configuration and all the Me groups will be located on the same side of the polymer chain. And the structure C is syndiotactic when the configuration of the stereo center alternates from one repeating unit to the next with the Me groups located alternately on the opposite sides of the plane of the polymer chain.

The properties of poly(α-olefin) are influenced strongly by their stereochemistry. Isotactic polypropylene is a crystalline thermoplastic, whereas

atactic polypropylene in an amorphous gum elastomer. Polypropylene consisting of blocks of atactic and isotactic stereosequences is a rubbery material with properties of a thermoplastic elastomer (see structure D). This kind of rubbery polypropylene was first produced by Natta and the elastomeric properties of this material was interpreted in terms of a stereoblock structure consisting of blocks of crystallized stereosequences and amorphous atactic stereosequences[3].

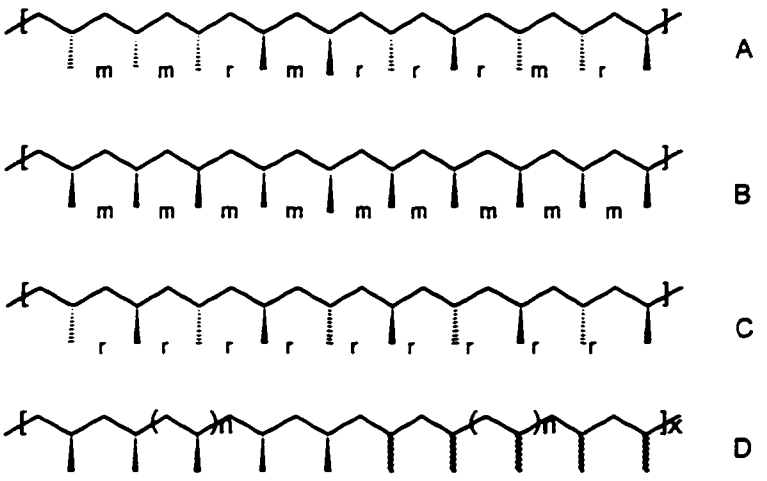

1.2 The Key to Control Stereochemistry--Catalysts

Polypropylene can be used widely today as a plastic because this polymer is dominated by only one type of tactic form (mainly isotactic form). The key to produce tactic polypropylene is the Ziegler-Natta catalyst. The chemistry begins with a fixed chiral (stereoregular) center found within the catalyst itself, and this center initiates a chain reaction of tens of thousands of propylene molecules to produce the polymer. The catalyst structure permits the insertion of the monomer molecules into the propagating species exclusively from one side of the

monomers. The amazing aspect of Zieglar-Natta chemistry is that each insertion of propylene occurs with nearly perfect stereochemical precision, thereby producing the same stereocenter each time in isotactic polymerization, and the alternating stereocenters in syndiotactic polymerization. An enormous amount of work has been done in this field since the Ziegler-Natta discovery[4]. However, it is not the end of the story.

We are experiencing an evolution of new generations of catalysts and polyolefin materials, which originate from studies on homogeneous, metallocene-based polymerization catalysts. Numerous subsequent studies on homogeneous catalysts and their polymerization have been summarized previousl[y5-8]. Chiral metallocenes were found to be able to produce highly isotactic polymers[9-15], some meso metallocenes can form highly syndiotactic polyolefins[16], and achiral meso metallocenes can get atactic polyolefins[17]. Since metallocene-based polymers range from crystalline to elastomeric materials, it is predicted to lead the plastics industry into a new era[18].

1.3 Oscillating Catalysts--A New Twist for Plastics[19]

It was mentioned before that the rubbery material polypropylene, consisting of blocks of atactic and isotactic stereosequences, was first produced by Natta. Subsequently, Collette et al reported improved catalysts for the synthesis of polypropylene with elastomeric properties based on the use of Zr and Ti alkyls on aluminum supports[20,21]. It was first reported by Chien et al that elastomeric polypropylene was synthesized using a stereorigid titanocene catalyst[22-24]. It was

proposed that polymerization occurs alternately at aspecific and isospecific coordination sites to give a stereoblock structure. Although these catalyst systems represent significant advances for the synthesis of elastomeric polypropylene, it has so far difficult to control the polymer structure and properties.

Oscillating stereocontrol is a strategy proposed by Waymouth and his co-workers for the synthesis of polypropylene rubbery material, which consists of blocks of atactic and tactic stereosequences[25]. As it has been described that chiral racemic ansa-metallocenes like **I** produce isotactic polyolefins, whereas achiral meso isomers as **II** form atactic polyolefins. If a metallocene can be

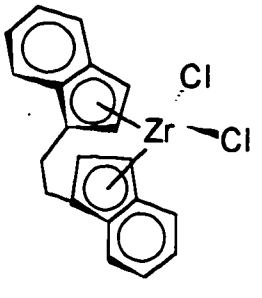

I

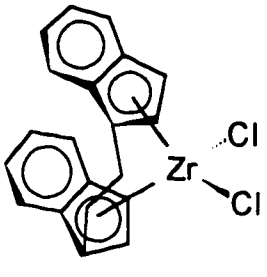

II

designed to oscillate between chiral rac-like and achiral meso-like geometries, which are called conformational isomers, stereoblock polymers can be produced under control. Since the rotation of the catalysts can be controlled through a rational modification of the catalysts or reaction conditions, the lengths of the stereoblocks in the polymers can be controlled. These kinds of catalysts were called oscillating metallocene catalysts. The first oscillating metallocene **III** was designed by Waymouth et al. In **III**, a phenyl substituent on the indene ligand

was chosen to inhibit the rate of ligand rotation between two extreme conformational isomers **IIIa** and **IIIb** such that it would be slower than that of monomer insertion yet faster than the time required to construct one polymer chain in order to produce atactic-isotactic stereoblock copolymers.

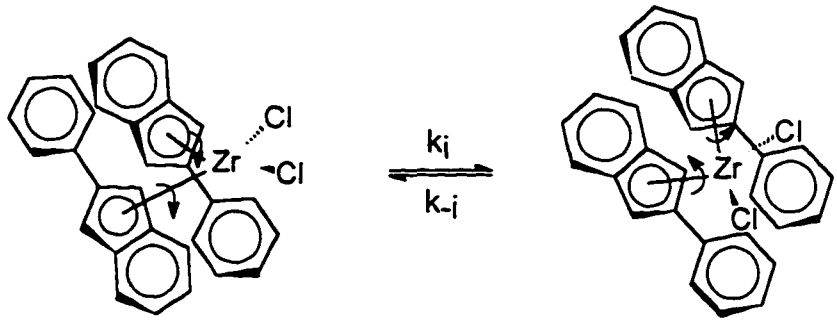

IIIa **IIIb**

k_{pi} k_{pa}

Isotactic block Atactic block

Although this catalyst did not show significant results in the polymerization of propylene, it did point the way for the development and application of metallocenes in a new direction.

1.4 Present work

To find metallocenes forming polyolefins with stereoblocks, a series of metallocenes were designed and synthesized. The basic modification is ligand substitution. **IV** is the general structure of ligands designed to be used in our work. Table B-1 summarizes the substituents we will put on indene rings.

The bonding orbitals on the center metal zirconium are sp^3 hybridized orbitals. The geometry of the compound $ZrX_1X_2X_3X_4$ should be tetrahedral if all

four ligands are identical. However, in zirconocenes, two of the ligands are bulky groups containing substituted cyclopentadienes, which form π-complex bonds with zirconium; and the other two ligands are small groups such as halides or

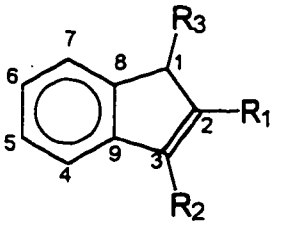

R_1 = -Ph, -Me
R_2 = -H, -Ph, -Me
R_3 = -H, -Ph

IV

small alkyl groups. The tetrahedral geometry is deformed and no longer symmetric. The angle between two bulky groups will be larger than 109.5° and smaller than 180°. Since the purpose is to slow down the rotation of the π-Zr bond and make the catalyst stay in one kind of conformational isomers longer, two effects of substituent groups should be considered. First, since the larger the size, the slower it rotates, a substituent group should be chosen to make the rotating radius longer and efficiently slow down the rotation. Based on this consideration, **III** was designed. The second effect we considered was: since two rings are not completely parallel, in fact, the angle of Ce-Zr-Ce is 131° for **III** (note: Ce means the center of the five member ring), rotation toward one direction can be stopped at certain positions if we put substituent groups on positions such as C1 and C3. Then the rotation will change its direction and turn toward the reverse direction. During this changing period, the polymerization can get enough time to produce certain length of one kind of stereoblocks. The purpose of our work is to put suitable substituents on the indene ring and set

Table B-1 Substituents on indene ring in different catalysts

Catalyst	Indene ring	Substituted position	Substituent
Cat.2	Indene ring 1	R_1	Ph
		R_2	Ph
		R_3	H
	Indene ring 2	R_1	Ph
		R_2	Ph
		R_3	H
Cat.3	Indene ring 1	R_1	Ph
		R_2	CH_3
		R_3	H
	Indene ring 2	R_1	Ph
		R_2	CH_3
		R_3	H
Cat.4	Indene ring 1	R_1	H
		R_2	Ph
		R_3	H
	Indene ring 2	R_1	Ph
		R_2	Ph
		R_3	Ph

Cat.5	Indene ring 1	R_1	CH_3
		R_2	CH_3
		R_3	H
	Indene ring 2	R_1	CH_3
		R_2	CH_3
		R_3	H

some restriction on the rotation.

1.4.1 Bis[1,2-Diphenylindenyl]zirconium Dichloride (Cat.2)

V is the structure of Cat. 2. The synthesis of this catalyst could cause two stereoisomers because the substituted indene ring here is no long symmetric and has two unidentical sides. The two stereoisomers have different structures as the following: in one of the stereoisomers, two indene rings coordinate with zirconium from the same side; and in the other stereoisomer, two indene rings coordinate with zirconium from different sides. **Va** and **Vb** are two extreme conformational isomers for the first stereoisomer, whereas, **Vc** and **Vd** are for the second stereoisomer. By examining the structures below, we can see that In **Va** substitution positions 3 on the bottom indene ring and substitution position 3' on the top indene ring are closest in space. Since there is not any substituent group on either of these two substitution positions, both indene rings rotate freely, either clockwise or counterclockwise. **Vb** is the structure when the top

indene ring stays in the position as it is in **Va**, but the bottom indene ring rotates 180°. In **Vb**, the substitution positions 1 on the bottom indene ring and 3' on the

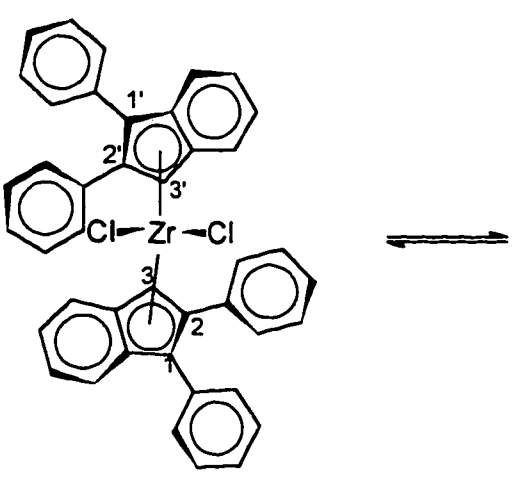

Va

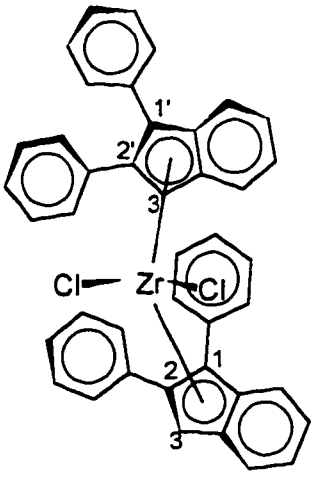

Vb

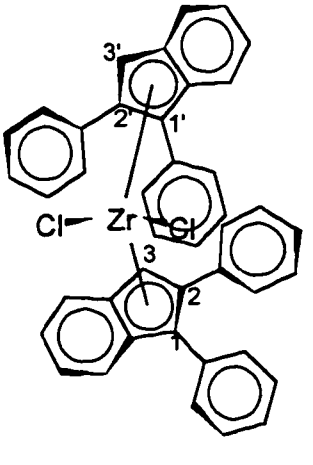

Vc

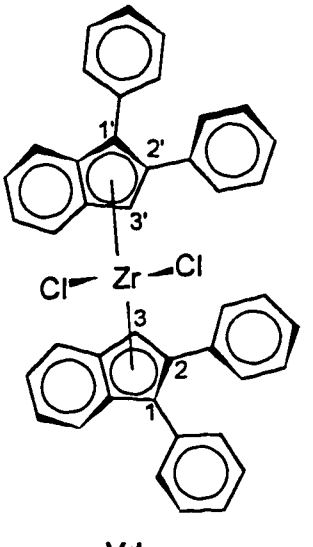

Vd

top indene ring are closest in space. So for **Vb**, the top indene ring can not rotate freely because whichever direction it rotates in, the rotation will be stopped by the phenyl group which is on substitution position 1 of the bottom indene ring. However, the rotation of the bottom indene ring towards either

direction is not restricted. Considering that **Va** and **Vb** are only two of the different conformational isomers for the same compound, the rotation of two indene rings will be slowed down as the total effect of the substitution of phenyl groups on substitution position 1 and 1'.

For the other stereoisomer, in **Vc**, substitution position 3 on the bottom indene ring and substitution position 1' on the top indene ring are closest in space. The top indene ring can rotate without any restriction. However, the rotation of the bottom indene ring towards either direction will be restricted by the phenyl group on substitution position 1'. Whenever the rotation of the bottom indene ring is stopped by the phenyl ring, it has to change direction in which it can also go nowhere. Whereas, in **Vd**, both rings can rotate freely.

The separation of two stereoisomers through the synthesis path has not been attempted in my project. But it is worthwhile to study because the polymerization result by this catalyst was a big improvement in stereochemistry compared with Waymouth's catalyst **III**.

1.4.2 Bis[2-Methyl-1-Phenylindenyl]zirconium Dichloride (Cat.3)

The structures of Cat.3 are shown on the next page. This catalyst is designed based on Cat.2. Since the activity of Cat.2 in the polymerization of 1-hexene was very low though it gave pretty good stereoblock sequences, we replaced one phenyl group with methyl group. The consideration of the rotation restriction of the indene rings is pretty much the same as that for Cat. 2, except

that the methyl group is smaller than the phenyl group and the restriction is decreased for **VI**.

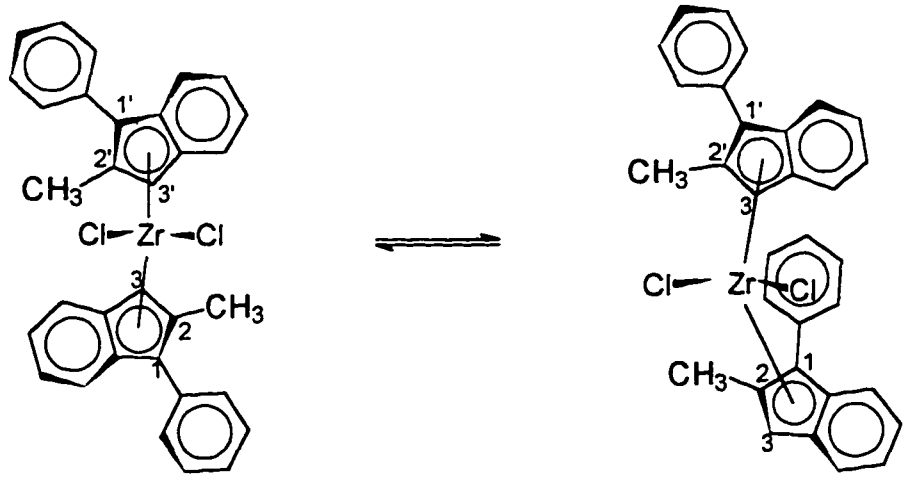

VIa **VIb**

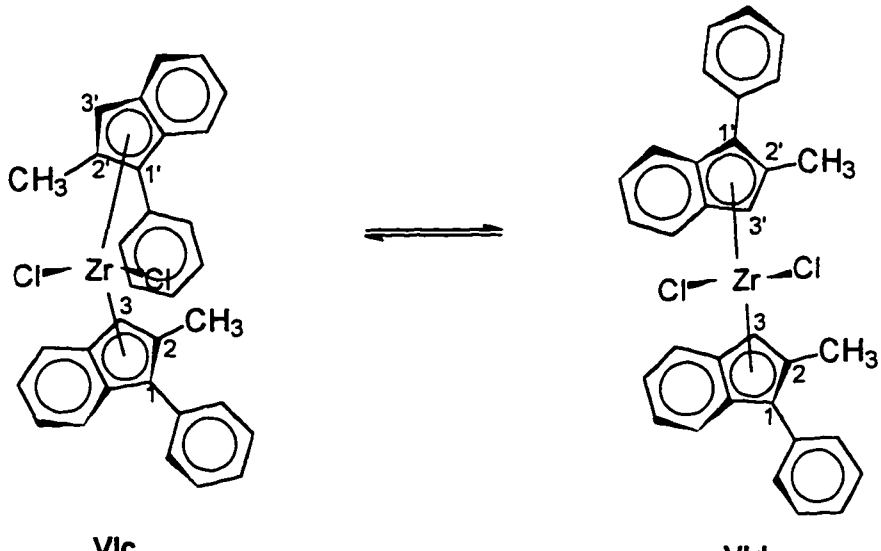

VIc **VId**

The same problem of the separation between the two stereoisomers of Cat.3 has also not been solved in this project.

1.4.3 [2-Phenylindenyl][1,2,3-Triphenylindenyl]zirconium Dichloride (Cat.4)

VII is the structure of Cat.4. This catalyst solved the problem in the synthesis of the previous two catalysts that there are two stereoisomers. Since both ligands in Cat.4 are symmetric, it is the same from which side the indene

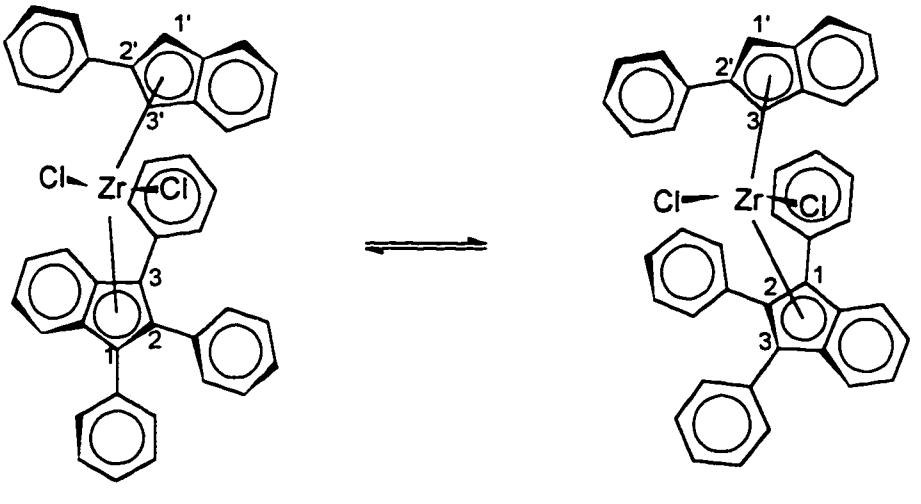

VIIa **VIIb**

rings coordinate with zirconium. In addition, the rotation of the top indene ring is restricted either in **VIIa** or in **VIIb**, whereas the bottom indene ring can rotate freely. As a total effect, the transformation from one isomer to the other is slowed down in a greater extent than that in **V** or **VI**.

1.4.4 Bis[1,2-Dimethylindenyl]zirconium Dichloride (Cat.5)

Cat.5 is designed to improve the catalyst activity in the polymerization of atactic polyolefin. It is assumed that the methyl group on position 1 are not long enough to block the rotation of two indene rings. The use of this catalyst is to prove if the assumption is reasonable or not.

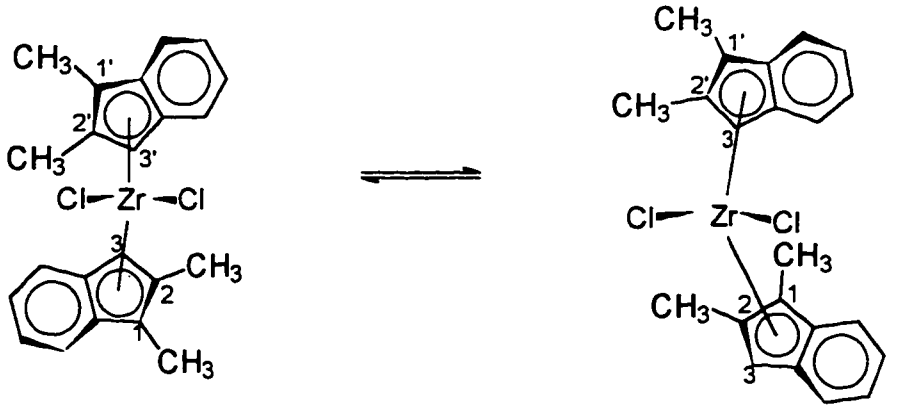

VIIIa VIIIb

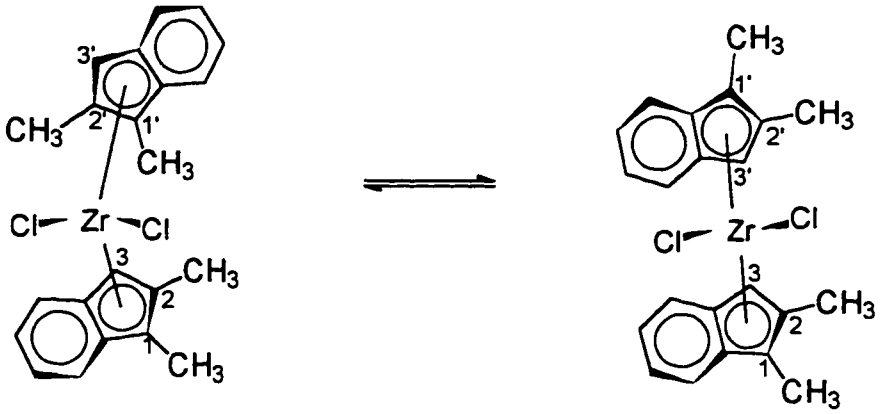

VIIIc VIIId

1.4.5 The Polymerization System

The polymerization of 1-hexene was chosen because the homogeneous isotactic polymerization of 1-hexene was studied in Part A. It is convenient to compare the results from the polymerization by new catalysts with that by the stereobridged metallocene catalyst.

2.0 Experimental

2.1 Materials and Their Purification

2-indone, 2,3-diphenyl-1-indenone, (±)-2-methyl-1-indone, methyllithium (1.4M solution in diethyl ether), n-butyllithium (1.6M solution in hexanes), methylmagnesium bromide (3.0M solution in Diethyl ether), phenylmagnesium bromide (3.0M solution in diethyl ether), sodium hydroxide, sodium chloride, magnesium sulfate, sodium, calcium hydride, zinc, mercury(II) chloride, aluminum oxide(activated, neutral), hydrochloric acid (37%, ACS reagent), hydrogen chloride (99+% gas) and 1,4-dioxane, were purchased from Aldrich Chemical Co. and were directly used without further purification. 4Å molecular sieves (1.6mm pellets) from Aldrich Chemical Co were activated by heating at ~320 °C for above 24 hours. Toluene (Aldrich, anhydrous reagent) used in polymerization and benzene (Aldrich, anhydrous reagent) were dried over 4Å molecular sieves for at least overnight. Tetrahydrofuran (THF) (Aldrich, anhydrous reagent) and toluene (Aldrich, anhydrous reagent) used in catalyst synthesis were refluxed and then distilled over calcium hydride and sodium, respectively. Polymerization monomer, 1-hexene (b.p 63 ~ 64 °C, J.T. Baker), was dried over a 3~4 : 1(%w/w) mixture of 4Å molecular sieves and aluminum oxide. Hexanes (GR reagent) was purchased from Fisher Scientific Co.. MAO (10% solution in toluene) was purchased from Ethyl Co. and used without further purification. Methylene-d_2 chloride (99.9% D) and Chloroform-d (99.8% D) were from Cambridge Isotope Laboratory.

2.2 Synthesis of catalyst ligands

2.2.1 Synthesis of 2-Phenylindene

Add a solution of 2-indone (13.47 g, 102 mmol) in a dried benzene (100 ml) into phenylmagnesium bromide (3.0 M in Et_2O, 50 ml, 150 mmol) at 3 ~ 5 °C over 2.5 hrs. Allow the reaction to warm to room temperature over 40 minutes. Cool down the solution to 0 °C and add water (100 ml). Dilute the resultant mixture with hexanes (200 ml). Add 5M HCl to neutralize it and wash it twice with brine (100 ml). Extract the aqueous layer twice with hexanes (50 ml). Combine all of the organic solvents and dry it over $MgSO_4$. Remove solvent in vacuo and get brown oil. Dissolve the above oil and p-toluenesulfonic acid (0.25 g) in benzene (200 ml) in a round-bottom flask below a Soxlet extractor containing 4Å molecular sieves. After refluxing the solution for 2.5 hrs, filter it and cool to 5 °C overnight. A white flaky solid, 2-phenylindene, was collected by filtration and was washed with cold benzene (50 ml). Additional product was obtained by removing the solvent from the filtrate, crystallizing the solid with acetone-water pair, and collecting the crystals (11.74 g, 60.0% yield based on 2-indone).

2.2.2 Synthesis of 1,2-Diphenylindene

Cover 20 g of Zn dust with 15% NaOH aqueous solution (~80 ml) and warm it until hydrogen is vigorously evolved. Dilute with water (50 ml) to slow down the reaction and decant the aqueous solution. Wash the zinc three times with water (100 ml). Add 60 ml of 1% $HgCl_2$ to cover the zinc and stand it for 30 ~ 60 minutes with occasional shaking. Pour off $HgCl_2$ aqueous solution and wash the

solid twice with water (100 ml). Add 50 ml of conc.HCl and 10 ml of water. The Zinc amalgam is ready to be used.

Into the above flask, introduce a bright red solution of 2,3-diphenyl indenone (5.00 g, 17.71 mmol) in dioxane (100 ml). Stir the mixture by mechanic stirring and pass in a slow stream of HCl gas while warming the flask by means of a small flame until the red color turns light yellow. It took about 6 hours. Allow the resulting mixture to stand for overnight. Steam distill the reaction mixture until a piece of yellow solid instead of oil was floating on the top of aqueous layer. Decant liquid. Wash the solid once with 5% of NaOH and twice with water. Crystallize and recrystallize the solid with hexanes. The product is white needle crystals (2.98 g, 63% yield based on 2,3-diphenylindenone).

2.2.3 Synthesis of 2-Methyl-3-Phenylindene

Add a solution of 2-methyl-1-indone (5.00g, 34.2mmol) in dried benzene (40 ml) into phenylmagnesium bromide (3.0 M in Et_2O, 19 ml, 57 mmol) at 3 ~ 5 °C over 1.5 hrs. Allow the reaction to warm to room temperature over 30 minutes. Cool down the solution to ~0 °C and add water (40 ml). Dilute the resulting mixture with hexanes (50 ml). Add 5M HCl to neutralize it and wash it twice with brine (100 ml). Extract the aqueous layer twice with hexanes (15 ml). Combine all of the organic solvents and dry it over $MgSO_4$. Remove solvent in vacuo and get yellow oil. Dissolve the above oil and p-toluenesulfonic acid (0.20 g) in benzene (120 ml) in a round-bottom flask below a Soxlet extractor containing 4Å molecular sieves. After refluxing the solution for 2.5 hrs, filter it and remove

solvent in vacuo. The brown oil was purified by crystallization from water/acetone and white crystals were obtained (4.18 g, 59% yield based on 2-methyl-1-indone).

2.2.4 Synthesis of 1,2,3-Triphenylindene

Dissolve 2,3-diphenylindenone (11.00 g, 38.96 mmol) into benzene (100 ml) and add PtO_2 (122 mg). Hydrogenation was carried out at room temperature and started from 4 atms of hydrogen pressure in a hydrogenator. Stop the reaction when the hydrogen pressure no longer decreased and the bright red solution turned into light yellow with a lot of white needle-like crystals. Filter and separate the solid and the solution. Concentrate the filtrate and cool it to 5 °C overnight. Filter and get white crystals, Dissolve the solid part into benzene and filer it to get rid of PtO_2. Concentrate the solution and cool to 5 °C overnight. Filter and get white crystals. The total product, 2,3-diphenylindone, is 10.23 g (93% yield based on 2,3-diphenylindenone).

Add a solution of 2,3-diphenylindone (4.03 g, 14 mmol) in anhydrous benzene (100 ml) to phenylmagnesium bromide (3.0 M in Et_2O, 10 ml, 30 mmol) at 3 ~ 5 °C over 2.5 hrs. Warm the reaction to room temperature over 30 minutes. Cool the solution to 0 °C and add water (20 ml). Dilute the resultant mixture with hexanes (40 ml) and add 5M HCl (25 ml). Wash the organic layer twice with brine (20 ml). Extract the aqueous layer twice with hexanes (10 ml), and dry the combined organic layers over MgSO4. Filter and remove solvent in vacuo and get a yellow solid residue. Dissolve the residue and p-toluenesulfonic

acid (0.11 g) in benzene (100 ml) in a flask below a Soxhlet extractor containing 4Å molecular sieves and keep the mixture refluxing for 3 hrs. Hot filter and cool it to 5 °C overnight. Filter and get dark orange yellow crystals (3.57 g, 74% yield based on 2,3-diphenylindone).

2.2.5 Synthesis of 2,3-Dimethylindene

Add a solution of 2-methyl-1-indone (5.00g, 34.2mmol) in dried benzene (40 ml) into methylmagnesium bromide (3.0 M in Et_2O, 20 ml, 60 mmol) at 3 ~ 5 °C over 1.5 hrs. Allow the reaction to warm to room temperature over 30 minutes. Cool down the solution to 0 °C and add water (40 ml). Dilute the resultant mixture with of hexanes (50 ml). Add 5M HCl to neutralize it and wash it twice with brine (100 ml). Extract the aqueous layer twice with hexanes (10 ml). Combine all of the organic solvents and dry it over $MgSO_4$. Remove solvent in vacuo and get light yellow oil. Dissolve the above oil and p-toluenesulfonic acid (0.2 g) in benzene (120 ml) in a round-bottom flask below a Soxlet extractor containing 4Å molecular sieves. After refluxing the solution for 2.5 hrs, filter it and remove solvent in vacuo. A orange oily liquid was obtained (4.93 g, 90% yield based on 2-methyl-1-indone).

2.3. Synthesis of Metallocene Catalysts

2.3.1 Bis[2-phenylindenyl]zirconium Dichloride (Cat. 1)

Add a solution of n-butyllithium (1.6 M in hexanes, 1.31 ml, 2.10 mmol) into a solution of 2-phenylindene (0.400 g, 2.10 mmol) in dried THF (20 ml) at -78 °C over 2 minutes. Warm the orange solution to room temperature over 35 minutes

and stir for 30 more minutes at room temperature. Remove solvent in vacuo and get light yellow solid. Add $ZrCl_4$ (0.246 g, 1.05 mmol) and mix them up. Suspend them in toluene (25 ml). Stir the suspension at room temperature overnight. Warm it to 80 °C and filter. Cool the solution to -20 °C overnight. Filter and get orange-colored crystals (0.182 g, 32% yield based on $ZrCl_4$).

2.3.2 Bis[1,2-diphenylindenyl]zirconium Dichloride (Cat. 2)

Following the procedure described for **Cat.1** (0.50 g (1.86 mmol) of 1,2-Diphenylindene, 12 ml Of THF, 1.32 ml of MeLi (1.4 M in Et_2O, 1.85 mmol), 0.216 g (0.93 mmol) of $ZrCl_4$, and 25 ml of toluene) yielded **Cat. 2** as a orange crystal (0.13 g, 50% yield based on $ZrCl_4$). **Cat. 2** has much smaller solubility in toluene. Another 45 ml of toluene was added to dissolve more product before hot filtration and the celite was washed twice with 5 ml of toluene for each time. Combine toluene solutions, concentrate it and cool it down to -20°C to get crystal.

2.3.3 Bis[1-phenyl-2-methylindenyl]zirconium Dichloride (Cat. 3)

Following the procedure described for **Cat.1** (0.52 g (2.50 mmol) of 2-methyl-3-phenylindene, 20 ml of THF, 1.78 ml of MeLi (1.4 M in Et_2O, 2.49 mmol), 0.291 g (1.25 mmol) of $ZrCl_4$, and 20 ml of toluene) yielded **Cat. 3** as a orange yellow crystal (0.13 g, 45% yield based on $ZrCl_4$).

2.3.4 [2-Phenylindenyl][1,2,3-Triphenylindenyl]zirconium Dichloride (Cat. 4)

Add a solution of MeLi (1.4 M in Et_2O, 0.72 ml, 1.0 mmol) into a solution of 2-phenylindene (0.19 g, 1.0 mmol) in dried THF (7 ml) in flask A at -78°C over 2 mins. Warm up the brown solution to room temperature over 30 mins and stir for 30 more minutes at room temperature. Remove solvent in vacuo and get yellow solid. Add $ZrCl_4$ (0.223 g, 1.0 mmol) and mix them up. Suspend them in toluene (15 ml). Stir the suspension at room temperature overnight.

In flask B, add a solution of MeLi (1.4 M in Et_2O, 0.72 ml, 1.0 mmol) into a solution of 1,2,3-triphenylindene (0.35 g, 1.0 mmol) in dried THF (10 ml) at -78°C over 2 mins. Warm up the dark red solution to room temperature over 30 mins and stir for 30 more minutes at room temperature. Remove solvent in vacuo and get a bright red solid. Transfer the red solid into flask A with 10 ml of toluene. Stir the mixture at room temperature overnight. Heat the mixture to 85°C and filter it through Celite. Wash the Celite with CH_2Cl_2. Precipitate product with hexanes and get a solid (NMR showed the solid was not pure).

2.3.5 Bis[1,2-dimethylindenyl]zirconium Dichloride (Cat. 5)

Following the procedure described for **Cat.1** (0.81 g (5.62 mmol) of 2,3-dimethylindene, 25 ml 0f THF, 4.0 ml of MeLi (1.4 M in Et_2O, 5.55 mmol), 0.654 g (2.81 mmol) of $ZrCl_4$, and 25 ml of toluene) yielded **Cat. 5** as a yellow crystal (0.50 g, 34% yield based on $ZrCl_4$).

2.4 Polymerization of 1-Hexene by the Synthesized Catalysts

2.4.1 Preparation of Solution

All of the procedures were completed in a glove box (Labconco).

MAO washing solution Add 0.5 ml of 10% MAO solution in toluene into 100 ml of dried toluene. Mix it throughout.

MAO spike solution Add 10 ml of 10% MAO solution in toluene into 100 ml of dried toluene. Mix it throughout.

Catalyst solution Add 1 ml of 10% MAO solution in toluene into 9 ml of dried toluene. Mix it throughout and then stay for 15 minutes. Dissolve mmol of catalyst into the above solution.

2.4.2 Polymerization of 1-Hexene

Rinse all the glassware with MAO washing solution right before each experiment. Add 1-hexene (5ml) into a 102 mm pressure tube, which is followed by the addition of the MAO spike solution (100 μl). After thorough mixing, add 10% MAO solution (180μl) and 100 μl of catalyst solution. Polymerization was carried at various temperatures (80°C, 50°C, room temperature and 0°C) for certain time and was quenched by the addition of 2% NaOH aqueous solution (5ml). The mixture was washed by 2% NaOH until no more white solid was left and then washed by water for three times. The left monomer and solvent were removed in a Speed Vac (Savant, SC110) at ~45°C for at least overnight. The poly(1-hexene) was weighted.

2.5 ^{1}H and ^{13}C NMR Spectroscopy

For ^{1}H NMR, samples were dissolved in CDCl3 as 10% (wt/vol) solution, 5mm probe, 40°C, 30° pulse, 1s acquisition time, 2s delay between pulses, 500 scans and TMS as internal reference were used on Varian Unity Plus 500 MHz spectrometer. For ^{13}C NMR, samples were dissolved in $CDCl_3$ as 10% (wt/vol) solutions with 15mg of $Cr(AcAc)_3$ per mililiter added, 10mm probe, 40°C, 90° pulse, inverse gated decoupling with 3s delay between pulses, 10,000 scans and $CDCl_3$ as internal reference were used on Varian Unity Plus 300 MHz spectrometer.

2.6 Infrared Spectroscopy (IR)

Fourier Transfer Infrared (FT-IR) spectra were recorded by a Nicolet FT-IR spectrometer, Model Magna-IR 550.

2.7 Elemental Analysis

The samples of Cat.1, Cat.2, Cat.3 and Cat.5 were sent to Desert Analytics Laboratory for elemental analysis.

3.0 Results and Discussion on the Catalyst Synthesis

3.1 Synthesis and Characterization of Bis[2-phenylindenyl]zirconium Dichloride (Cat.1)

3.1.1 Synthesis of 2-Phenylindene

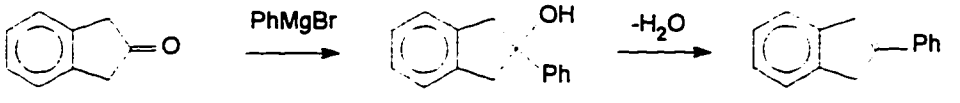

IX **X** **XI** (1)

2-Phenylindene (**XI**) was prepared from 2-indone (**IX**) and phenyl-magnesium bromide (**X**) followed by a dehydration step. 2-Phenylindene was a purplish white flaky crystal after crystallization from acetone-water solvent pair. The crystal changed color to dark brown after staying in air for a couple of weeks, but the NMR spectra did not show any difference.

3.1.2 Characterization of 2-Phenylindene

The chemical structure of 2-phenylindene was determined by ^{1}H and ^{13}C NMR spectroscopy and FT-IR spectroscopy.

The ^{1}H NMR spectrum in CD_2Cl_2 (Figure B-1) supports structure **XI**.

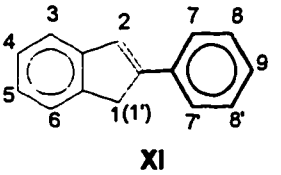

XI

The singlet at δ3.78 ppm is assigned to proton 1 and 1' because these two proton are the only protons which are not on aromatic rings or double bond which is conjugated with aromatic. All the signals between δ7.64 - 7.25 ppm are belong to those protons on aromatic rings or on the double bond which is

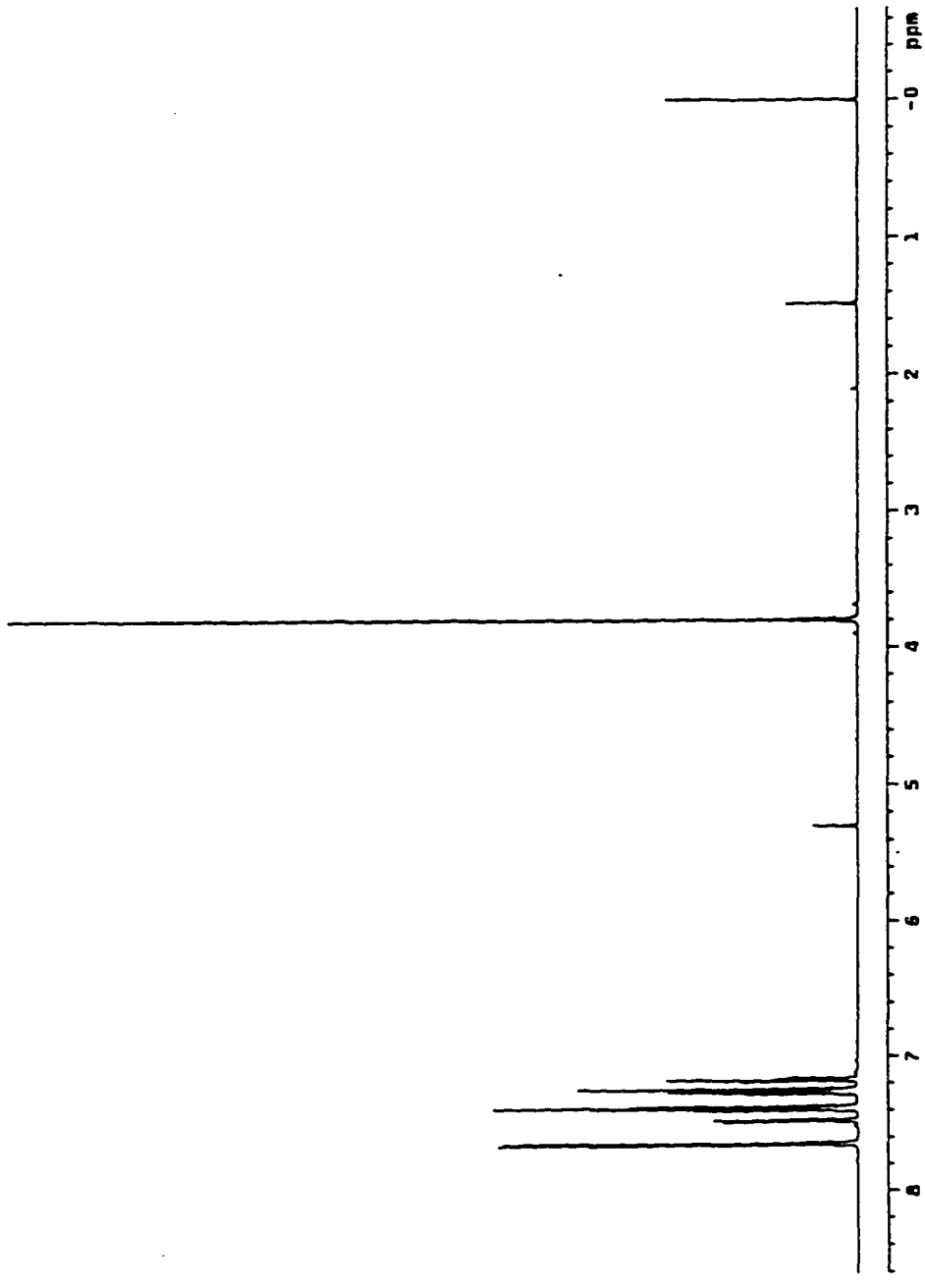

Figure B-1 ^{1}H NMR spectrum of 2-phenylindene

conjugated with aromatic rings. The integral ratio of the signals between δ7.64 - 7.25 ppm : the signal at δ3.78 ppm is 10 : 2.

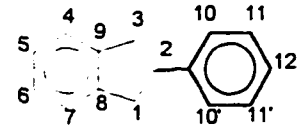

XI

Table B-2 Chemical Shifts of the Signals in ^{13}C NMR Spectrum of 2-Phenylindene

Carbon Numbers	Chemical Shift (ppm)
1	146.65
1	145.60
1	143.38
1	136.26
2	128.89
1	127.74
1	126.84
1	126.75
2	125.88
1	124.98
1	123.88
1	121.19
1	39.23

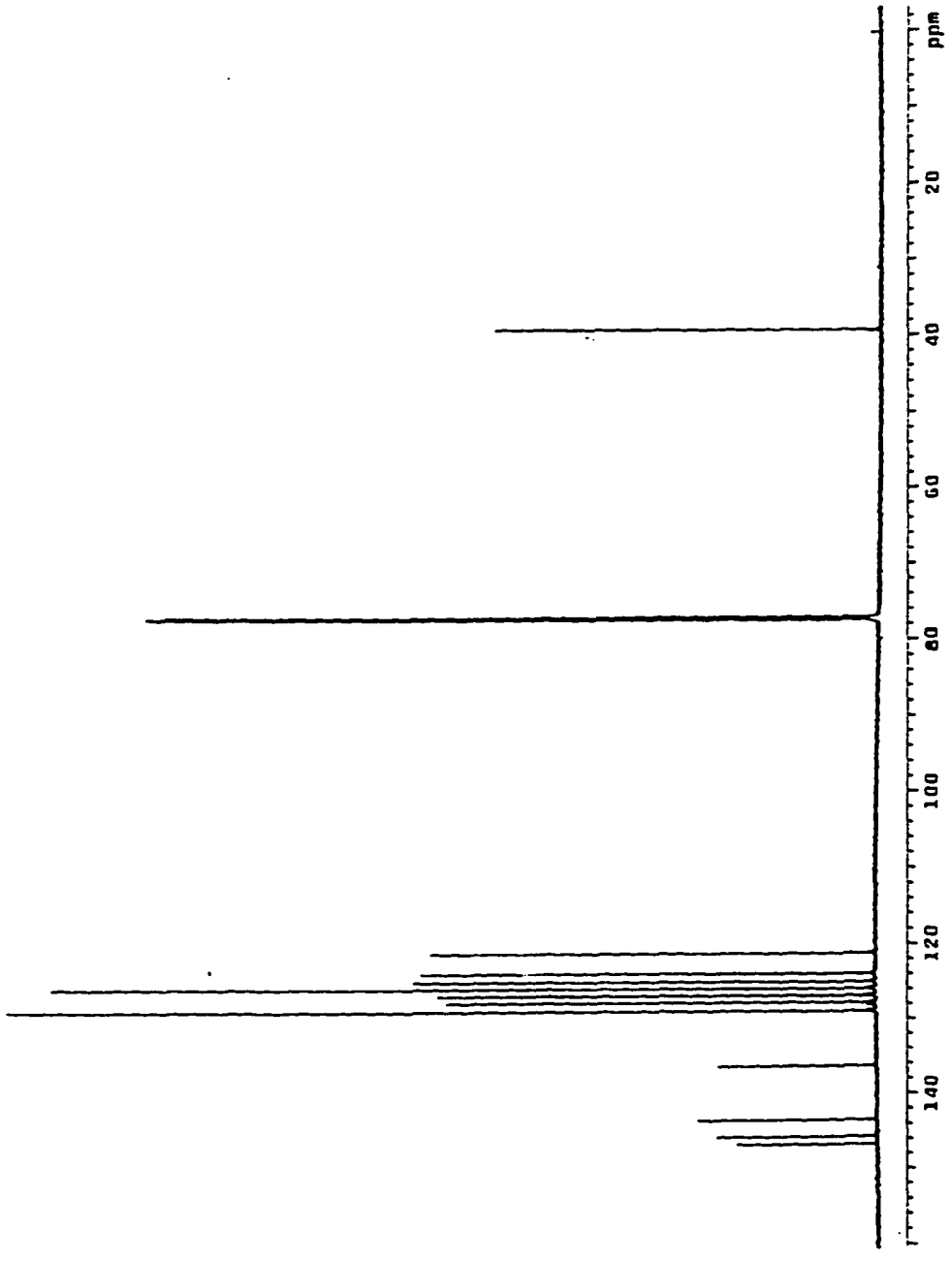

Figure B-2 ^{13}C NMR spectrum of 2-phenylindene

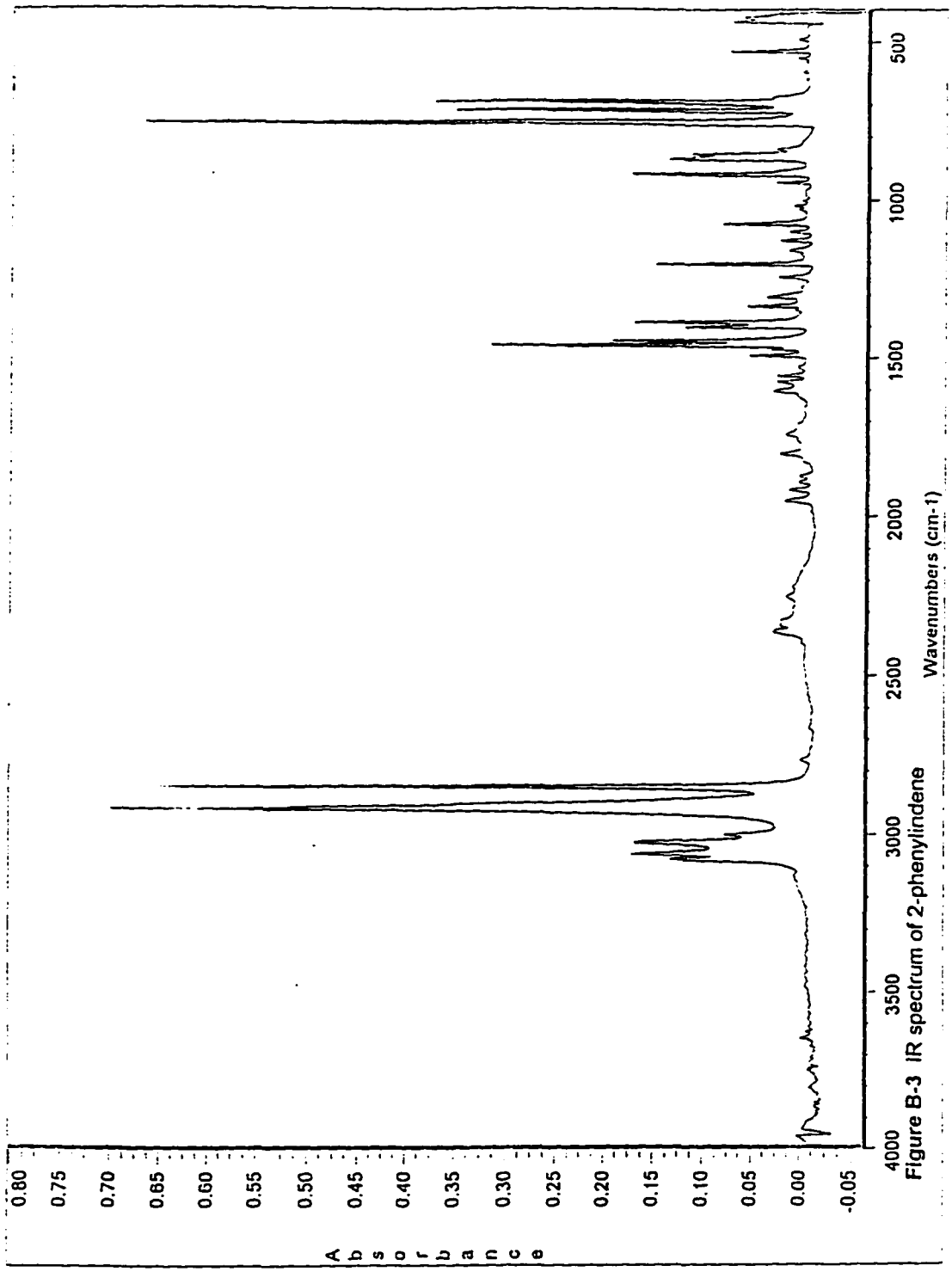

Figure B-3 IR spectrum of 2-phenylindene

The ^{13}C NMR spectrum (Figure B-2) in $CDCl_3$ supports the structure X as shown in Table B-2.

IR spectrum (Figure B-3) proves the completion of the reduction of ketone. There is no absorption at around 1700 cm^{-1} (>C=O stretching) in 2-phenylindene IR spectrum. The absence of the absorption at 3200 ~ 3550 cm^{-1} (-O-H stretching) showed the completion of dehydration from 2-phenyl-2-indenol to 2-phenylindene.

3.1.3 Synthesis of Bis[2-phenylindenyl]zirconium Dichloride (Cat. 1)

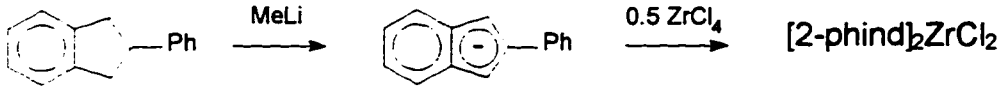

(2)

XI **XII** **III**

One proton on 2-phenylindene (**XI**) was taken away by a strong base MeLi and an aromatic anion (**XII**) was formed. **XII** continued to react with $ZrCl_4$ in a ratio of 2 : 1 without purification. A dark yellow powder of bis[2-phenylindenyl] zirconium dichloride (**III**) was obtained and separated by crystallization.

3.1.4 Characterization of Bis[2-phenylindenyl]zirconium Dichloride

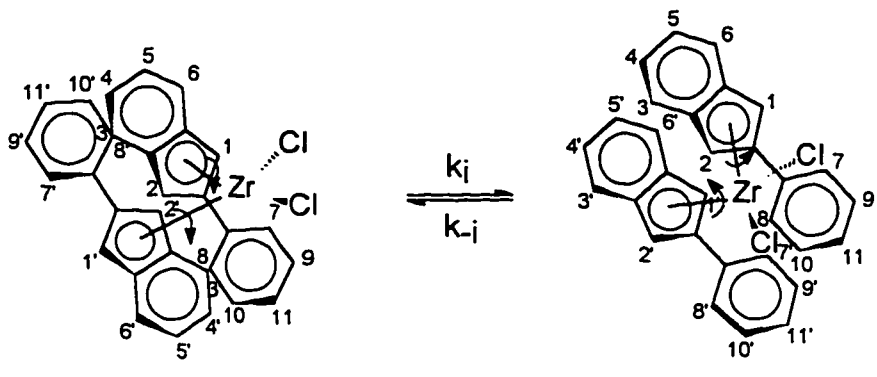

IIIa **IIIb**

^{1}H NMR spectrum in CD_2Cl_2 (Figure B-4) supports structure **IIIa** and **IIIb**. Comparing the ^{1}H NMR spectrum of 2-Phenylindene (Figure B-1) with Figure B-4, a significant change can be found between these two spectra that the signal at δ3.78 ppm in Figure B-1 almost disappears in Figure B-4 and a new signal appears at δ6.64. One of the proton 1 and 1' in **X** was taken away and the five member ring became an aromatic ring in which proton 1 and 2 in **III** are symmetric. The new signal of proton 1 and 2 in **III** should show at the location between the two signals of proton 1(1') and 2 in **XI**. The integral ratio of the peaks at δ7.55 - 7.12 ppm to the peak at δ6.64 ppm is 9 : 2. Because of the quick rotation of the Zr-cetroid single bond, **IIIa** and **IIIb** cannot be distinguished here.

The elemental analysis of C and H percent compositions is in agreement with structure **III (Cat.1)**:

	C (%)	H (%)
Elemental Analysis Result	66.12	4.08
Theoretical Value	65.46	4.07

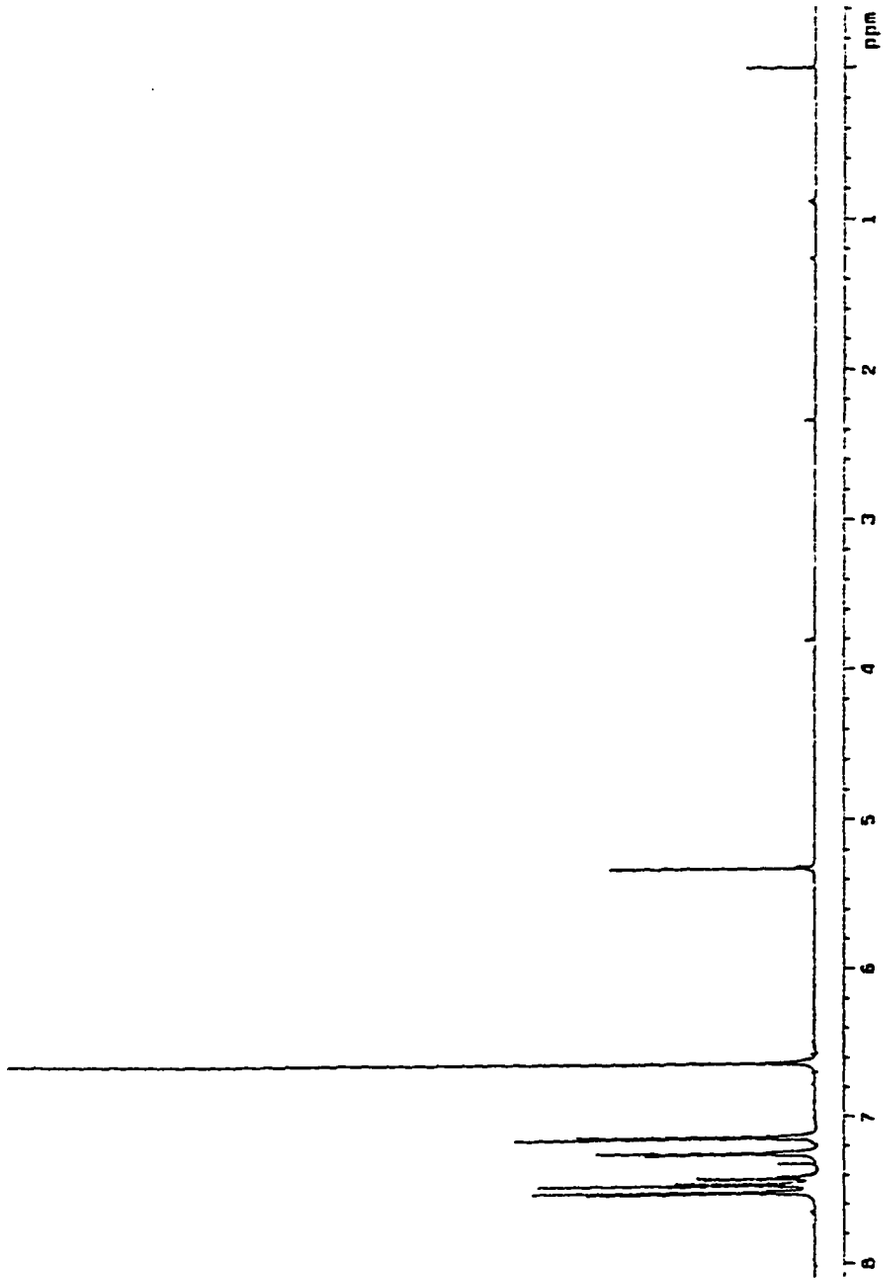

Figure B-4 ^{1}H NMR spectrum of bis[2-phenylindenyl]zirconium dichloride

3.2 Synthesis and Characterization of Bis[1,2-diphenylindenyl]zirconium Dichloride (Cat.2)

3.2.1 Synthesis of 1,2-Diphenylindene

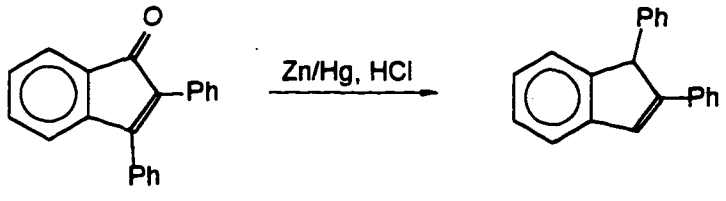

(3)

XIII XIV

1,2-Diphenylindene (**XIV**) was prepared from 2,3-diphenylindenone by the Clemmensen reduction of carbonyl group. 2,3-Diphenylindene was supposed to obtained as the product of this reduction step. However, it is very interesting that the double bond was completely shifted after the reduction and 1,2 diphenylindene was obtained as the product. This was caused by the very strong acidity in the reaction system. The yield of this step depended seriously on the control of reaction condition such as temperature, the current speed of HCl gas, stirring rate and the quality of the zinc amalgam. 1,2-Diphenylindene was a white fine needle-like crystal after crystallization from hexanes with melting point of 178.3-179.6 °C.

3.2.2 Characterization of 1,2-Diphenylindene

The chemical structure of 1,2-phenylindene was determined by melting point, ^{1}H and ^{13}C NMR spectroscopy and FT-IR spectroscopy.

The melting point of our product was 178.3-179.6 °C. This is the first evidence that we can confirm our product is 1,2-diphenylindene instead of 2,3-

diphenylindene. According to the reference[26], the melting point of 1,2-diphenylindene is 177-178 °C and the melting point of 2,3-diphenylindene is 108-109 °C.

The ^{1}H NMR spectrum in CD_2Cl_2 (Figure B-5) supports structure **XIV**.

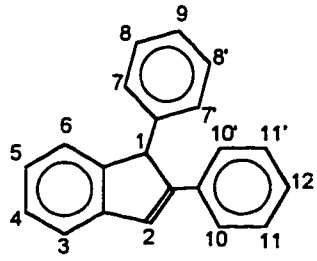

XIV

Proton 1 is the only proton on a saturated carbon. All the other protons are connected with aromatic carbons or with carbons on a conjugated double bond with aromatic rings. The only signal shown at higher field is at δ5.03 ppm, which is assigned to proton 1. The overlapped signals in aromatic region from δ7.55 to δ7.07 ppm are proton 2-13. The integral ratio of the signals between δ7.55 - δ7.07 ppm to the singlet signal at δ5.03 ppm is 15 : 1. Figure B-5 is the second evidence which proves our product is 1,2-diphenylindene instead of 2,3-diphenylindene. Proton 1 in of 2,3-diphenylindene should show at higher field

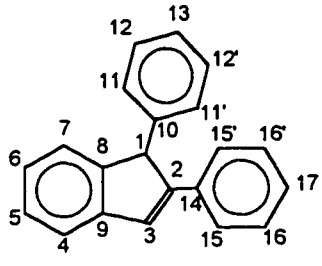

XIV

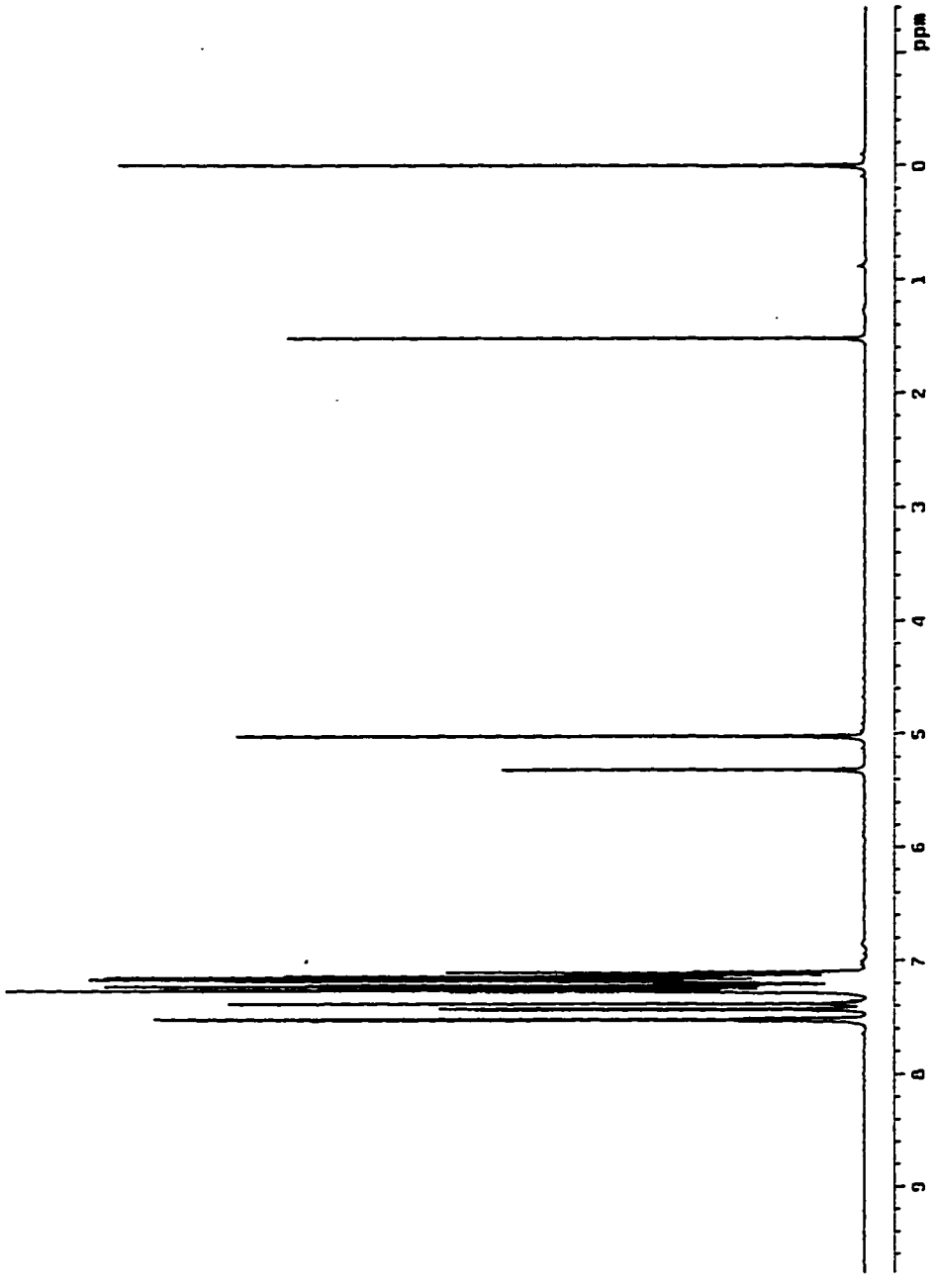

Figure B-5 ^{1}H NMR spectrum of 1,2-diphenylindene

around δ4.00 ppm according to the ^{1}H NMR spectrum of model compound, 1,2,3,4-tetraphenyl-1,3-cyclopentadiene[27].

Table B-3 Chemical Shifts of the Signals in ^{13}C NMR Spectrum of 1,2-Diphenylindene

Carbon Numbers	Chemical Shift (ppm)
1 (4°)	150.14
1 (4°)	149.39
1 (4°)	143.47
1 (4°)	140.28
1 (4°)	135.27
2 (3°)	129.07
2 (3°)	128.66
1 (3°)	128.24
2 (3°)	128.08
1 (3°)	127.55
1 (3°)	127.20
1 (3°)	126.87
2 (3°)	126.91
1 (3°)	125.68
1 (3°)	124.07
1 (3°)	121.30
1 (3°)	56.52

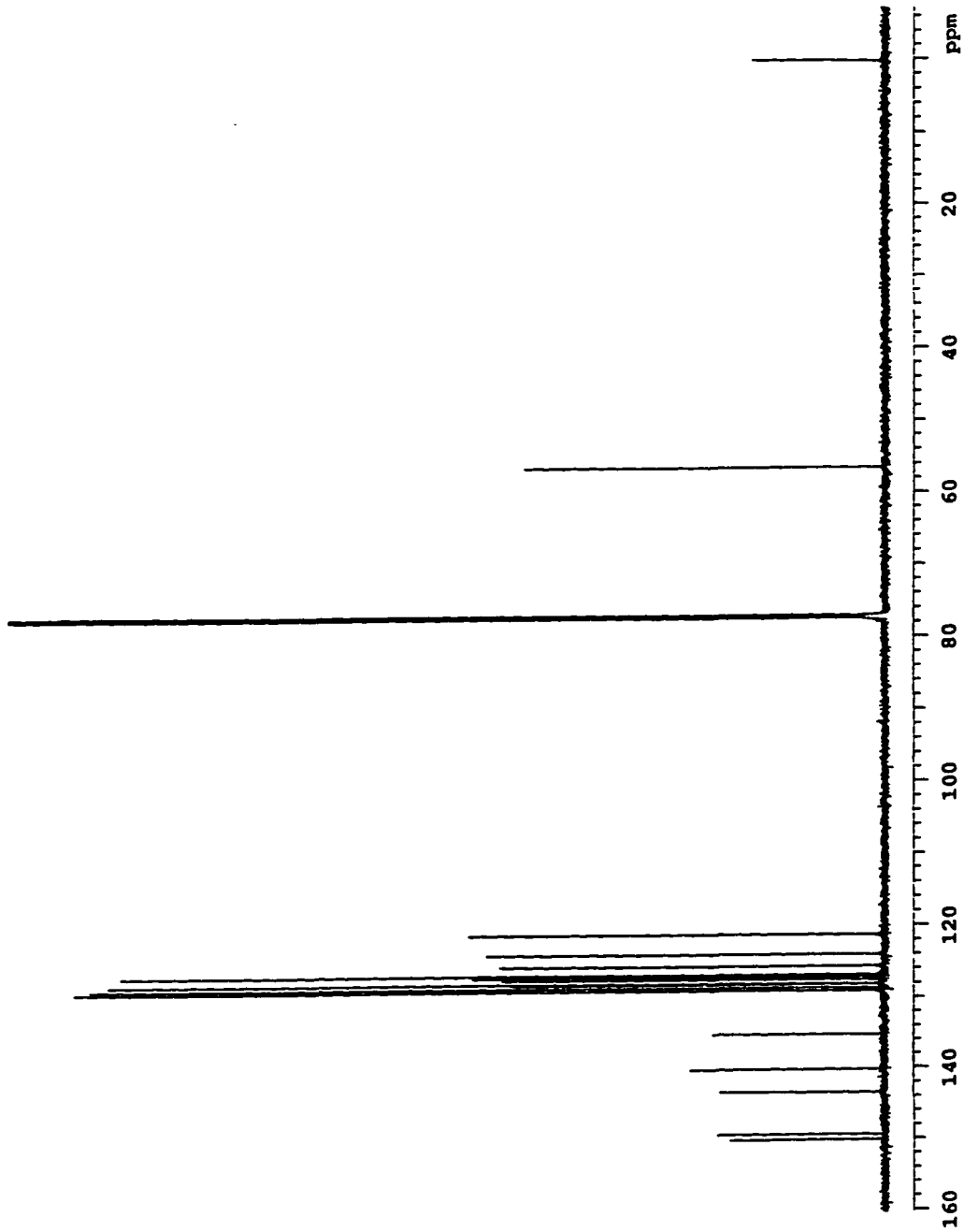

Figure B-6a ^{13}C NMR spectrum of 1,2-diphenylindene

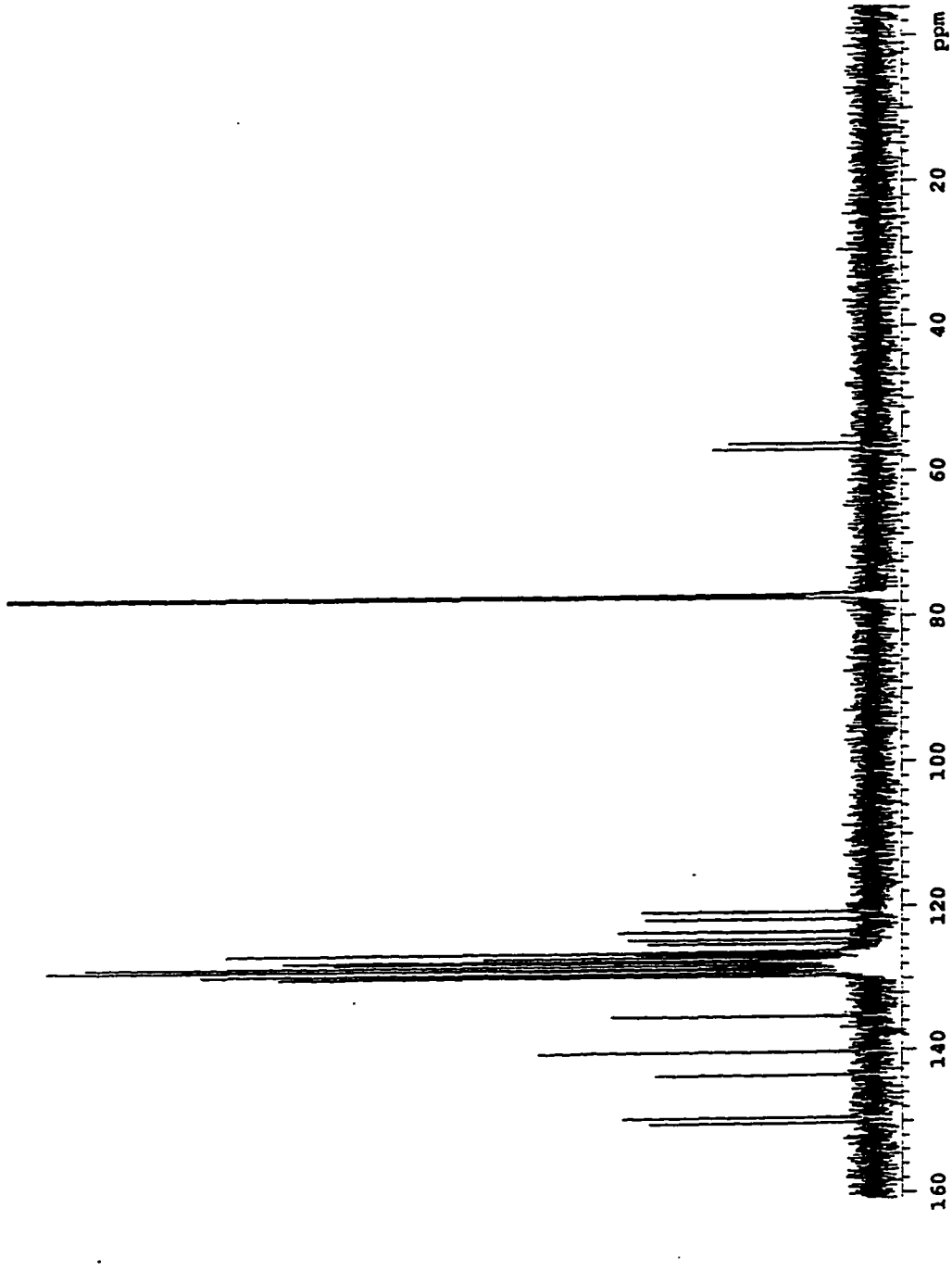

Figure B-6b ^{13}C NMR spectrum of 1,2-diphenylindene w/o decoupling

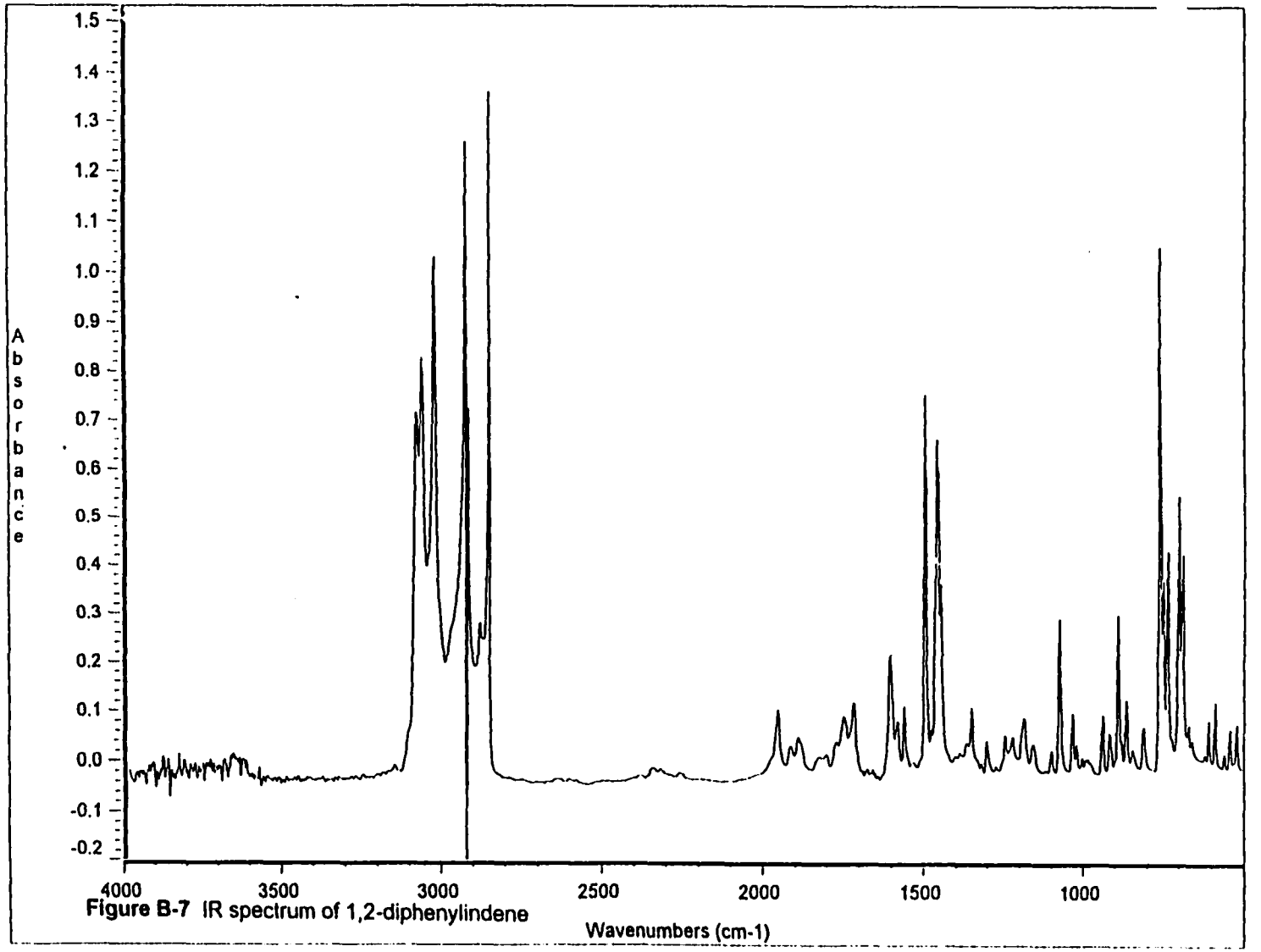

Figure B-7 IR spectrum of 1,2-diphenylindene

The ^{13}C NMR spectrum in $CDCl_3$ (Figure B-6a) supports structure **XIV** as shown in Table B-3. Figure B-6b is the ^{13}C NMR spectrum of **XIV** without heteronuclear decoupling. It supplies another evidence that our product is 1,2-diphenylindene instead of 2,3-diphenylindene. The signal of saturated carbon 1 at δ56.52 ppm is split to a doublet instead of a triplet because there is only one proton connected with it.

IR spectrum (Figure B-7) proves the completion of the reduction of ketone. There is no absorption at around 1700 cm^{-1} (>C=O stretching) in 1,2-diphenylindene IR spectrum.

The elemental analysis of C and H percent compositions also supports the completion of Clemmensen reduction step.

	C (%)	H (%)
Elemental Analysis Result	94.03	6.12
Theoretical Value	93.99	6.01

3.2.3 Synthesis of Bis[1,2-diphenylindenyl]zirconium Dichloride (Cat. 2)

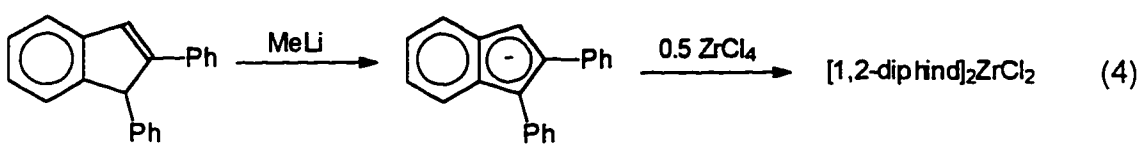

XIV **XV** **V** (4)

One proton on 1,2-phenylindene (**XIV**) was taken away by a strong base MeLi and an aromatic anion (**XV**) was formed. **XV** continued to react with $ZrCl_4$ in a ratio of 2 : 1 without purification. An orange powder of bis[1,2-diphenylindenyl]

zirconium dichloride (**V**) was obtained and separated by crystallization. The reaction itself is very easily completed. Since **V** has pretty small solubility in toluene, more toluene should be added to dissolve the product before filtration. Otherwise, only very low yield can be obtained.

3.2.4 Characterization of Bis[1,2-diphenylindenyl]zirconium Dichloride

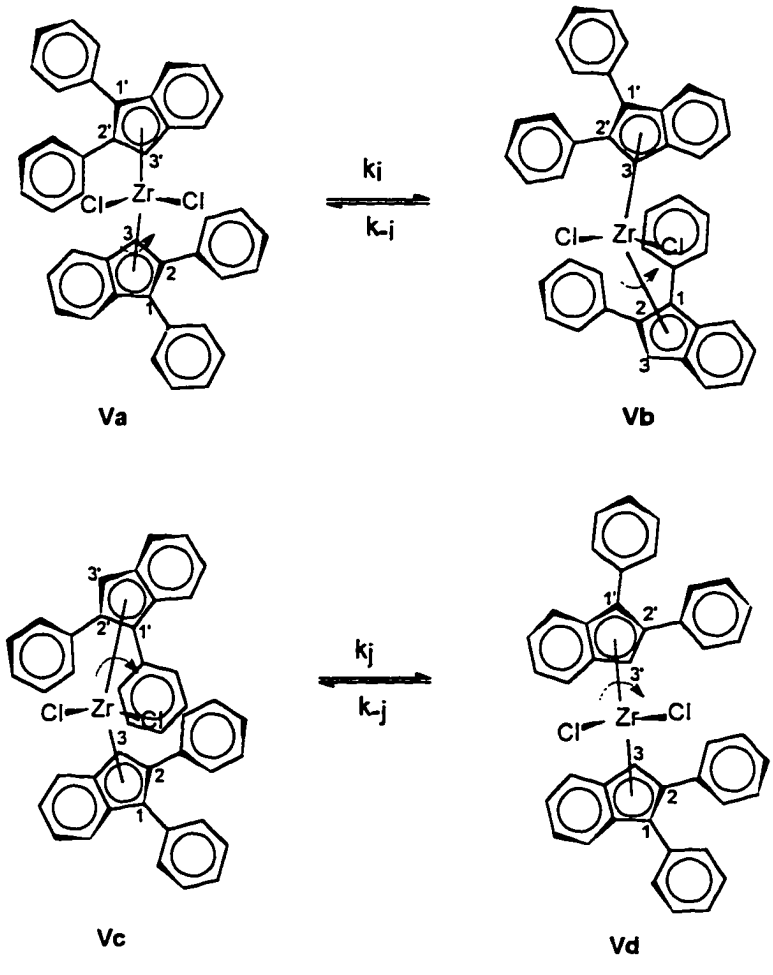

^{1}H NMR spectrum (Figure B-8) supports the structure **V**. Theoretically, **Va** & **Vb** are stereoisomers of **Vc** & **Vd**. They are supposed to be distinguished in NMR spectra. However, **Va** and **Vb**, or **Vc** and **Vd** are conformational isomers for each other and should be identical in NMR spectra when the rotation

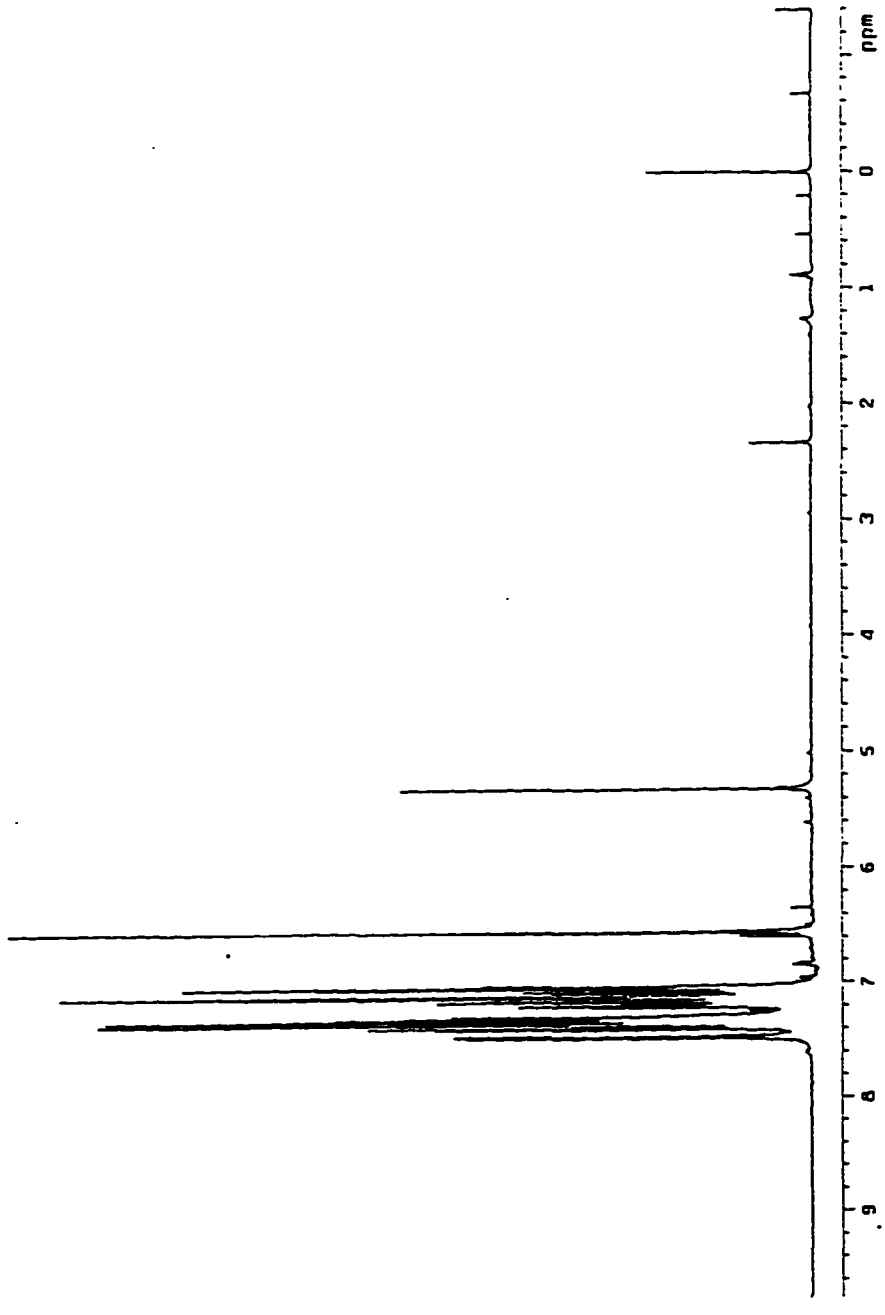

Figure B-8 ^{1}H NMR spectrum of bis[1,2-diphenylindenyl]zirconium dichloride

is fast. In fact, Figure B-8 shows that there are two stereoisomers formed during the synthesis. One isomer is in predominating amount.

Comparing the ^{1}H NMR spectrum of 1,2-diphenylindene (Figure B-5) with Figure B-8, it can be seen that the proton 1 signal in **XIV** at δ5.03 ppm disappears in Figure B-8. Proton 1 was taken away by MeLi to form anion **XV**. The negative charge on the five member ring makes the chemical shift of proton 2 in **XV** shifted to higher field (from above δ7.00 ppm shifted to around δ6.60 ppm). A big peak at δ6.54 ppm and a tiny peak at δ6.58 ppm show that there are two stereoisomers in which proton 2 is in different chemical circumstance. The reason that we say these two isomers are stereoisomers instead of conformational isomers is that the integral ratio of these two peaks is almost constant within a big range of temperature. This experiment will be discussed separately later.

Since **V** is very unstable in CD_2Cl_2 and $CDCl_3$, we could not set up a longer NMR experiment to confirm which isomer is predominating.

The elemental analysis of C and H percent compositions proves the synthesis of **V (Cat.2)**.

	C (%)	H (%)
Elemental Analysis Result	72.39	4.35
Theoretical Value	71.87	4.17

3.3 Synthesis and Characterization of Bis[2-methyl-1-phenylindenyl] zirconium Dichloride (Cat.3)

3.3.1 Synthesis of 2-Methyl-3-phenylindene

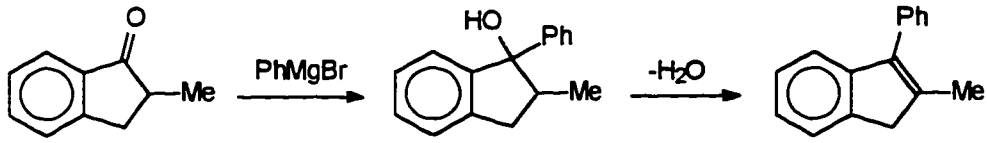

(5)

XVI XVII XVIII

2-Methyl-3-phenylindene (**XVIII**) was prepared from 2-methyl-1-indone (**XVI**) and phenylmagnesium bromide followed by a dehydration step. 2-Methyl-1-phenylindene was a white crystal after crystallization from acetone-water solvent pair. The melting point of this crystal was 57.21 - 59.00 °C. The product was not stable in air and was kept in vacuum.

3.3.2 Characterization of 2-Methyl-3-phenylindene

The chemical structure of 2-methyl-3-phenylindene was determined by ^{1}H and ^{13}C NMR spectroscopy and FT-IR spectroscopy.

The ^{1}H NMR spectrum in CD_2Cl_2 (Figure B-9) supports structure **XVIII**.

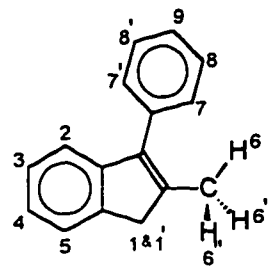

XVIII

The singlet signal at δ3.45 ppm is assigned to proton 1 and 1' because these two protons are in identical chemical circumstance. The singlet signal at δ2.13

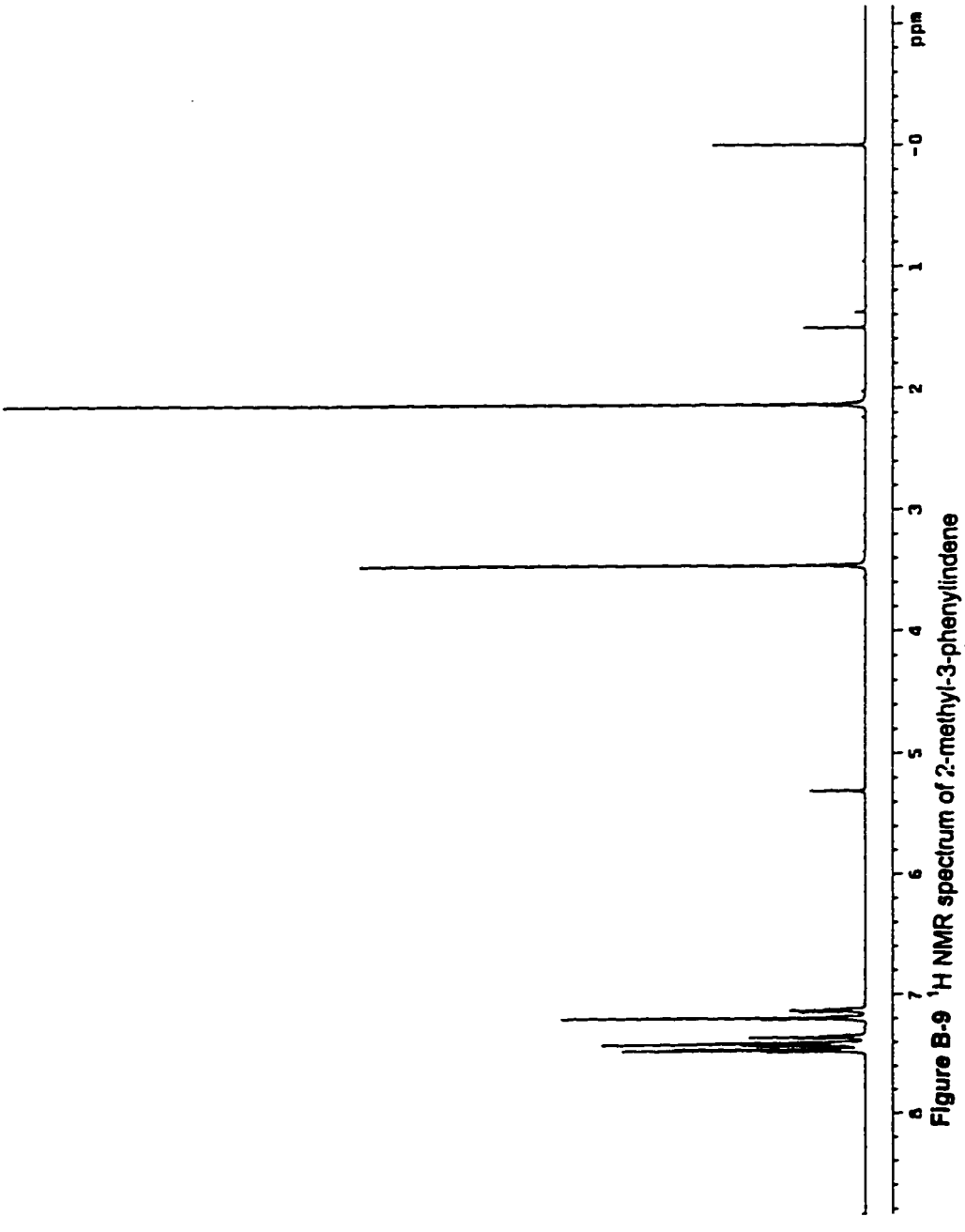

Figure B-9 ^{1}H NMR spectrum of 2-methyl-3-phenylindene

ppm should be proton 6, 6' and 6". The overlapped signals between δ7.50 to δ7.20 ppm are all those protons on aromatic rings (proton 2 - 5 and proton 7 - 9). The integral ratio of signals at δ7.50 - δ7.20 ppm : signal at δ3.45 ppm : signal at δ2.13 ppm is 9 : 2 : 3.

Table B-4 Chemical Shifts of the Signals

in ^{13}C NMR Spectrum of 2-Methyl-3-Phenylindene

Carbon Numbers	Chemical Shift (ppm)
1 (4°)	146.66
1 (4°)	142.64
1 (4°)	140.74
1 (4°)	138.95
1 (4°)	135.81
2 (3°)	129.38
2 (3°)	128.62
1 (3°)	127.21
1 (3°)	126.39
1 (3°)	124.20
1 (3°)	123.59
1 (3°)	119.52
1 (2°)	43.37
1 (1°)	15.03

The ^{13}C NMR spectrum in $CDCl_3$ (Figure B-10) supports structure **XVIII** as shown in Table B-4.

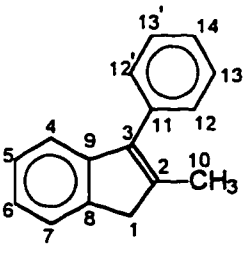

XVIII

The carbon types were determined by ^{13}C NMR spectrum without heteronuclear decoupling.

IR spectrum (Figure B-11) proves the completion of the reduction of ketone. There is no absorption at around 1700 cm^{-1} (>C=O stretching) in 2-methyl-3-phenylindene IR spectrum. The absence of the absorption at 3200 ~ 3550 cm^{-1} (-O-H stretching) showed the completion of dehydration from 2-methyl-1-phenyl-1-indenol **XVII** to 2-methyl-3-phenylindene **XVIII**.

3.3.3 Synthesis of Bis[2-methyl-1-phenylindenyl]zirconium Dichloride (Cat. 3)

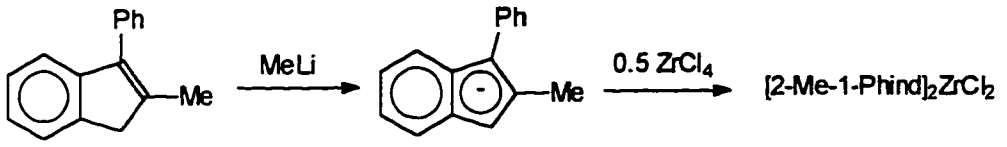

XVIII **XIX** **VI** (6)

One proton on 2-methyl-3-phenylindene (**XVIII**) was taken away by a strong base MeLi and an aromatic anion (**XIX**) was formed. **XIX** continued to react with $ZrCl_4$ in a ratio of 2 : 1 without purification. An yellow orange powder of bis[2-

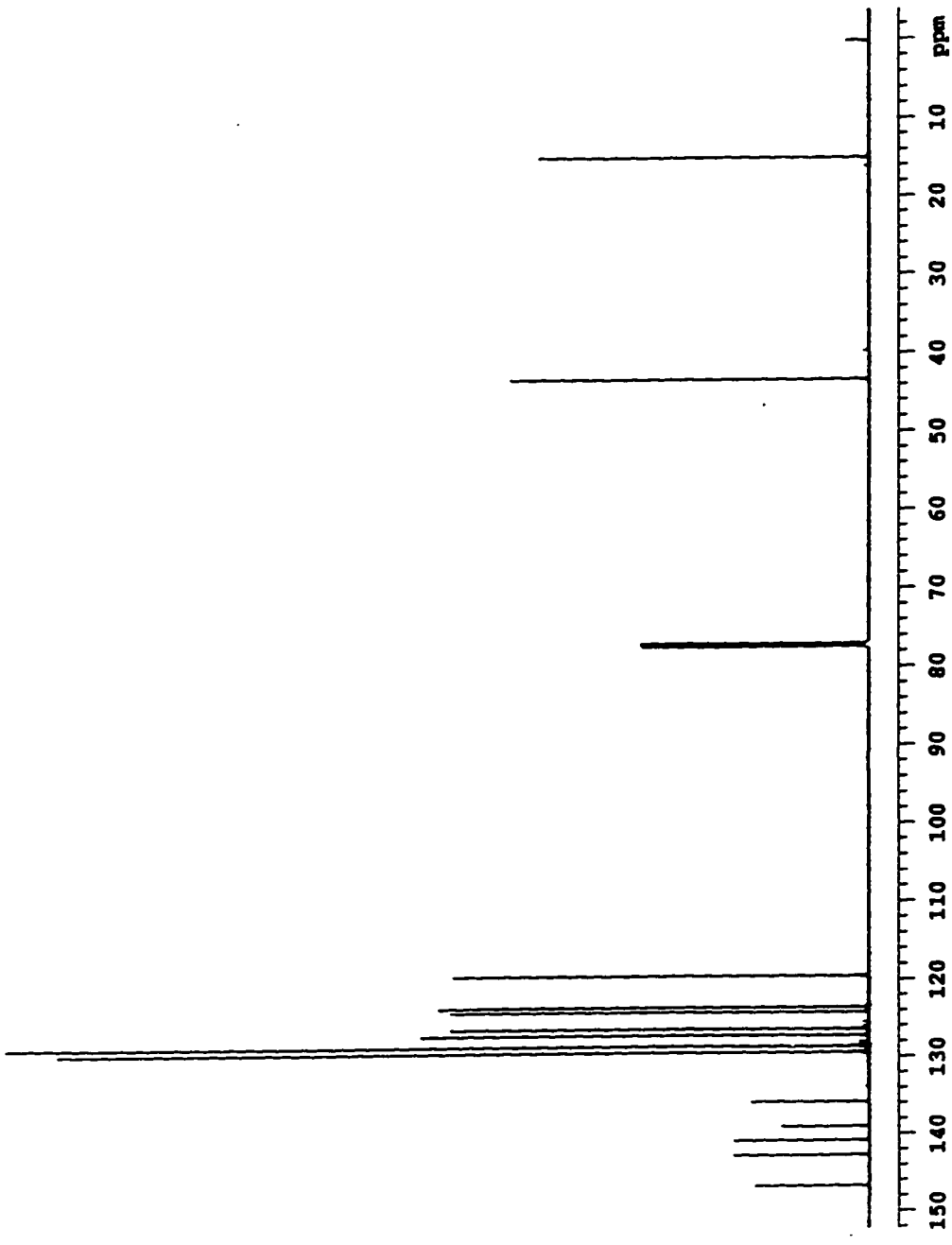

Figure B-10 ^{13}C NMR spectrum of 2-methyl-3-phenylindene

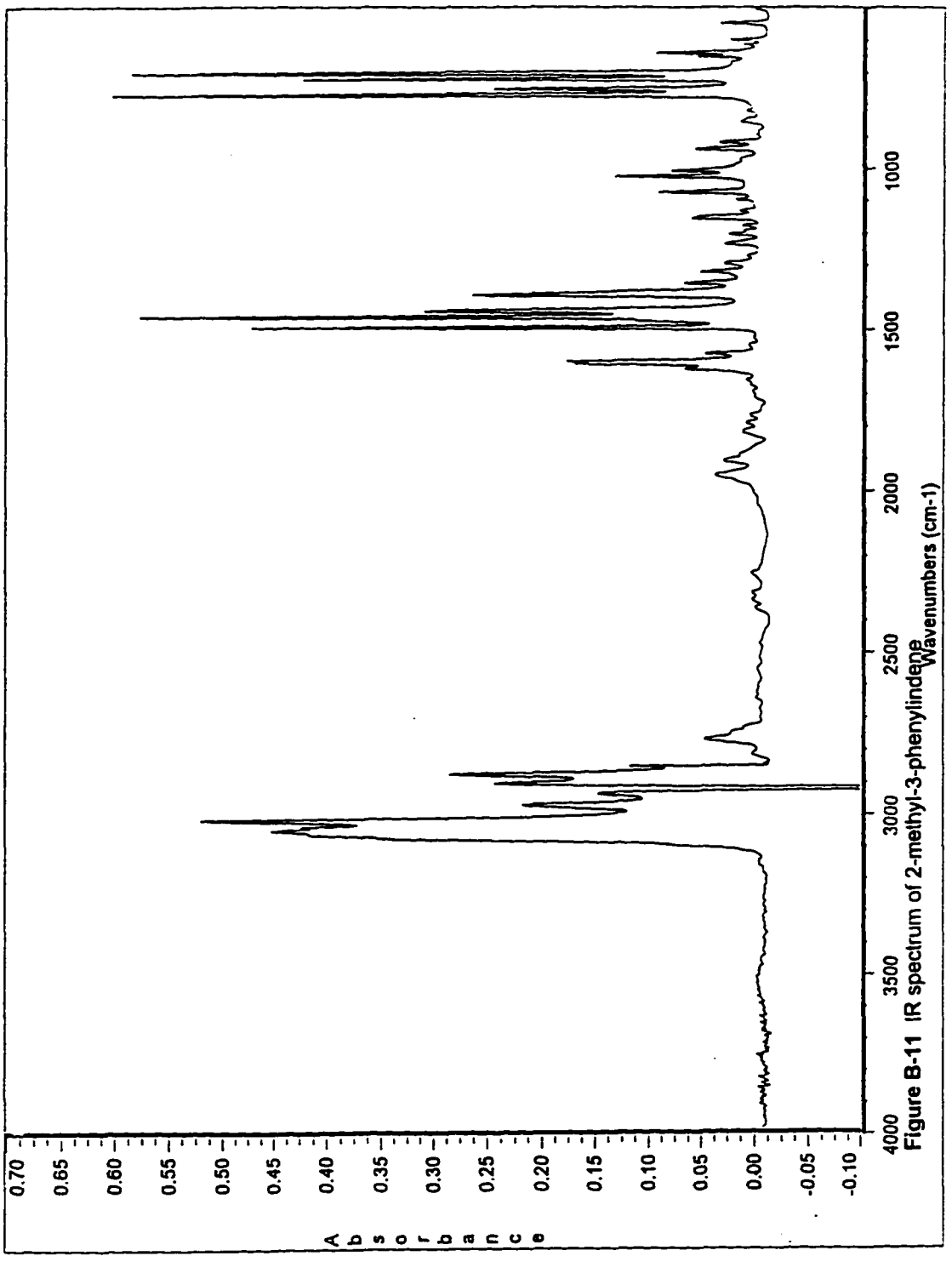

Figure B-11 IR spectrum of 2-methyl-3-phenylindene

methyl-1-phenylindenyl] zirconium dichloride (**VI**) was obtained and separated by crystallization. The product was fractional crystallized by toluene.

3.3.4 Characterization of Bis[2-methyl-1-phenylindenyl] zirconium Dichloride

^{1}H NMR spectrum in CD_2Cl_2 (Figure B-12) supports the structure **VI**. It is like structure **V** that theoretically, **VIa** & **VIb** are stereoisomers of **VIc** & **VId**.

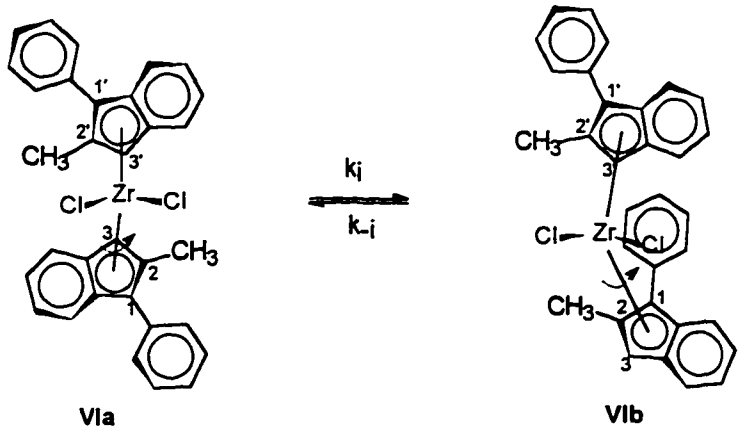

VIa **VIb**

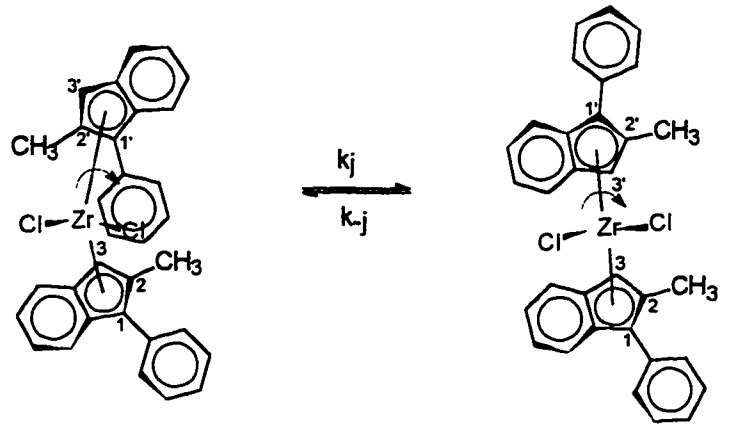

VIc **VId**

They are supposed to be distinguished in NMR spectra. However, **VIa** and **VIb**, or **VIc** and **VId** are conformational isomers, respectively, for each other and should be identical in NMR spectra when the rotation is fast. In fact, Figure B-

12a shows that there are two stereoisomers formed during the synthesis. One isomer is in predominating amount. After fractional crystallization by toluene, only one isomer can be obtained (see Figure B-12b). There is no further evidence to prove which stereoisomer is the main product because the catalyst will decompose in CD_2Cl_2 and $CDCl_3$. Low temperature ^1H NMR was performed to see whether two conformational isomers can be distinguished when the rotation of centroid-Zr bond was slowed down. This experiment will be discussed separately later.

Comparing the ^1H NMR spectrum of 2-methyl-3-phenylindene **XVIII** (Figure B-9) with Figure B-12, it can be seen that the proton 1&1' signal in **XVIII** at δ3.45 ppm disappears in Figure B-12. Either one of proton 1 or 1' was taken away by MeLi to form anion **XIX**. The five member ring with one negative charge on became aromatic, which made the chemical shift of the left proton shifted to lower field. Meanwhile, the proton signal of the methyl group shifted to higher field because in **XVIII**, the methyl group is connected with a double bond, but it is connected with an aromatic ring in **VI**. In Figure 12a, we can see a big signal at δ5.91 ppm and a small signal at δ5.44 ppm. Both of them should be signed to proton 1 (or 1') in **VI**. And there is a big signal at δ1.92 ppm and a small signal at δ2.18 ppm, which are signed to be methyl group in **VI**. However, both small peaks disappear after fractional crystallization in Figure B-12b. The signals between δ7.90 - 7.30 ppm are assigned to all the protons on aromatic rings. The

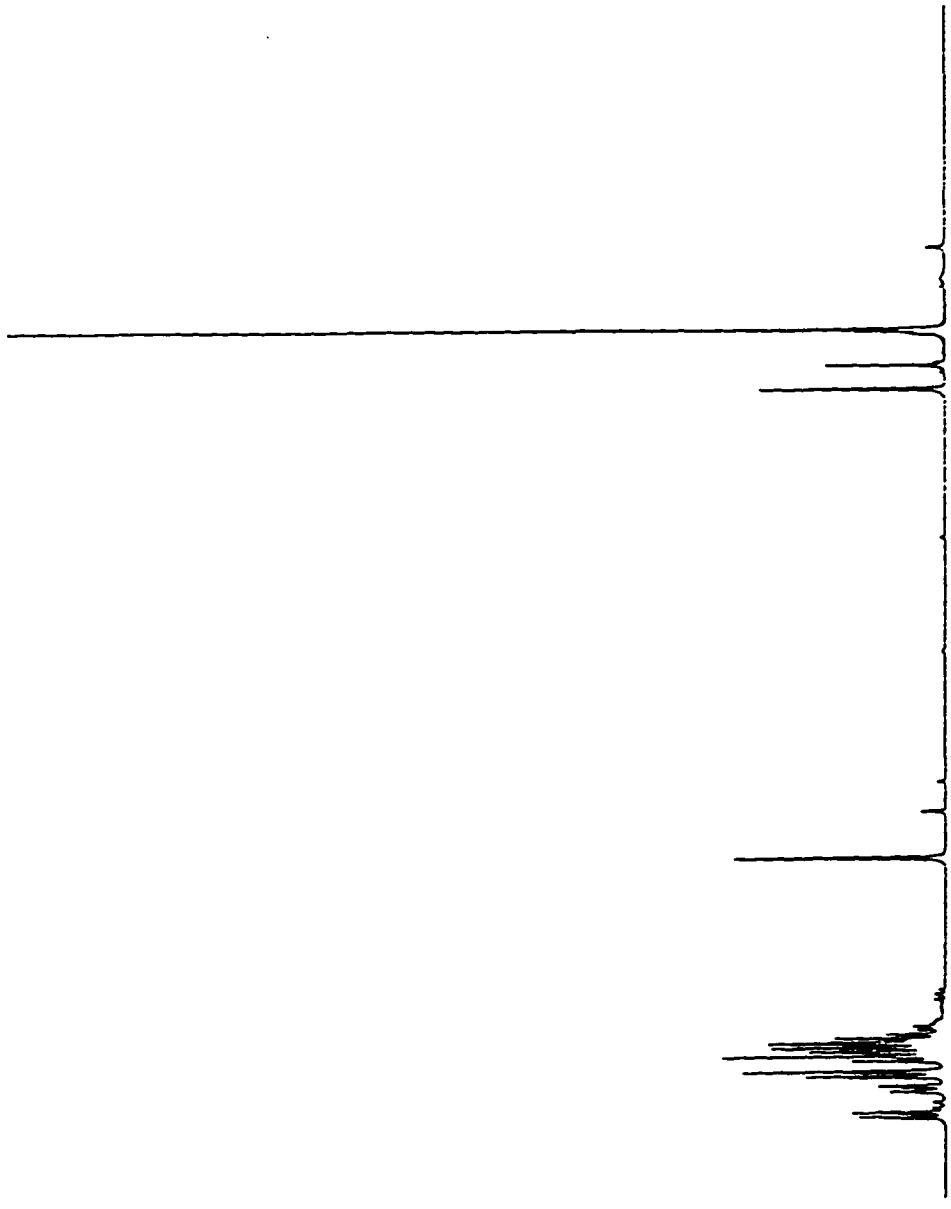

Figure B-12a ^{1}H NMR spectrum of bis[2-methyl-1-phenylindenyl]zirconium dichloride before fractional crystallization

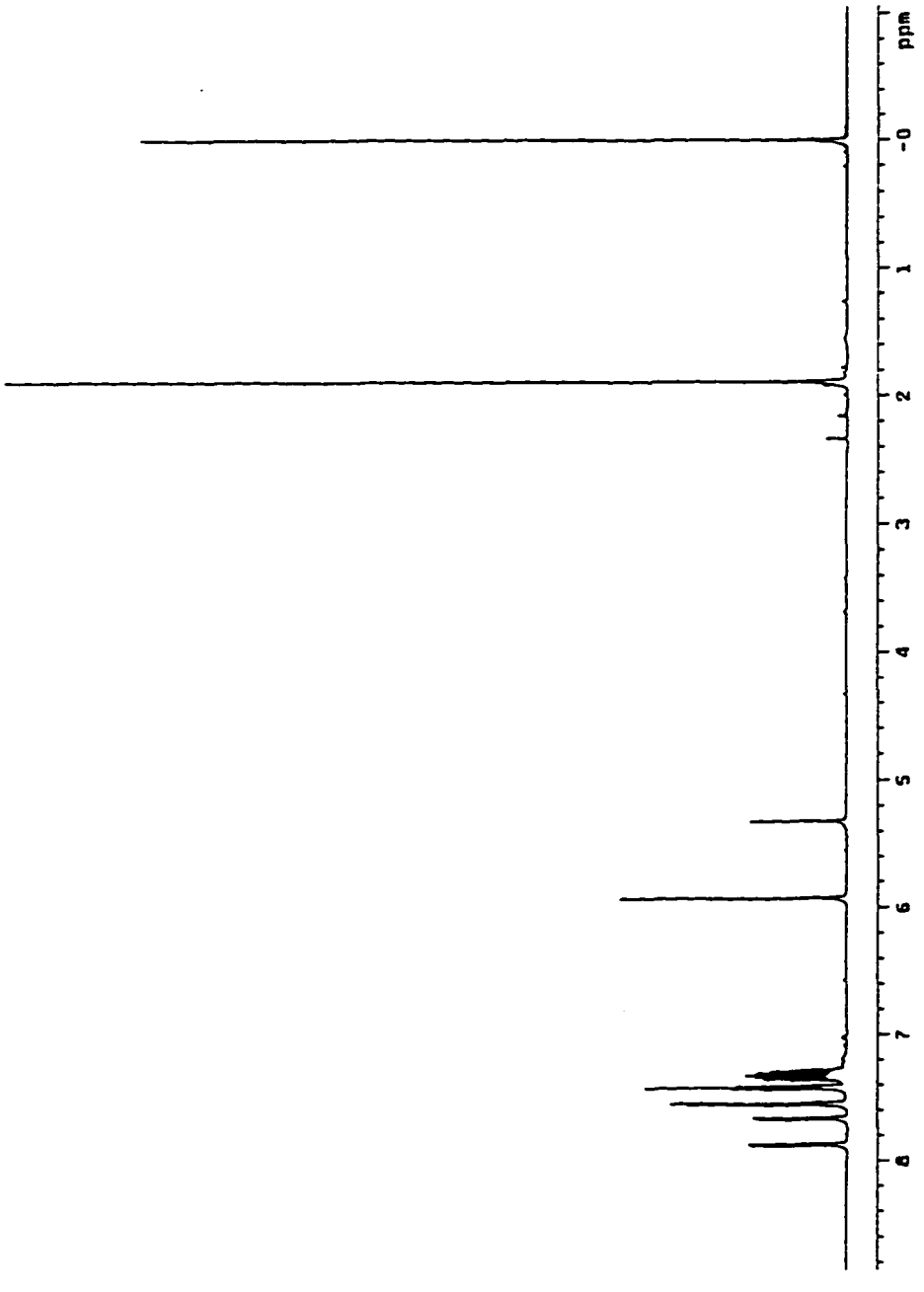

Figure B-12b ^{1}H NMR spectrum of bis[2-methyl-1-phenylindenyl]zirconium dichloride after fractional crystallization

integral ratio of the signals between δ7.90 - 7.30 ppm : signal at between δ5.91 ppm : signal at δ1.92 ppm is 9 : 1 : 3.

The elemental analysis of C and H percent compositions proves the synthesis of **VI (Cat.3)**.

	C (%)	H (%)
Elemental Analysis Result	67.38	4.86
Theoretical Value	67.11	4.60

3.4 Synthesis and Characterization of [2-Phenylindenyl][1,2,3-Triphenyl-indenyl] zirconium Dichloride (Cat.4, an unsuccessful experiment)

3.4.1 Synthesis of 1,2,3-Triphenylindene

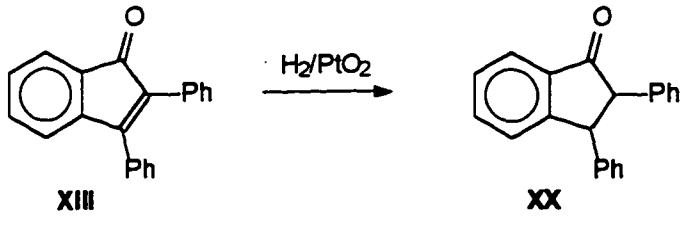

XIII XX (7)

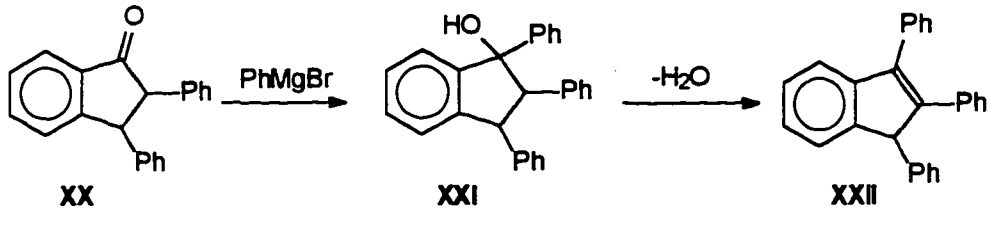

XX XXI XXII (8)

1,2,3-Triphenylindene (**XXII**) was prepared from 2,3-diphenyl-1-indenone (**XIII**) through two steps. The first step is reduction of 2,3 carbon-carbon double bond by hydrogen under the catalysis of platinum dioxide. The second step is the carbonyl group reaction with a Grignard reagent (PhMgBr) and followed by a dehydration step. 2,3-diphenyl-1-indone **XX** was a white crystal after crystallized from benzene. The melting point of this crystal was 159.26 - 167.39 °C. And 1,2,3-triphenylindene **XXII** was a dark yellow crystal after recrystallization from acetone/water solvent pair with a melting point of 129.14 - 132.01 °C.

3.4.2 Characterization of 2,3-Diphenyl-1-indone

The ^1H NMR spectrum in $CDCl_3$ (Figure B-13) supports structure **XX**. The doublet signal at δ5.06 ppm is assigned to proton 1 and the doublet signal at

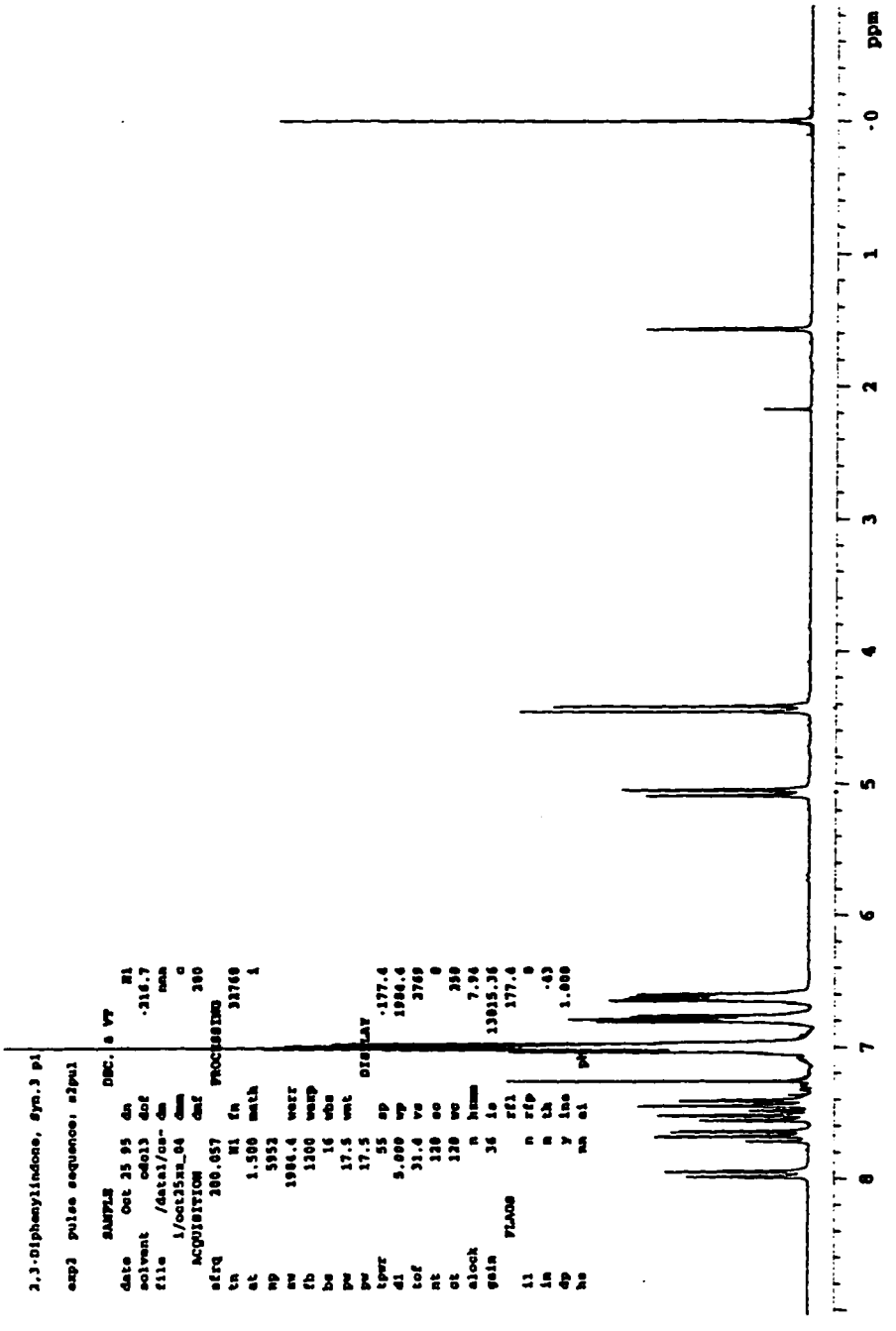

B-13 ^{1}H NMR spectrum of 2,3-diphenylindone

δ4.43 ppm should be proton 2. The signals around δ8.00 - δ6.30 ppm are assigned to all the aromatic protons. the integral ratio of the signals around δ8.00 - δ6.30 ppm : the signal at δ5.06 ppm : the signal at δ4.43 ppm is 14 : 1 : 1.

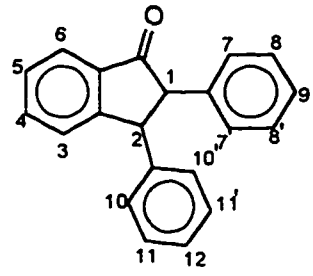

XX

The ^{13}C NMR spectrum in $CDCl_3$ (Figure B-14) supports structure **XX** as shown in Table B-5.

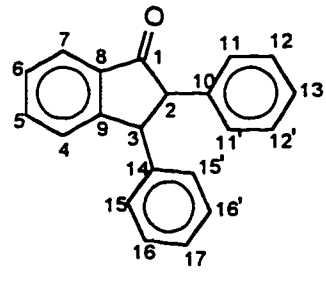

XX

According to structure **XX**, some of the carbons can be easily assigned. The signal at δ205.95 ppm is assigned to carbon 1 which is a carbonyl carbon. The signals at δ155.54 ppm and δ140.49 ppm should be carbon 8 and 9, respectively. The signals at δ137.81 ppm and δ137.00 ppm are carbon 10 and 14, respectively. The signals at δ60.90 ppm and δ51.83 ppm are carbon 2 and 3, respectively. All the signals corresponding to 3° carbons on aromatic rings cannot be assigned directly from the structure without further experiments.

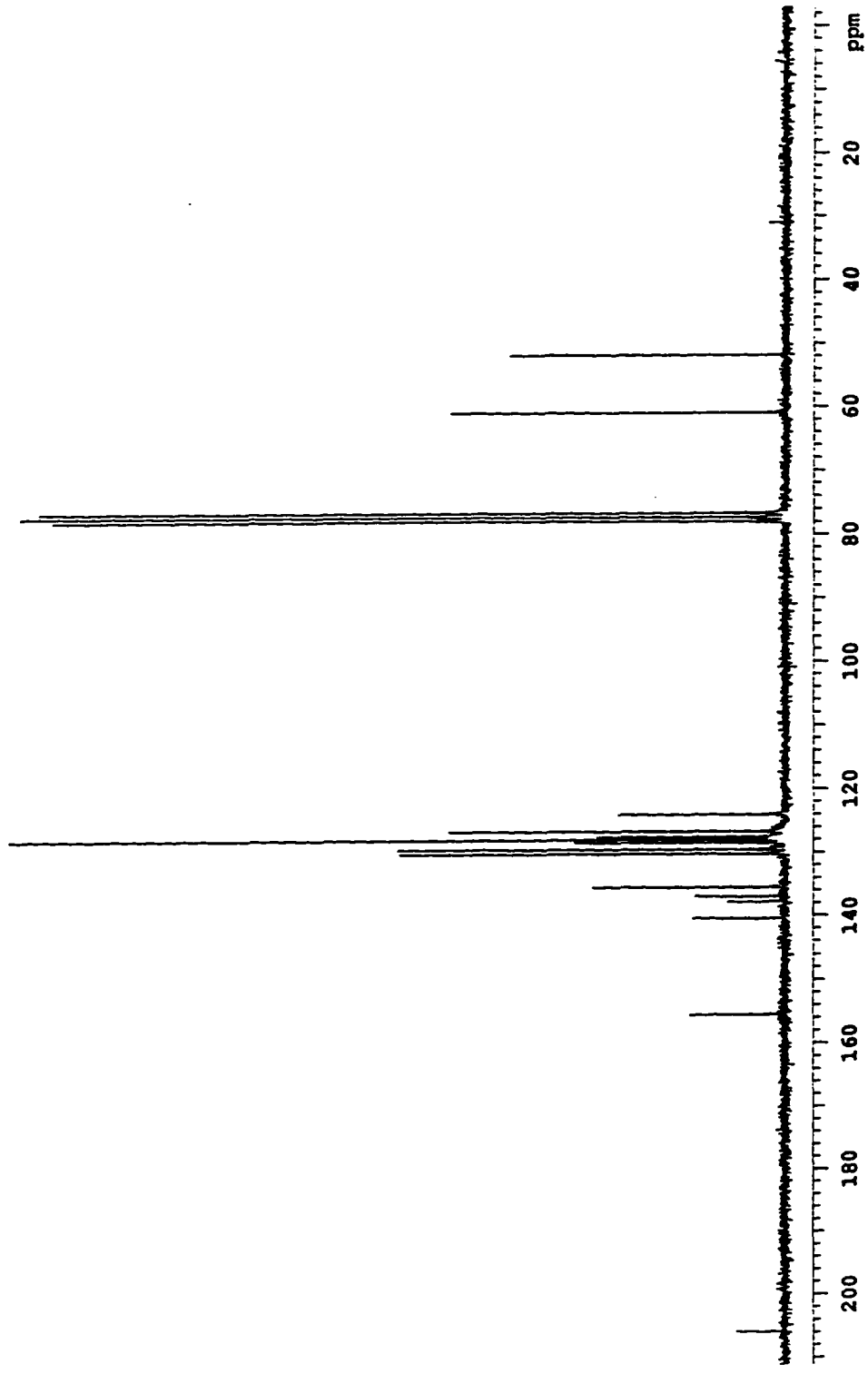

Figure B-14 ^{13}C NMR spectrum of 2,3-diphenyl-1-indone

Table B-5 Chemical Shifts of the Signals

in ^{13}C NMR Spectrum of 2,3-Diphenylindone

Carbon Numbers	Chemical Shift (ppm)
1 (4°)	205.95
1 (4°)	155.54
1 (4°)	140.49
1 (4°)	137.81
1 (4°)	137.00
1 (3°)	135.52
2 (3°)	130.25
2 (3°)	129.57
1 (3°)	128.48
4 (3°)	128.02
1 (3°)	127.62
2 (3°)	126.71
1 (3°)	124.03
1 (3°)	60.90
1 (3°)	51.83

3.4.3 Characterization of 1,2,3-Triphenylindene

The ^1H NMR spectrum in CD_2Cl_2 (Figure B-15) supports structure **XXII**. Two doublets at δ5.06 ppm and δ4.43 ppm in Figure B-13 disappear in Figure B-15

and only one singlet at δ5.17 ppm can been assigned as proton 1 in structure **XXII**. In structure **XXII**, the chemical circumstances of these protons are pretty close, and so, the spread range of aromatic proton signal is much narrower than structure **XX**. The integral ratio of aromatic proton signals between δ7.45 - δ7.05 ppm : the signal at δ5.17 ppm is 19 : 1.

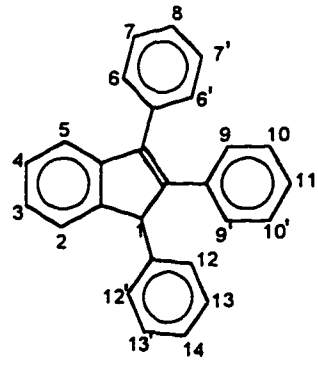

XXII

The ^{13}C NMR spectrum in $CDCl_3$ (Figure B-16) supports structure **XXII** as shown in Table B-6. Total carbon number is twenty seven, including seven 4° unsaturated carbons, nineteen 3° unsaturated carbons and one 3° saturated carbon.

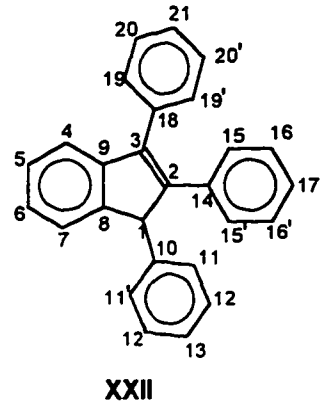

XXII

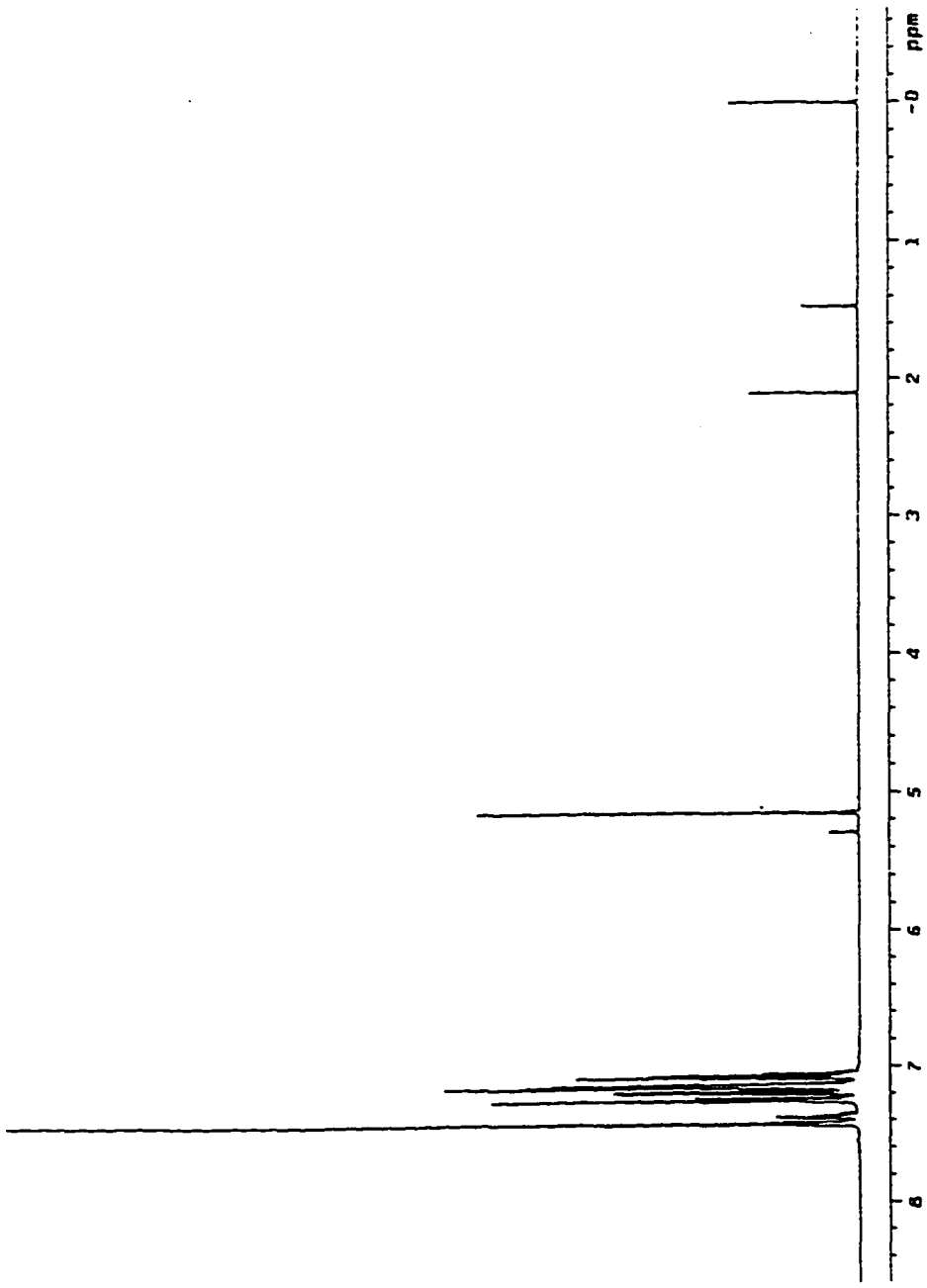

Figure B-15 ^{1}H NMR spectrum of 1,2,3-triphenylindene

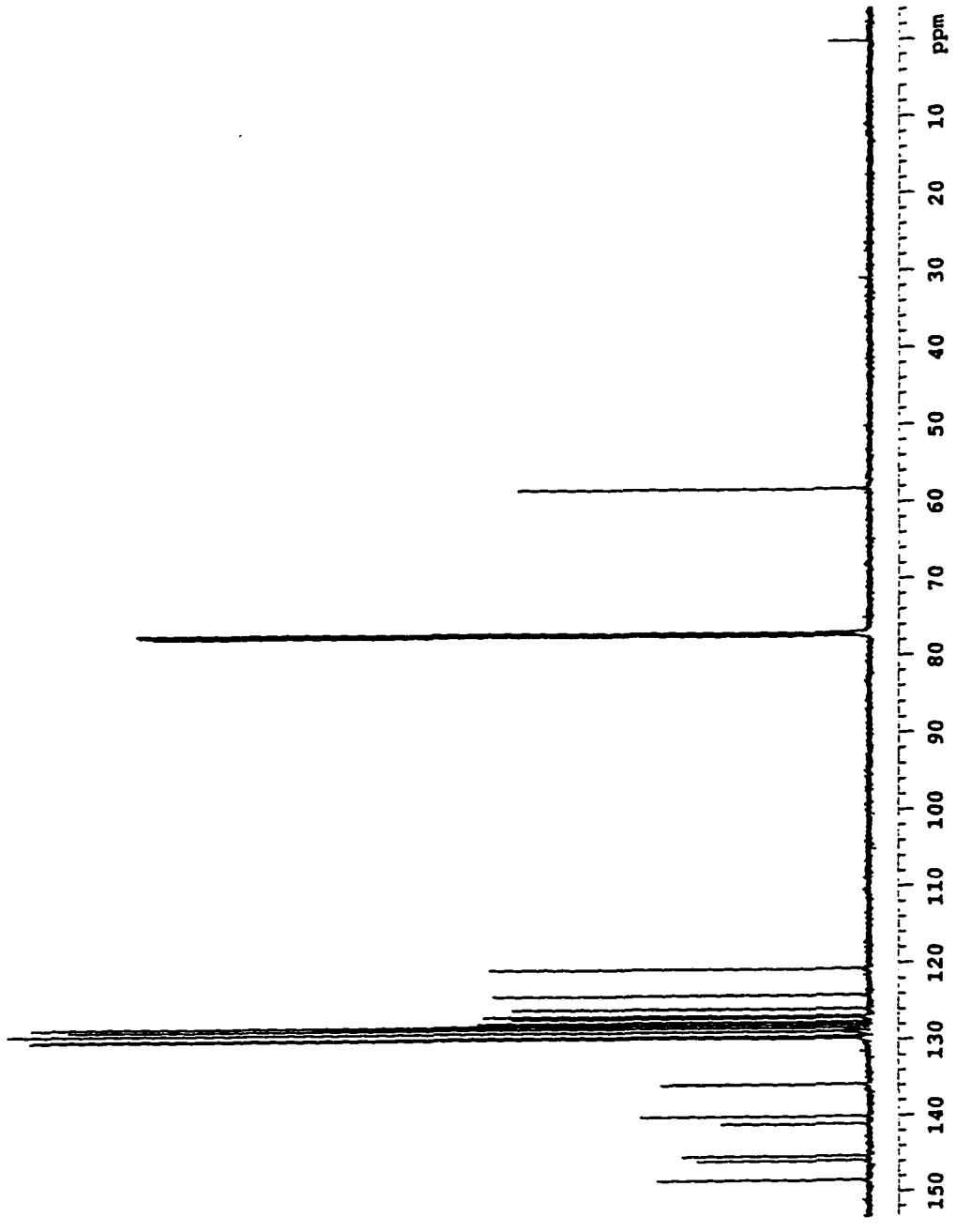

Figure B-16 ^{13}C NMR spectrum of 1,2,3-triphenylindene

Table B-6 Chemical Shifts of the Signals

in ^{13}C NMR Spectrum of 1,2,3-Triphenylindene

Carbon Numbers	Chemical Shift (ppm)
1	148.47
1	145.88
1	145.29
1	141.07
1	140.07
1	135.88
1	135.80
2	129.77
2	129.55
2	128.92
2	128.88
2	128.43
2	128.05
1	127.68
1	127.13
1	126.91
1	126.86
1	125.93
1	124.15

Table B-6 (continued)

1	120.75
1	58.36

Figure B-17 shows the IR spectrum of 1,2,3-triphenylindene. The disappearance of >C=O stretching band at around 1700 cm-1 show the complete of the reduction of ketone to alkene.

3.4.4 Synthesis of [2-phenylindenyl][1,2,3-triphenylindenyl]zirconium Dichloride (Cat. 4)

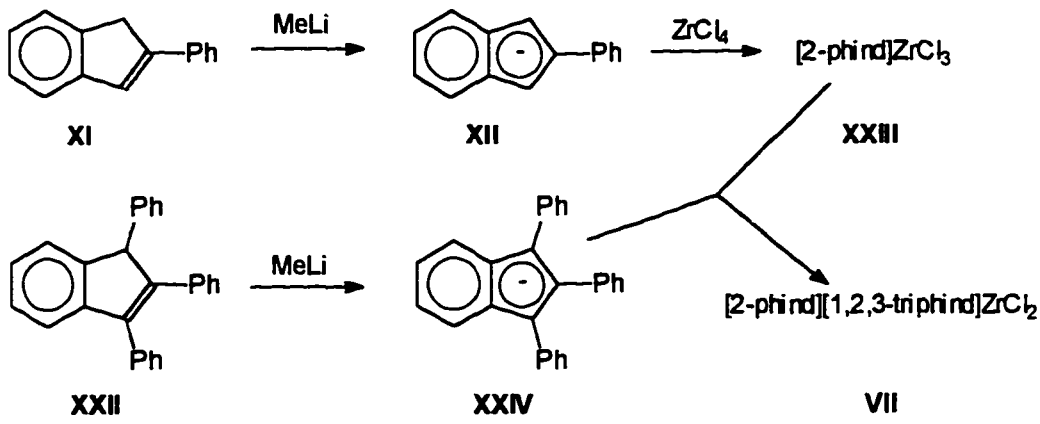

(9)

[2-Phenylindenyl][1,2,3-triphenylindenyl]zirconium dichloride was prepared by two steps. In the first step, one of the four chloride anions was replaced by a 2-phenylindene anion **XII** and [2-phenylindenyl]zirconium trichloride **XXIII** was formed. This step is similar with section 3.1.1 except that the molar ratio of **XII** : $ZrCl_4$ is 1 : 1 instead of 2 : 1. **XXIII** was used in the second step without isolation. In the second step, **XXIII** was mixed with 1,2,3-triphenylindene anion **XXIV** in molar ratio of 1 : 1. Unfortunately, this synthesis was not that successful

because most anion returned back to indene form. It is probably because the phenyl substituent is too big and it is hard to coordinate with Zr. We mention here because a tiny bit of this kind of catalyst can also make polymer with steroeblocks.

3.4.5 Characterization of [2-phenylindenyl][1,2,3-triphenylindenyl] zirconium Dichloride

Pure [2-phenylindenyl][1,2,3-triphenylindenyl] zirconium dichloride has not been separated so far. The ^{1}H NMR showed that we obtained a mixture of Cat. 5 and its two ligands, 2-phenylindene and 1,2,3-triphenylindene. The polymerization with this mixture showed that there was active catalyst in this mixture and the polymer microstructure was different from Cat.1 whose ligands were two 2-phenylindene molecules.

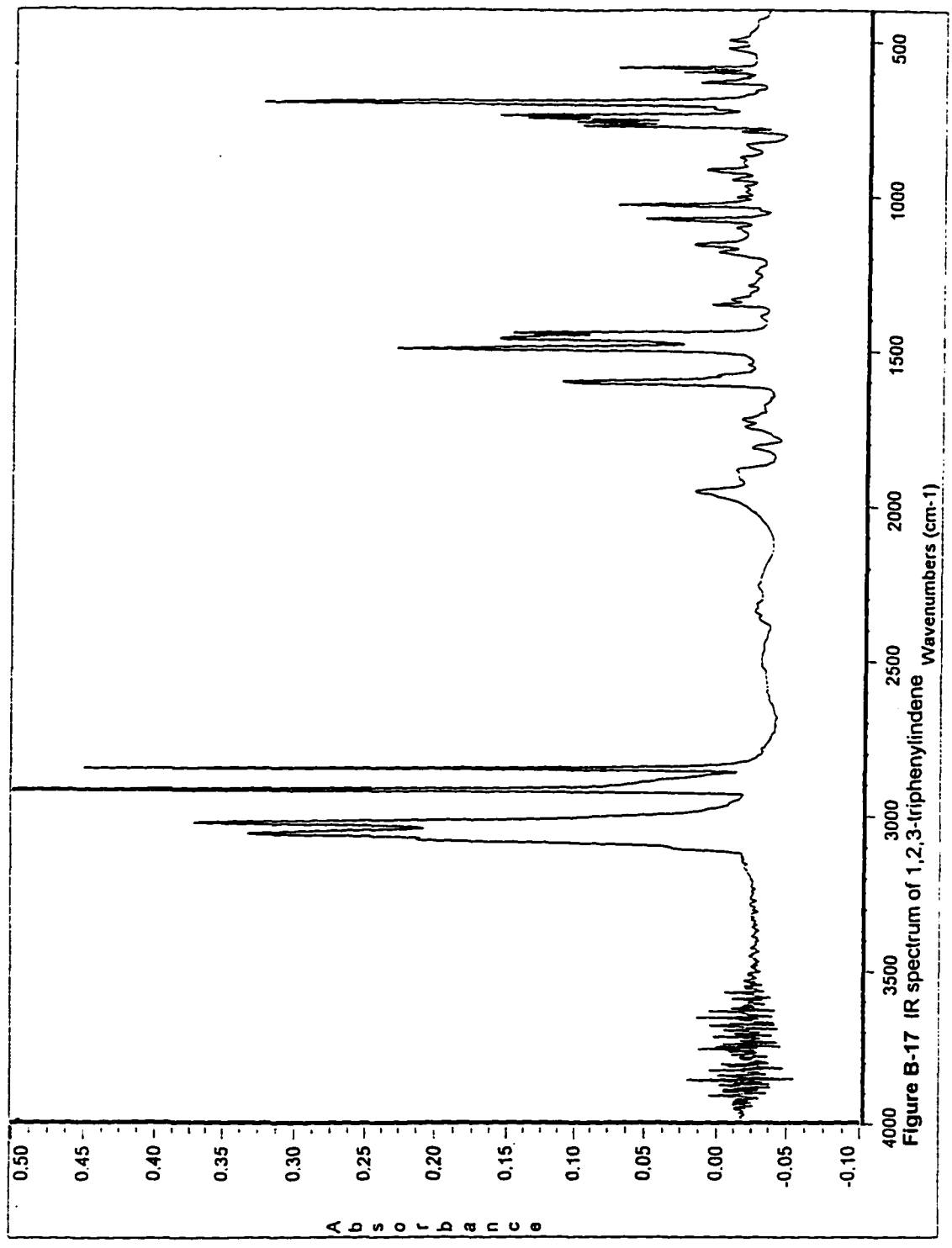

Figure B-17 IR spectrum of 1,2,3-triphenylindene

3.5 Synthesis and Characterization of Bis[1,2-dimethylindenyl]zirconium Dichloride (Cat.5)

3.5.1 Synthesis of 2,3-Dimethylindene

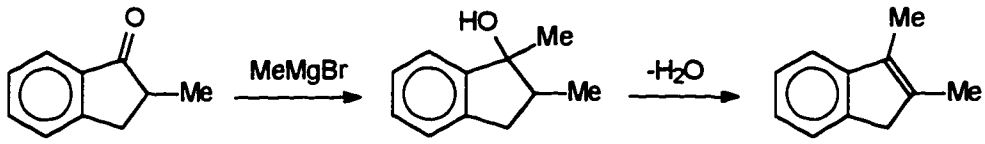

(10)

XVI **XXV** **XXVI**

2,3-Dimethylindene (**XXVI**) was prepared from 2-methyl-1-indone (**XVI**) and methylmagnesium bromide followed by a dehydration step. 2,3-dimethylindene was a light brown liquid.

3.5.2 Characterization of 2,3-Dimethylindene

The ^1H NMR spectrum in $CDCl_3$ (Figure B-18(a)) supports structure **XXVI**.

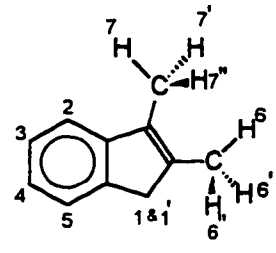

XXVI

The singlet signal at δ3.22 ppm is assigned to methylene proton 1 and 1'. The split signals at δ2.03 ppm and δ2.01 ppm are protons on two methyl groups. Four aromatic protons show between δ7.33 - 7.09 ppm. The integral ratio of the signals between δ7.33 - 7.09 ppm : δ3.22 ppm : δ2.03 ppm : δ2.01 ppm is 4 : 2 : 3 : 3. The singlet at δ7.33 ppm is the signal of benzene.

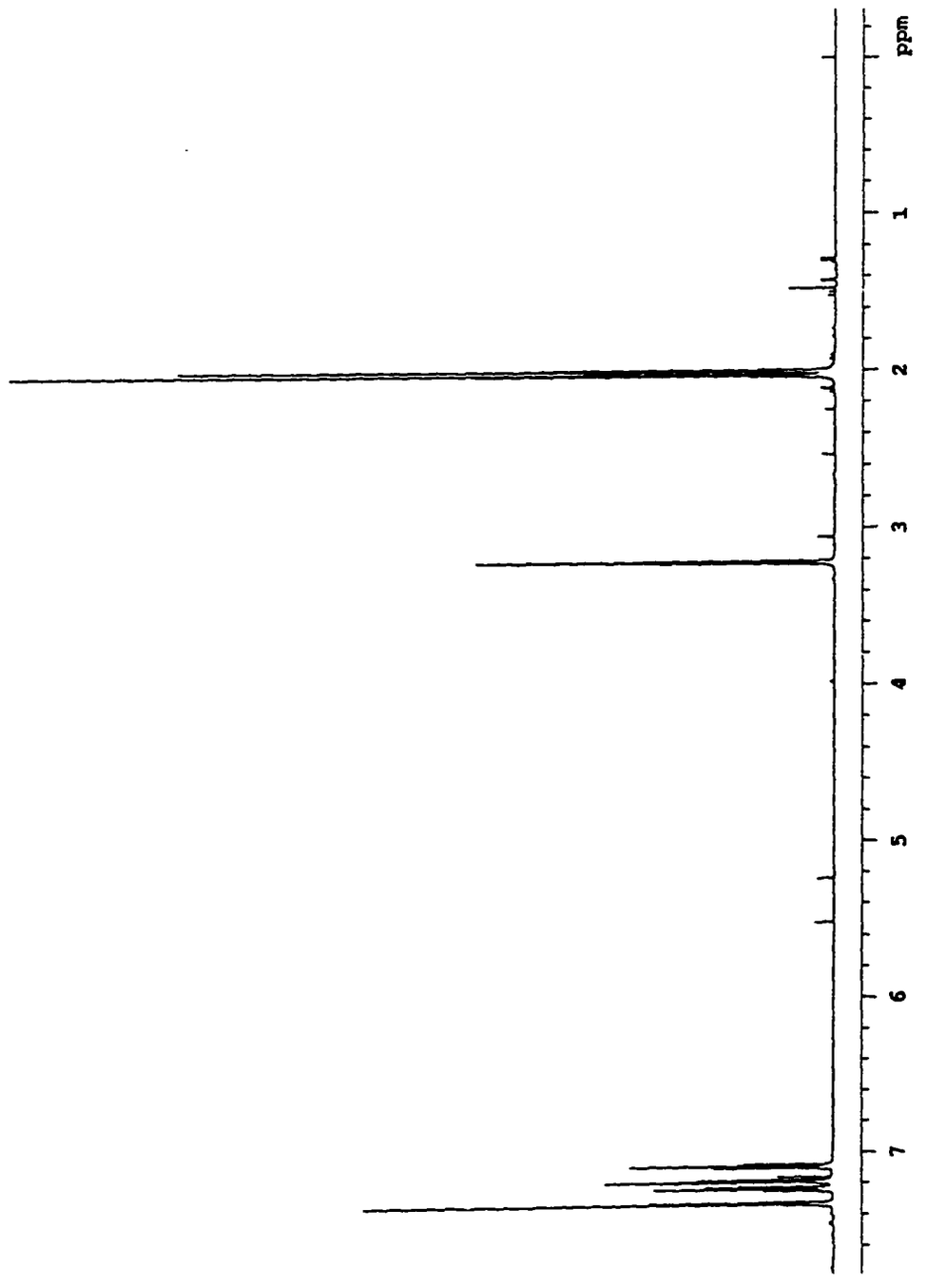

Figure B-18a ^{1}H NMR spectrum of 2,3-dimethylindene

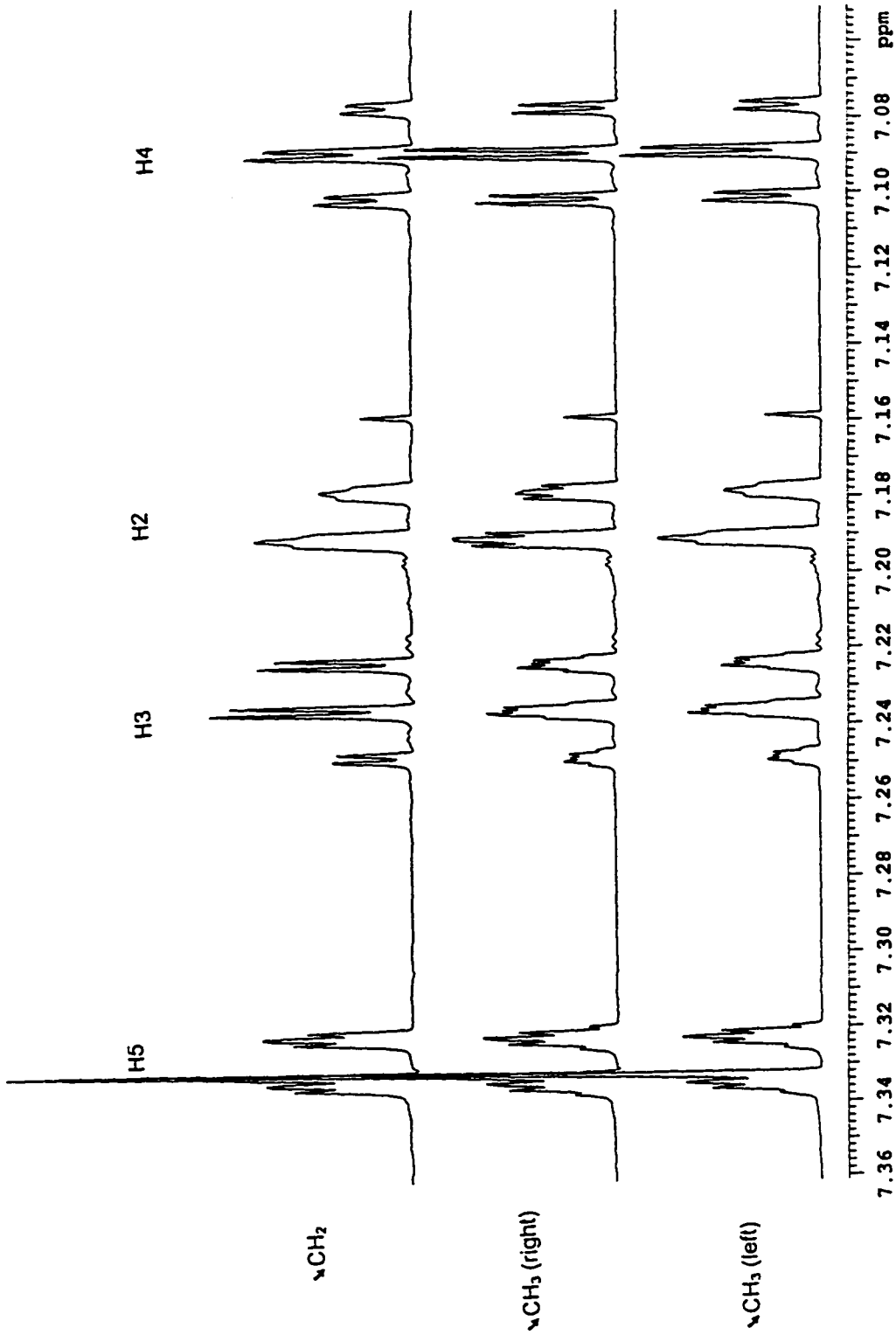

Figure B-18b ^{1}H NMR spectrum of 2,3-dimethylindene in aromatic region when CH_3 and CH_2 are irradiated

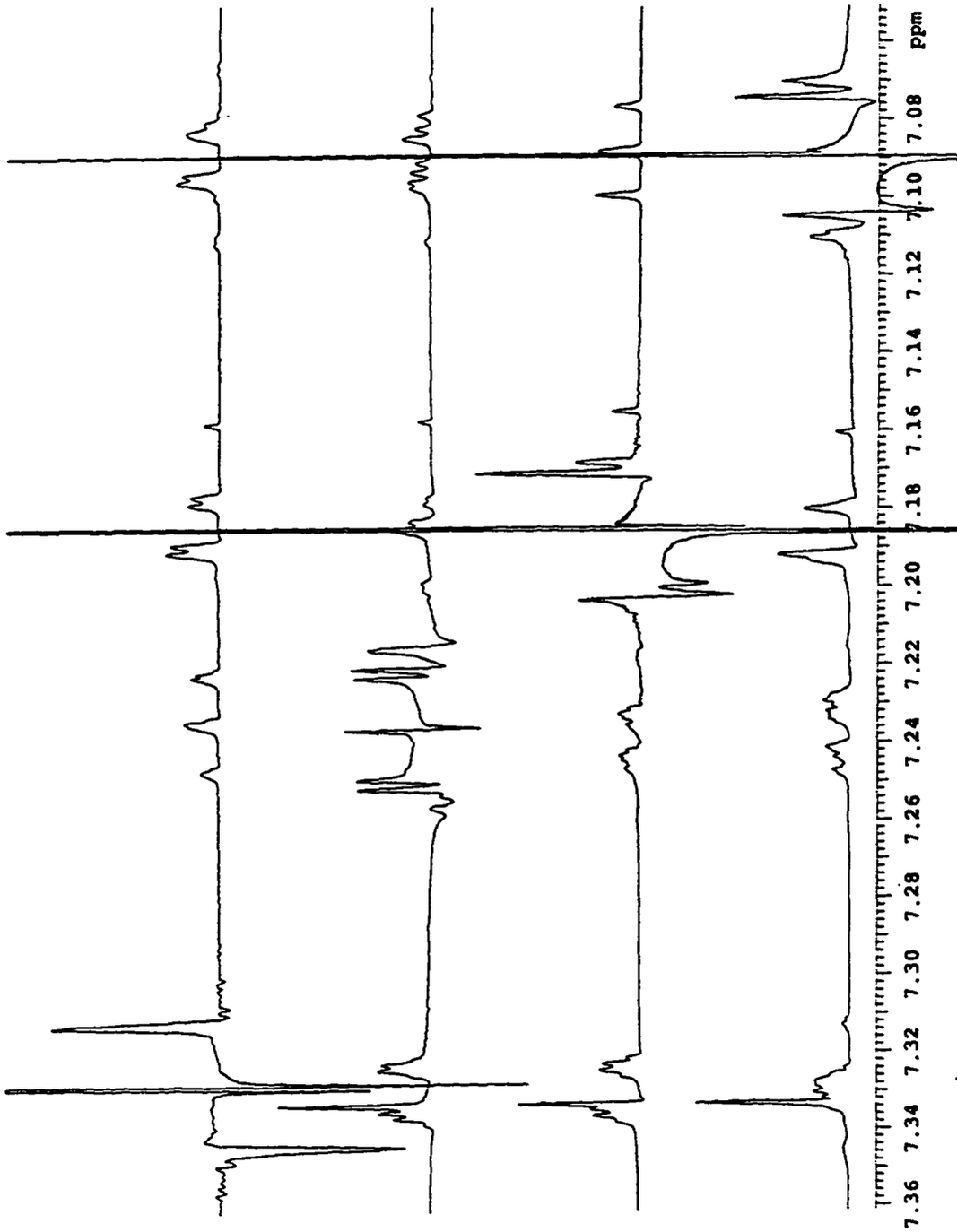

Figure B-18c ^{1}H NMR spectrum of 2,3-dimethylindene in aromatic region when they are irradiated respectively

A series of selective homonuclear decoupling experiments were performed for the complete assignment of the ^{1}H NMR spectrum. Figure B-18(b) shows the signal changes of aromatic protons when methylene and methyl are irradiated. The basic idea of this experiment is that when one proton is irradiated, its coupling on other protons disappears. When methylene is irradiated, the couplings of doublet signal at δ7.33 ppm and triplet signal at δ7.24 ppm decrease. So the doublet at δ7.33 ppm should be proton 5 and the triplet at δ7.24 ppm should be proton 3 because protons on the methylene have long range coupling to the protons on ortho- and para- positions. The doublet at δ7.18 ppm should be proton 2 and the triplet at δ7.09 ppm is proton 4 because the irradiation on methyl groups decreases their coupling. The assignment of the two methyl groups can be done by the irradiation on methylene. The split singlet at δ2.03 ppm is protons 7, 7' and 7" and the split singlet at δ2.01 ppm is protons 6, 6' and 6", because the irradiation on methylene causes the reduced coupling on the signal at δ2.01 ppm. This assignment can be confirmed by Figure-18(c) in which the four protons on the benzene ring are irradiated. When the proton at δ7.33 ppm was irradiated, the coupling on the signal at δ7.09 ppm decreased which told us that these two protons are adjacent. When the proton at δ7.24 ppm was irradiated, the coupling on the signals at δ7.18 ppm and δ7.09 ppm decreased which told us that these three protons are adjacent. And When the proton at δ7.18 ppm was irradiated, the coupling on the signal at δ7.24 ppm decreased which told us that these two protons are adjacent.

The ^{13}C NMR spectrum in $CDCl_3$ (Figure B-19(a))) supports structure **XXVI** as shown in Table B-7. The signal at δ128.53 ppm is benzene. The detail assignment was finished by the selective hetereonuclear decoupling experiment. This experiment only decoupled the selected protons and the carbon connected

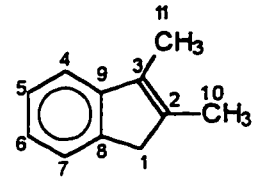

XXVI

Table B-7 Chemical Shifts of the Signals in ^{13}C NMR Spectrum of 2,3-Dimethylindene

Carbon Assignments	Chemical Shift (ppm)
C9	147.75
C8	142.53
C2	138.15
C3	132.68
C5	126.26
C6	123.77
C7	123.16
C4	118.11
C1	42.66
C11	14.06
C10	10.30

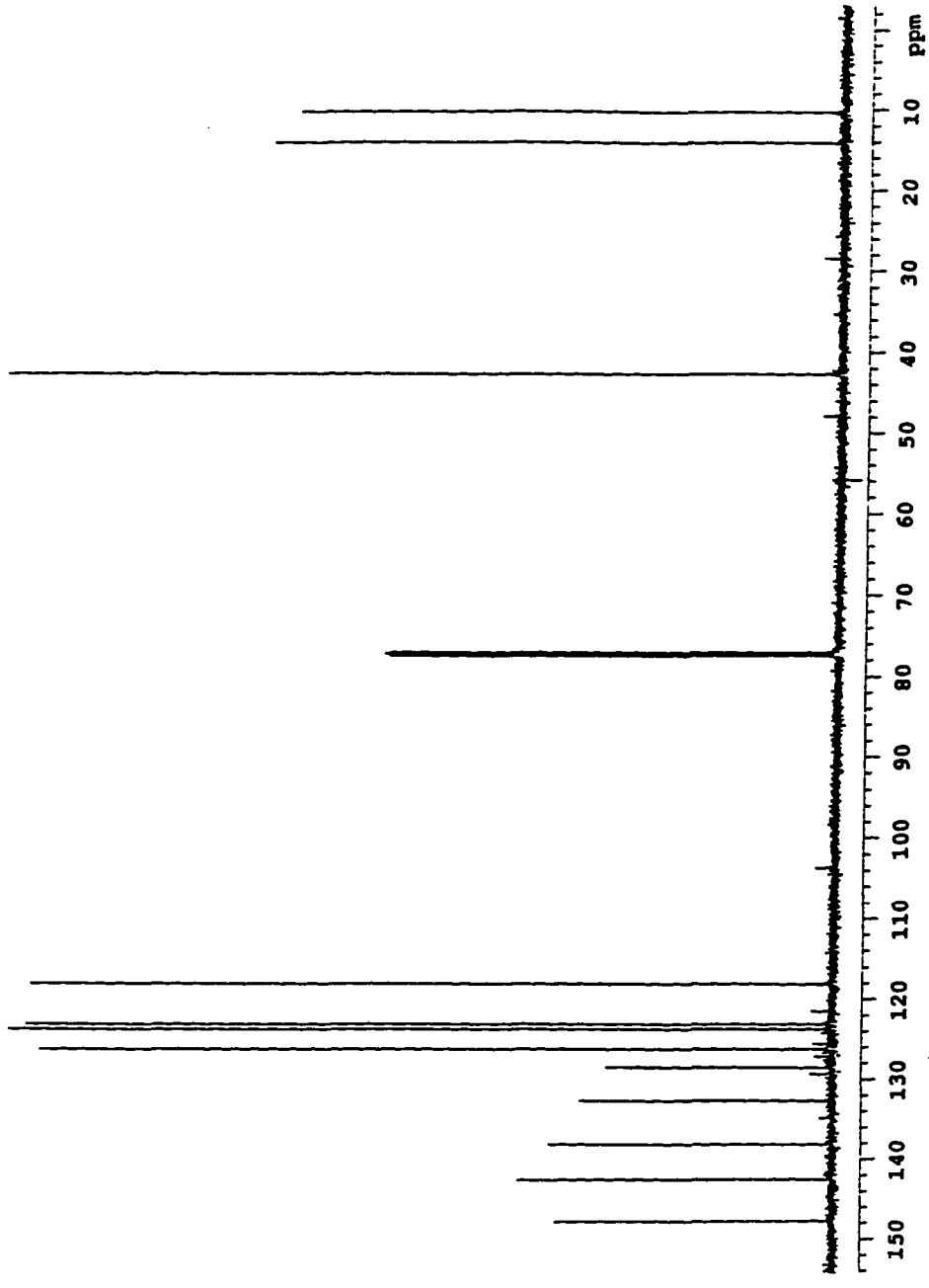

Figure B-19a ^{13}C NMR spectrum of 2,3-dimethylindene

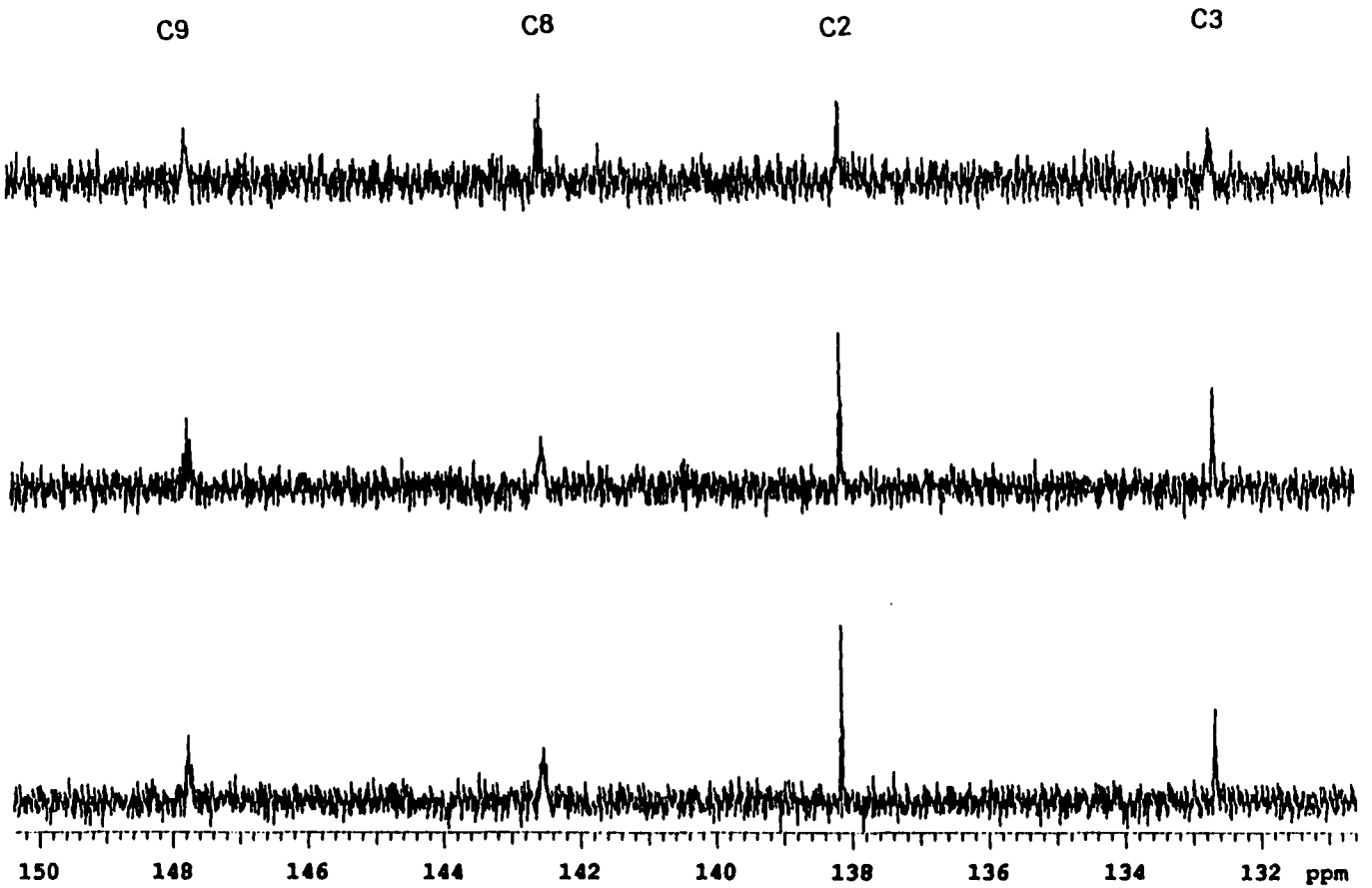

Figure B-19b selective decoupling ^{13}C NMR spectrum of 2,3-dimethylindene (> 130 ppm)

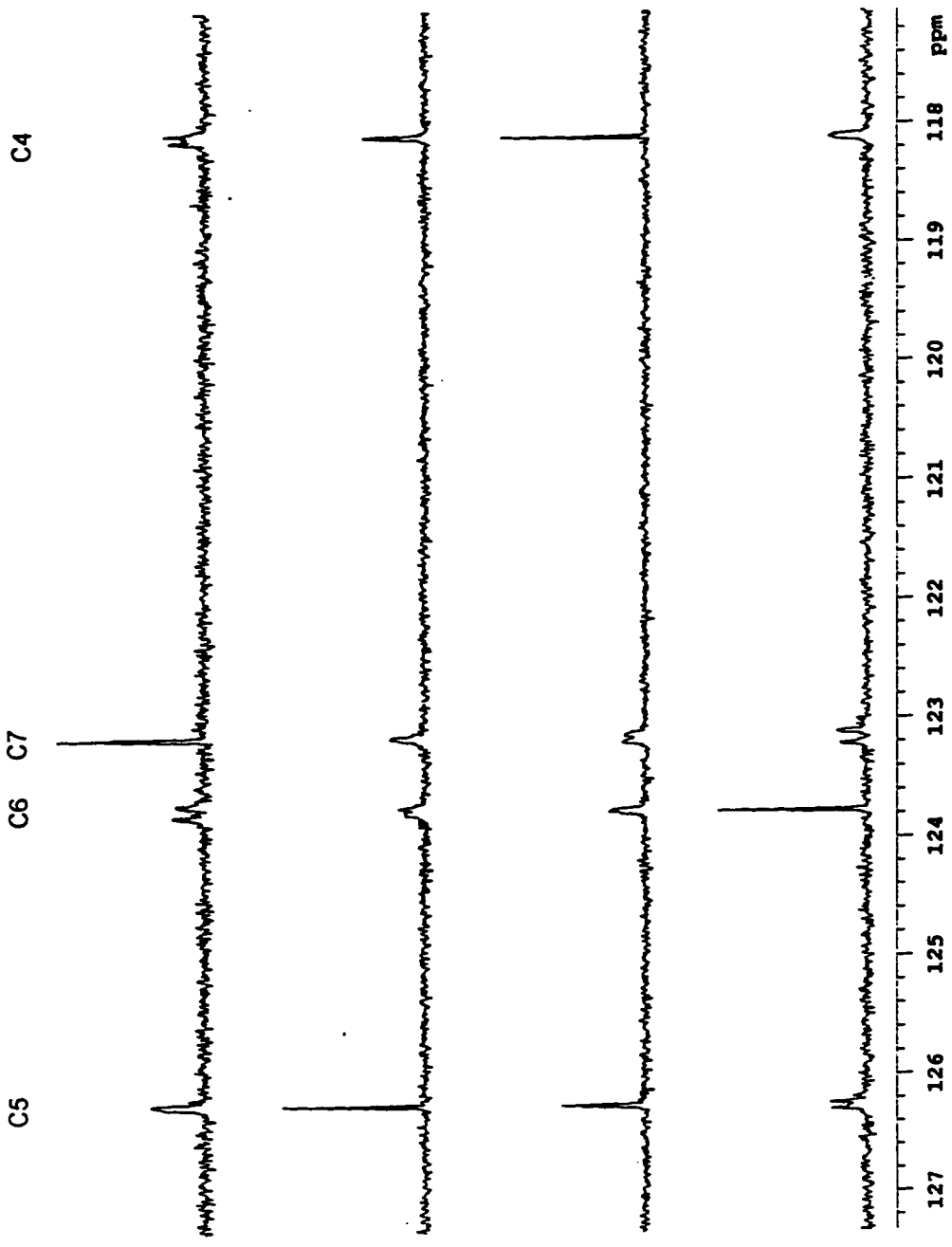

Figure B-19c selective decoupling ^{13}C NMR spectrum of 2,3-dimethylindene (127 - 117 ppm)

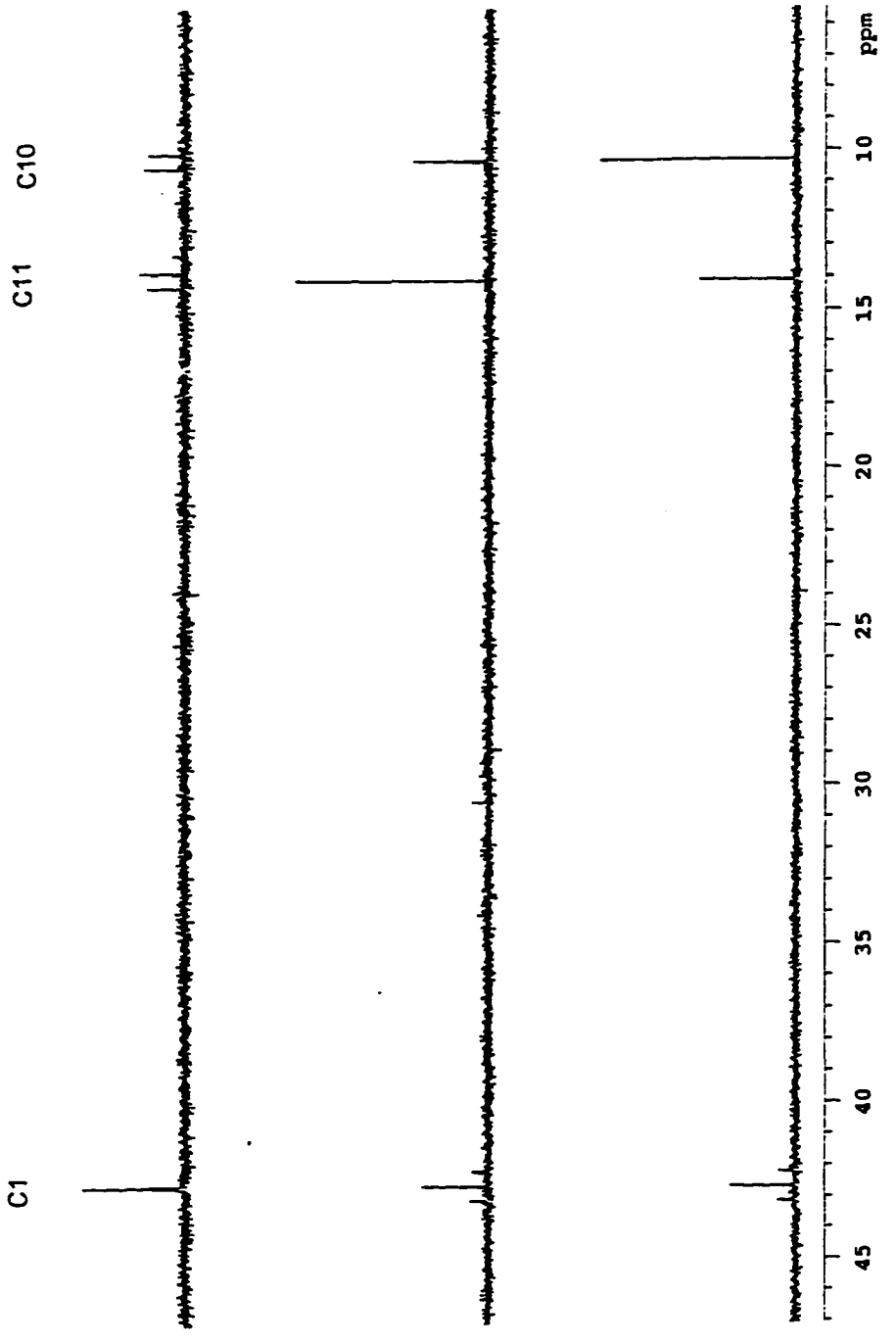

Figure B-19d selective decoupling ^{13}C NMR spectrum of 2,3-dimethylindene (< 45 ppm)

coupled by these protons would get stronger decoupling and the other carbons do not have decoupling. Figure B-19(b) shows the selective decoupling effect on these four 4° carbons. The assignment of 4° carbons is more difficult than the others because they can only get long range coupling from protons instead of direct coupling. Decoupling of protons 1 and 1' makes the signal at δ142.53 ppm stronger, which is assigned to carbon 8. The signal at δ132.68 ppm gets stronger when protons 7, 7' and 7" are decoupled, which should be carbon 3. Since the long range coupling from protons 7, 7' and 7", the intensity of carbon 9 should be increased without this coupling. This occurs on the signal at δ147.75 ppm. The signal at δ138.15 ppm is carbon 2 because it is much stronger with the decoupling of protons 6, 6' and 6". Figure B-19(c) shows the selective decoupling effect on these four -CH- carbons on the benzene ring. It is very obviously that the signal at δ123.16 ppm is carbon 7, the signal at δ126.26 ppm is carbon 5, the signal at δ118.11 ppm is carbon 4 and the signal at δ123.77 ppm is carbon 6. Figure B-19(d) shows the selective decoupling on these saturated carbons. The signal at δ42.66 ppm should be carbon 1, the signal at δ14.06 ppm is carbon 11 and the signal at δ10.30 ppm is carbon 10.

Figure B-20 is the IR spectrum of 2,3-dimethylindene which proves the complete reaction of reducing ketone to alkene.

3.5.3 Synthesis of Bis[1,2-dimethylindenyl]zirconium Dichloride (Cat. 5)

One proton on 2,3-dimethylindene (**XXVI**) was taken away by a strong base MeLi and an aromatic anion (**XXVII**) was formed. **XXVII** continued to react with

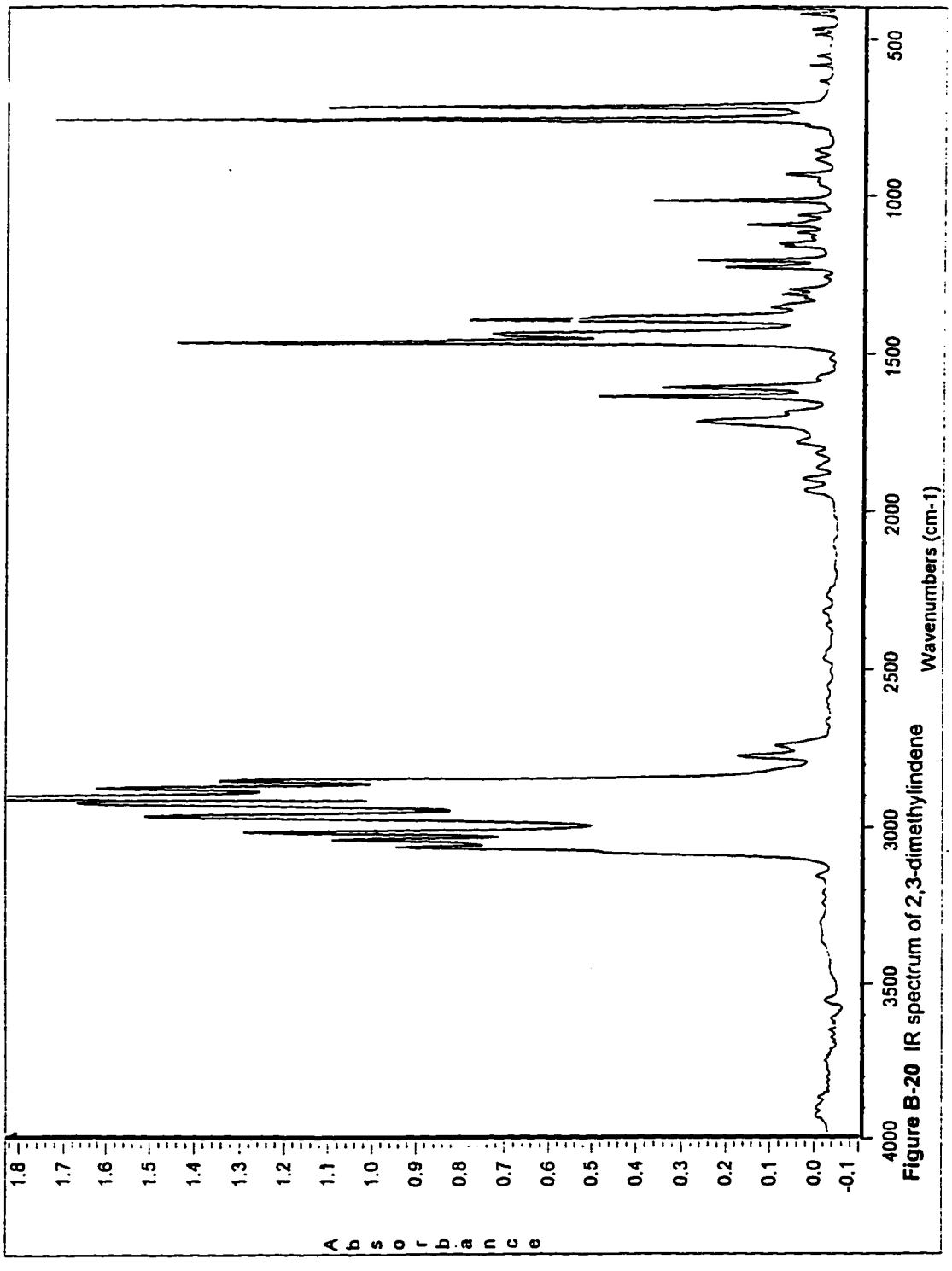

Figure B-20 IR spectrum of 2,3-dimethylindene

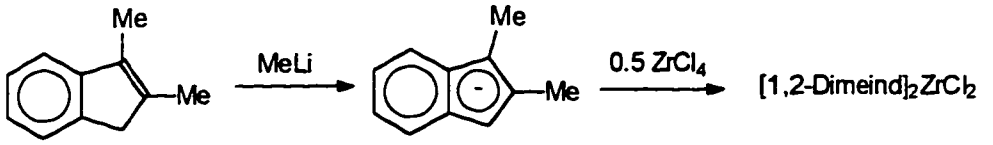

$ZrCl_4$ in a ratio of 2 : 1 without purification. An yellow orange powder of bis[1,2-dimethylindenyl] zirconium dichloride (**VIII**) was obtained and separated by crystallization.

3.5.4 Characterization of Bis[1,2-dimethylindenyl] zirconium Dichloride

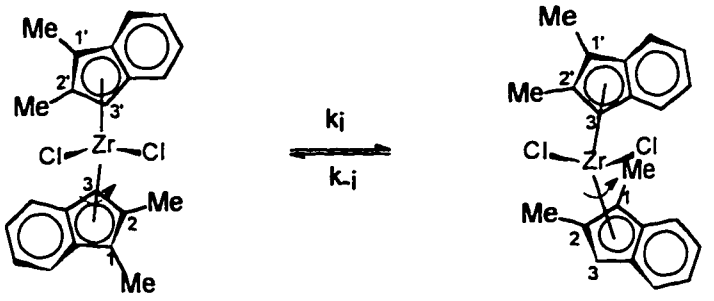

VIIIa VIIIb

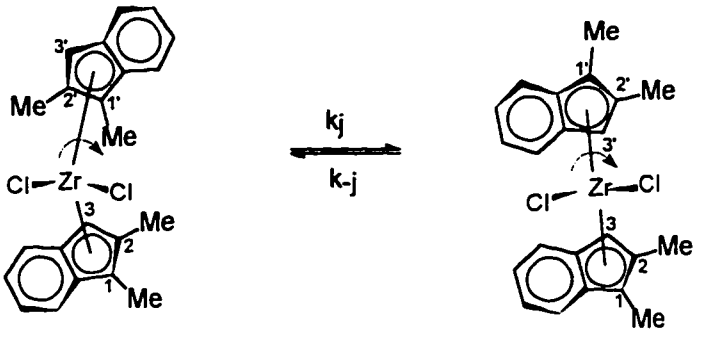

VIIIc VIIId

^1H NMR spectrum in CD_2Cl_2 (Figure B-21) supports the structure **VIII**. It is like structures **V** and **VI** that theoretically, **VIIIa** & **VIIIb** are stereoisomers of **VIIIc** & **VIIId**. They are supposed to be distinguished in NMR spectra. However,

VIIIa and **VIIIb**, or **VIIIc** and **VIIId** are conformational isomers for each other and should be identical in NMR spectra when the rotation is fast. Especially for this catalyst, since methyl group is a small group, the rotation of Zr-centroid bond is faster than that in the above catalysts.

Figure B-21 shows the ^{1}H NMR spectrum of Bis[1,2,-dimethylindenyl] zirconium dichloride. It can be seen that two isomers were obtained because there are two signals at δ5.76 ppm and δ5.49 ppm which are assigned to protons on 3 and 3' positions of the catalyst. Four methyl group protons are found in the spectrum which are corresponding to these two isomer. The ratio of these two isomers can be determined according to the integral ratio of the signals at δ5.76 ppm : δ5.49 ppm, which is 45% : 55% in this spectrum. According to the integrals, the proton at δ5.76 ppm and the methyl protons at δ2.23 and δ1.74 belong to one isomer; And, the proton at δ5.49 ppm, the methyl protons at δ2.16 ppm and δ2.09 ppm belong to the other. All the aromatic protons show between δ7.80 - 7.05 ppm. The overall integral ratio of the signals within the aromatic range between δ7.80 - 7.05 ppm : summation of signals at δ5.76 ppm : δ5.49 ppm : total summation of four methyl signals is 4 : 1 : 6.

The elemental analysis of C and H percent compositions also supports the completion of Clemmensen reduction step.

	C (%)	H (%)
Elemental Analysis Result	58.78	5.11
Theoretical Value	59.18	4.97

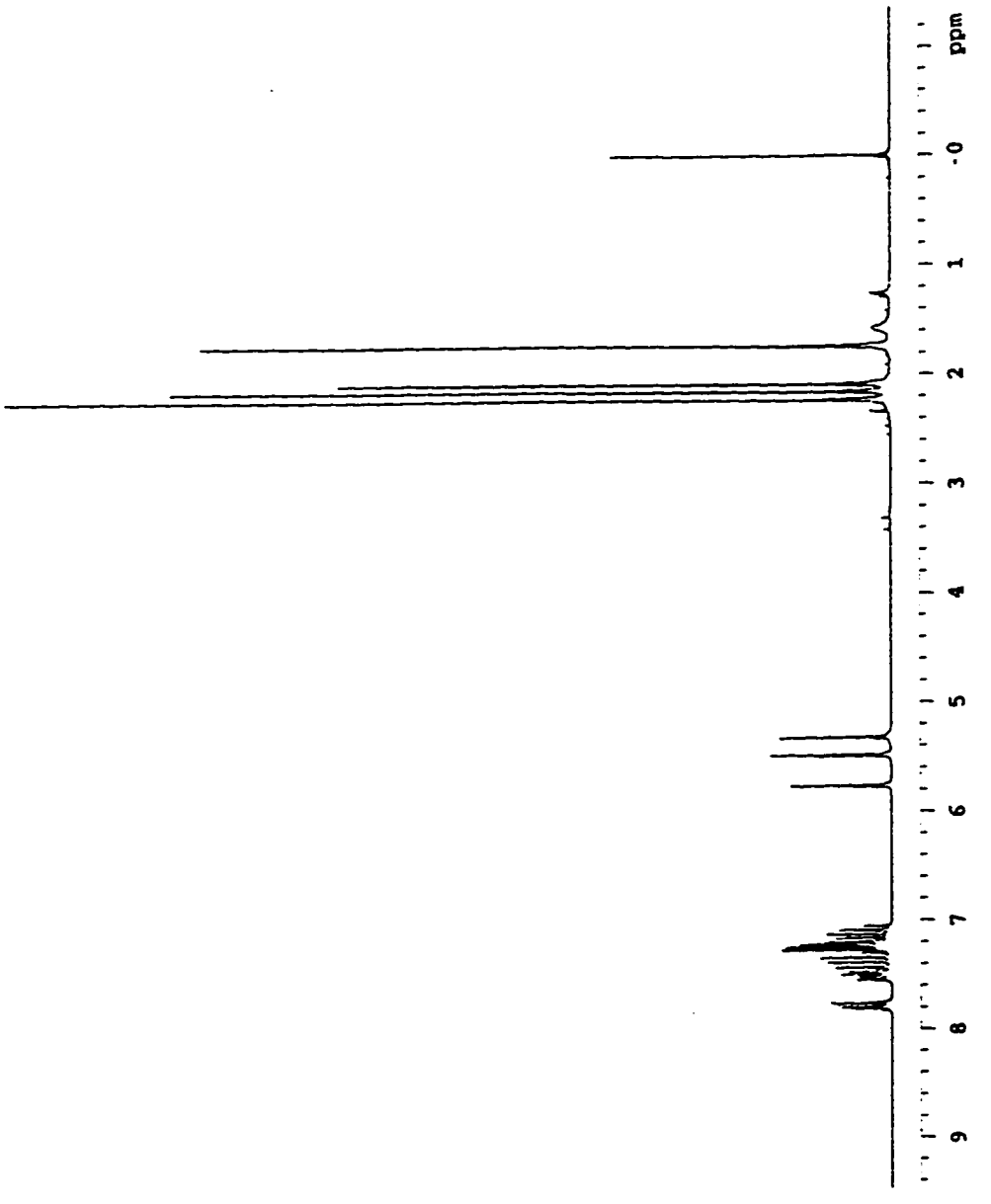

Figure B-21 ^{1}H NMR spectrum of bis[1,2-dimethylindenyl]zirconium dichloride

4.0 Catalyst Conformation Study

The catalyst conformation study was performed by ^{1}H NMR. The rotation of Zr-centroid bond should be slowed down when temperature is decreased. Cat. 2 and 3 were studied.

4.1 Conformation Study on Cat. 2 (bis[1,2-diphenylindenyl]zirconium dichloride)

It has been discussed in section 3.2.3 about the isomers of bis[1,2-diphenyl indenyl]zirconium dichloride. Figure B-22 shows two proton 3 (3') signals of the Cat. 2 at different temperatures. The relative integral does not change with temperature, which means that these two signals show two structural isomers. The chemical shifts of these two signals are changing with temperature. Even at low temperature, there is no obvious signal splitting except that at -50°C, The minor peak seems to be split into two. There are two conformational isomers possibly existing. However the evidence from this experiment is not efficient to prove the exist of conformational isomers.

4.2 Conformation Study on Cat. 3 (bis[2-methyl-1-phenylindenyl]zirconium dichloride)

Figure B-23 shows the proton 3 (3') signal of Cat. 3. It can been seen that when the temperature decreases, the signal is split into two. This means that there are two conformational isomers existing. At low temperature, the rotation of the Zr-centroid bond slows down to such a significant extent that these two

isomers can be "frozen". The proton 3 (3') on different isomers can be distinguished.

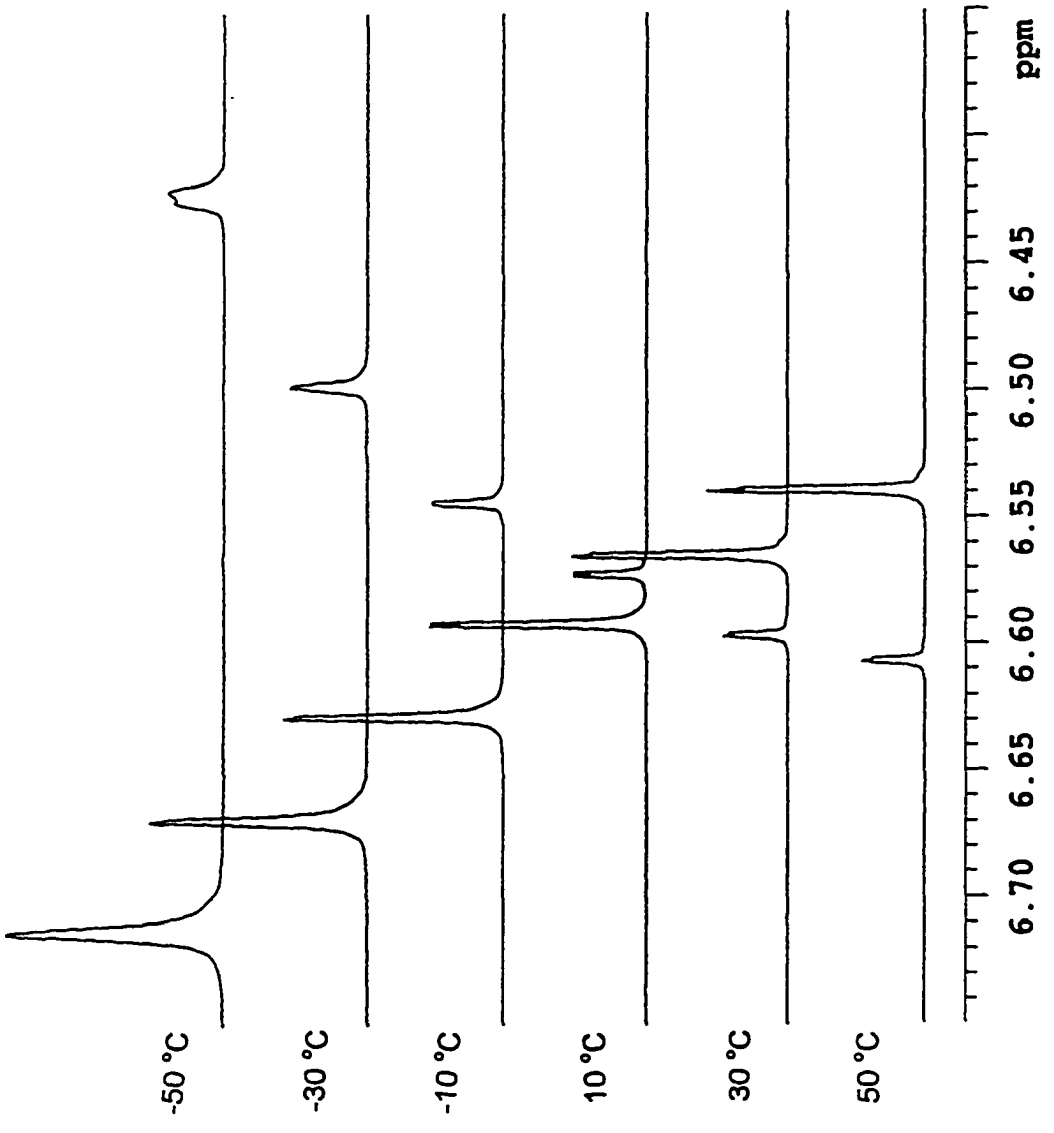

Figure B-22 H3 signal of Cat.2 at different temperatures

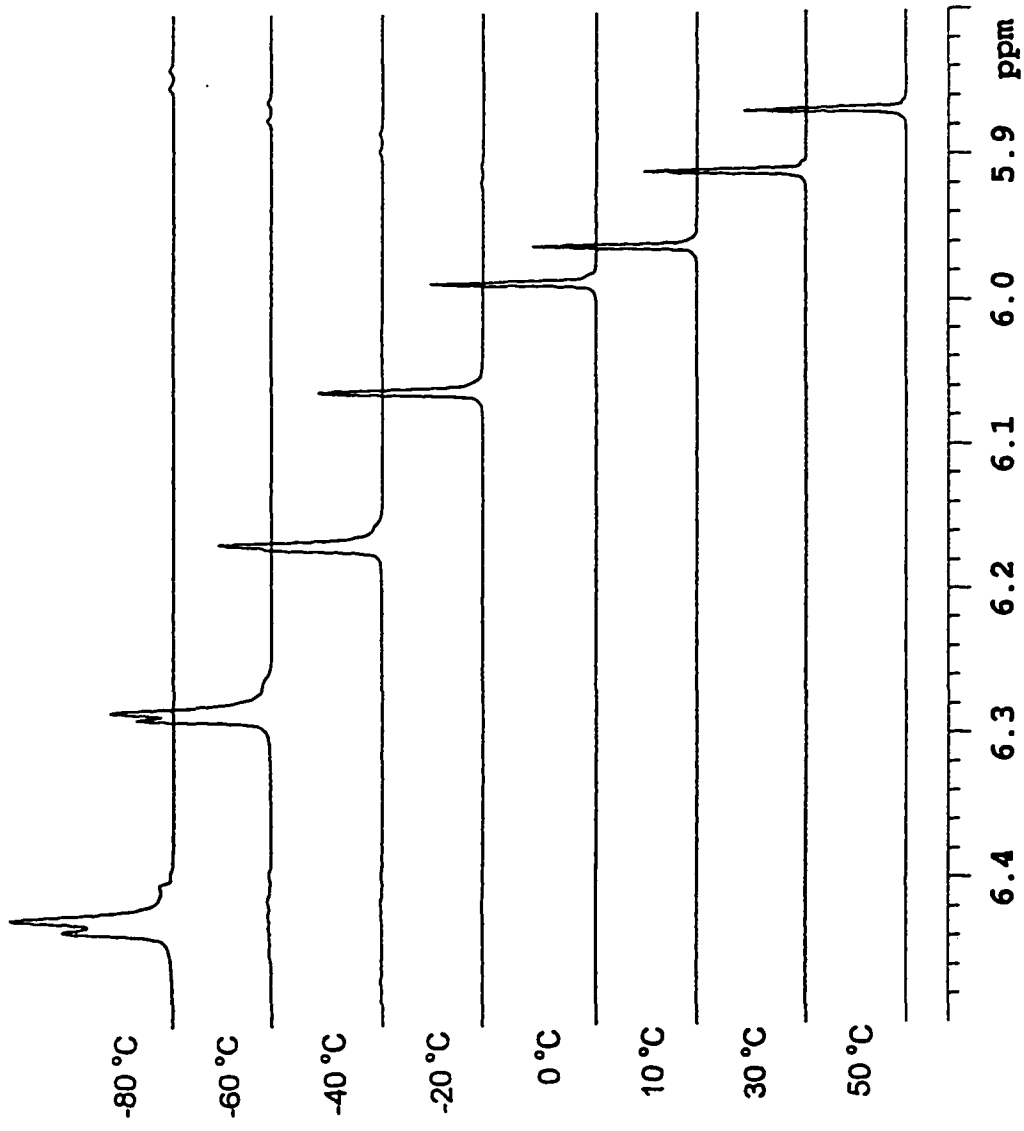

Figure B-23 H3 signal of Cat.3 at different temperatures

5.0 Polymerization of 1-Hexene by These New Catalysts

5.1 Catalyst Activity

Polymerizations of 1-hexene with these new catalysts were performed. Table B-7 shows the activity of these catalysts in polymerization of 1-hexene. It seems that the substituents on C1 (or C3) of the five member ring make the catalyst activity decreased.

Table B-7 Catalyst Activity in the Polymerization of 1-Hexene[a]

Catalyst	T (°C)	Activity (kg polymer/mol Zr/hr)
Cat. 1	80	450
	50	250
	20	210
Cat. 2	80	2
	50	1
	20	0.4
Cat. 3	80	0.1
	20	5
	0	2
Cat. 5	80	100
	0	13

[a] Other polymerization conditions: [M] = 8.0 M (bulk); [Zr] = 100 μM, [MAO] = 62 mM

Generally, catalyst activity increases with the increase of temperature. However, it is very interesting that the activity of Cat. 3 is higher at 20°C and 0°C

than 80°C. It is possible that this catalyst is not stable at high temperature.

The activity of Cat. 4 could not be determined because we could not get pure Cat. 4. The polymerization was performed by two ways. The first was that a small piece of the catalyst mixture product was directly added into the monomer and MAO solution; The second was that the catalyst was used as in toluene solution. Polymerization occurred at 80°C in both ways and the polymer had good stereoblock microstructure.

5.2 Microstructure of Poly(1-hexene) Synthesized by These New Catalysts

The ^{13}C NMR assignment of poly(1-hexene) has been described in detail in section 6.1, Part A of this thesis. Since our attention is on the isotacticity of the polymer, we only studied the C3 carbon signal of poly(1-hexene), which is the first methylene on the substituent chain and next to the chiral center. We are going to observe C3 for the poly(1-hexene) we synthesized on pentad level and possibly heptad level. Because our purpose is to make stereoblock polymer by these new catalysts, the higher tacticity level we can get, the longer the stereoblock of the polymer will consist of.

Figure B-24 shows the C3 ^{13}C NMR of poly(1-hexene) synthesized by Cat. 1. The polymer synthesized at 80°C is completely atactic and the isotacticity on pentad level mmmm% increases with the decrease of polymerization temperature. Heptad level of mmmmmm% + mmmmmr% cannot be determined until the polymerization below 20 °C.

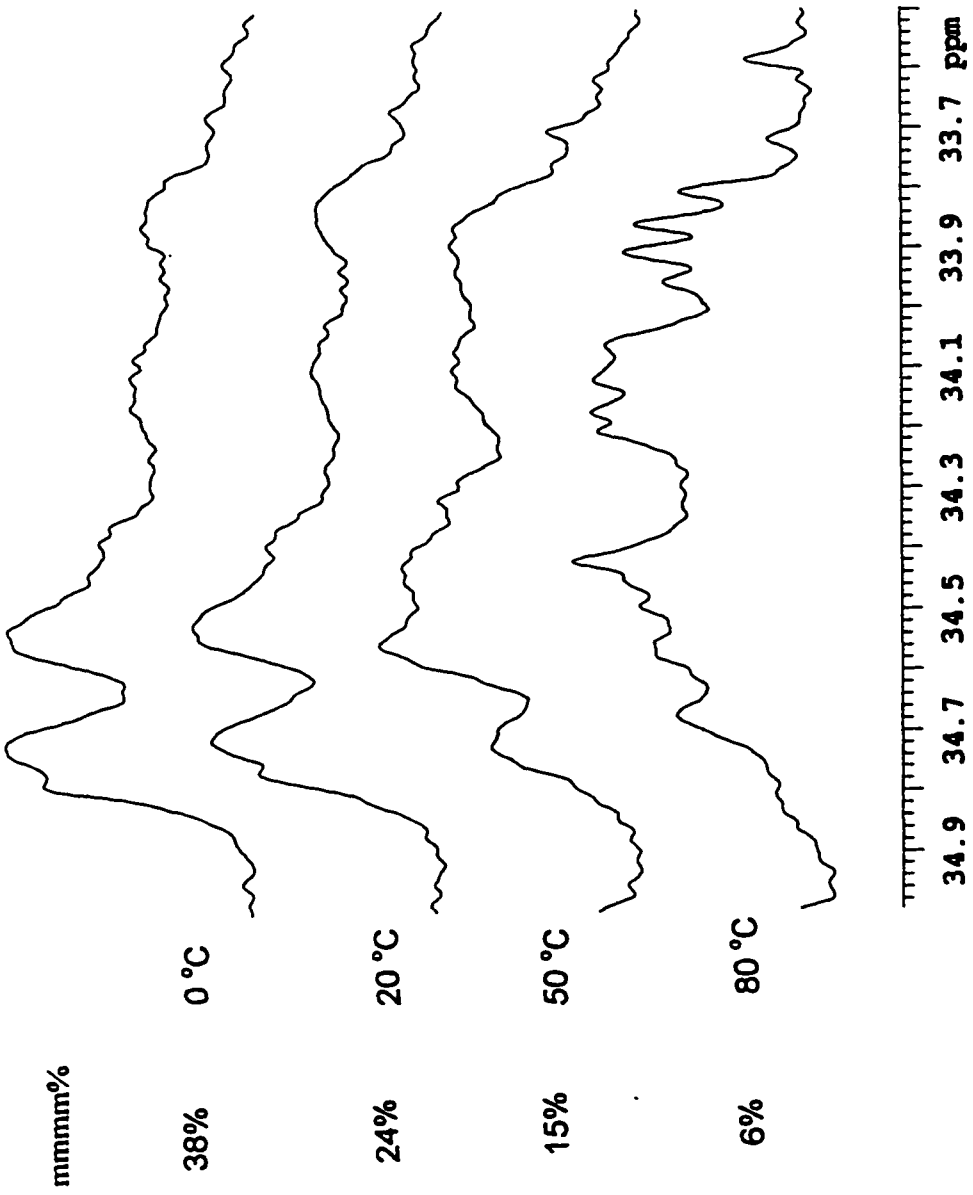

Figure B-24 C3 signal of poly(1-hexene) synthesized by Cat. 1 at different temperature

Cat. 1 was designed and synthesized first by Waymouth[25]. It was used in the polymerization of 1-propylene. The isotacticity of polypropylene increased with the decrease of temperature. mmmm% was only 6.3 at 45°C, 9.2 at 25°C, and then increased to 12.3 at 0°C and 16.1 at -25°C when the pressure of propylene was 1 atm.

Figure B-25 shows the C3 ^{13}C NMR of poly(1-hexene) synthesized by Cat. 2. Although the phenyl substituent on C3 on the indene ring decreases the catalyst activity substantially by comparing with Cat. 1, it increases the isotacticity on both pentad level and heptad level greatly. It can be also found that the isotacticity almost does not change with the polymerization temperature within the range of 20°C to 80°C. This means that the rotation rate of the centroid-Zr bond does not change that much within this temperature range. Figure B-25 shows that stereoblock (isotactic block + atactic block) polymer can been successfully synthesized by Cat. 2.

Figure B-26 shows the C3 ^{13}C NMR of poly(1-hexene) synthesized by Cat. 3. It is shown that Cat. 3 is an interesting catalyst. At 20°C, it produces poly(1-hexene) with major signals at syndiotactic regions; However at 0°C, major signals show at both isotactic region and syndiotactic region but very little signals in atactic region; And at 80°C, signals can be seen in all three regions. From the polymer microstructure, we can predict the rotation of centroid-Zr bond in this catalyst. At 20°C, one conformation of this catalyst, which produces syndiotactic polymer, has the lowest potential energy and the rotation of the

mmmmmm% + mmmmmr%	mmmm%
25%	47%
23%	45%
23%	43%

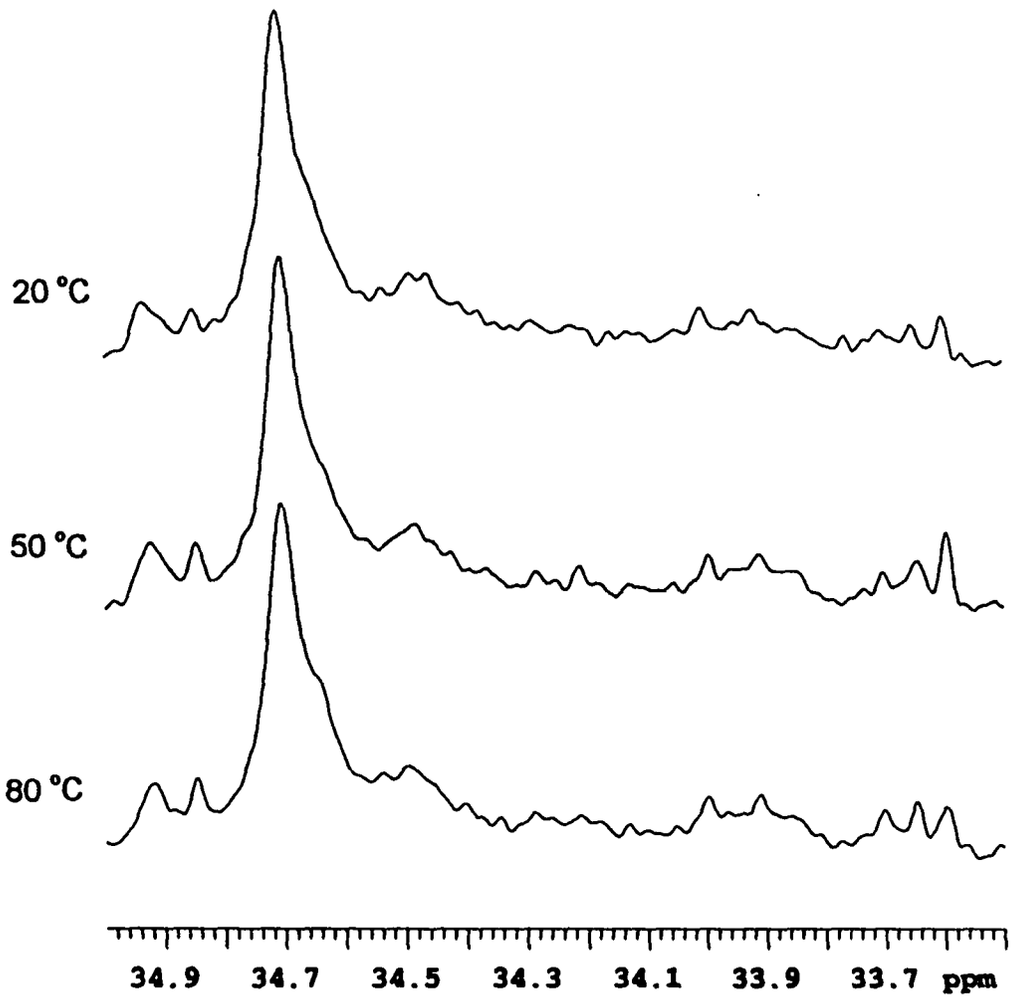

Figure B-25 C3 signal of poly(1-hexene) synthesized by Cat. 2 at different temperature

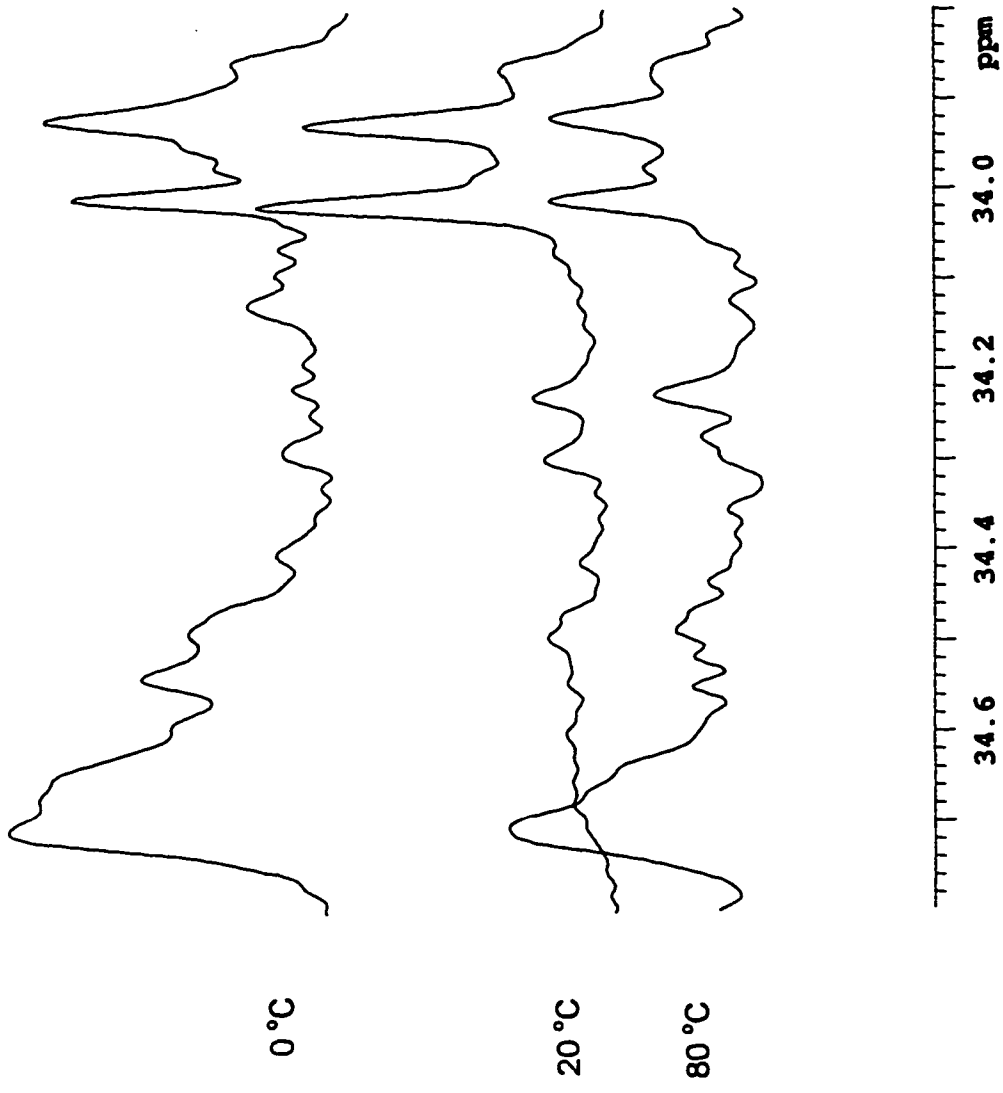

Figure B-26 C3 signal of poly(1-hexene) synthesized by Cat. 3 at different temperature

centroid-Zr bond is restricted around this conformation. At 0°C, the catalyst becomes an absolute oscillating catalyst which oscillates between the two conformations, one is to produce isotactic structure and the other is to produce syndiotactic. Because these two conformations have much lower potential energies than all the other intermediate conformations, the catalyst can only oscillate between two conformation and most of the time the catalyst's conformation should be one of these two and produce either isotactic or syndiotactic polymer. At 80°C, these two conformations still have lower potential energies than other intermediate conformations but the potential energy differences between these two conformations and other conformations are much smaller than at 0°C. So, besides these two conformations, the catalyst spends certain time on some intermediate conformations, which produce atactic structure.

Figure B-27 shows the C3 ^{13}C NMR of poly(1-hexene) synthesized by Cat. 4. Like we had mentioned above, although we cannot get this pure catalyst, the polymer synthesized by it gives good stereoblock microstructure. Isotacticity of this polymer on the pentad level is lower than that synthesized by Cat. 2, however, they are close on the heptad level.

Figure B-28 shows the C3 ^{13}C NMR of poly(1-hexene) synthesized by Cat. 5. At 80°C, it can only produce atactic polymer. However, at 0°C, it can produce stereoblock (isotactic + atactic) polymer.

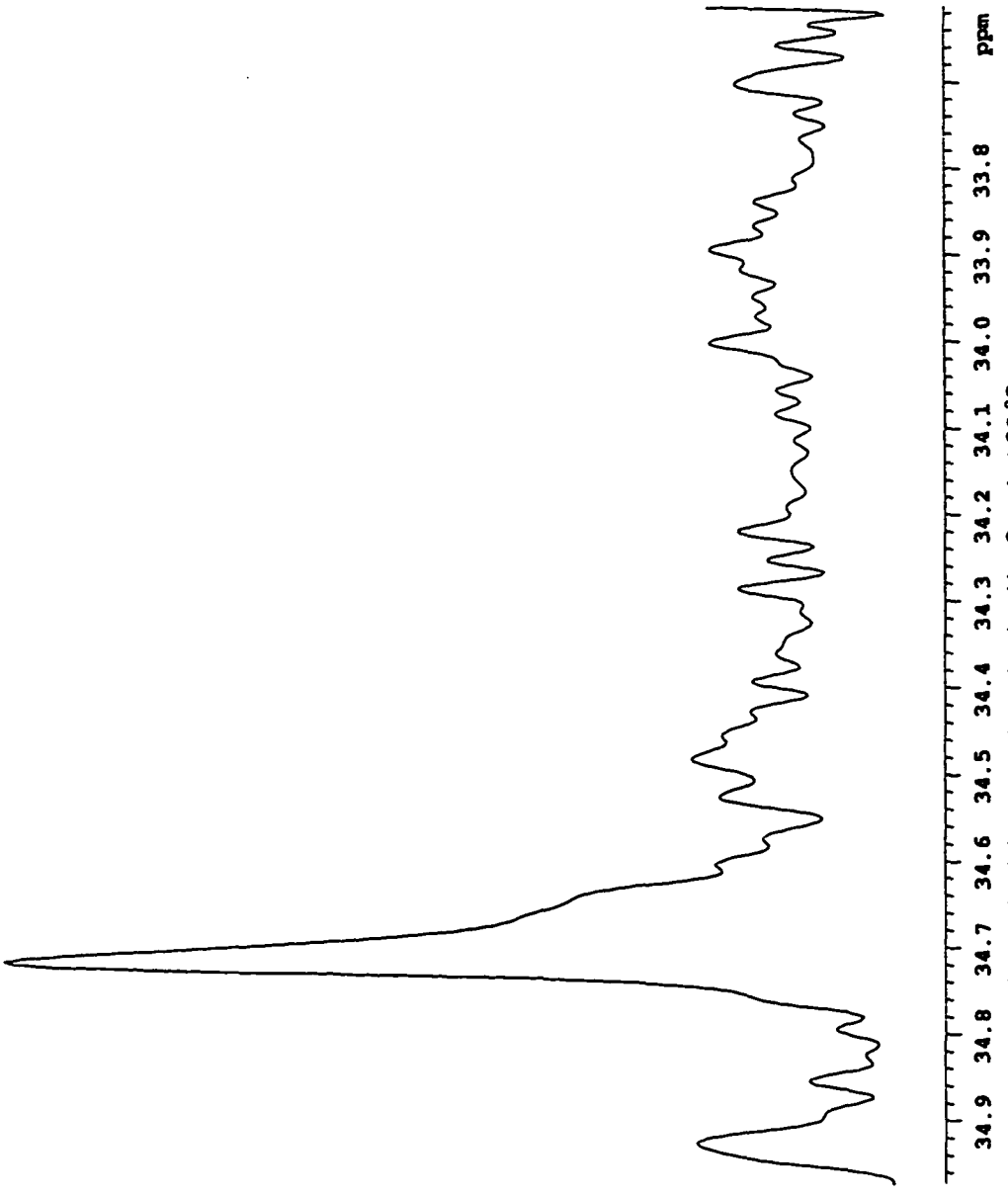

Figure B-27 C3 signal of poly(1-hexene) synthesized by Cat. 4 at 80 °C

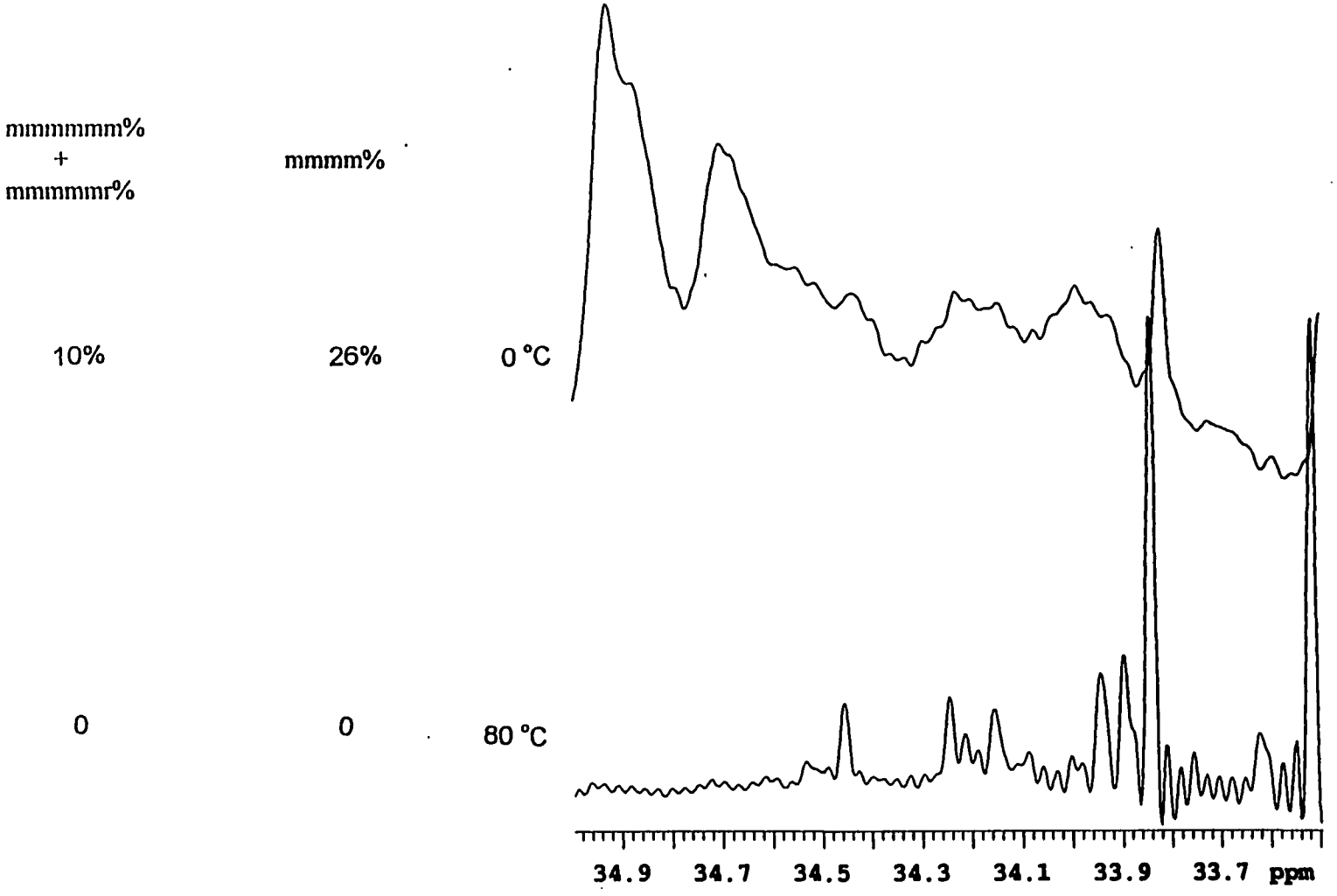

Figure B-28 C3 signal of poly(1-hexene) synthesized by Cat. 5 at different temperature

6.0 References

1. a) K. Ziegler, E. Holzkamp, H. Breil and H. Martin, *Angew. Chem.*, 1955, **67** 426, 541;

b) G. Natta, *J. Am. Chem. Soc.*, 1955, **77**, 1708.

2. G. Odian, *Principles of Polymerization*, 3rd ed., John Wiley & Son, Inc., 1991, 607.

3. a) G. Natta, G. Mazzanti, G. Crespi and G. Moraglio, *Chim. Ind. Milan*, 1957, **39**, 275;

b) G. Natta, *J. Polym. Sci.*, 1959, **34**, 531.

4. Y. V. Kissin, *Isospecific Polymerization of Olefins with Hetereogeneous Ziegler-Natta Catalysts*, Springer-Verlag, New York, 1985.

5. H. Sinn and W. Kaminsky, *Adv. Organomet. Chem.*, 1980, **18**, 99;

6. P. Pino and R. Mülhaupt, *Angew. Chem.*, 1980, **92,** 869; *Angew. Chem. Int. Ed. Engl.*, 1980, **19**, 857.

7. W. Kaminsky, S. Niedoba, N. Möller-Lindenhof and O. Rabe, 'Catalysts in Pooymer Synthesis", pp63, *ACS Symposium Series 496*, E. J. Vandenberg and J. C. Salamone, Eds., 1992.

8. H. H. Brintzinger, D. Fischer, R. Mülhaupt, B. Rieger and R. M. Waymouth, *Angew. Chem. Int. Ed. Engl.*, 1995, **34**, 1143.

9. F. R. W. P. Wild, L. Zsolnai, G. Hutter and H. H. Brintzinger, *J. Organomet. Chem.*, 1982, **232**, 233.

10. J. A. Ewen, L. Haspeslagh, J. L. Atwood and H. Zhang, *J. Am. Chem. Soc.*, 1987, **109**, 6544.

11. B. A. Kuntz, N. J. Taylor and D. C. Ward, *J. Organomet. Chem.*, 1988, **342**, 21.

12. R. B. Grossman, R. A. Doyle and S. L. Buchwald, *ibid.*, 1991, **10**, 1501.

13. F. Piemontesi, I. Camurati, L. Resconi, D. Balboni, A. Sironi, M. Moret, R. Ziegler and N.Piccolrovazzi, *ibid.*, 1995, **14**, 1256.

14. J. A. Ewen, *J. Am. Chem. Soc.*, 1984, **106**, 6355.

15. W. Kaminsky, K. Külper, H. H. Brintzinger and F. R. W. P. Wild, *Angew. Chem. Int. Ed. Engl.*, 1985, **24**, 507.

16. T. Asanuma, Y. Nishimori, M. Ito, N. Uchikawa and T. Shiomura, *Polymer Bulletin*, 1991, **25**, 567.

17. G. Erker, *J. Am. Chem. Soc.*, 1993, **115**, 4590.

18. A. M. Thayer, *C&E News,* 1995, Sep. 11, 15.

19. K. B. Wagener, *Science*, 1995, **267**, 191.

20. J. W. Collete and C. W. Tullock, U. S. *Patent*, 1982, **4,335**, 225.

21. J. W. Collete, *Macromolecules,* 1989, **22**, 3851.

22. D. T. Mallin, M. D. Rausch, Y. G. Lin, S. Dong and J. C. W. Chien, *J. Am. Chem. Soc.*, 1990, **112**, 2030.

23. J. C. W. Chien, G. H. Llinas, M. D. Rausch, Y. G. Lin, H. H. Winter, J. L. Atwood and S. G. Bott, *J. Am. Chem. Soc.*, 1991, **113**, 8569.

24. G. N. Babu, R. A. Newmark, H. N. Cheng, G. H. Llinas and J. C. W. Chien, *Macromolecules,* 1992, **25**, 7400.

25. G. W. Coates and R. W. Waymouth, *Science*, 1995, **267**, 217.

26. "*Physical constants of organic compounds*" in "CRC Handbook of Chemistry and Physics," 68th Ed., R. C. Weast, M. J. Astle and W. H. Beyer, Eds., Chemical Rubber Publishing Company, 1987-1988, ppC-323.

27. "*Aromatic Hydrocarbons: 3)Non-fused multiple ring*" in "The Aldrich Library of ^{13}C and ^{1}H FT-NMR Spectra", 1st Ed., C. J. Pouchert and J. Behnke, **Vol. 2**, 39A.